THE MEASUREMENT OF THE BOEING 747 TRAILING VORTEX SYSTEM USING THE TOWER FLY-BY TECHNIQUE

Leo J. Garodz, et al

National Aviation Facilities Experiment Center

Prepared for:

Federal Aviation Administration

June 1974

NOTICE

This document is disseminated under the sponsorship of the Department of Transportation in the interest of information exchange. The United States Government assumes no liability for its contents or use thereof.

Technical Report Documentation Page

1. Report No.	2. Government Accession No.	3. Recipient's Catalog No.
FAA-RD-73-156		AD 782 046

4. Title and Subtitle	5. Report Date
THE MEASUREMENT OF THE BOEING 747 TRAILING VORTEX SYSTEM USING THE TOWER FLY-BY TECHNIQUE	June 1974
	6. Performing Organization Code
	8. Performing Organization Report No.
7. Author(s)	
Leo J. Garodz, David Lawrence, and Nelson J. Miller	FAA-NA-73-73
9. Performing Organization Name and Address	10. Work Unit No. (TRAIS)
Federal Aviation Administration National Aviation Facilities Experimental Center Atlantic City, New Jersey 08405	11. Contract or Grant No. 214-531-070
	13. Type of Report and Period Covered Final September - October 1972
12. Sponsoring Agency Name and Address	14. Sponsoring Agency Code
Department of Transportation Federal Aviation Administration Systems Research and Development Service Washington, D. C. 20590	

15. Supplementary Notes

COLOR ILLUSTRATIONS REPRODUCED IN BLACK AND WHITE

16. Abstract

The characteristics of the trailing vortex system of the Boeing 747 airplane have been investigated by the National Aviation Facilities Experimental Center (NAFEC), Atlantic City, N. J., during a series of flight tests conducted in September and October 1972. This investigation is part of a long-term program, started in February 1970 with flight tests conducted by NAFEC at the Atomic Energy Commission site at Idaho Falls, Idaho, devoted to the study of the overall wake turbulence problem. The present tests were conducted using improved flow measurement and meteorological instrumentation, permitting greater resolution than had been possible in earlier testing. Principal findings were that the peak tangential velocity decays as the reciprocal of the square root of the time elapsed since vortex generation; that the peak velocity is unaffected by the throttling back of the adjacent outboard engine; and that the lateral transport velocities correlate quite well with theory. Vortex descent rates did not correlate with theory, being up to three times greater than theoretical values. It was further determined that the velocity distribution in the Boeing 747 trailing vortices is strongly affected by the wing flap setting. At small settings, the vortex core diameter is small and peak tangential velocities are high, and as the flap deflection is increased, the core diameters increase and peak velocities diminish.

17. Key Words	18. Distribution Statement
Wakes Turbulence Trailing Vortices Full-Scale Flight Tests Hot-Film Anemometry	Document is available to the public through the National Technical Information Service, Springfield, Virginia 22151

19. Security Classif. (of this report)	20. Security Classif. (of this page)	21. No. of Pages	22. Price
Unclassified	Unclassified	238	6.00 - 1/45

Form DOT F 1700.7 (8-72) Reproduction of completed page authorized

TABLE OF CONTENTS

	Page
INTRODUCTION	1
Purpose	1
Background	1
DISCUSSION	1
Flight Test Program	1
Test Airplane	1
Test Procedure	1
Test Tower	6
Instrumentation	6
Aircraft	6
Tower Vortex Measurement	8
Tower Atmospheric Measurements	8
Photography	8
Time	8
Test Site	8
Data Processing	8
Data Presentation	12
Data Analysis	12
CONCLUSIONS	56
REFERENCES	57
APPENDIXES	
A - Instrumentation	
B - Data Processing	
C - Tangential Velocity Distributions	
D - Summary Flight Test Data Sheets	
E - Vortex Lateral Transport Velocity vs. X-Wind Component Peak Recorded Velocity vs. Altitude at Tower	
F - Low-Altitude Meteorological Data	
G - Windspeed and Direction at 140 feet, Airplane Track, Date, and Time of Runs	

LIST OF ILLUSTRATIONS

Figure		Page
1	Boeing 747 Airplane - Landing Configuration - Underview Showing Flap Arrangement	2
2	Boeing 747 Airplane - Landing Configuration - Three Quarter Front View	3
3	General Arrangement and Major Dimensions - Boeing 747	4
4	Boeing 747 Flaps at Full Deflection (25°)	5
5	Closeup of Boeing 747 Abeam of the Tower - Minimum Lateral Clearance	7
6	NAFEC Full-Scale Flight Test Vortex Measurement Facility - Looking Northwest	9
7	NAFEC Full-Scale Flight Test Vortex Measurement Facility - Looking West	10
8	Boeing 747 - Colored Smoke Flow Visualization of Upwind (i.e., Second) Vortex	11
9	Computer Expanded Time History of Tangential Velocity	13
10	Peak Recorded Tangential Velocity vs. Age (Landing Configuration) (2 Pages)	15
11	Data Sample Indicates Second Vortex Core Reached Sensor at 67 Seconds, at or Close to the 62-Foot Level	17
12	Data Sample Indicates Second Vortex Core Reached Sensor at 27 Seconds, at or Close to the 70-Foot Level	18
13	Resultant Velocity Distribution Through Vortex When Core Registers Exact "Hit" on Sensor. $V_w = .125\ V_{\theta_{max}}$	19
14	Expanded Time History of Recorded Velocity at a Sensor	20
15	Geometric Relationship for Sensor Velocities	21
16	Peak Recorded Tangential Velocity vs. Age (All Available Data)	23
17	Peak Recorded Tangential Velocity vs. Age (Takeoff Configuration)	25

LIST OF ILLUSTRATIONS (continued)

Figure		Page
18	Peak Recorded Tangential Velocity vs. Age (Holding Configuration)	26
19	Peak Recorded Tangential Velocity vs. Age (Landing Configuration - Upwind Vortices)	27
20	Peak Recorded Tangential Velocity vs. Age (Landing Configuration - Downwind Vortices)	28
21	Derived Vortex Core Diameter as a Function of Peak Recorded Tangential Velocity (Takeoff Configuration)	30
22	Derived Vortex Core Diameter as a Function of Peak Recorded Tangential Velocity (Holding Configuration)	31
23	Derived Vortex Core Diameter as a Function of Peak Recorded Tangential Velocity (Downwind Vortices - Landing Configuration)	32
24	Derived Vortex Core Diameter as a Function of Peak Recorded Tangential Velocity (Upwind Vortices - Landing Configuration)	33
25	Derived Vortex Core Diameter vs. Vortex Age (Landing Configuration - Diameter Determined From V_θ - h Plots)	34
26	Derived Vortex Core Diameter vs. Vortex Age (Takeoff and Holding Configurations - Diameter Determined from V_θ - h Plots)	35
27	Comparison of Theoretical and Actual Vortex Mean Descent Rates (2 Pages)	40
28	Peak Recorded Tangential Velocity vs. Windspeed (Takeoff Configuration - Downwind Vortices)	42
29	Peak Recorded Tangential Velocity vs. Windspeed (Takeoff Configuration - Upwind Vortices)	43
30	Peak Recorded Tangential Velocity vs. Windspeed (Holding Configuration - Downwind Vortices)	44
31	Peak Recorded Tangential Velocity vs. Windspeed (Holding Configuration - Upwind Vortices)	45
32	Peak Recorded Tangential Velocity vs. Windspeed (Landing Configuration - Downwind Vortices)	46

LIST OF ILLUSTRATIONS (continued)

Figure		Page
33	Peak Recorded Tangential Velocity vs. Windspeed (Landing Configuration - Upwind Vortices)	47
34	Hoffman-Joubert Logarithmic Distribution of Tangential Velocity (Small Core Vortex)	49
35	Hoffman-Joubert Logarithmic Distribution of Tangential Velocity (Large Core Vortex)	50
36	Correlation of Vortex Core Diameter as Determined by Two Methods	54
A-1	Vortex Tower Location NAFEC/Atlantic City Airport	A-2
A-2	Sensor Locations on Tower	A-3
A-3	Directional Location of Sensors	A-4
A-4	Constant Resistance Hot-Film Anemometer System	A-6
A-5	Wakes and Vortices Checkoff Sheet	A-8
A-6	Block Diagram - Data System Wakes and Vortices	A-9
A-7	Wakes and Vortices VCO Assignments	A-10
A-8	Wakes and Vortices Checkoff Sheet	A-12
B-1	Schematic of Information Flow	B-2
B-2	Data Retrieval Program (3 Pages)	B-3
B-3	Schematic of Plot II Program Series	B-7
E-1	Vortex Lateral Transport Velocity vs. Crosswind Velocity Component. Takeoff Configuration	E-1
E-2	Vortex Lateral Transport Velocity vs. Crosswind Velocity Component. Holding Configuration	E-2
E-3	Vortex Lateral Transport Velocity vs. Crosswind Velocity Component. Landing Configuration - Upwind Vortices	E-3
E-4	Vortex Lateral Transport Velocity vs. Crosswind Velocity Component. Landing Configuration - Downwind Vortices	E-4

LIST OF ILLUSTRATIONS (continued)

Figure		Page
E-5	Peak Recorded Tangential Velocity vs. Aircraft Altitude Abreast of Tower. Landing Configuration - Downwind Vortices, Zero to 10 Seconds Age	E-5
E-6	Peak Recorded Tangential Velocity vs. Aircraft Altitude Abreast of Tower. Landing Configuration - Upwind and Downwind Vortices, 10 to 15 Seconds Age	E-6
E-7	Peak Recorded Tangential Velocity vs. Aircraft Altitude Abreast of Tower. Landing Configuration - Upwind and Downwind Vortices, 15 to 20 Seconds Age	E-7
E-8	Peak Recorded Tangential Velocity vs. Aircraft Altitude Abreast of Tower. Landing Configuration - Upwind Vortices, 20 to 25 Seconds Age	E-8
E-9	Peak Recorded Tangential Velocity vs. Aircraft Altitude Abreast of Tower. Landing Configuration - Upwind and Downwind Vortices, 25 to 30 Seconds Age	E-9
E-10	Peak Recorded Tangential Velocity vs. Aircraft Altitude Abreast of Tower. Landing Configuration - Upwind and Downwind Vortices, >30 Seconds Age	E-10

LIST OF SYMBOLS AND DEFINITIONS

h	=	Height from base of tower, feet.
r	=	Radial distance from vortex axis, feet.
r_c	=	Vortex core radius, feet.
S	=	Airplane reference wing area, square feet.
AR	=	Aspect ratio, span $\div$ geometric mean chord.
$\Lambda_{.25c}$	=	Wing sweepback angle at quarter chord point, degrees.
V_θ	=	Vortex tangential velocity, feet per second.
$\hat{V}$	=	Peak recorded velocity, uncorrected for wind, feet per second.
V_w	=	Wind velocity at time zero at height where $\hat{V}$ is recorded.
Γ	=	Median circulation, based on elliptical lift distribution, square feet per second.
ν	=	Kinematic viscosity term in Prandtl vortex model, square feet per second.
ρ	=	Density of the air, slugs per cubic foot.

INTRODUCTION

PURPOSE.

The work described in this report was performed to gain information on the wake turbulence characteristics of the Boeing 747 airplane, to aid in the development of improved terminal area traffic control procedures, needed to minimize the wake turbulence hazard.

BACKGROUND.

It became apparent, early in 1970, that there was a need to further investigate the wake characteristics of large jet transport airplanes in conditions representative of terminal area operations. An investigation was conducted, involving the Federal Aviation Administration (FAA)/National Aviation Facilities Experimental Center (NAFEC), the National Aeronautics and Space Administration (NASA), The Boeing Company, and the United States Air Force. The airplanes involved, flight test techniques used, and results obtained are reported on in references 1, 2, and 3.

NAFEC's part in that operation included the acquisition of quantitative data on the characteristics of the Boeing 747 wake, using the tower fly-by technique. At the time a very limited number of sensors was available for the measurement of vortex flow velocities. However, in view of the currently-accepted theory of vortex phenomena of fixed-wing aircraft (reference 4), namely that core diameter is initially equal to 15 percent of the wing span, the available instrumentation appeared to suffice for achieving the objective of the planned tests. It has subsequently been shown (reference 5) that core diameters are much smaller than were originally predicted, especially in certain configurations, and the need for further tests, utilizing closer sensor spacing, became apparent.

DISCUSSION

FLIGHT TEST PROGRAM.

TEST AIRPLANE. The Boeing 747 airplane, figures 1, 2, and 3, used in this test program was leased from Pan American Airways. It is a large four-engine commercial jet transport airplane powered by Pratt and Whitney JT9D-3A turbo-fan engines. The wing has an area of 5,500 square feet, aspect ratio 6.95, and a 37 1/2° sweep angle at the quarter chord. The flaps are triple-slotted, in four segments, with cutouts at the fuselage and behind the inboard engines. Full-span leading-edge flaps are also fitted. A closeup of the trailing edge flaps is shown in figure 4.

TEST PROCEDURE. The flight test procedure used in the present tests has been described in reference 6 and will not be discussed further in this report, with the exception of certain changes as follows:

FIGURE 1. BOEING 747 AIRPLANE - LANDING CONFIGURATION - UNDERVIEW SHOWING FLAP ' \NGEMENT

FIGURE 2. BOEING 747 AIRPLANE - LANDING CONFIGURATION - THREE QUARTER FRONT VIEW

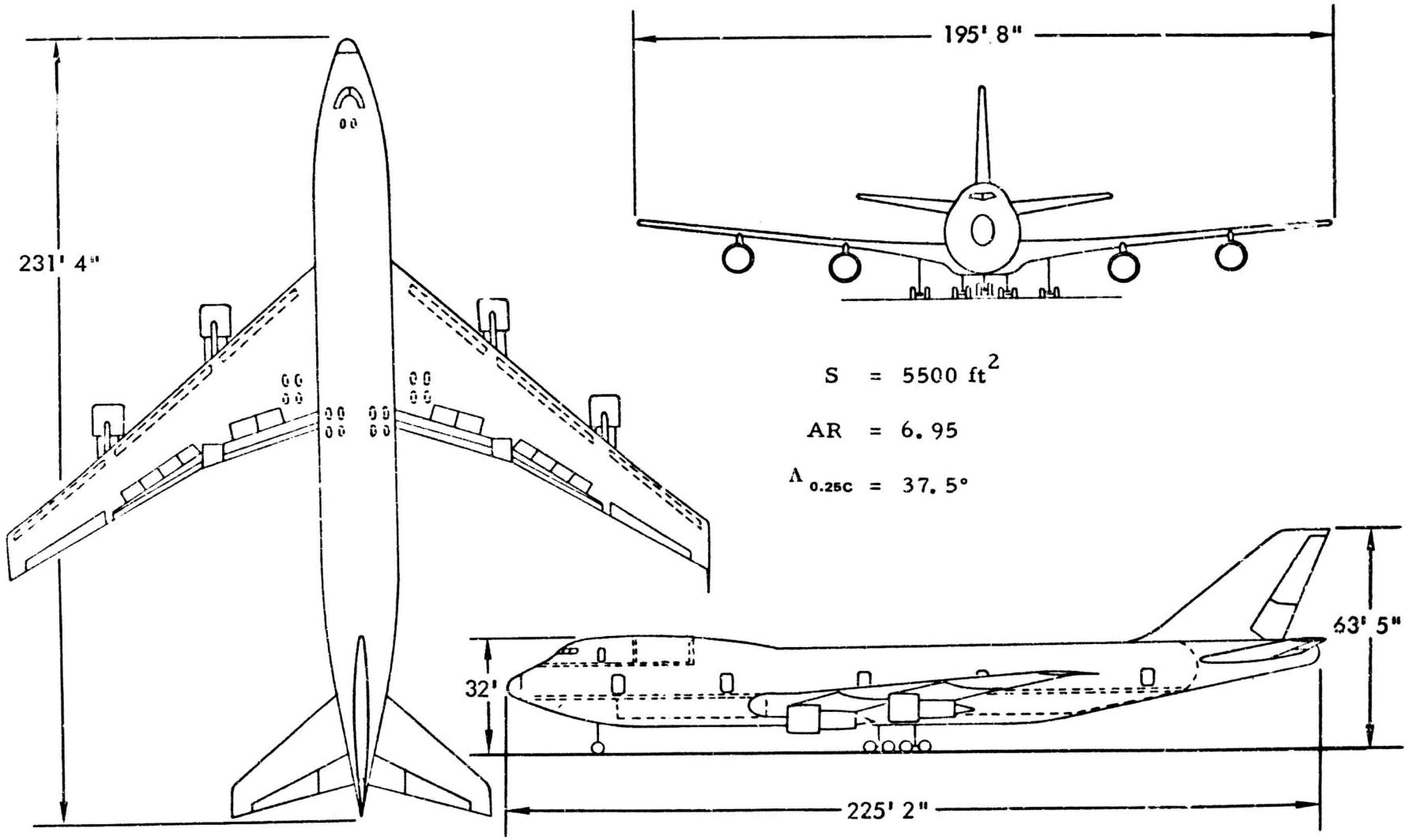

FIGURE 3. GENERAL ARRANGEMENT AND MAJOR DIMENSIONS - BOEING 747

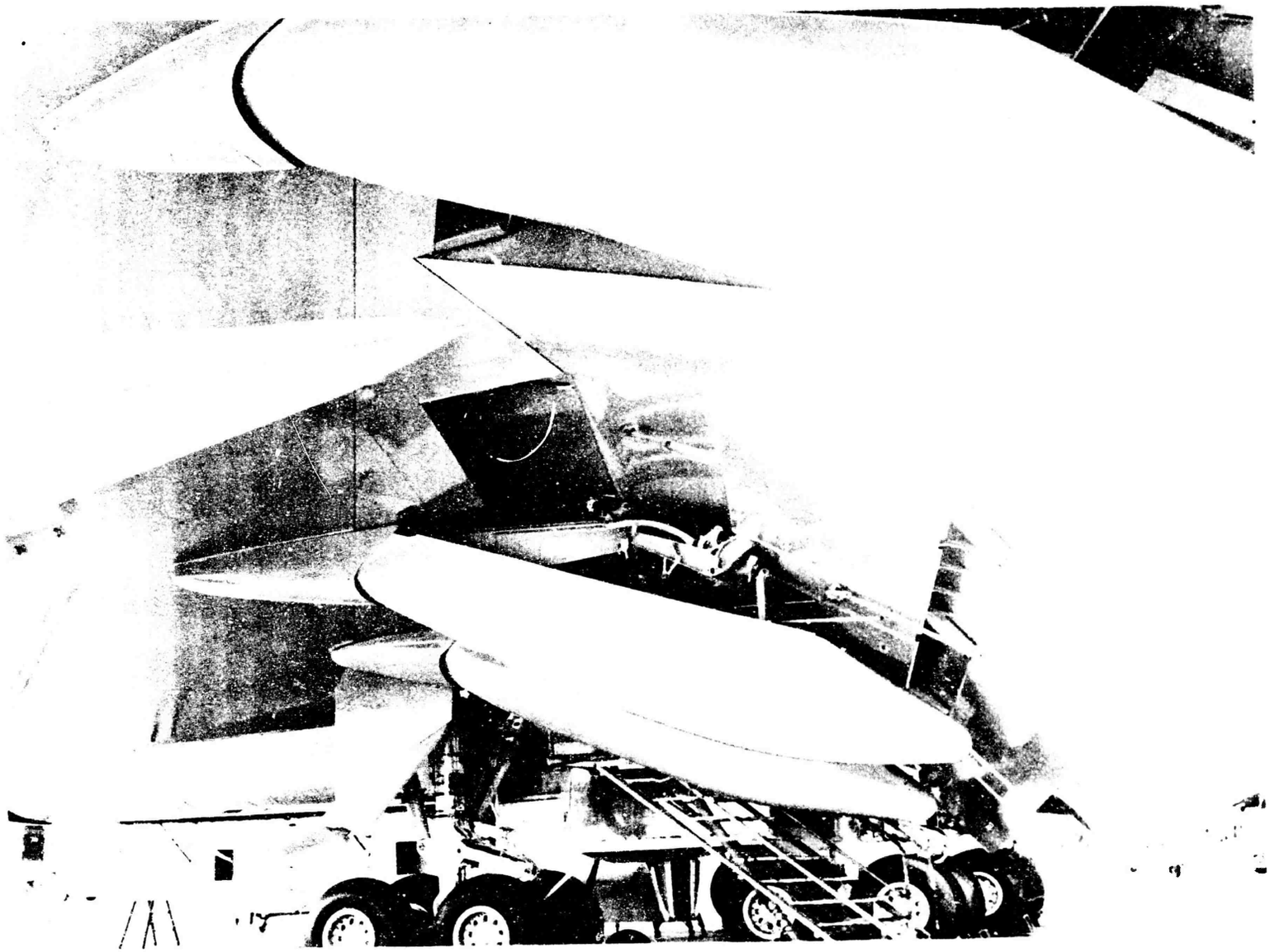

FIGURE 4. BOEING 747 FLAPS AT FULL DEFLECTION (25°)

- "Zoom" climbs were scheduled for certain runs to simulate a wave-off/go-around condition from a landing-approach maneuver (see figure 5).

- Several runs were made with an outboard engine (i.e., No. 1 or No. 4) throttled back to flight idle.

TEST TOWER. The test tower used in these tests is the same tower used in previous tests of this type, described in detail in reference 6.

INSTRUMENTATION.

AIRCRAFT. The airplane needed no special instrumentation. A pilot's log sheet was used to record the following information when the airplane was approximately abreast of the tower:

- Time.

- Airplane configuration (landing, takeoff, or holding).

- Gross weight.

- Indicated airspeed.

- Radar altitude.

- Pressure altitude.

- Magnetic track.

- Lateral offset from test tower.

- Engine performance.

- Subjective evaluation of atmospheric turbulence.

For data reduction purposes, phototheodolite data on aircraft altitude above ground level (AGL), lateral offset, track, and groundspeed was used whenever it was available. Groundspeed was corrected to true airspeed using wind velocity data gathered at a height of 140 feet.

Since the test pressure altitude was so low, it was not considered necessary to account for the difference between true airspeed and equivalent airspeed in any data reduction or calculations dependent on these quantities (such as calculation of lift coefficient or estimation of the strength of the tip vortices).

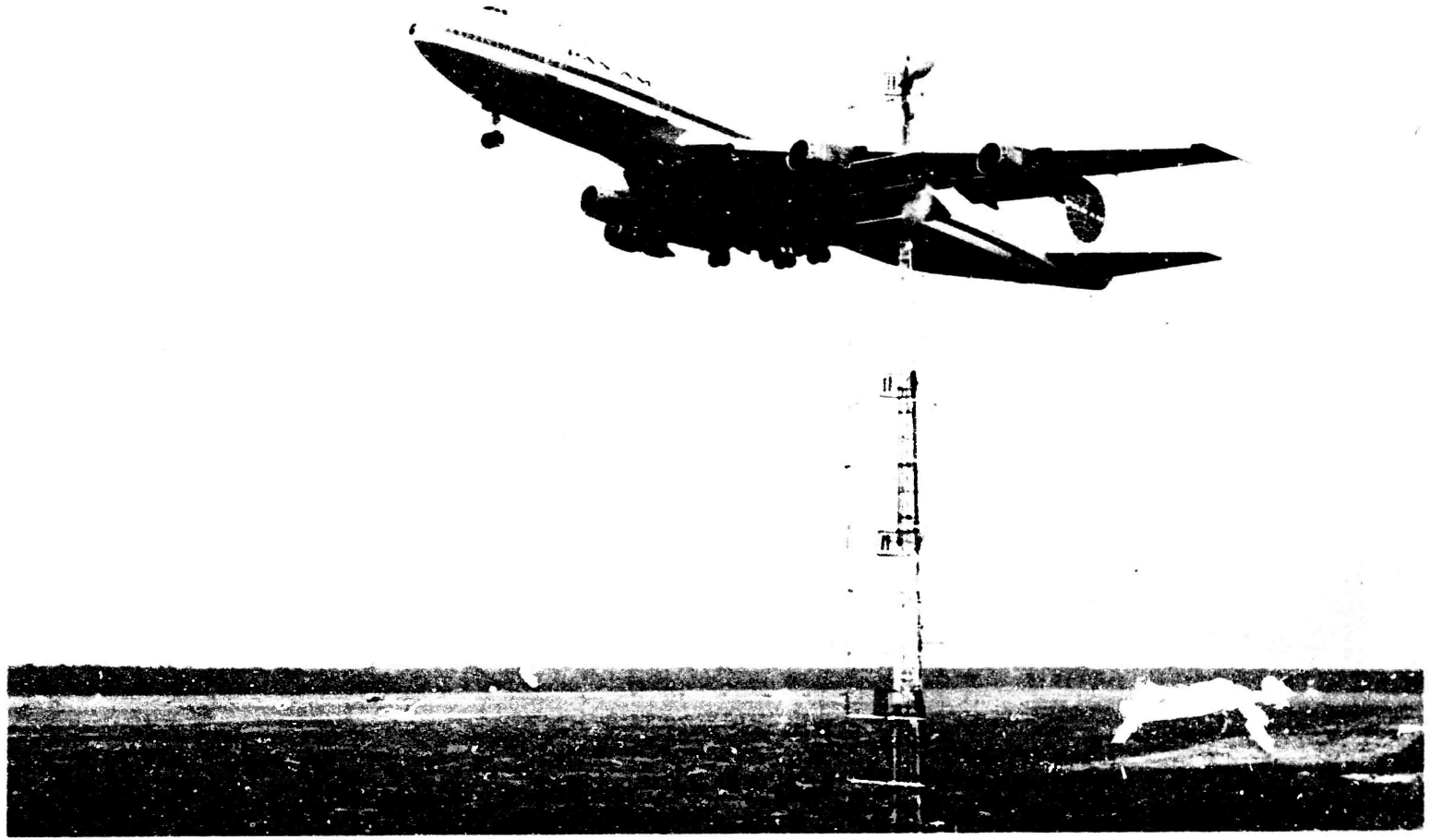

FIGURE 5. CLOSEUP OF BOEING 747 ABEAM OF THE TOWER - MINIMUM LATERAL CLEARANCE

TOWER VORTEX MEASUREMENT. The airflow measurement instrumentation used in the current test series represents a considerable improvement over that used in earlier tests (reference 6). Closer spacing of the sensors (at 2-foot intervals from 8 to 40 feet, 1-foot intervals from 40 to 142 feet) resulted in enhanced resolution. The same type of hot-film sensor was used, however, capable only of yielding scalar magnitude of the air flow velocity impinging on it. Further details of the instrumentation may be found in reference 6 and in appendix A of this report.

TOWER ATMOSPHERIC MEASUREMENTS. The instrumentation used in the present test series was the same as that used for and discussed in reference 6.

PHOTOGRAPHY. Colored smoke grenades were used to provide flow visualization, and motion picture photography was used to record the results. This made it possible to determine when and at what level the vortex systems intercepted the tower and is a valuable aid in confirming the interpretation of sensor data. Two 16 mm motion picture cameras, normally located on 325 feet radii, 90° apart, centered at the tower, were used to provide this coverage. A third 16 mm motion picture camera, using a zoom lens was set on a "HI-RANGER" crane to provide closeup coverage of the vortices.

TIME. All data runs were time correlated as discussed in reference 6.

TEST SITE. The NAFEC aircraft vortex measurement facility was used for these tests. It consists of: (1) A 140-foot test-tower suitably instrumented for vortex flow and meteorological measurements, (2) Colored smoke dispensers (racks holding easily replaceable grenades) for vortex flow visualization, mounted on both the 140-foot tower and the movable 88-foot telescopic towers, (3) Motion picture photography (16 mm) stations, (4) Three concentric circles marked on the ground, centered at the base of the tower, in yellow, with radii of 100, 200, and 300 feet, for pilot site identification, and (5) High-intensity strobe lights for pilot assistance in alignment of the aircraft track abeam of the tower. Figures 6, and 7 show overall views of the test site. Figure 8 shows a good example of the flow visualization - in this case, of the upwind (second) vortex.

DATA PROCESSING.

The signals from the hot-film airflow velocity sensors were recorded on magnetic tape and subsequently digitized at the NAFEC Central Data and Recovery System (CENDAR) facility (see reference 7 for details of CENDAR) for automatic data processing. The data processing, handling, and computations were performed on the IBM 7090 computer. The special software programs for data conversion supplied information for a large flatbed plotter, which produced sensor velocity time histories. Appendix B presents details of the data processing techniques.

FIGURE 6. NAFEC FULL-SCALE FLIGHT TEST VORTEX MEASUREMENT FACILITY - LOOKING NORTHWEST

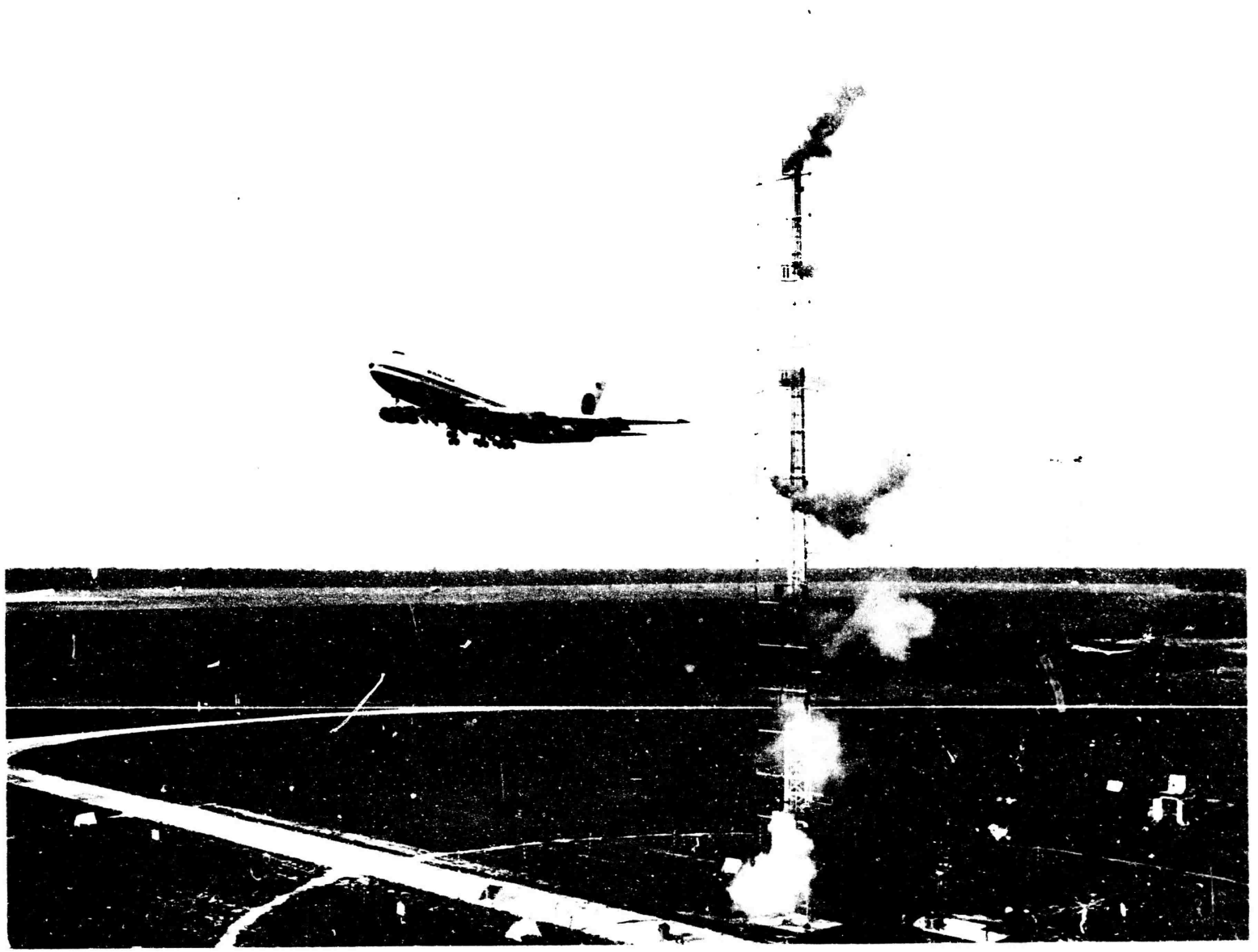

FIGURE 7. NAFEC FULL-SCALE FLIGHT TEST VORTEX MEASUREMENT FACILITY - LOOKING WEST

FIGURE 8. BOEING 747 - COLORED SMOKE FLOW VISUALIZATION OF UPWIND (i.e., SECOND) VORTEX

DATA PRESENTATION.

The data output and presentation consisted primarily of:

1. Computer printout (tabular) of peak recorded vortex tangential velocity with associated vortex ages as recorded by the hot-film sensors on the tower.

2. Printout of atmospheric data on temperature, wind direction, and relative humidity, as recorded by appropriate sensors located on the tower at the 23-, 45-, 70-, 100- and the 140-foot levels.

3. Plots of recorded tangential velocity scalar magnitude against time for the hot-film sensors.

4. Plots of recorded tangential velocity versus time, using an expanded time scale for enhanced data resolution (as required) for detailed vortex analysis. A sample of such a plot depicting a core penetration is presented in figure 9.

Most flight test runs were further analyzed to generate vortex velocity profiles, presenting vortex tangential velocity (corrected for wind), as a function of sensor height above ground level. The resultant velocity profiles are presented in appendix C.

DATA ANALYSIS.

The general flow pattern generated behind the Boeing 747 does not, for the purposes of data reduction, differ significantly from that generated behind the DC7, as discussed in reference 6. The change in airplane size is one obvious difference, but not of fundamental importance. Of greater significance is the difference in wing plan-form and the associated load distribution. The Boeing 747 wing, furthermore, has segmented flaps - two segments per side - with a fuselage cut-out (as can be seen in figures 1, 2, and 4), while the DC7 flap system features a continuous flap on each side, again with a fuselage cut-out. These differences are felt to the greatest extent in the near-flow field, but do not completely disappear as the wake develops downstream. Far downstream, it is generally considered that the wake behind any lifting surface tends to resolve itself into a pair of oppositely rotating vortices that produce downwash in the center of the wake, and upwash at the edges. Differences still remain however, between the wake of a flapped wing - and that of an unflapped wing - that result in the more rapid breakup (into random turbulence) of the wake of the flapped wing. With the present anemometry, no directional information is obtained, and the interpretation of tangential velocity time histories (to produce velocity distributions across the diameter of the vortex) has necessarily proceeded on the assumption of a single-centered circulatory motion about the vortex axis, though this may not be strictly correct when the wing flaps are appreciably deflected. Reference 6, gives consideration to the effects of outboard slip-stream rotation, and it appeared from the data on the takeoff configuration that where rotation

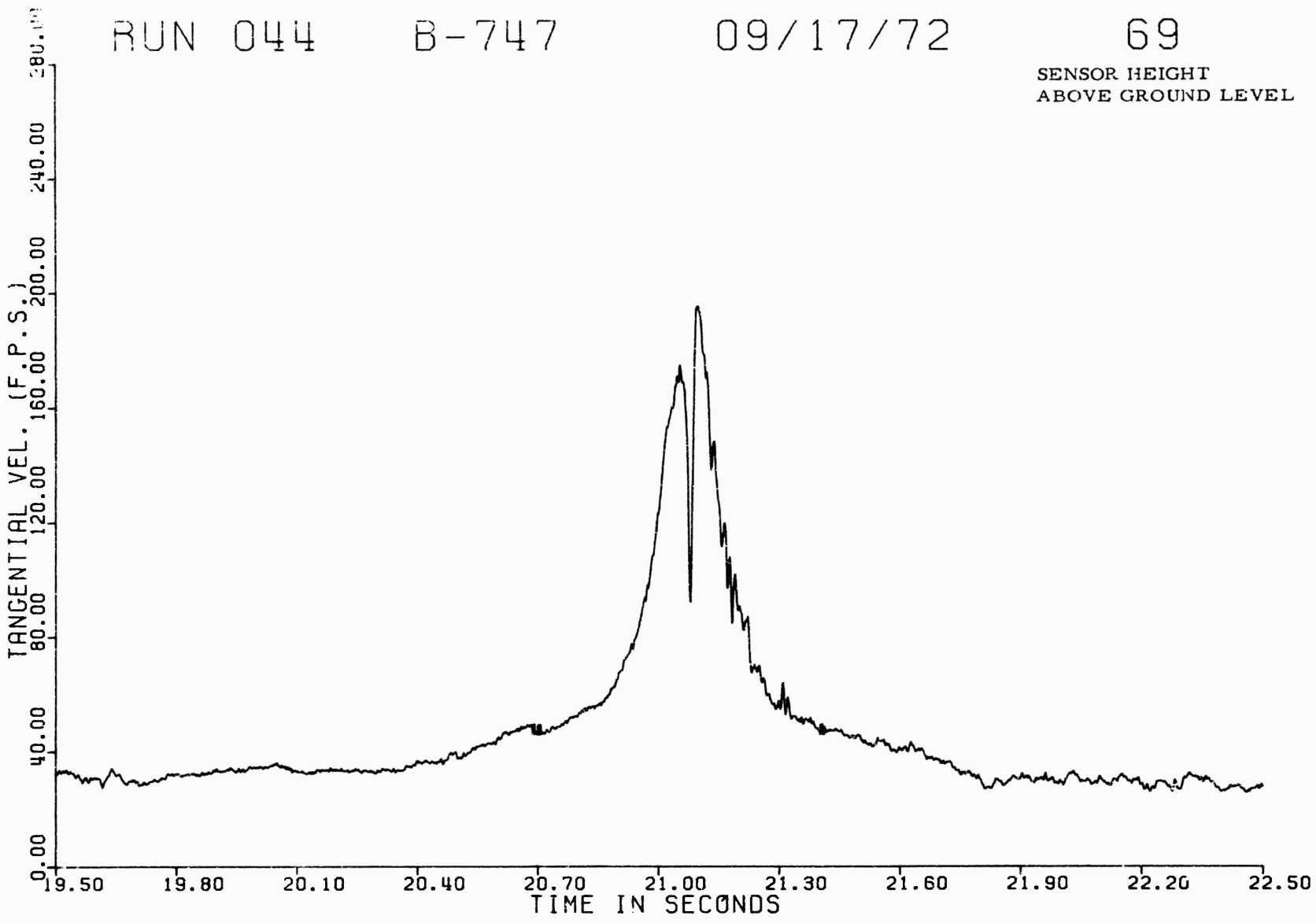

FIGURE 9. COMPUTER EXPANDED TIME HISTORY OF TANGENTIAL VELOCITY

was against the tip vortex, the peak tangential velocity was noticeably diminished. While rotation still exists in the efflux of a turbo-fan engine, it is not thought to be as significant, but the longitudinal momentum of the efflux, injected into the wake at a point near where there occurs a large and rapid change in circulation (such as at the extremity of a deflected flap), is thought to be possible cause of detectable changes in the near-field wake. For this reason then, certain data runs in this series were made with an outboard engine throttled back to flight idle (figure 10).

Interpreting the Boeing 747 data has been a simpler task than that presented by the DC7 data of reference 6 - largely because of the closer sensor spacing and greater ease of vortex core identification. The problem of ambiguity still arises in those parts of each vortex where the induced velocities are in opposition to the ambient wind. In that situation, a measured velocity of 10 feet per second (ft/s), for example, could be the difference between 20 ft/s wind velocity and either a 10 ft/s vortex tangential velocity, or a 30 ft/s vortex tangential velocity. The resolution of the ambiguity is dependent on knowledge of the direction of the 10 ft/s resultant, and this is not available.

The closer spacing of sensors has resulted in the more frequent capture of peak or near-peak velocities, and many instances occurred where a "core-hit" can be identified. Examples of this phenomenon are shown in figures 11 and 12. As the vortex core approaches the sensor, the measured tangential velocity rises, until it reaches a peak value, at the outer extremity of the core. Within the core, velocity diminishes linearly to zero at the axis, and the more closely the axis passes to the sensor, the steeper the dip - then as the core passes through, the velocity rises sharply again at the point where the sensor detects the velocity at the extreme core radius once more (see figures 13, 14, and 15). The time interval that elapses between adjacent peaks of this kind is a direct measure of core diameter, so long as the vortex axis can be located with reasonable accuracy. If the instantaneous vortex lateral transport velocity were known, then the core diameter could be determined. The instantaneous velocity cannot be determined by the existing experimental method, however, although the mean value, between time zero and the vortex hit on the tower, can be determined fairly accurately. The question of core diameter, its relationship to peak tangential velocity and its dependence on airplane configuration and variation as a function of time, are discussed in a separate subsection of this analysis.

Seventy-six data runs were made, of which approximately 80 percent were successful in yielding usable data - usable, that is, in the sense of being capable of interpretation to yield tangential velocity distribution plots. Of the 76 runs, 9 were made in the takeoff configuration, 17 in the holding and cruise configurations, and the balance (50) in the landing configuration. The emphasis on the landing configuration is appropriate, in view of the operational regime in which airplane wake turbulence is considered to be the greatest hazard. The configuration terminology used here relates to the aerodynamic configuration. The power settings were those appropriate to the maintenance of level flight at the selected airspeed. Flight test data,

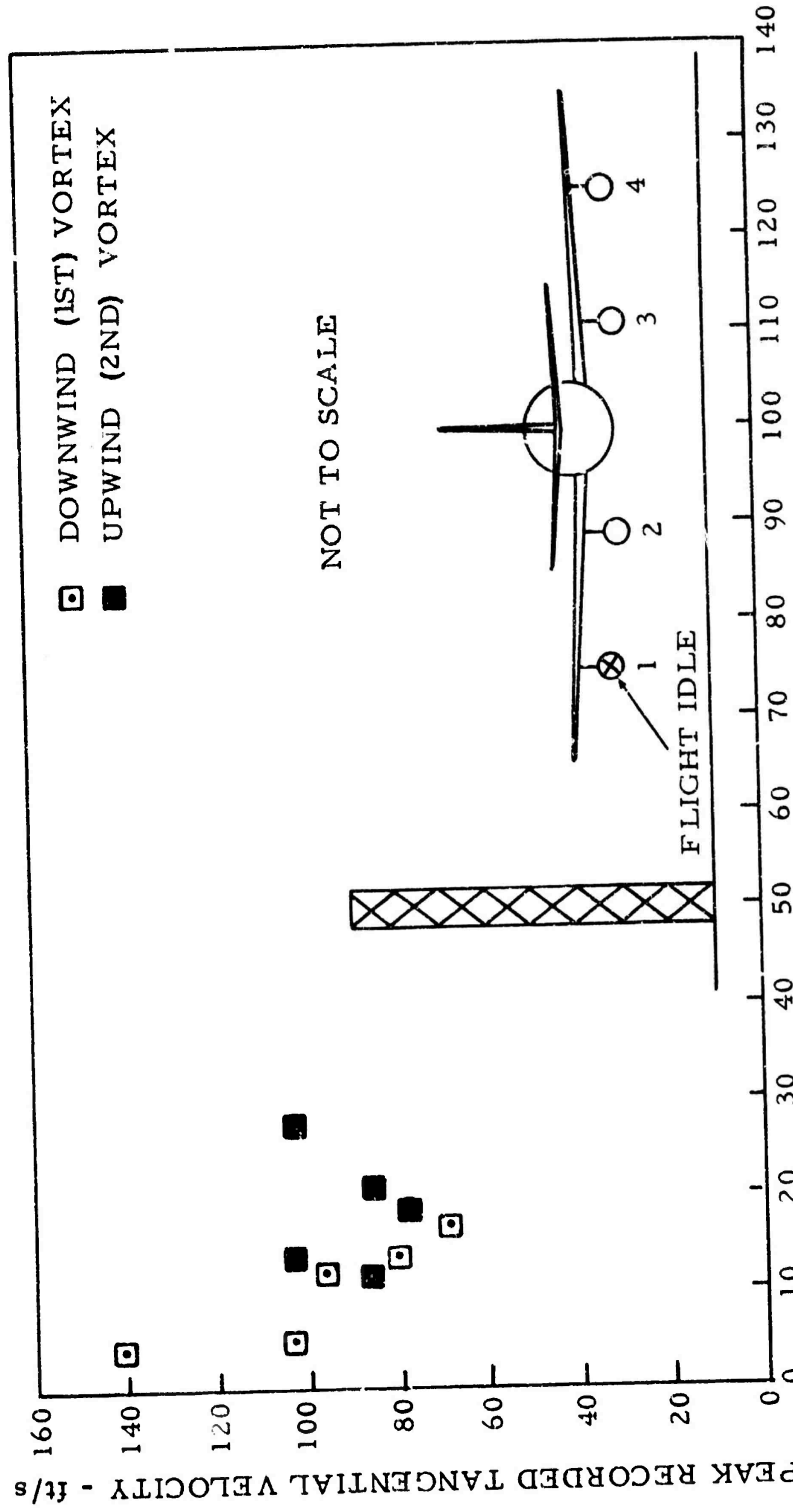

FIGURE 10. PEAK RECORDED TANGENTIAL VELOCITY VS. AGE (LANDING CONFIGURATION)
(Sheet 1 of 2)

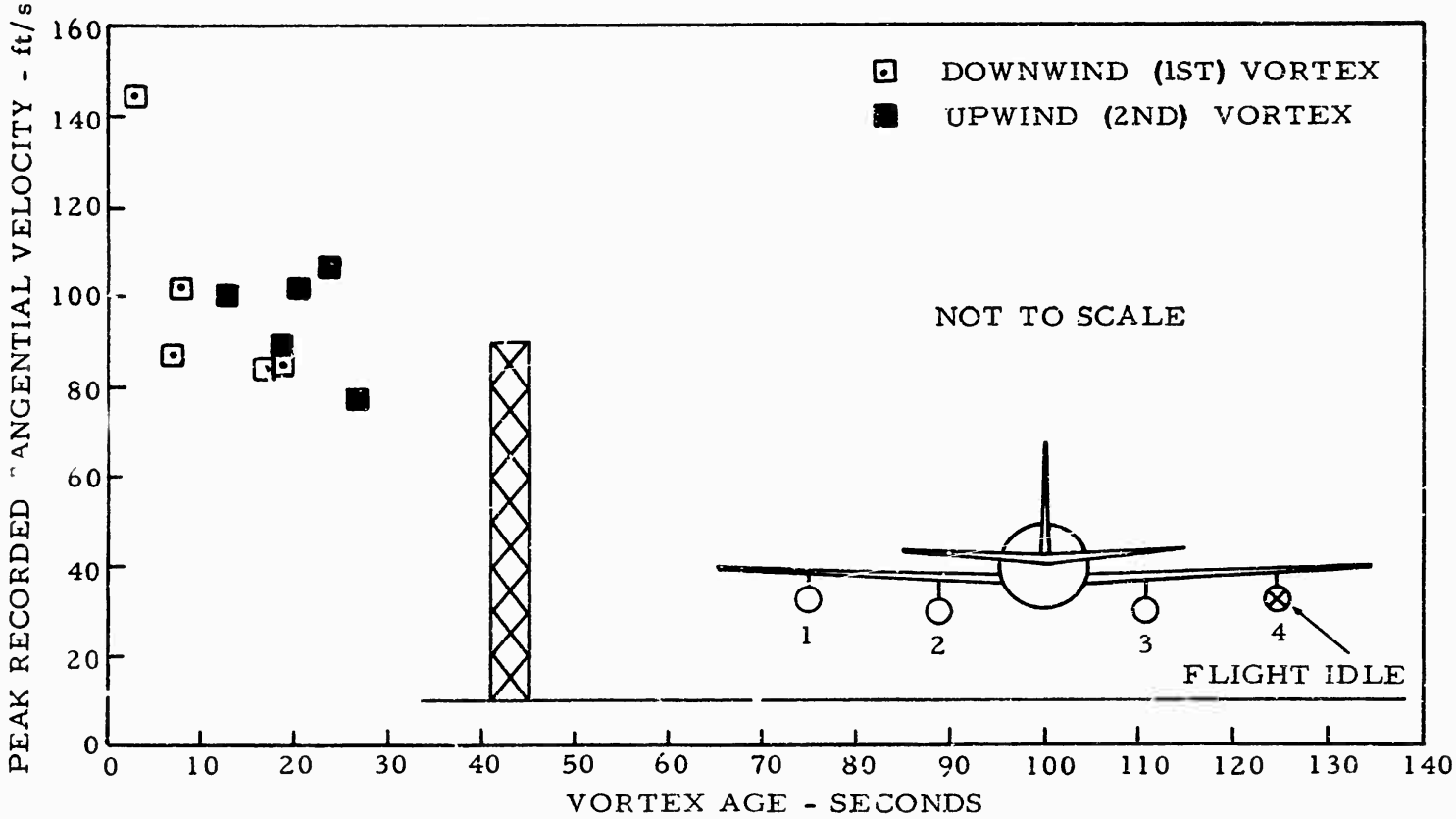

FIGURE 10. PEAK RECORDED TANGENTIAL VELOCITY VS. AGE (LANDING CONFIGURATION)
(Sheet 2 of 2)

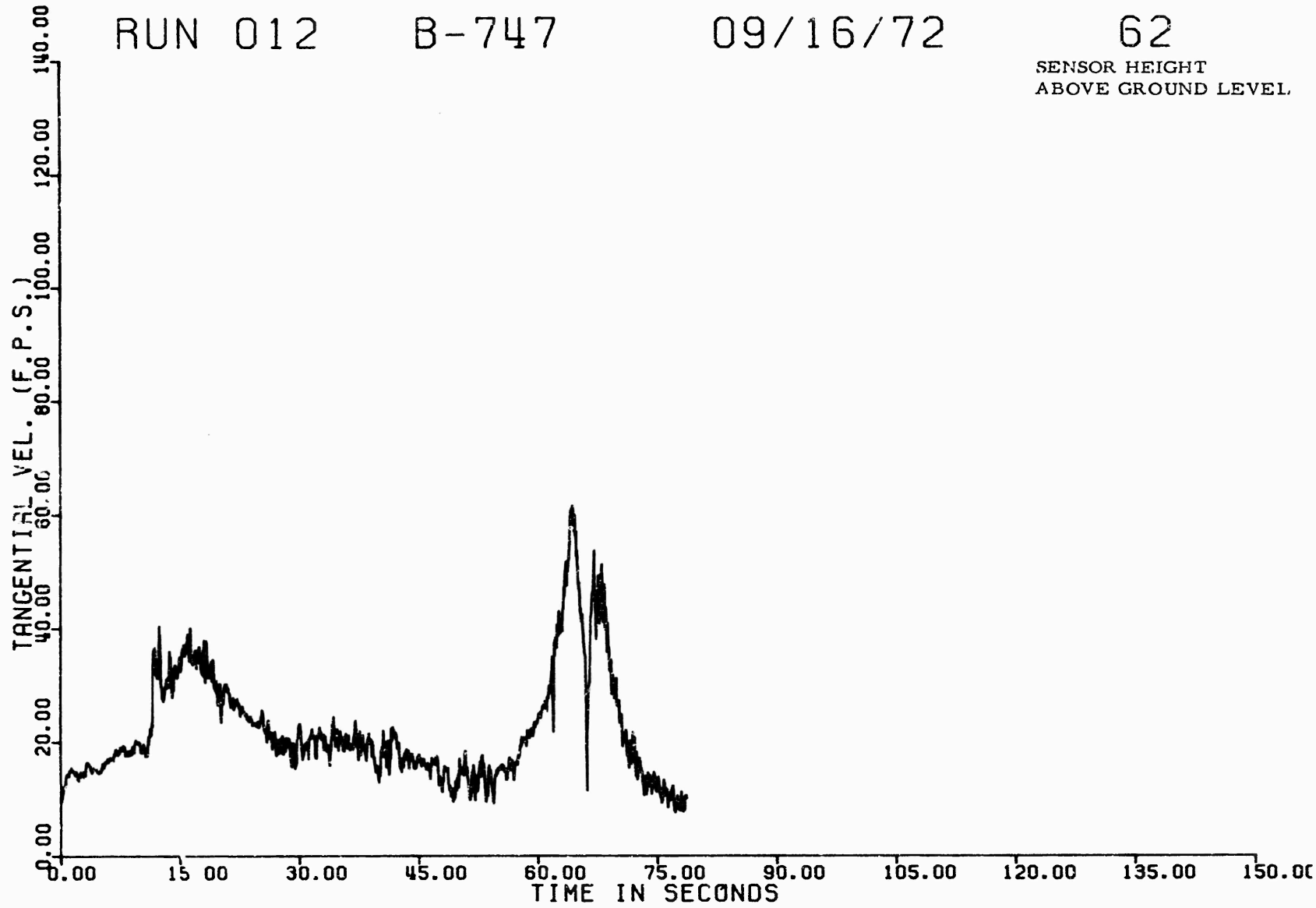

FIGURE 11. DATA SAMPLE INDICATES SECOND VORTEX CORE REACHED SENSOR AT 67 SECONDS, AT OR CLOSE TO THE 62-FOOT LEVEL

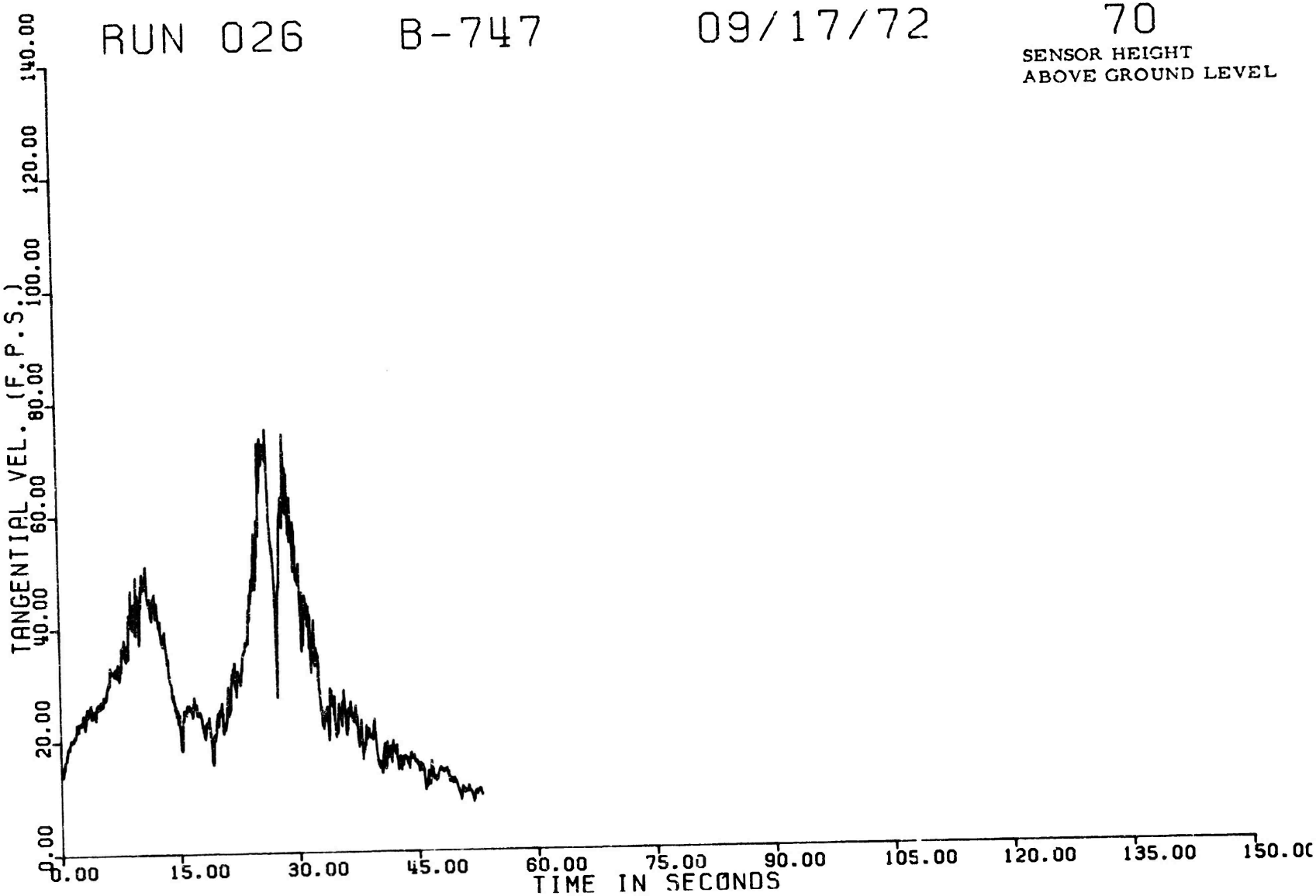

FIGURE 12. DATA SAMPLE INDICATES SECOND VORTEX CORE REACHED SENSOR AT 27 SECONDS, AT OR CLOSE TO THE 70-FOOT LEVEL

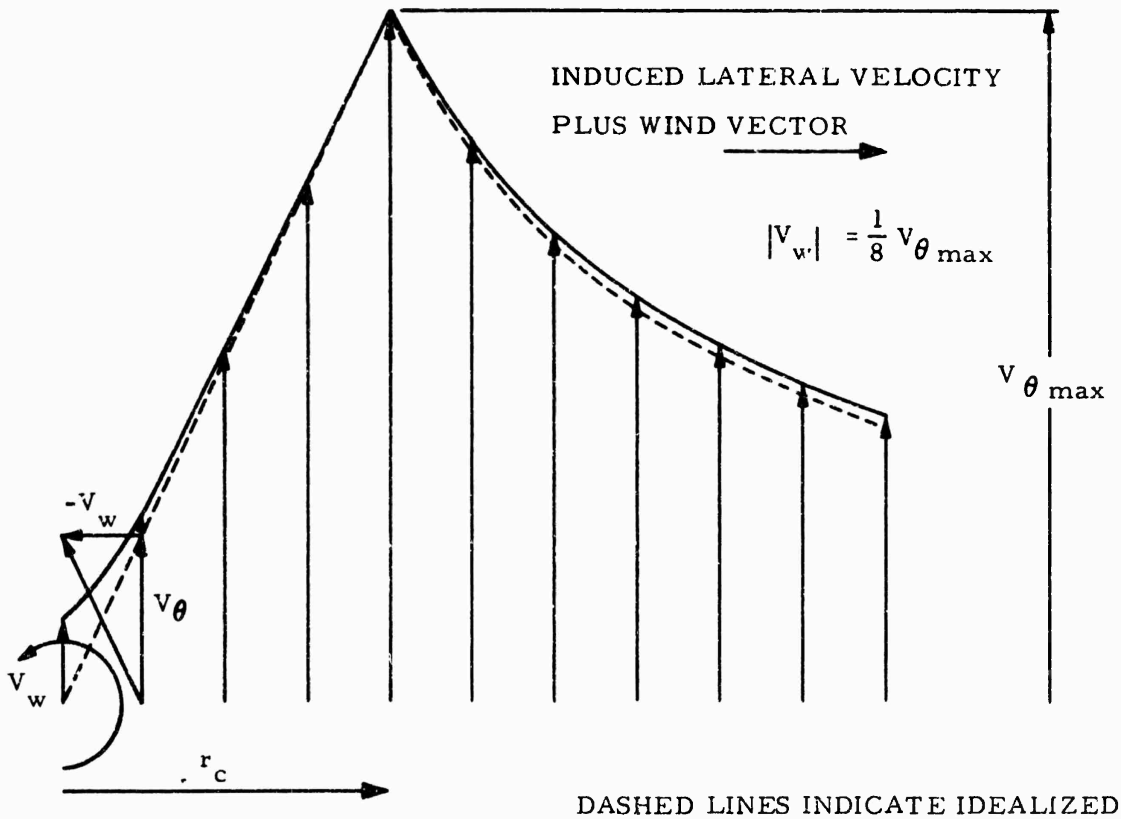

DASHED LINES INDICATE IDEALIZED VELOCITY DISTRIBUTION IN VORTEX

SOLID LINES INDICATE MAGNITUDE OF RESULTANT VELOCITY VECTOR WHEN WIND VELOCITY IS ONE-EIGHTH V_{θ} MAX

$0 < r < r_c \qquad V_\theta = \frac{\Gamma}{2\pi r_c} \frac{r}{r_c}$

$r \geq r_c \qquad V_\theta = \frac{\Gamma}{2\pi r}$

FIGURE 13. RESULTANT VELOCITY DISTRIBUTION THROUGH VORTEX WHEN CORE REGISTERS EXACT "HIT" ON SENSOR. $V_w = .125\ V_{\theta_{max}}$

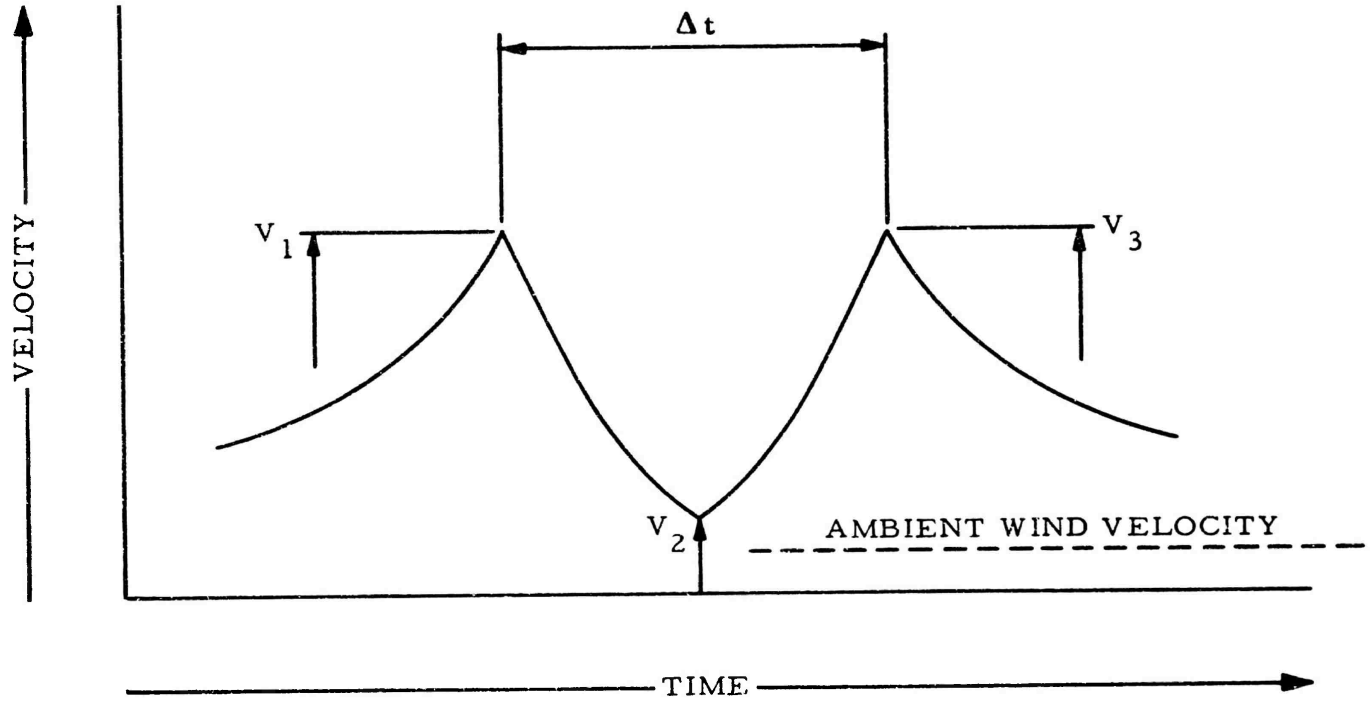

FIGURE 14. EXPANDED TIME HISTORY OF RECORDED VELOCITY AT A SENSOR

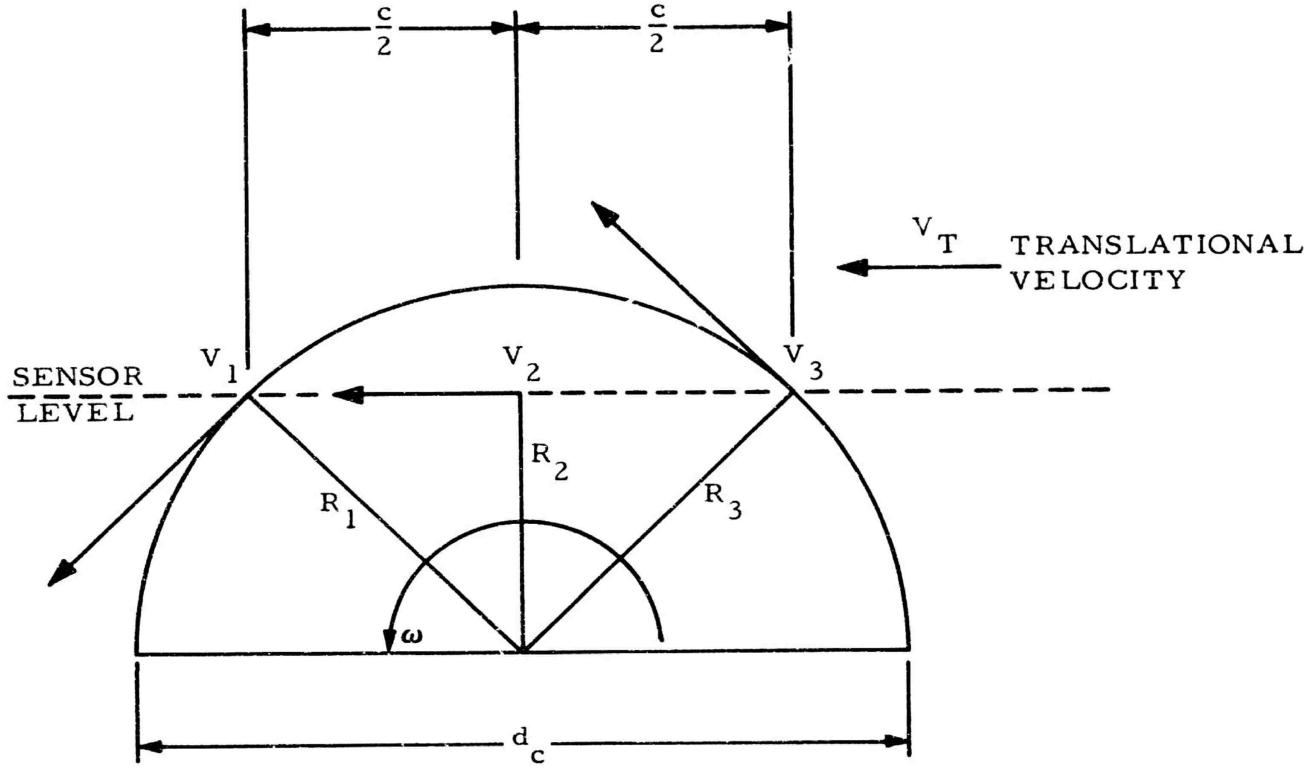

FIGURE 15. GEOMETRIC RELATIONSHIP FOR SENSOR VELOCITIES

presented in appendix D includes the pertinent parameters for each test run. The most significant configuration variable is flap setting - for some of the runs, one outboard engine was throttled back to flight idle in an attempt to determine if any significant change in vortex characteristics is induced by the removal from the airplane's wake of that engine's efflux. This was done on Runs 56-61 and 69-74, all of which were flown in the landing configuration. The results are shown as a separate plot of the relevant data, differentiated to indicate whether the idling engine is adjacent to the specific vortex or not. This data appears in figure 10, and it is apparent that as far as peak velocity, as a function of time, is concerned, it makes little difference whether the engine is throttled back, or at power for level flight.

The peak recorded tangential velocities for the entire series of test runs have been plotted (figure 16), to show that, regardless of airplane configuration or weather conditions, it is evidently possible with available data to define a definite boundary, above which the peak recorded velocity will not pass, and to define that boundary value as a function of time. The empirical curve fit obtained follows the law:

$$V_{\theta_{max}} = 336.5 \exp(-.0173t) \qquad (1)$$

This exponential function has a half-life of 40 seconds. While it may be argued that this decay law has no theoretical basis, the function fits the data quite well between vortex age limits of 10 and 80 seconds, and the constant half-life could be a useful index in defining vortex hazard. Prandtl's vortex model (reference 8) leads to a peak velocity decay that follows an inverse square root law (inverse square root of time elapsed since generation of vortex). The derivation of this result is presented at a later point in this report. Its application leads to the following decay law:

$$V_{\theta_{max}} = 886t^{-1/2} \qquad (2)$$

where the constant, 886, is determined empirically.

In the previous work (reference 6), over the time period during which the exponential decay was considered operative (between 30 and 90 seconds after the passage of the airplane), the data exhibited a great deal of scatter which was at the time attributed to the wide spacing of sensors (4 feet), and it was also noticed that the peak recorded velocity was never less than approximately 30 ft/s. For the present work, a closer sensor spacing (1 foot) was used with the idea of obtaining greater resolution, yet the amount of scatter in the data has not greatly altered, though the lower limiting value of peak recorded velocity is now approximately 50 ft/s. We might perhaps suspect that the scatter in the data arises either from extreme variability in the phenomenon itself, or from the data processing. The first supposition is difficult to support, since it necessitates that the peak velocity vary between wide limits, over a series of data runs during which ambient conditions varied but little. In the data processing, the analog signal put out by the sensors is digitized 1,000 times per second, and each normal plotted point is the

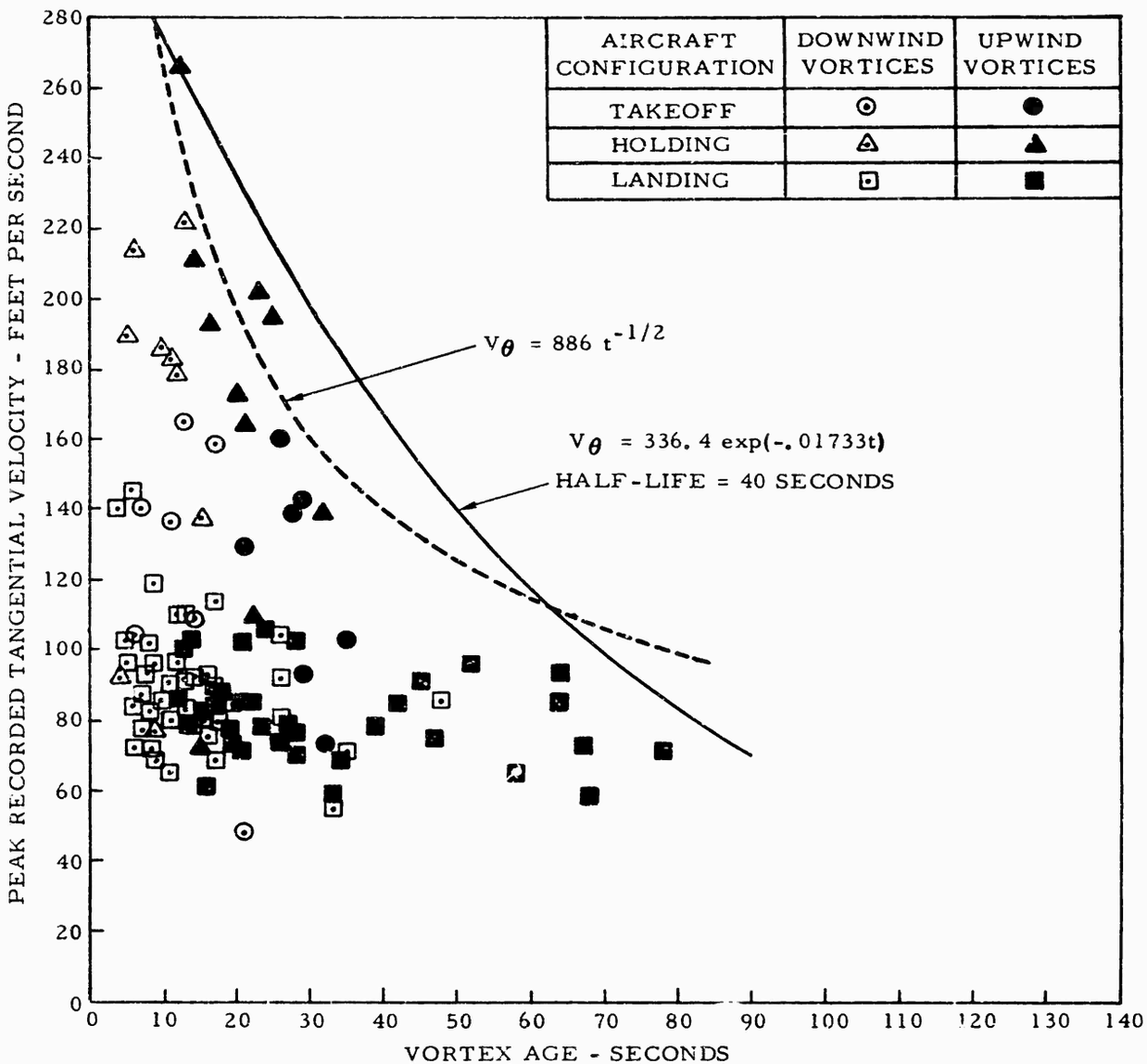

FIGURE 16. PEAK RECORDED TANGENTIAL VELOCITY VS. AGE (ALL AVAILABLE DATA)

average of 50 data values (representing a mean over a time interval of .050 second). It seems unlikely that this resolution is too coarse, or that it could account for the 5 to 1 scatter shown in figure 16. If we examine figures 17, 18, 19, and 20 separately, the scatter ratio for any one configuration is much less - about 3.5:1.0 for takeoff, about 3.8:1.0 for holding, and 2.7:1.0 for landing. If this is an accurate reflection of what is happening, then it indicates that the absolute peak velocity within a vortex is extremely localized, since in general, the peak is never more than 6 inches away from the nearest sensor. This seems at least plausible for the takeoff and holding configurations, where the data indicates a small vortex core diameter and a high peak velocity. For the landing configuration, however, the data indicates large core diameters and lower peak velocities, not consistent, apparently, with the scatter in figure 20 (downwind vortices) - though considerably less scatter appears in figure 19 (upwind vortices).

In figures 17 through 20, the peak recorded velocities have been categorized according to airplane configuration and plotted against time. For the takeoff and holding configurations, the data are rather sparse, so upwind and downwind vortex points have been plotted on the same graph. The bulk of the data gathered on the Boeing 747 airplane was for the landing configuration and is shown in figures 19 and 20. There are enough data points to warrant separating the upwind and downwind vortices and there appears to be some indication that the decay rate is less for upwind vortices than for downwind - a result that may be attributable to the wind velocity profile between ground level and the top of the tower. The upwind vortex is turning in such a sense that the wind is additive to the upper part of the vortex, and counter to the lower part. The wind strength is thus greater in that part of the vortex where it assists, and is of lesser strength in the lower part, where it detracts from the vortex. This is a possible explanation for the differences between figures 19 and 20. However, it should be noted that in figure 20, the majority of data points are for vortex ages, less than 20 seconds, whereas in figure 19, a great many data points are for ages greater than 20 seconds.

The peak tangential velocities in the holding configuration (figure 18) are clearly higher than those for any other configuration, while those for takeoff (figure 17) are greater than those for landing (figures 19 and 20). The corresponding flap angles for these configurations are holding 1.0°, takeoff 10°, and landing 25°. There appears to be a definite progression according to which, as flap angle is increased, the peak velocity diminishes. The relationship between flap angle and peak tangential velocity can be best explained in terms of induced drag and the mechanism by which it appears as the result of the generation of lift. An infinite, or two-dimensional wing of constant chord, section and angle of attack, has a constant spanwise lift distribution, and since the wing either terminates in a solid boundary or extends to infinity (doubly infinite), no trailing vortices are shed and there is no induced drag (drag due to lift). A finite wing, on the other hand, must have the lift fall to zero at each wingtip, and since this requires the existence of a spanwise gradient in lift and, hence in circulation, vortices are shed from the trailing edge. The strength and sense of the vortices is

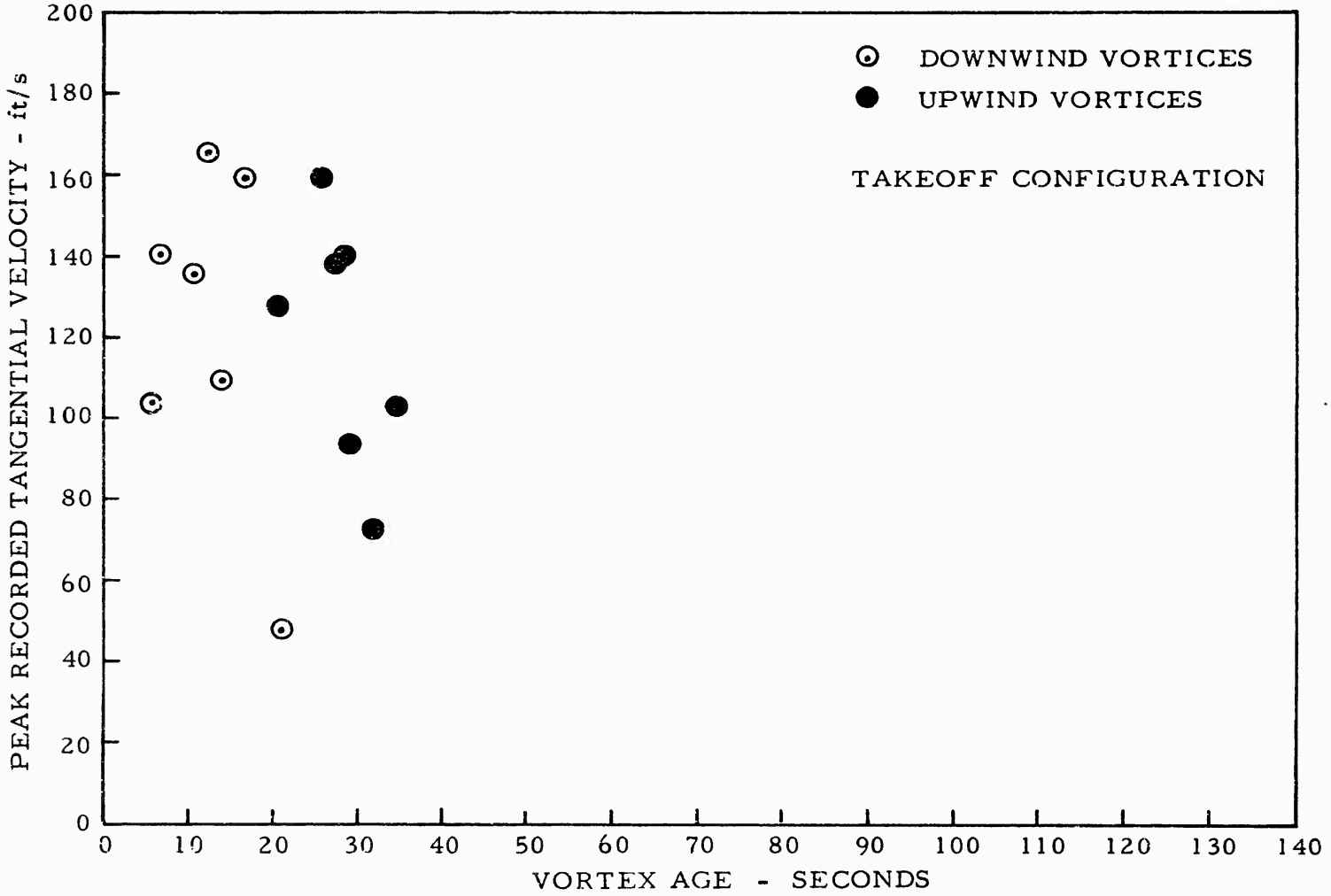

FIGURE 17. PEAK RECORDED TANGENTIAL VELOCITY VS. AGE (TAKEOFF CONFIGURATION)

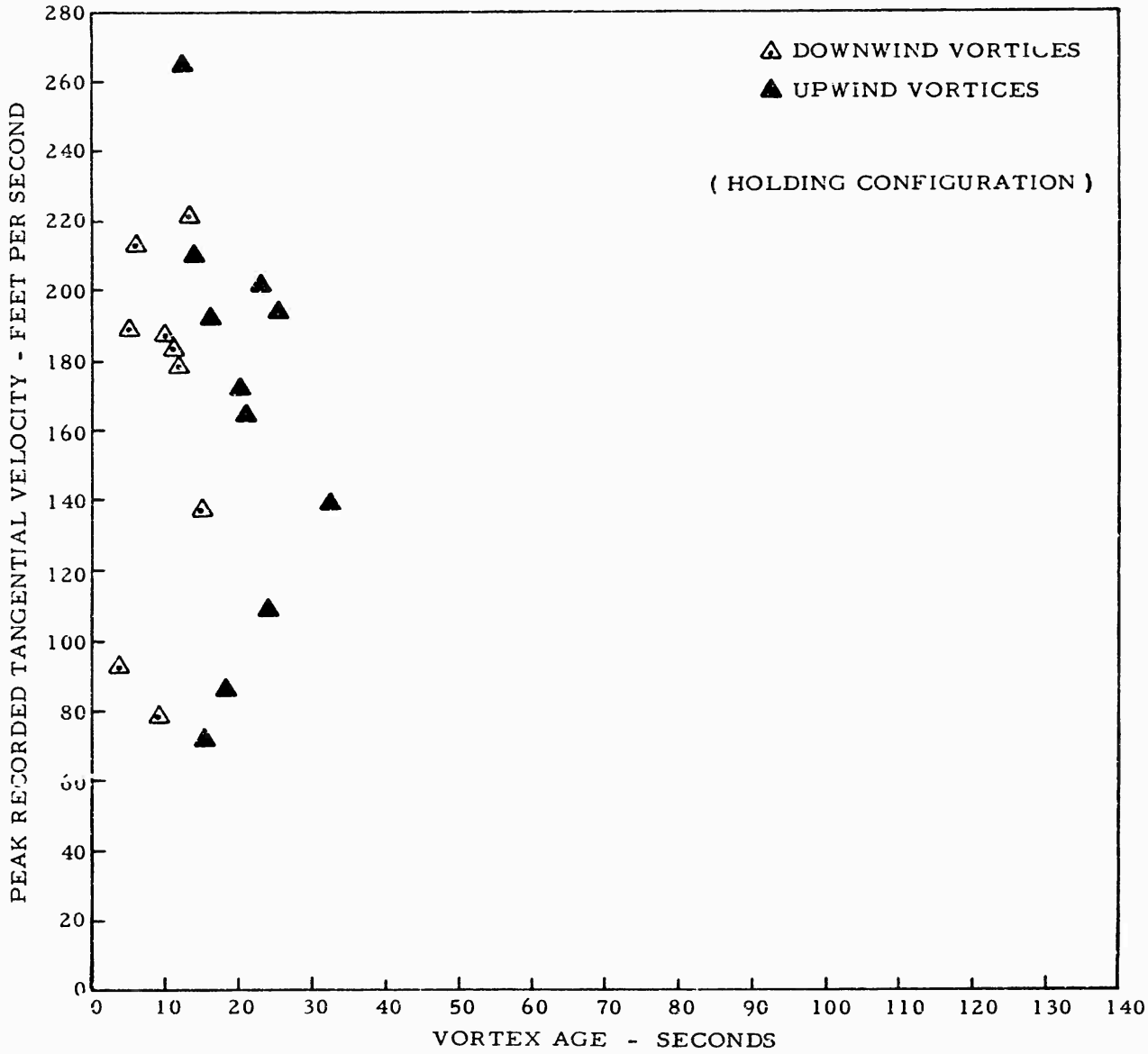

FIGURE 18. PEAK RECORDED TANGENTIAL VELOCITY VS. AGE (HOLDING CONFIGURATION)

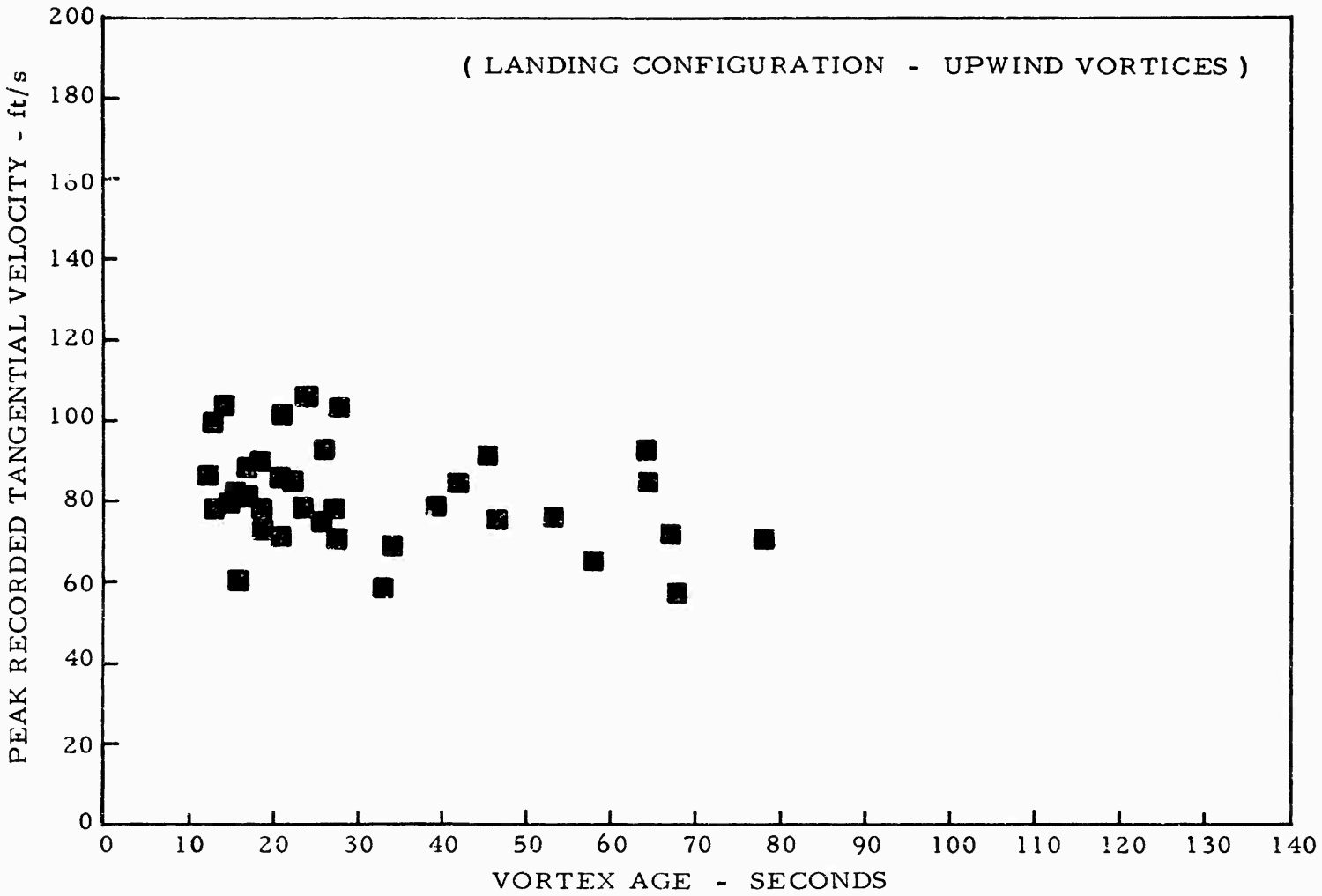

FIGURE 19. PEAK RECORDED TANGENTIAL VELOCITY VS. AGE (LANDING CONFIGURATION - UPWIND VORTICES)

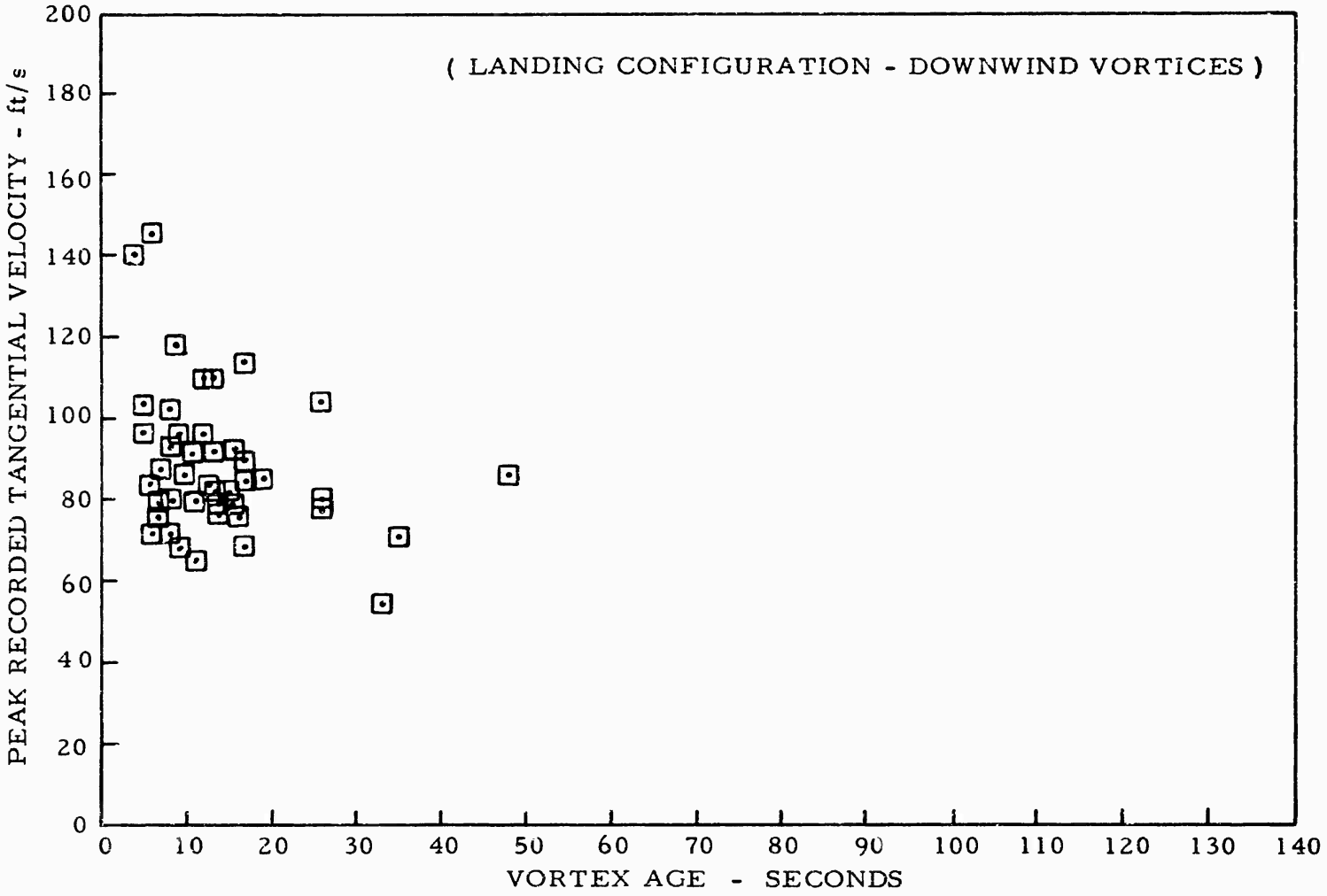

FIGURE 20. PEAK RECORDED TANGENTIAL VELOCITY VS. AGE (LANDING CONFIGURATION - DOWNWIND VORTICES)

determined by the magnitude and sense of the local gradient in the circulation. The result of the vortices being shed along the trailing edge is the creation of a downwash field behind the wing and a small backward rotation of the lift vector, the horizontal component of which is defined as the induced drag. Two factors act to increase or decrease the induced drag - the more closely the flow over the wing approaches the two dimensional ideal the lower the induced drag, and in fact, the induced drag coefficient is inversely proportional to the aspect ratio. The other factor, of course, is the form of the lift distribution - if the wing is so designed that the lift distribution is elliptical, then the induced drag is minimized, while the greater the extent to which the lift distribution departs from the elliptical, then the greater the induced drag. While the Boeing 747 wing was not designed to give an elliptical lift distribution in any configuration, and induced drag is only a small part of the total at cruise lift coefficients, so it is not the prime design consideration, it is nevertheless at a minimum in the cruise configuration, and the lift distribution approaches the condition whereby it decreases without inflection (second derivative does not change sign) from root to tip. As the flap angle is increased, for a given lift coefficient, the wing is more heavily loaded inboard and correspondingly less heavily outboard. The lift distribution curve develops one or more inflections (sign changes in the second derivative) and at the same time, the local gradient increases in the vicinity of the inflections. The result of this disruption of the smoothly decreasing lift is the production of a downwash field that, in the immediate area behind the wing, varies rapidly spanwise. This leads to a large increase in induced drag and a corresponding increase in the rotational energy of the wake. The rollup of the wake into a pair of oppositely rotating vortices occurs more directly when it starts with the near uniform downwash field generated by the clean wing. Under these conditions, the vortex cores are small in diameter and their rotational speed is high, but due to the smallness, the kinetic energy of rotation is not large. As the flap angle increases, the rollup is less clearly defined and in the resulting trailing vortices, though their core rotational speed is much less, the cores become very large with a resulting increase in rotational kinetic energy.

The derived vortex core diameter, as a function of peak-recorded tangential velocity is presented in figures 21 to 24. The constant circulation of 6,000 feet squared per second (ft^2/s) is based on a typical gross weight and airspeed (536,000 lb, 145 knots indicated airspeed, being the median circulation generated assuming an elliptical lift distribution). Core diameter as a function of age is shown in figures 25 and 26.

There is too small a velocity spread in the data to determine whether or not a trend exists to indicate a constant circulation, but it appears for the landing configuration that core diameter decreases with increasing tangential velocity much more rapidly than is required by constancy of circulation.

In the takeoff and holding configurations, the resolution possible with 1-foot sensor spacing is still too coarse to permit the vortex core diameters to be determined with confidence, especially since the anemometers used in these

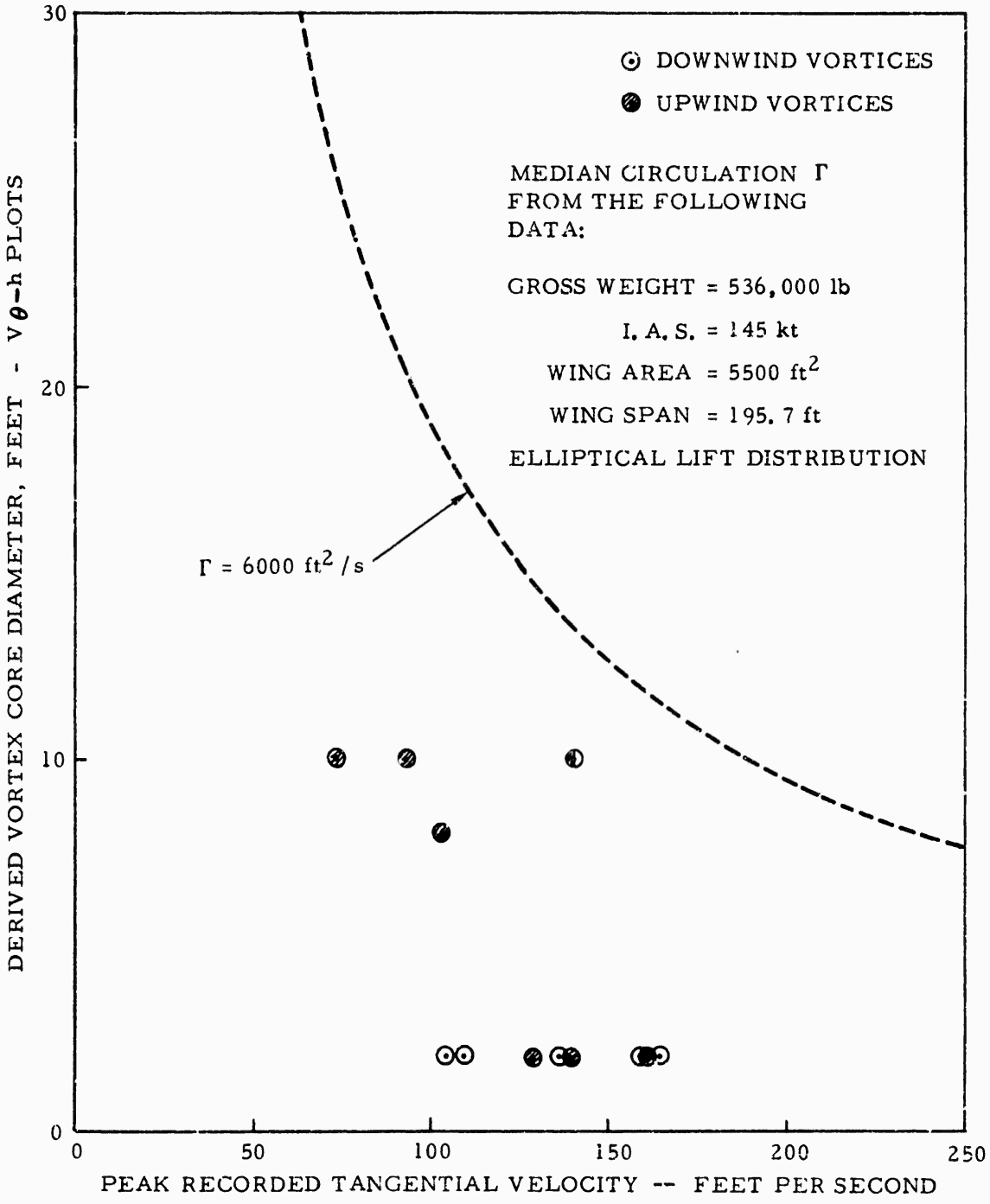

FIGURE 21. DERIVED VORTEX CORE DIAMETER AS A FUNCTION OF PEAK RECORDED TANGENTIAL VELOCITY (TAKEOFF CONFIGURATION)

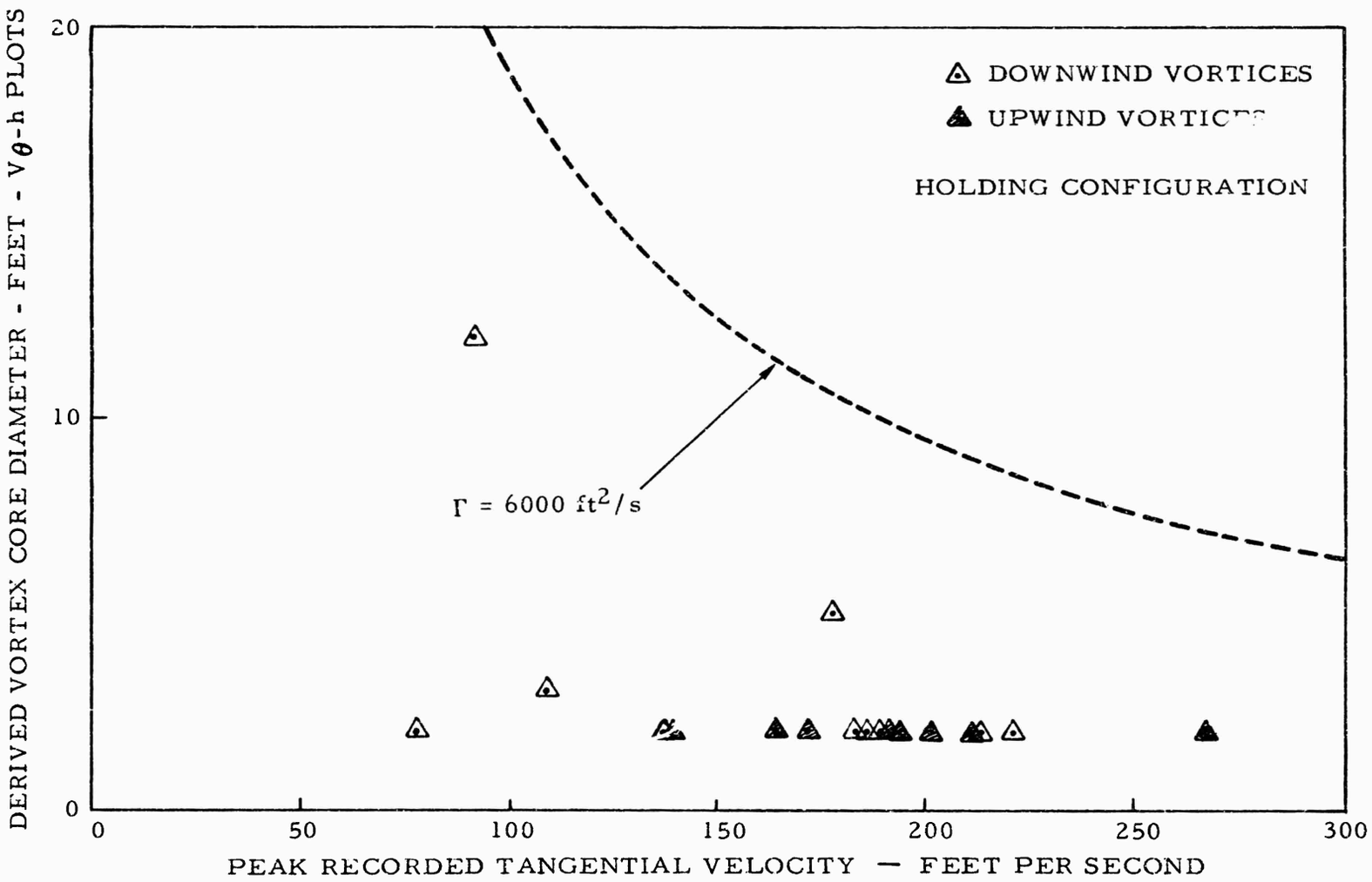

FIGURE 22. DERIVED VORTEX CORE DIAMETER AS A FUNCTION OF PEAK RECORDED TANGENTIAL VELOCITY (HOLDING CONFIGURATION)

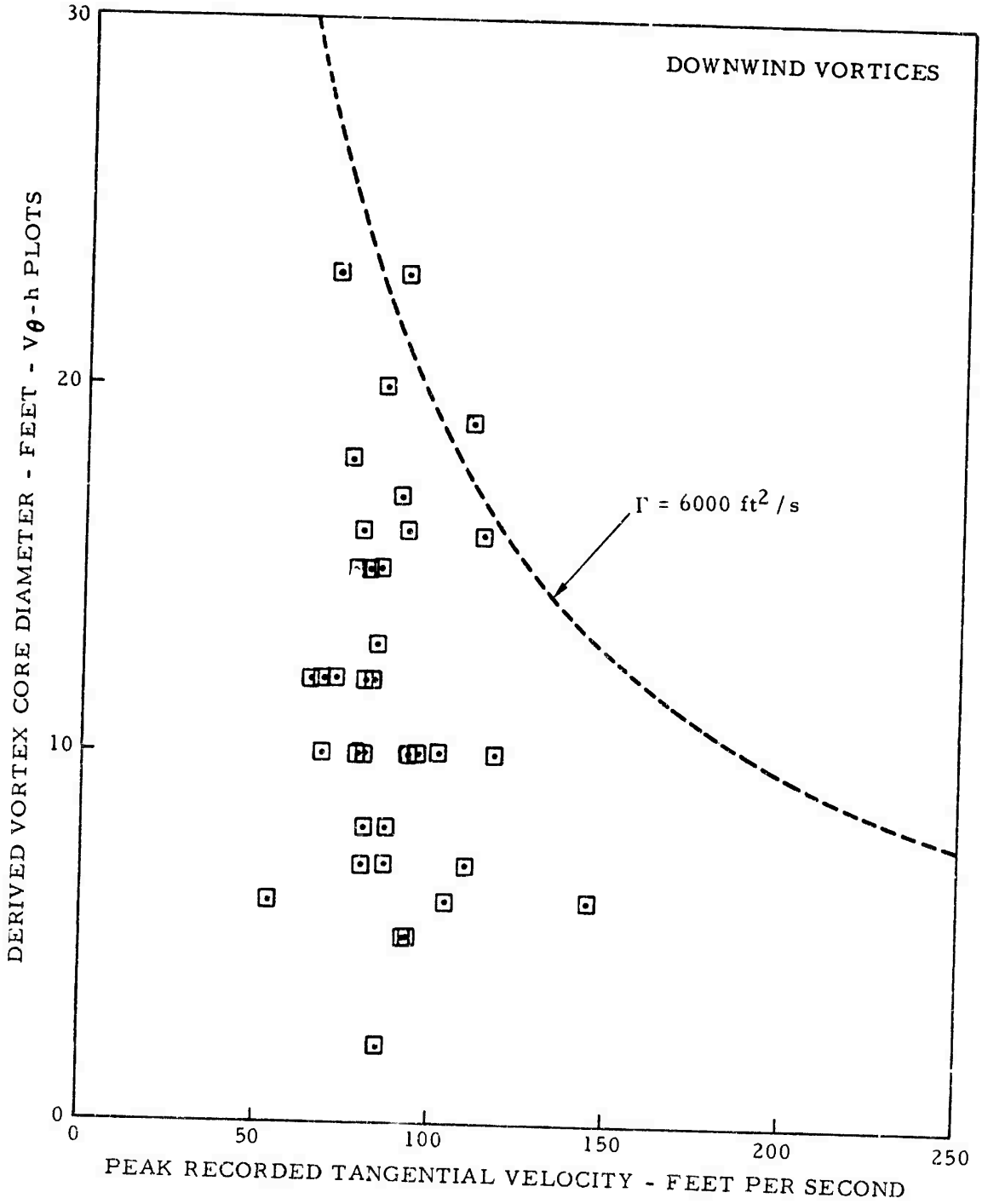

FIGURE 23. DERIVED VORTEX CORE DIAMETER AS A FUNCTION OF PEAK RECORDED TANGENTIAL VELOCITY (DOWNWIND VORTICES - LANDING CONFIGURATION)

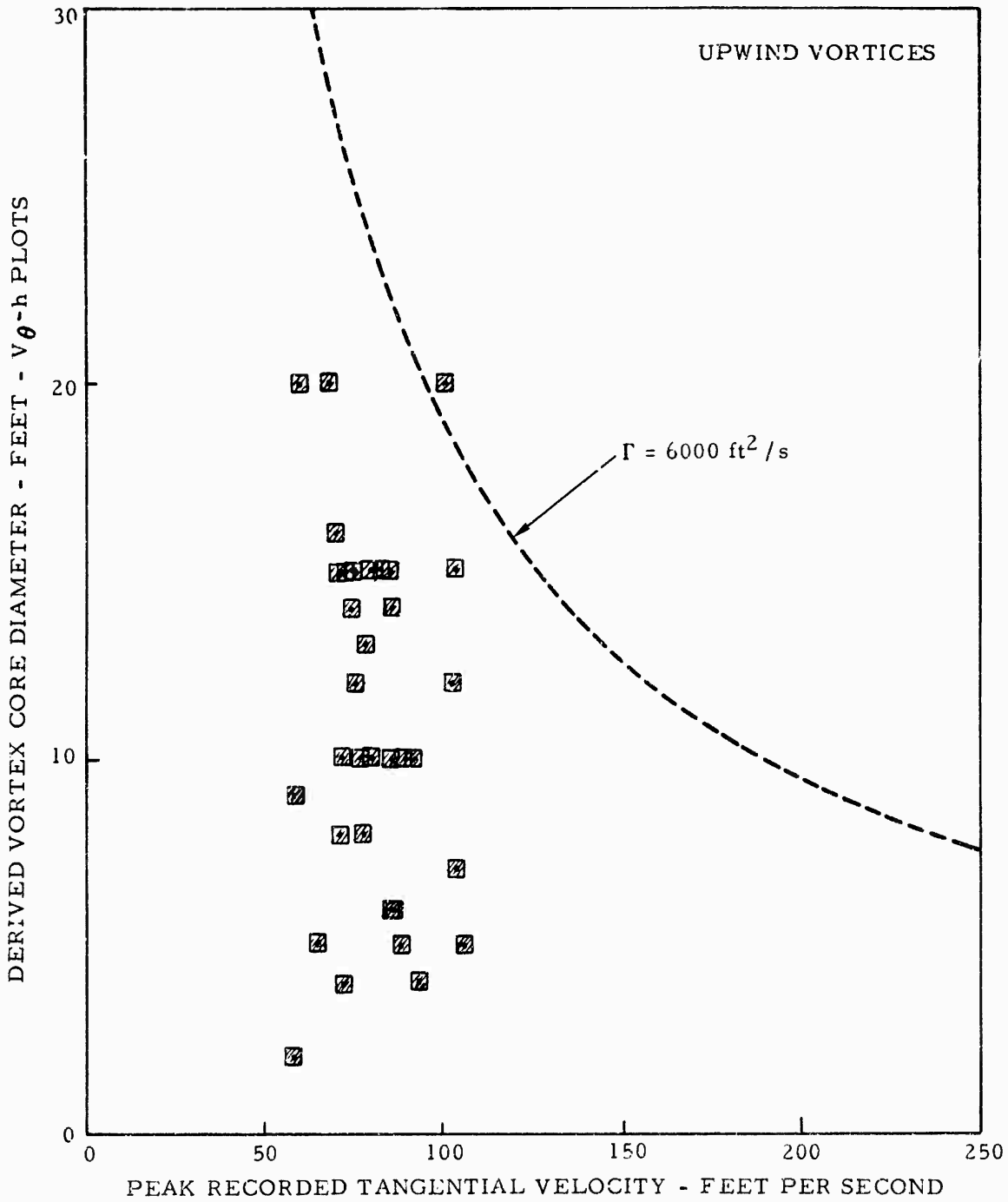

FIGURE 24. DERIVED VORTEX CORE DIAMETER AS A FUNCTION OF PEAK RECORDED TANGENTIAL VELOCITY (UPWIND VORTICES - LANDING CONFIGURATION)

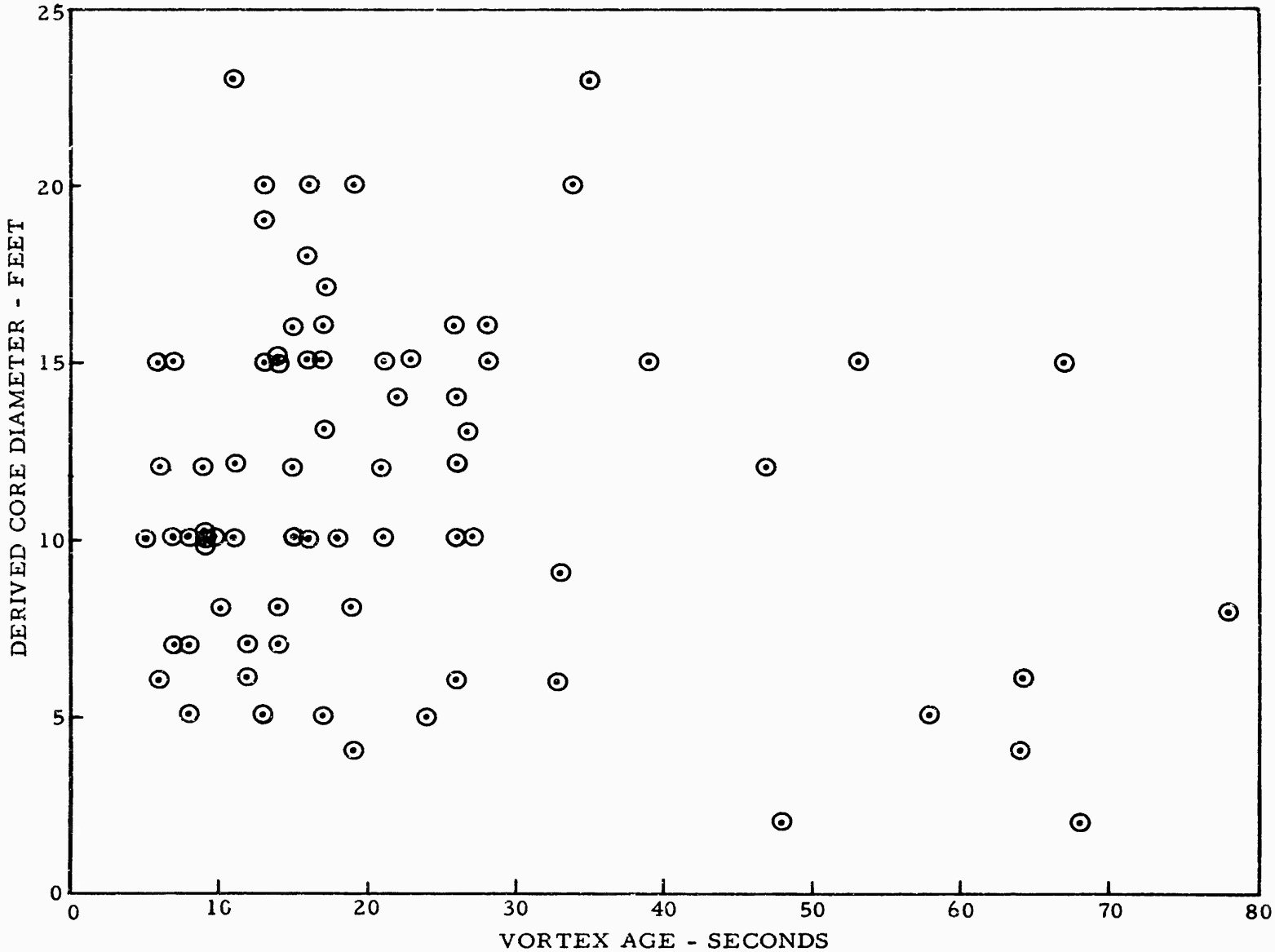

FIGURE 25. DERIVED VORTEX CORE DIAMETER VS. VORTEX AGE (LANDING CONFIGURATION - DIAMETER DETERMINED FROM V_θ - h PLOTS)

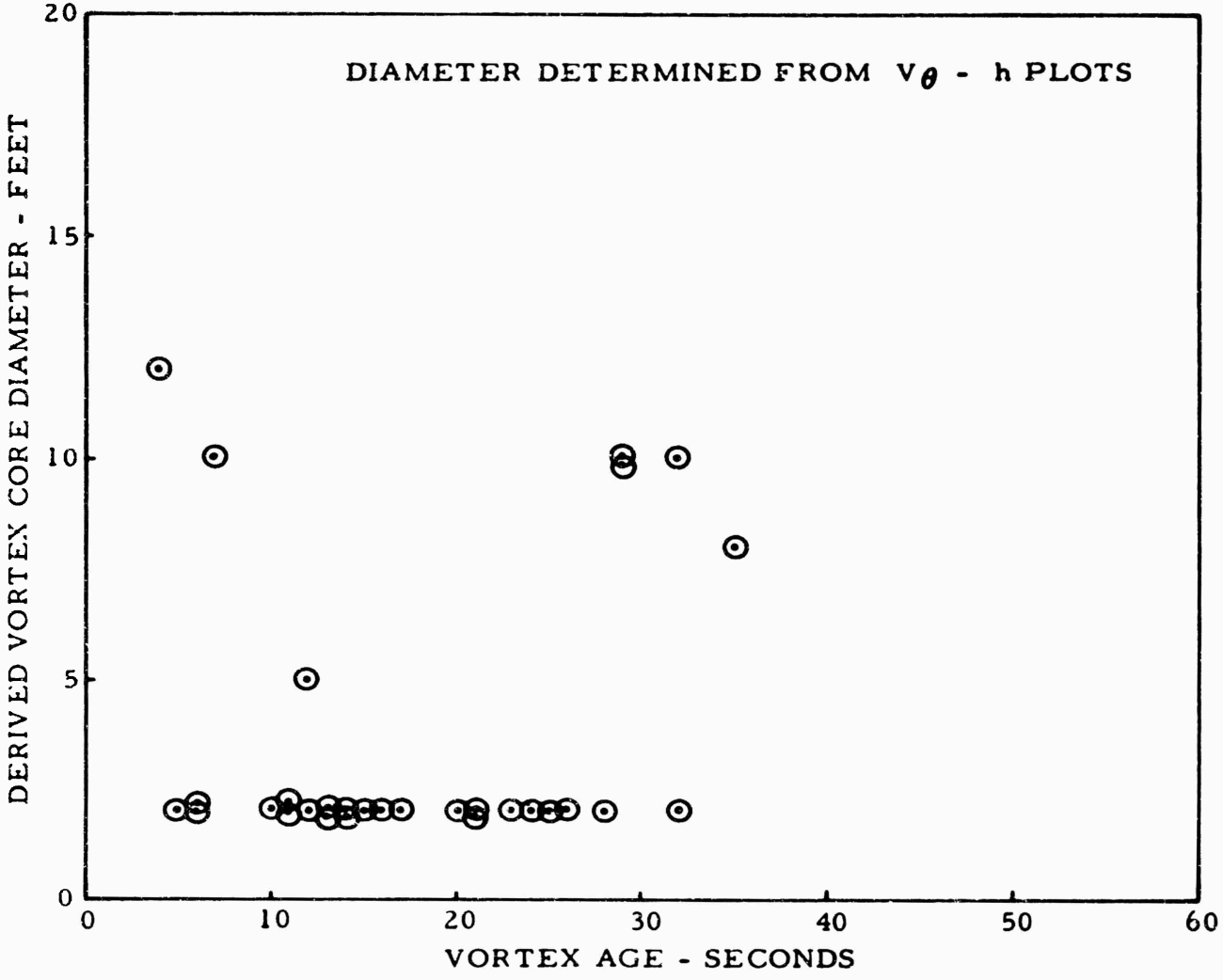

FIGURE 26. DERIVED VORTEX CORE DIAMETER VS. VORTEX AGE (TAKEOFF AND HOLDING CONFIGURATIONS - DIAMETER DETERMINED FROM V_θ - h PLOTS)

tests do not yield directional information. The velocity distribution plots do indicate, however, that the diameter is extremely small, but the value shown for many cases, namely, 2 feet, is a nominal value being equal to twice the spacing between adjacent sensors.

To the extent that little difference has been detected in the associated vortex structures, the above two configurations are quite similar. For small flap settings, the most significant change relative to the clean wing is the increased wing chord, this being particularly noticeable in the holding configuration for which the deflection is 1.0°, and even in the landing configuration, the flap deflection is only 25°.

It is apparent that in the landing configuration vortex core circulation values at least approach the calculated median values, while in the relatively clean takeoff and holding configurations, core circulation is much less than the median value.

The circulation, angular momentum (per unit length) and kinetic energy (per unit length) of the vortex core are given by the following expressions:

$$\Gamma = 2\pi r_c V_\theta \tag{3}$$

$$AM = \Gamma \frac{\rho r_c^2}{4} \tag{4}$$

$$KE = \frac{\rho \Gamma^2}{16\pi} \tag{5}$$

Rewriting circulation and kinetic energy in terms of angular momentum,

$$\Gamma = \frac{4\ AM}{\rho r_c^2} \tag{6}$$

$$KE = \frac{(AM)^2}{\rho \pi r_c^4} \tag{7}$$

In other words, with angular momentum AM held constant, the circulation "Γ" varies as the inverse square of the core radius and the kinetic energy varies as the inverse of the fourth power of the radius.

Now, according to Prandtl (reference No. 8), the dissolution of a vortex filament through fluid friction is analogous to the conduction of heat from a point of concentration in a uniform, flat conducting plane. The analogy leads to the following equation describing the distribution of rotation "ω" as a function of radius and time:

$$\omega = \frac{A}{t} e^{-r^2/4\nu t} \tag{8}$$

The circulation around any simple closed curve is given by:

$$\Gamma = 2\int_s \omega \, ds \tag{9}$$

where the surface integral is taken over the surface enclosed by the curve. The circulation around a circle of radius "r" is then equal to twice the surface integral of ω inside the circle. Let the surface element be

$$ds = 2\pi r dr$$

then

$$\Gamma = \int_o^r 4\omega\pi r.dr$$

$$= 4\pi \int_o^r \omega r.dr$$

$$= \frac{4\pi A}{t}\int_o^r e^{-r^2/4\nu t}.r.dr \quad ,$$

Evaluating the integral, we obtain:

$$\Gamma = 8\pi A\nu(1 - e^{-r^2/4\nu t}) \tag{10}$$

The value of "A" is expressible in terms of $\Gamma_1 = 8\pi a\nu$, the circulation around an infinitely large circle. The final result is:

$$\Gamma = \Gamma_1 \, (1 - e^{-r^2/4\nu t}) \tag{11}$$

and the tangential velocity at any given radius r is given by

$$V_\theta = \frac{\Gamma_1}{2\pi r} \, (1 - e^{-r^2/4\nu t}) \tag{12}$$

For large values of the exponent, the quantity $e^{-r^2/4\nu t}$ tends to zero very rapidly, and V_θ approaches the potential flow value. For small values of r, tangential velocity approaches a value

$$V_\theta = \frac{\Gamma_1 \, r}{2\pi.4\nu t} \, , \tag{13}$$

which of course vanishes as r approaches zero.

MAXIMUM VALUE OF u.

Differentiating u (from equation (12)) with respect to r,

$$\frac{dV_\theta}{dr} = \frac{\Gamma_1}{2\pi}\left\{-\frac{1}{r^2} + e^{-r^2/4\nu t}\left(\frac{1}{r^2} + \frac{1}{2\nu t}\right)\right\}$$

Setting the derivative to zero, we obtain:

$$e^{r^2/4\nu t} = \frac{2\nu t + r^2}{2\nu t} \qquad (14)$$

or

$$\frac{r^2}{4\nu t} = \ln\left(1 + \frac{r^2}{2\nu t}\right)$$

Let $\frac{r^2}{4\nu t} = \chi$, then equation (14) becomes

$$\chi = \ln(1 + 2\chi)$$

or

$$e^{\chi} = 1 + 2\chi$$

Solving this numerically,

$$\chi = 1.26$$

Thus V_θ is a maximum for $r^2/4\nu t = 1.26$.

If we identify $V_{\theta_{max}}$ with core radius r_c,

$$\frac{r_c^2}{4\nu t} = 1.26$$

$$r_c = 2.246\ (\nu t)^{\frac{1}{2}} \qquad (15)$$

Thus the peak tangential velocity, corresponding to the core radius, occurs at a constant value of $\frac{r^2}{4\nu t}$ - namely, 1.26. From equations (12) and (15), $V_{\theta_{max}}$ varies as the inverse square root of the time. Applying this decay law to the data of figure 16, with an initial value of 280 ft/s at t = 10 seconds, a curve is obtained that, between t = 10 and t = 80 seconds, fits the data better than the exponential function which was chosen originally because of the conveniently constant "half-life" that it yields.

Using the potential theory result quoted in reference 6, the theoretical vortex descent rates for each data run were calculated, and the results are shown in figure 27. The only configuration for which it is possible to draw a conclusion is the landing configuration, and it appears that the actual mean vortex descent rate may exceed the theoretical value by a factor of two. One source of discrepancy is in the estimation of the median circulation - the theory is based on a value determined from an assumed elliptical lift distribution, an assumption that is not only reflected in the strength of the trailing vortex pair, but in the lateral spacing between the members of this pair downstream from the point of generation. There is a great deal of scatter in the experimental data - due mostly, it is believed, to irregularities in the descent rates of individual vortices. It has been noticed in the field that a vortex, far from descending uniformly, "snakes" markedly, due to instability inherent in the vortex itself, and interaction with a nonhomogeneous atmosphere.

Figures 28 through 33 show the effect of ambient wind on peak velocity. There appears to be a trend towards lower peak velocities in higher ambient winds, consistent with the hypothesis that the presence of wind, especially wind shear in close proximity to the ground, introduces sufficient turbulence to promote an earlier breakup of the vortex system and a more rapid decay of the extreme peak velocities. The vortex tangential velocity distributions presented in appendix C are grouped according to airplane flight configuration, and within each group, are arranged in ascending order of vortex age. The quantities $\hat{V}$ and V_w are, respectively, the peak recorded absolute velocity for the vortex in question, and windspeed at the height at which the vortex in question struck the tower.

Takeoff, holding, and cruise configurations use flap settings of 10°, 1°, and zero, respectively, and at these settings, it is found that vortex core diameters are small, and peak velocities high (figures 21 and 22). Tangential velocity distributions C-1 through C-33, with few exceptions exhibit a consistent pattern - high-peak velocity, small-core diameter, and a rapid decline in tangential velocity at radii beyond the core, in an approximately logarithmic manner, as described in reference 3. This law is:

$$\frac{\Gamma}{\Gamma(r_c)} = \ln \frac{r}{r_c} + 1 \qquad (16)$$

or

$$V_\theta = \frac{r_c}{r} V_\theta(r_c) \left(\log r/r_c + 1 \right) \qquad (17)$$

where
- r_c = Core radius
- r = General radius
- V_θ = Tangential velocity at radius r
- $V_\theta(r_c)$ = Tangential velocity at core radius
- Γ = Circulation at radius r
- $\Gamma(r_c)$ = Circulation at core radius r_c

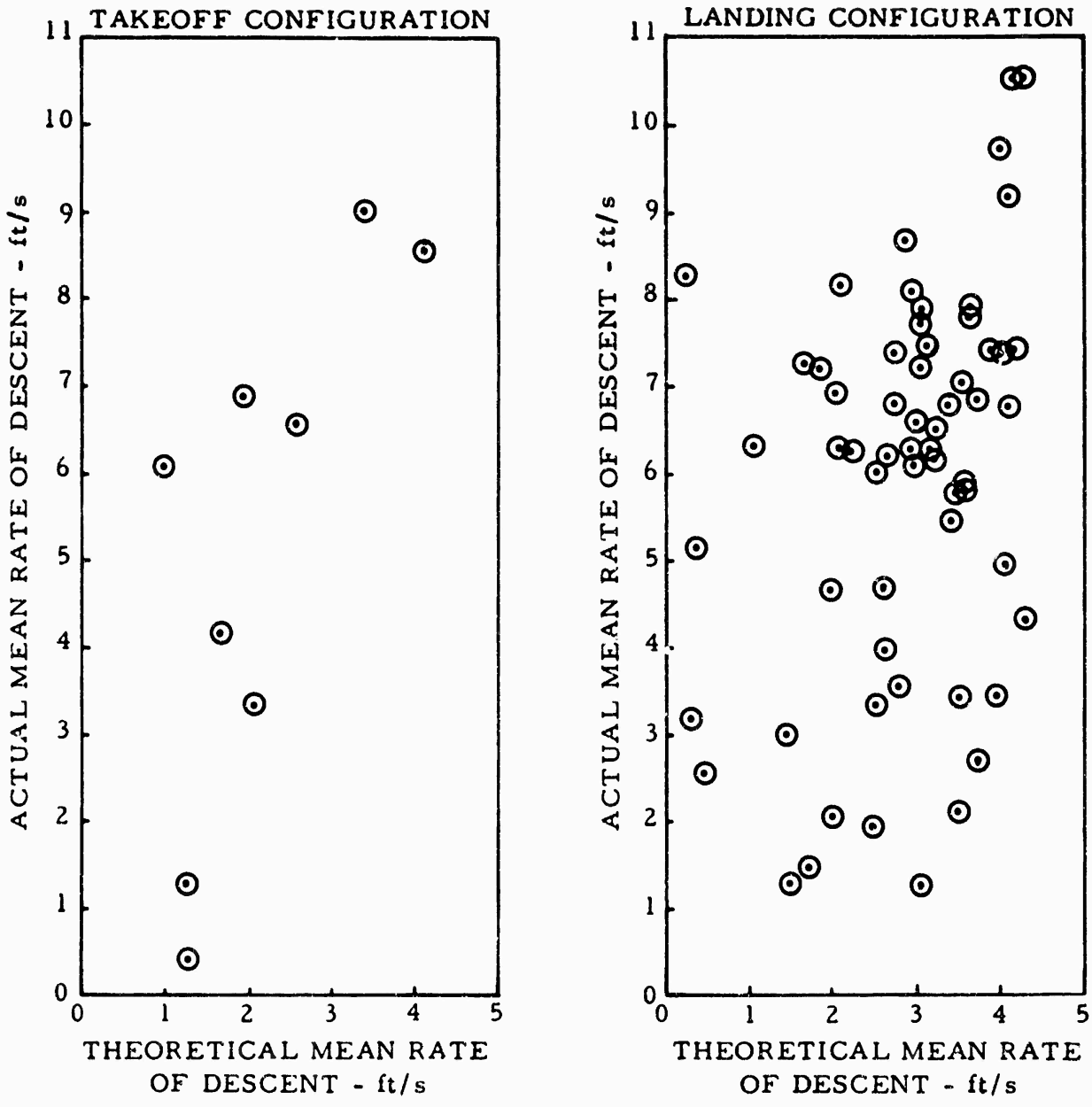

FIGURE 27. COMPARISON OF THEORETICAL AND ACTUAL VORTEX MEAN DESCENT RATES
(Sheet 1 of 2)

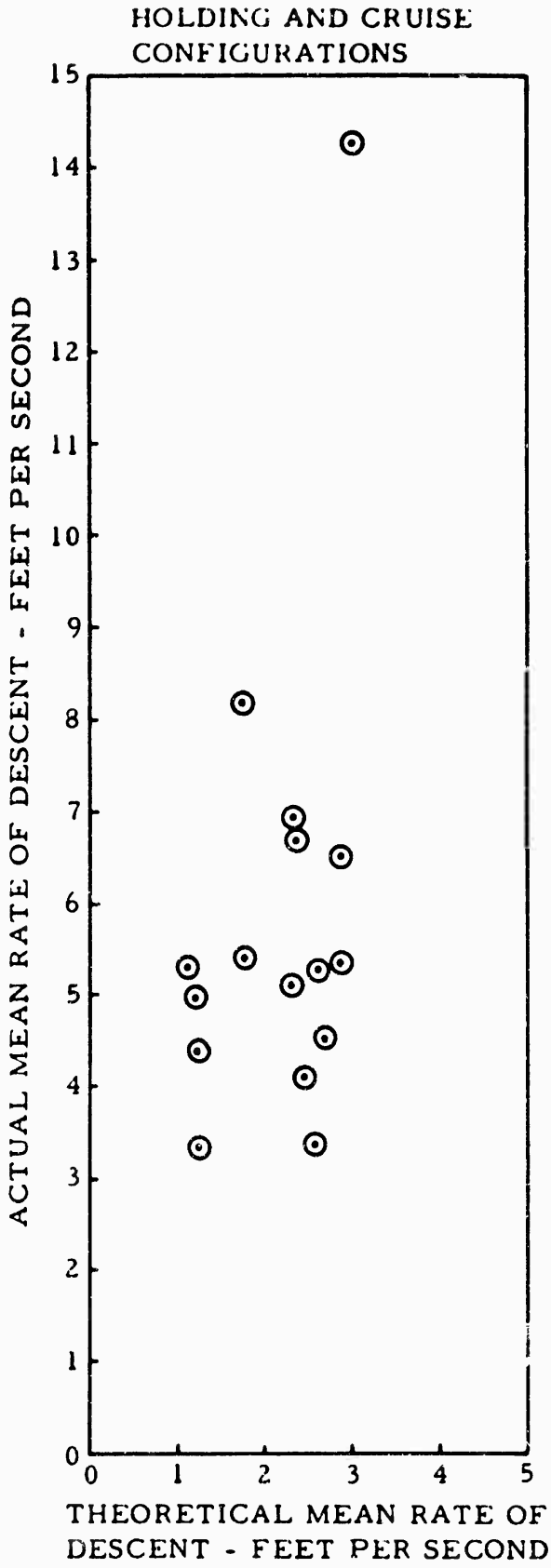

FIGURE 27. COMPARISON OF THEORETICAL AND ACTUAL VORTEX MEAN DESCENT RATES (Sheet 2 of 2)

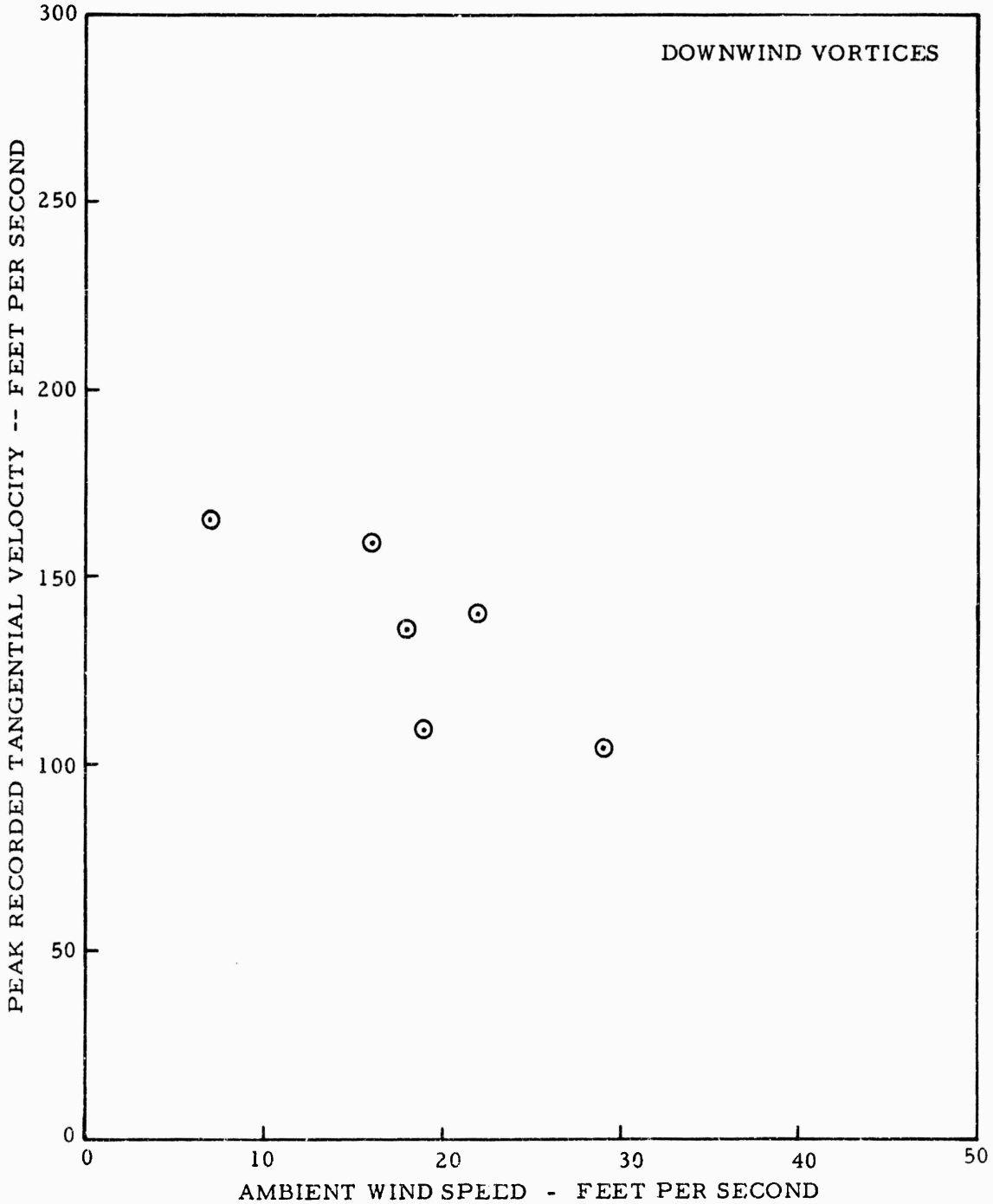

FIGURE 28. PEAK RECORDED TANGENTIAL VELOCITY VS. WINDSPEED (TAKEOFF CONFIGURATION - DOWNWIND VORTICES)

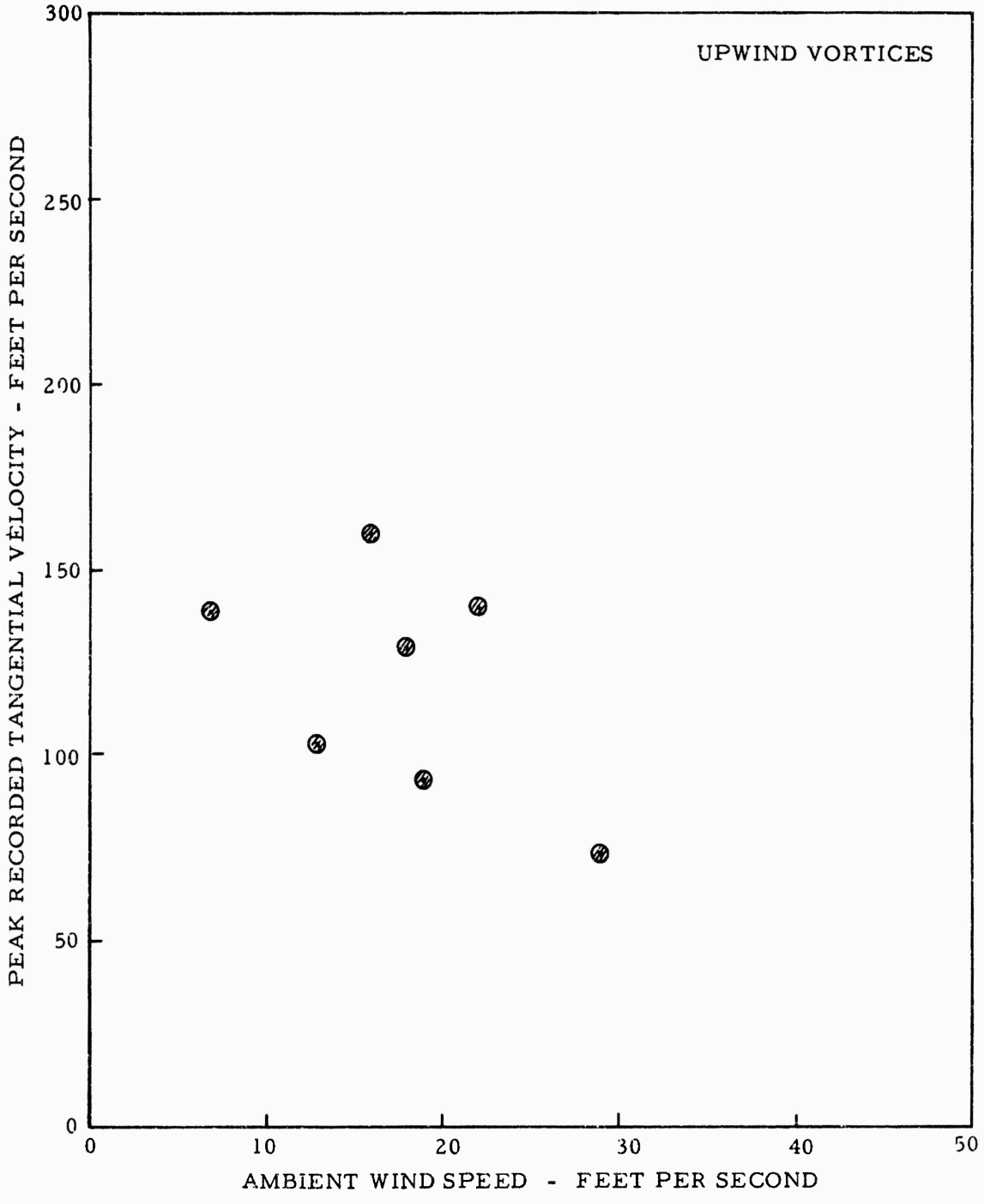

FIGURE 29. PEAK RECORDED TANGENTIAL VELOCITY VS. WINDSPEED (TAKEOFF CONFIGURATION - UPWIND VORTICES)

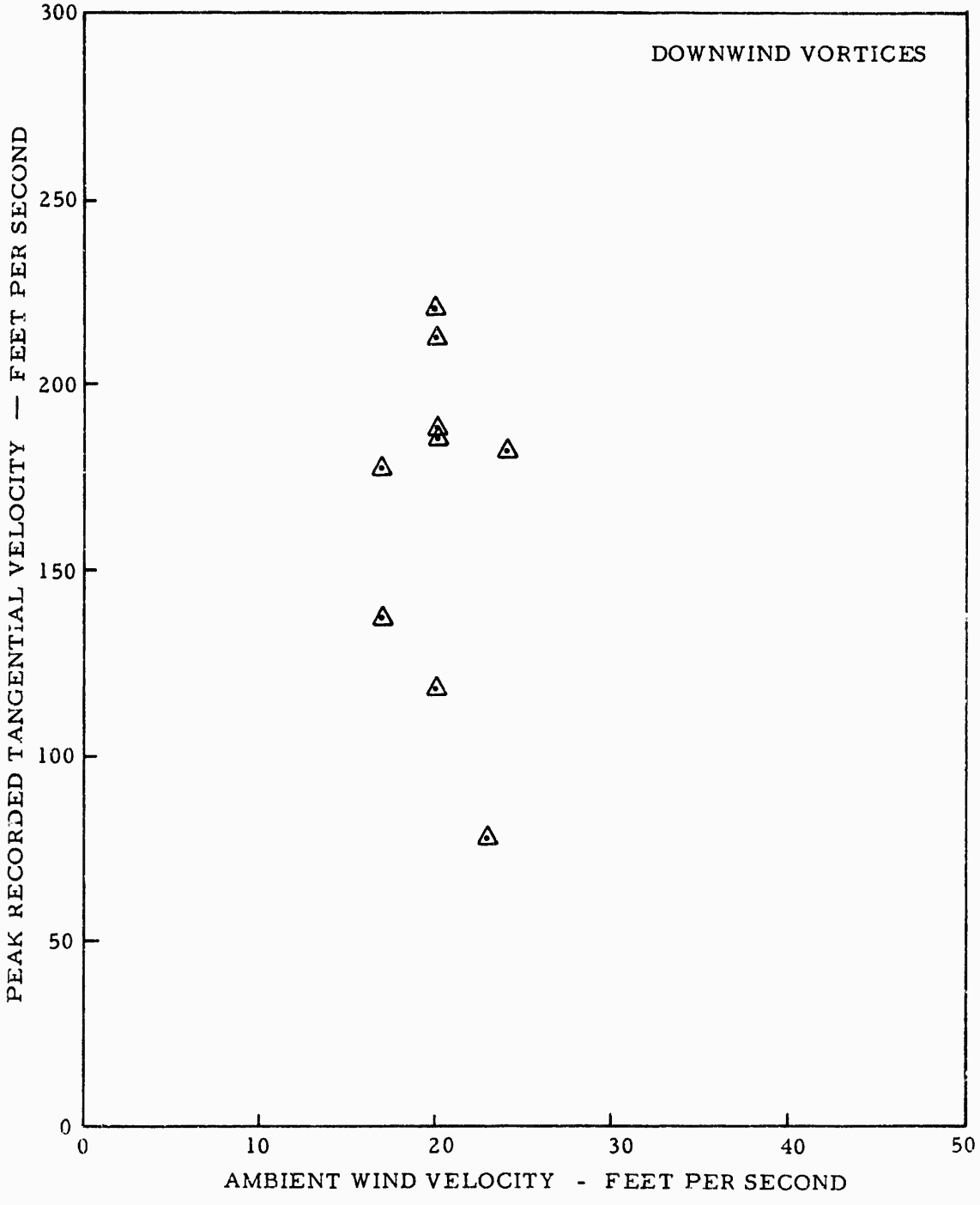

FIGURE 30. PEAK RECORDED TANGENTIAL VELOCITY VS. WINDSPEED (HOLDING CONFIGURATION - DOWNWIND VORTICES)

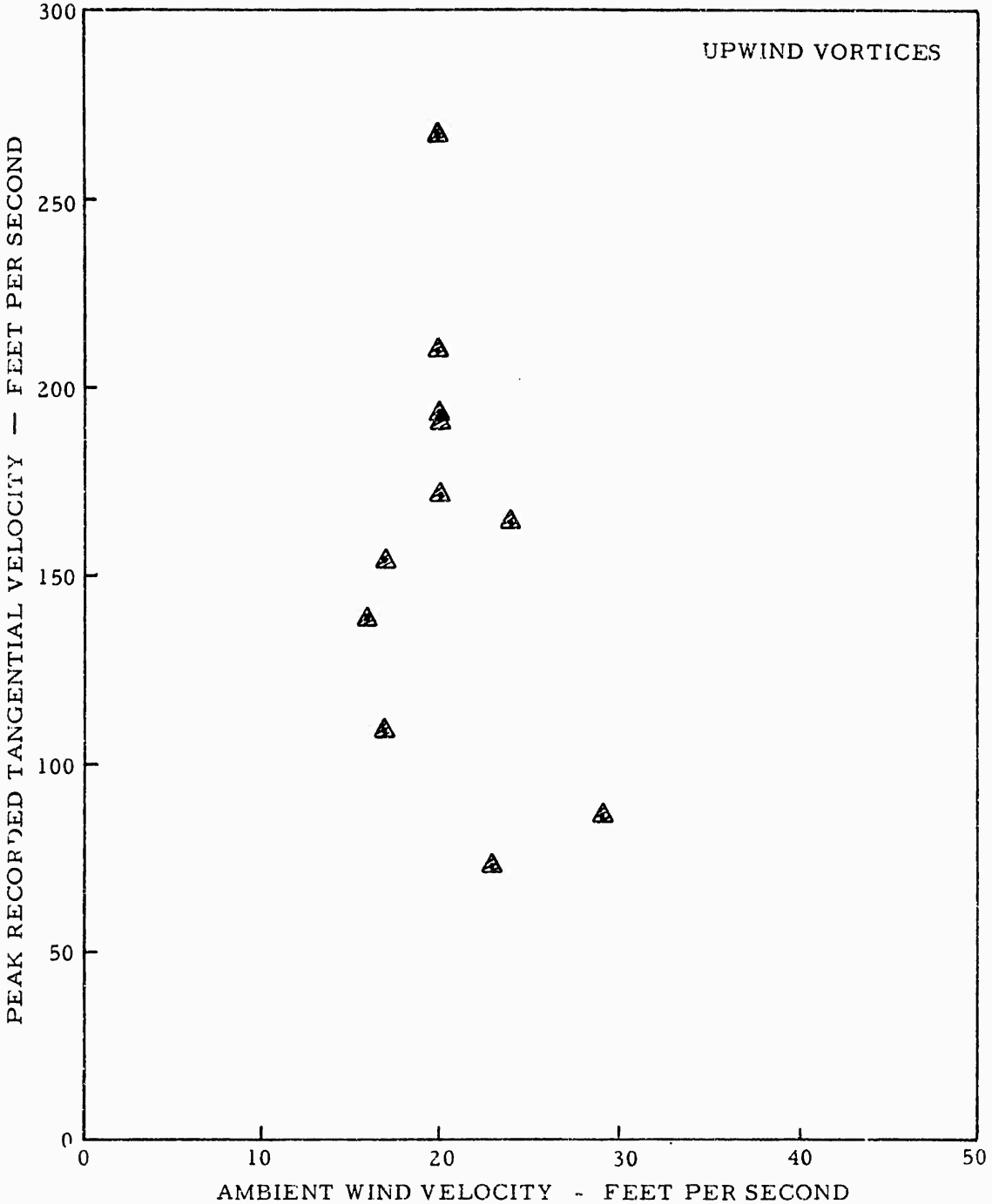

FIGURE 31. PEAK RECORDED TANGENTIAL VELOCITY VS. WINDSPEED (HOLDING CONFIGURATION - UPWIND VORTICES)

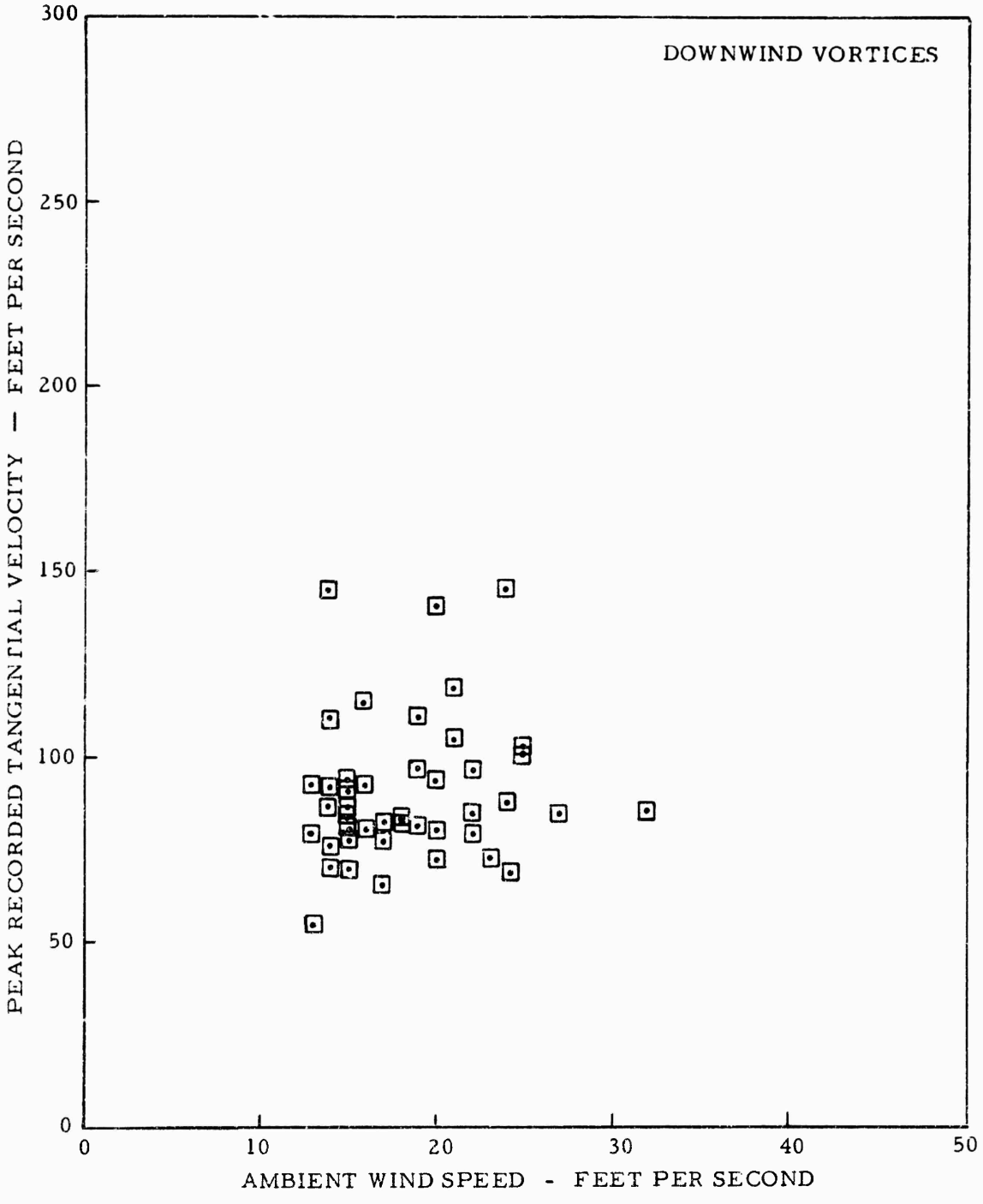

FIGURE 32. PEAK RECORDED TANGENTIAL VELOCITY VS. WINDSPEED (LANDING CONFIGURATION - DOWNWIND VORTICES)

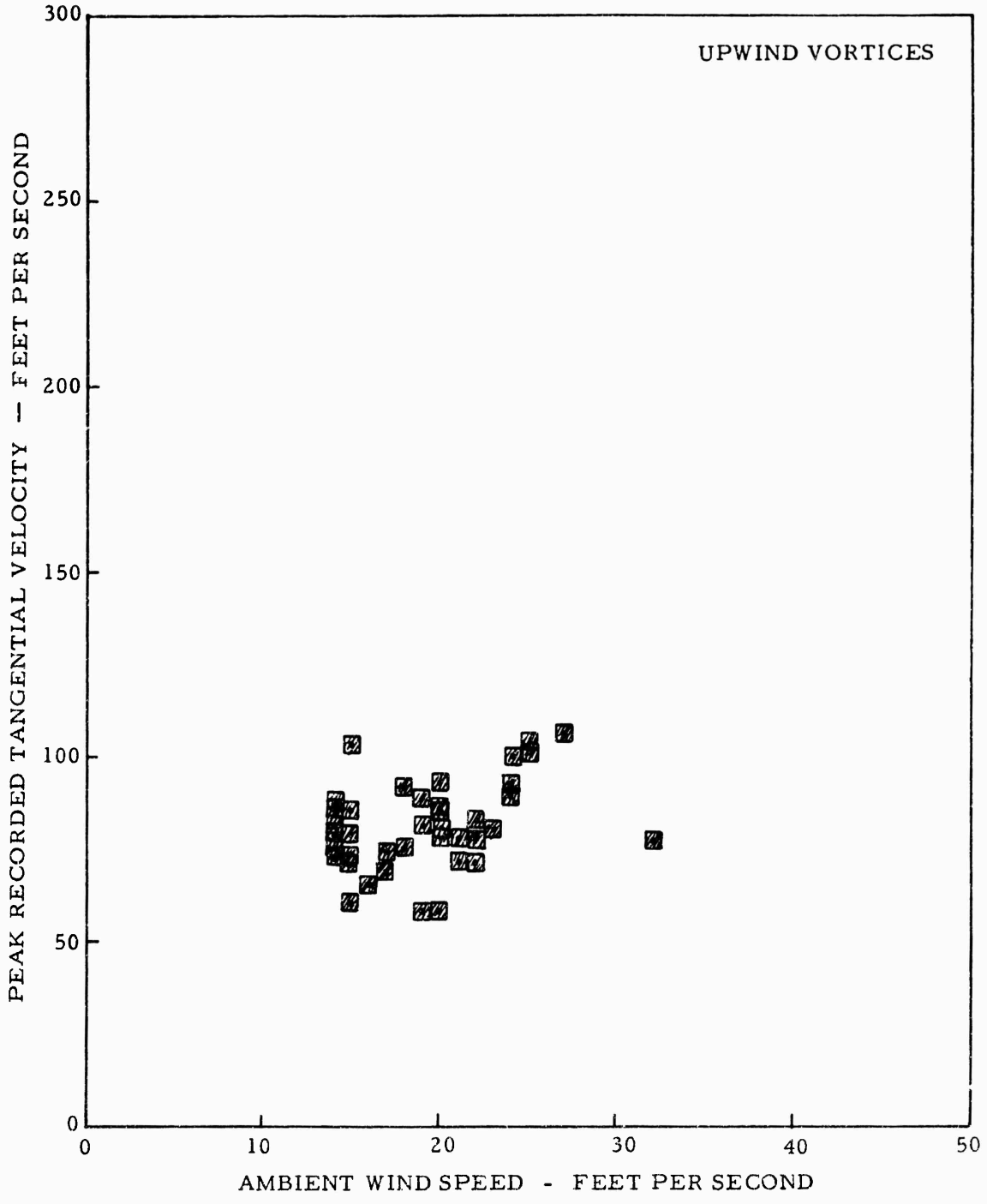

FIGURE 33. PEAK RECORDED TANGENTIAL VELOCITY VS. WINDSPEED (LANDING CONFIGURATION - UPWIND VORTICES)

Figure 34 shows two typical logarithmic velocity distributions, calculated for core radius of half a foot, with peak velocities of 100 and 140 ft/s.

In a few instances, i.e., pages C-2, 11, 12, 13, 14, 17, 25, 27, and 31 the velocity distribution does not fit the general pattern, though there is no apparent reason why this should be so - the only distributions for which test conditions were in any way atypical are pages C-17, 25, 27, and 31 which are for runs made at 300 knots or more, while most of the runs in this test series were made at speeds between 140 and 220 knots. The higher airspeed, and correspondingly reduced circulation is not the explanation however, since there is an example, (page C-24), in the group, of a high-speed run (350 knots) for which the velocity distribution is normal.

The balance of the velocity distributions presented (pages C-34 through C-115) are for the landing configuration. They exhibit consistently lower peak velocities, larger core radii and a less well-defined structure. Together with the larger core radius, it is also evident that an appreciable tangential velocity is maintained at greater radii, beyond the core, than is evident in any of the other configurations. Figure 35 shows the calculated logarithmic velocity distributions for a core radius of 10 feet, with peak velocities of 50, 100 and 140 ft/s. Qualitatively, this fits a great many of the experimental velocity distributions - e.g., pages C-38, 39, 41, 42, 50, 51 and 53 - to cite a few of them, and significantly, predicts the maintenance of sizeable tangential velocities, out to quite large radii, as was frequently found to occur in the landing configuration.

It should be remarked that the interpretation of the sensor velocity time histories to produce the tangential velocity distributions is not free of ambiguity and uncertainty. The vortex "hit" on the tower is identified by the presence of a peak in the velocities recorded by sensors in close proximity - usually with one peak being larger than those above or below it. At the instant at which this occurs, it is assumed that the vortex axis is no more than half a foot away from the nearest sensor, and so assuming that the flow is axi-symmetric, the velocity experienced by each sensor is essentially horizontal, normal to the airplane flight path, either into the tower or away from it. The velocities are corrected for wind by adding or subtracting the flow velocity recorded at time zero. It is then assumed that the resultant is the tangential velocity due to vortex rotation, which is approximately true, but does nevertheless ignore interference between the two vortices, and between this pair and the ground. A further correction may also be required for complete rigor - that due to simply to the displacement caused by the physical volume of the airplane, on the order of 100,000 cubic feet, travelling at speeds in excess of 200 ft/s. The airplane's dimensions in this particular case, are large in comparison with the linear dimensions defining the equipment used and airspace occupied in this experiment. It is difficult with such a large airplane to obtain data out of ground effect and free of the displacement effect, without employing a much taller tower than the 140-foot one used in this series of tests.

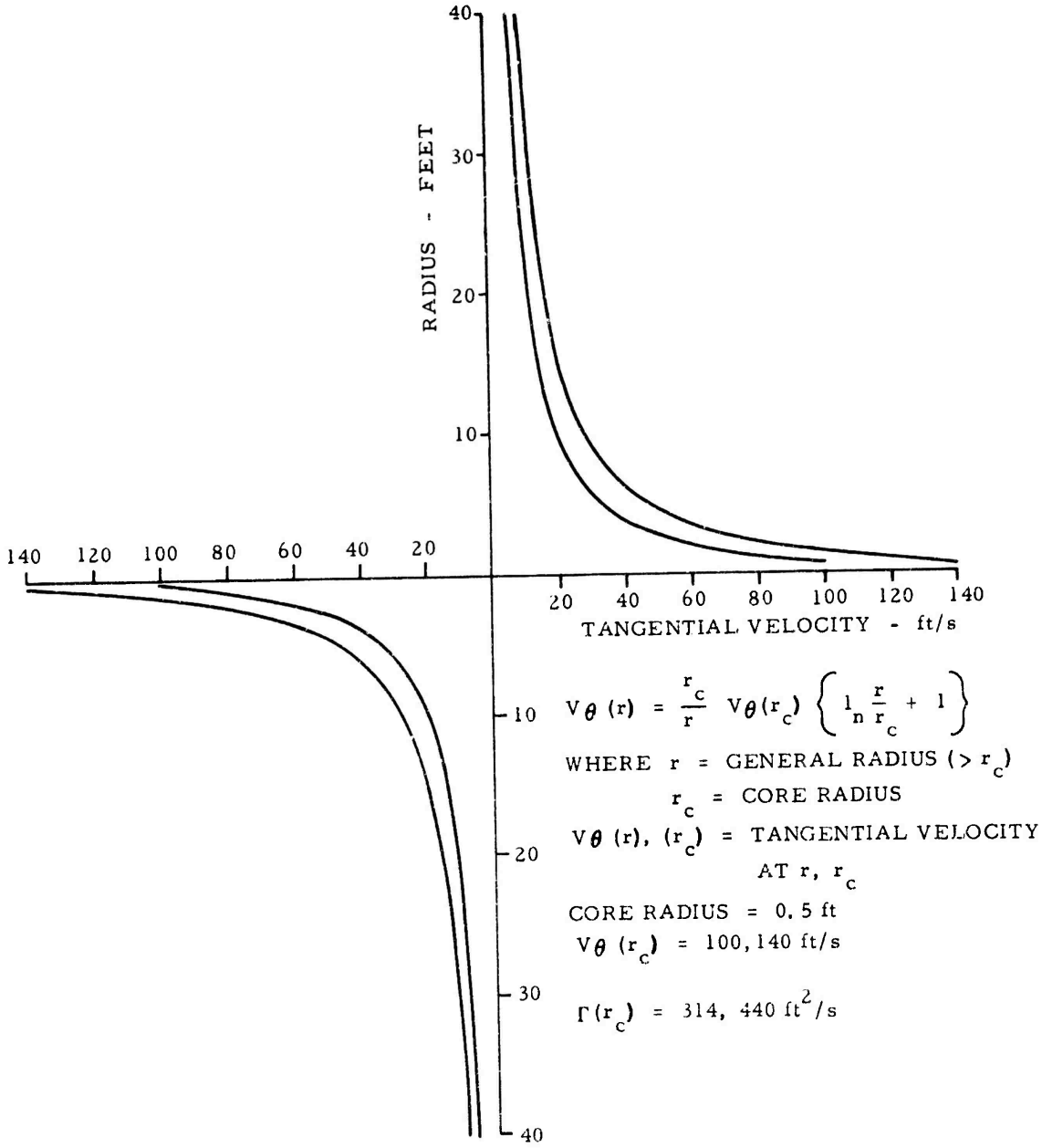

FIGURE 34. HOFFMAN-JOUBERT LOGARITHMIC DISTRIBUTION OF TANGENTIAL VELOCITY (SMALL CORE VORTEX)

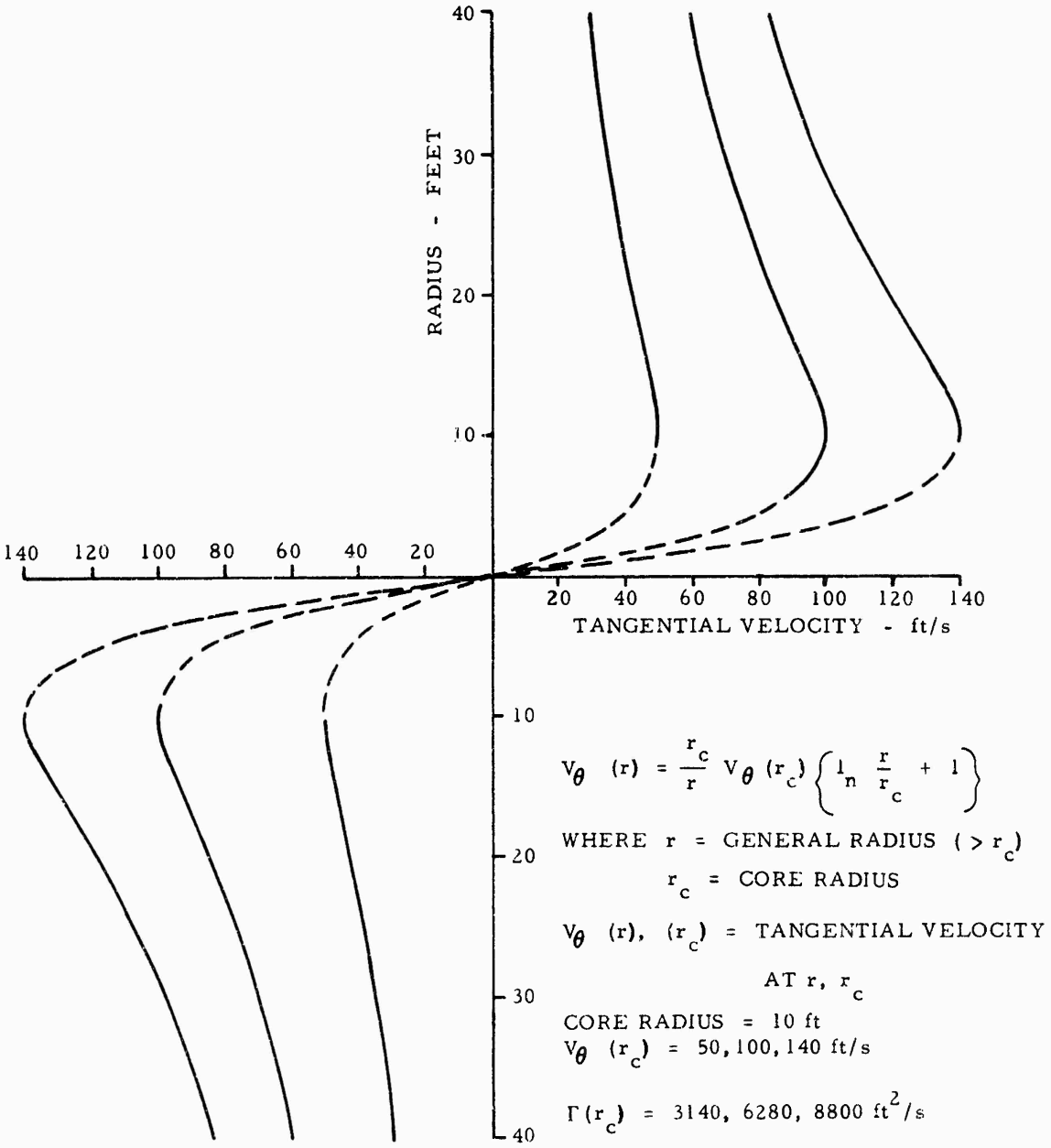

FIGURE 35. HOFFMAN-JOUBERT LOGARITHMIC DISTRIBUTION OF TANGENTIAL VELOCITY (LARGE CORE VORTEX)

Vortex lateral transport velocities as a function of crosswind velocity component are presented in appendix E, figures E-1 through E-4. Crosswind velocity component is based on the data presented in appendix F. In this case, the data for the 140-foot level is used. Information on the airplane track is presented in appendix G. Only in landing configuration were enough data points gathered to present the data separately for upwind and downwind vortices. In both cases, the positive sense of lateral velocity is defined by the wind, and ideally, one would expect to find that:

1. The upwind and downwind vortex lateral transport velocities would have the same slope when plotted as functions of the crosswind velocity component.

2. On extrapolating the data to zero crosswind, a positive intercept would occur on the vertical axis for the downwind vortex.

3. A negative intercept would occur on the vertical axis for the upwind vortices, since their natural motion is opposite to that of the wind and the downwind vortex.

The two slopes obtained are within experimental error, and the expected negative intercept for upwind vortices was obtained.

In figures E-5 through E-10, peak recorded velocity has been plotted as a function of airplane altitude abreast of the tower - with the data points grouped according to vortex age. A similar plot was made in reference 6, with the intent of determining whether close proximity to the ground, would lead to a measurable reduction in peak velocity. That plot failed to yield any significant result, as does the present data.

The use of 1-foot sensor spacing in the current tests has permitted a more accurate determination (than was possible in reference 6) of the tangential velocity profile through the entire vortex, especially in those areas where the velocity changes rapidly with radius, which occurs within the core and in the area immediately outside it. The maximum velocity within the vortex occurs at the core circumference, and with the closer spacing, it now can be no further than 6 inches from the nearest sensor. It is usually possible to identify (by inspection of the sensor velocity time-history plots) the sensor at which the peak velocity occurs. At these sensor levels, velocity time-history data was replotted on an expanded time scale. Vortex core diameters can be determined from these expanded plots, as described in reference 10, as follows:

When a direct vortex core hit on a sensor occurs, the tangential velocity time-history exhibits the following characteristics:

1. Initial velocity, at time zero will simply be the ambient wind velocity.

2. As the vortex approaches the sensor under the influence of the wind, the velocity at the sensor rises progressively - slowly at first and finally very rapidly, until it achieves its first peak value. At this point, the vortex axis is level with the sensor, separated from it by one core radius.

The velocity "seen" by the sensor is the vector sum of the circumferential velocity (which at this point is either vertically up or down), the lateral transport velocity and any residual vertical transport velocity.

3. As the vortex core passes through the sensor, the tangential velocity falls to a minimum value equal to the ambient wind velocity. This occurs when the axis of the vortex is situated exactly at the sensor.

4. The velocity rises to a second peak, occurring when the upstream boundary of the core passes through the sensor. Beyond that point, velocity falls at first rapidly, then more slowly, back down to ambient wind velocity.

Reference to figures 13, 14, and 15 will show how the velocities are generated as the vector sums of the circumferential velocities inherent in the vortex, the induced lateral transport velocity and the ambient wind velocity. The region separating the velocities V_1 and V_3 is referred to as the vortex core, the distance between them being the core diameter.

In reality, the velocity V_2 does not reduce exactly to ambient wind velocity during a vortex passage - lateral and vertical transport velocities exist even in the absence of any wind, and it is extremely rare for an exact hit to occur.

For a direct core hit" at the vortex center, the core diameter is given by:

$$d_c = \Delta t \cdot V_t \tag{18}$$

where V_t = Vortex lateral transport velocity
Δ_t = Time interval between velocity peaks

The core diameter cannot be determined with any reliability unless the core center passes through the sensor. On the assumption of solid body rotation within the vortex core, constant angular velocity ω yields the following:

$$\frac{V_1}{R_1} = \frac{V_2}{R_2} = \frac{V_3}{R_3} = \omega \tag{19}$$

As can be seen from figure 15 with the chord length, C,

$$\left(\frac{C}{2}\right)^2 = R_1^2 - R_2^2 = R_3^2 - R_2^2 \tag{20}$$

Substituting $R_1 = R_3$ and solving for R_2 from equation (19), and substituting into equation (20), the following are obtained:

$$R_1^2 = \frac{\left[(V_T \cdot \Delta t)\right]^2}{4\left[1 - \left(\frac{V_2}{V_1}\right)^2\right]} \tag{21}$$

$$R_3^2 = \frac{\left[(V_T \cdot \Delta t)\right]^2}{4\left[1 - \left(\frac{V_2}{V_3}\right)^2\right]} \tag{22}$$

Referring again to figures 14 and 15, and assuming $V_2 = V_{min}$, and V_1, $V_3 = V_{max}$ (whichever is greater),

$$d_c^2 = \frac{\left[V_T \cdot \Delta t\right]^2}{\left[1 - \left(\frac{V_{min}}{V_{max}}\right)^2\right]} \tag{23}$$

A problem arises in the application of the method - the quantity V_t, vortex lateral transport velocity cannot be accurately estimated. The quantity required for the determination of core diameter is the instantaneous value appropriate to the interval of time during which the core is passing through the sensor. The only transport velocities readily measurable in the present experiment are the mean values, determined between time "zero" (airplane abreast of the tower) and the time a vortex reaches a sensor. The initial and final lateral velocities are essentially zero, or no more than that of the ambient wind, with a peak value occurring in between.

An alternative method to determine core radius is by inspection of the V_θ - h plots (appendix C). The results of applying the two methods are presented in:

- Figure 25 - derived core diameter vs vortex age. Landing configuration diameter determined from V_θ - h plots.
- Figure 26 - as above, takeoff and holding configurations.
- Figure 36 - correlation of core diameters as determined by the two methods cited above.

The correlation between the two methods is poor and it is probably due to the shortcomings of employing average transport velocities and the time interval between adjacent peaks, and of the simple process of inspection of V_θ - h plots, which is subject to possible errors in interpretation of the sensor time histories and is evidently not completely reliable, though gross errors should essentially be precluded by the condition that the final plot have a reasonable degree of axi-symmetry. Figure 25 (landing configuration) shows that even for recently formed vortices (approximately 15 seconds), very wide variations in estimated vortex diameter are possible, at least in this configuration.

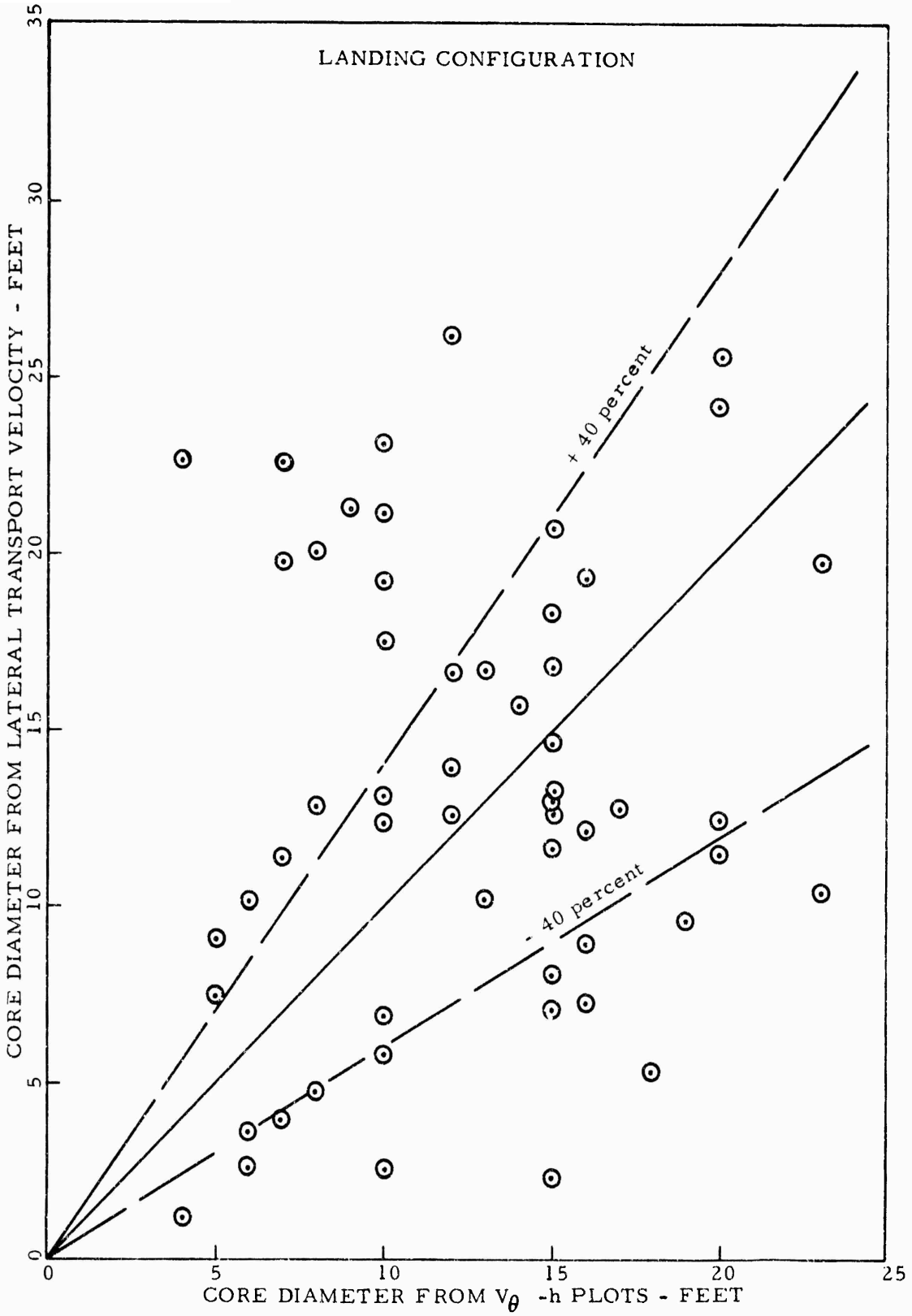

FIGURE 36. CORRELATION OF VORTEX CORE DIAMETER AS DETERMINED BY TWO METHODS

In figure 26, takeoff and holding configurations, the majority of points show a very small core diameter, and it is difficult to see how values as large as 12 feet can exist as little as 5 seconds after generation. The value of 2 feet, found for the majority of runs in these two configurations is a nominal one, indicating small diameter. The sensor spacing (1 foot between adjacent sensors) does not justify any smaller diameter being shown.

CONCLUSIONS

1. All data points on peak recorded tangential velocity fall on or under an exponential curve defined by the equation

$$V_{\theta_{max}} = 336.4 \exp(-.0173t)$$

This function has a half-life of 40 seconds, and fits the data between 15 and 80 seconds.

A more correct decay law, based on a vortex mathematical model due to Prandtl is

$$V_{\theta_{max}} = 886t^{-1/2}$$

This law fits the data more closely than the exponential law.

2. The use of a close sensor spacing (1 foot) has confirmed the existence of very small core diameters, coupled with high peak velocities, in the takeoff and holding configurations, while the landing configuration is characterized by large core diameters and lower peak velocities.

3. No difference in peak vortex velocity has been found attributable to throttling back the adjacent outboard engine to flight idle.

4. Mean vortex descent rates do not correlate well with the values yielded by potential theory. They may exceed the theoretical values by as much as three times.

5. Lateral transport velocities, as a function of crosswind velocity component, correlate quite well with theory.

REFERENCES

1. Garodz, Leo J., Measurements of the Vortex Wake Characteristics of the Boeing 747, Lockheed C5A and Other Aircraft, Data Report, Project 177-621-03X (Special Task No. 1), April 1970 (Final Report in preparation).

2. Condit, Philip M., Results of the Boeing Wake Turbulence Test Program, Boeing Document No. D6-30851, April 1970.

3. Andrews, William H., Robinson, Glenn H., Krier, Gary E., and Drinkwater, Fred J., III, Flight-test Evaluation of the Wing Vortex Wake Generated by Large Jet Transport Aircraft, FWP-18, April 1970.

4. Spreiter, John R., and Sacks, Alvin H., The Rolling Up of the Trailing Vortex Sheet and its Effect on the Downwash Behind Wings, Journal of the Aerospace Sciences, Volume 18, No. 1, January 1951.

5. Eisenhuth, Joseph J., McCormick, B. W., Nelson, Robert C., Aero Engineering Associates, State College, Pa., and Garodz, Leo J., FAA, NAFEC, Analysis of Experimental Measurements of Trailing Vortex Systems of Large Jet Transport Aircraft, NAECON, 1971 Record.

6. Garodz, Leo J., Miller, N. J., and Lawrence, D. M., The Measurement of the DC7 Vortex System Using the Tower Fly-by Technique, September 1971 FAA/SRDS, FAA-RD-73-141.

7. Anon, Central Data and Recovery System (CENDAR), SRDS/FAA Report, September 1964.

8. Prandtl, L., Aerodynamic Theory, Volume 3, Division G, Section 10, Editor-in-Chief, W. F. Durand, Dover Publications, Inc., New York.

9. McCormick, Barnes W., Tampler, James L., and Sherrieb, Harold E., Structure of Trailing Vortices, American Institute of Aeronautics and Astronautics, Journal of Aircraft, May-June 1968.

10. Garodz, Leo J., Investigation of Jet Transport Aircraft Vortex Systems Descending Into and Generated in Ground Effect, November 1970, FAA/SRDS Data Report, Special Task No. 2.

APPENDIX A

INSTRUMENTATION

INSTRUMENTED TOWER.

The tower is 140 feet high, with its base 76 feet above sea level. It is self-supporting, of triangular cross section and designed to produce a minimum of aerodynamic interference. The location is at a point 2,456 feet from the centerline of Runway 13-31 (figure A-1).

The tower was instrumented with hot-film anemometers to measure vortex airflow velocity. Flow patterns were observed through the use of colored motion pictures and colored smoke dispensers. The smoke was entrained in the passing vortex system, producing a visual indication of its movement and structure. Instrumentation and smoke dispensers were located as shown in figure A-2.

INSTRUMENTATION ROOM.

An underground room, located at the base of the tower, was used to house the recording equipment, necessary electronic accessories, and served as a central control room for recording during flight tests.

TEST INSTRUMENTATION.

The sensors mounted on the tower were divided into two groups. Group one consisted of 120 hot-film single-axis anemometers, capable of sensing velocities up to 370 feet per second at frequencies well above 1,000 Hz. The anemometers were installed at 2-foot increments, between 8 and 40 feet and 1-foot increments from 41 to 142 feet. They were mounted on the end of a movable boom that extended approximately 10 feet from the center of the tower, and were aligned in a single vertical line. The anemometers were mounted on a protractor fixture that was installed on the end of the boom and were adjustable over a $\pm 90°$ range, from 130° to 310° (magnetic) - figure A-3.

The hot-film sensors were mounted with the axis parallel to the ground. They were aligned through the use of the protractor fixture so that the axis was perpendicular to the direction of the ambient wind. This position allows the tangential velocity of the vortex to impact the hot-film sensor normal to the sensor axis. Axial flow velocities are not detectable by this system. In the event that the ambient wind was in the range of 310° through 130°, the sensors were aligned downwind, with the axis still perpendicular to the wind. The turbulence around the sensor resulted in what appeared to be a noisy output. However, this noise disappeared or was minimized when the vortex penetrated the hot-film area. The hot-film anemometers used in these tests were manufactured by Thermo-Systems, Inc. They utilize the "constant resistance" mode of operation in which a voltage is a measure of the cooling effect of the wind, which is directly related to wind velocity. The output

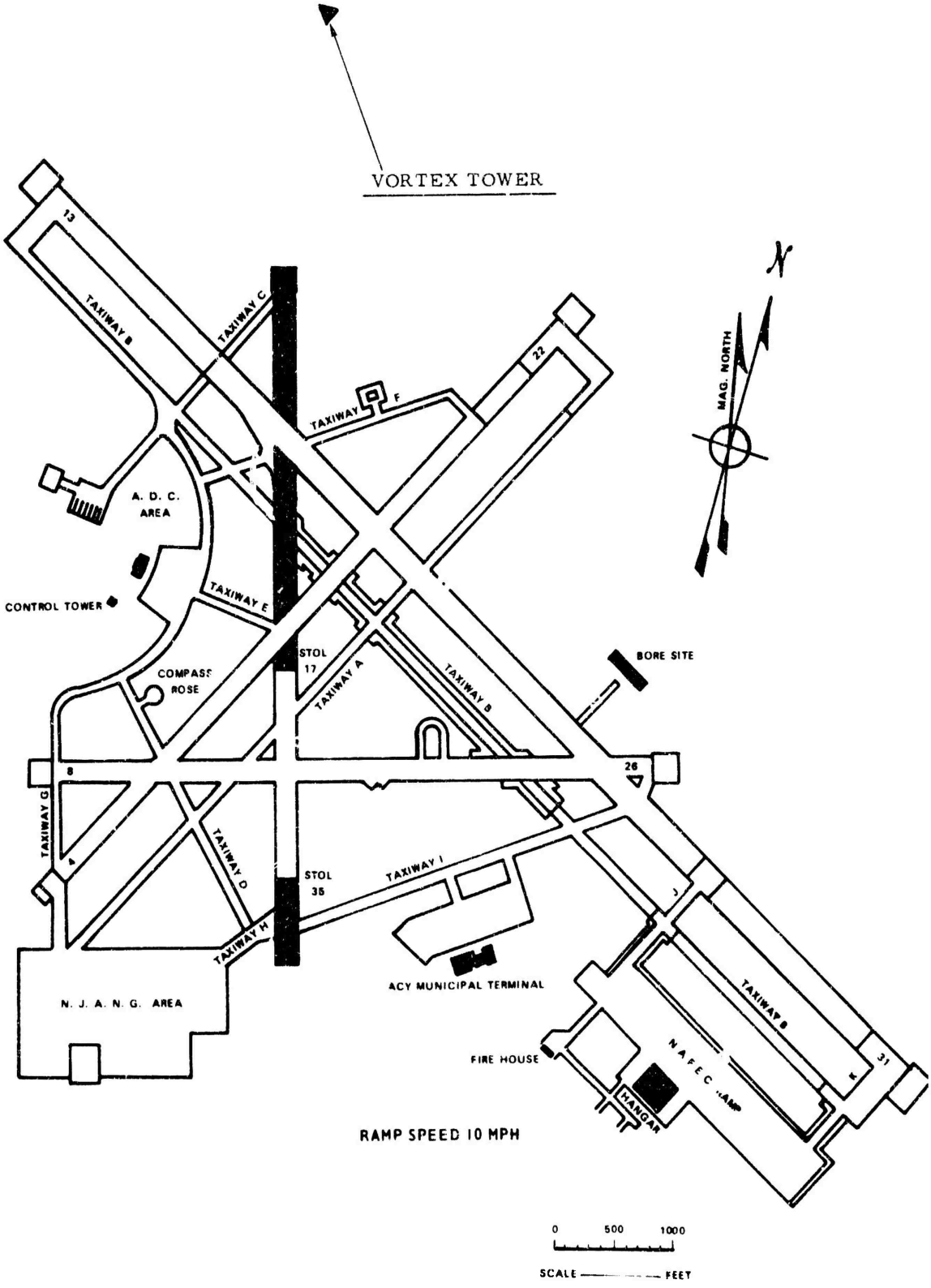

FIGURE A-1. VORTEX TOWER LOCATION NAFEC/ATLANTIC CITY AIRPORT

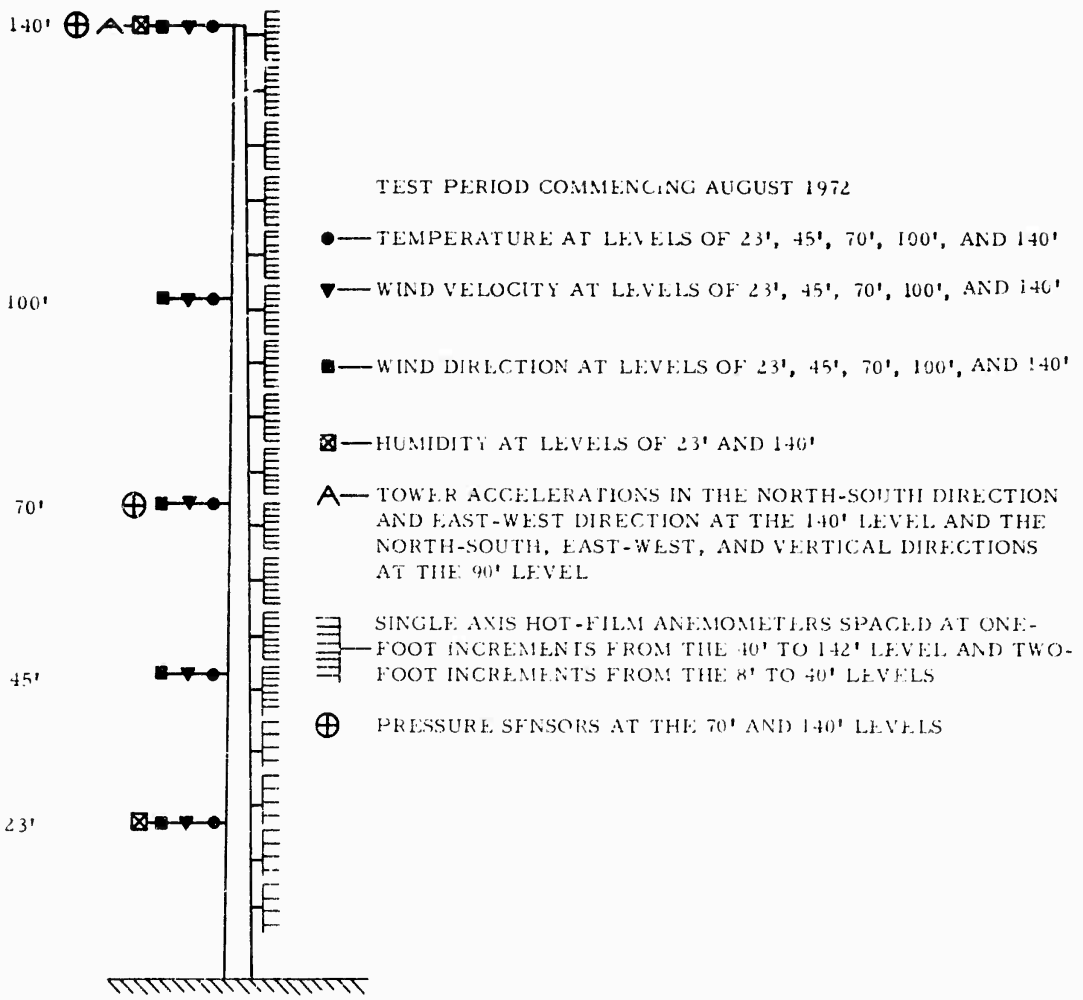

FIGURE A-2. SENSOR LOCATIONS ON TOWER

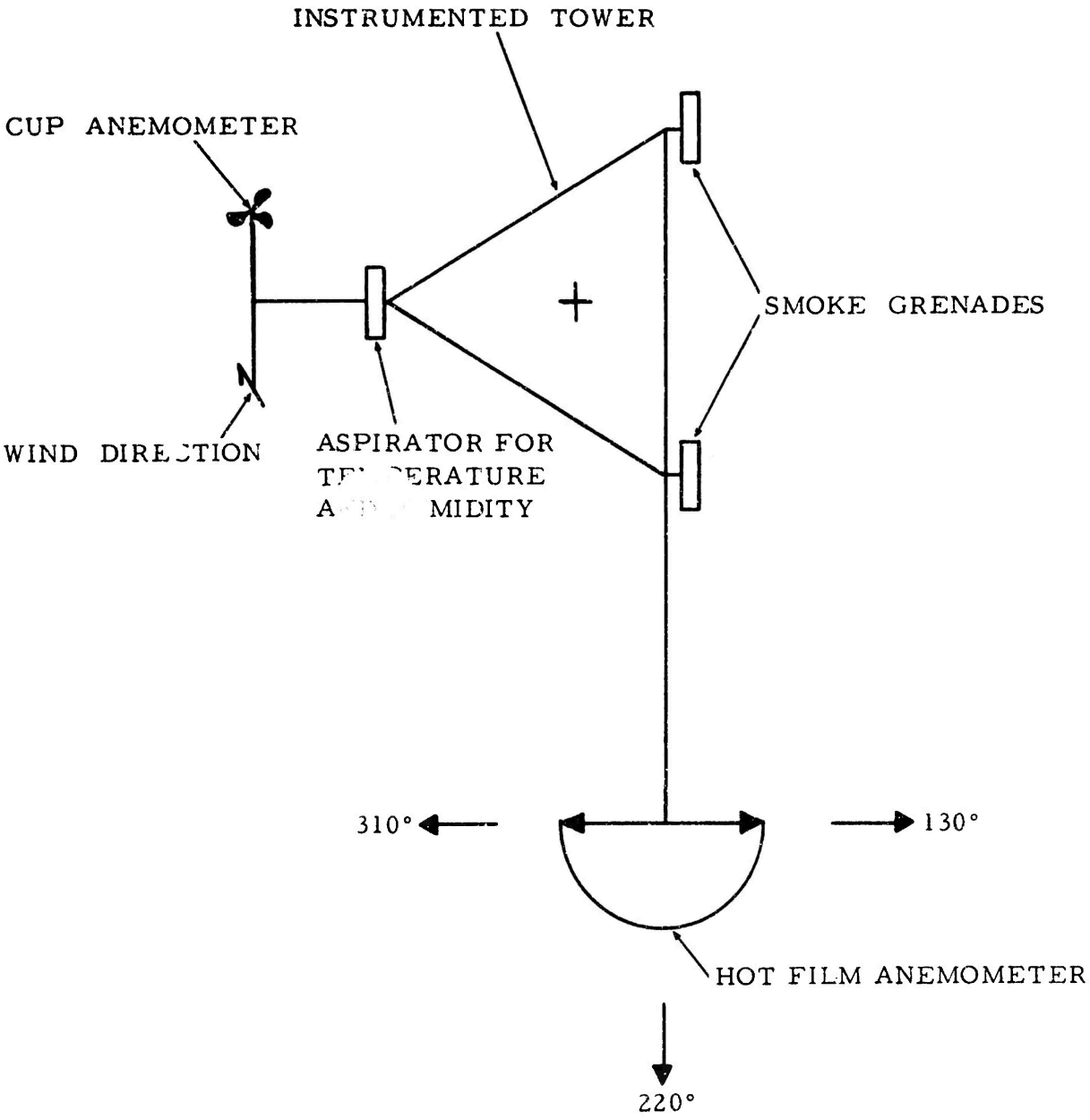

FIGURE A-3. DIRECTIONAL LOCATION OF SENSORS

voltage of the bridge is in the range of 4 to 14 volts, which represents wind velocities of zero to 370 feet per second. Figure A-4 is a schematic of the basic circuit. In order to have the anemometer output compatible to normal recording system standards, a zero suppression circuit and a gain control circuit was added to have a zero to 5 volts output for zero to 370 feet per second velocity.

Group two sensors consisted of standard meteorological instruments to measure the low frequency components of the required atmospheric variables. Cup-type anemometers, wind direction sensors, and temperature sensors were located on five levels, with approximately logarithmic spacing. Two humidity sensors were installed, one at the 23-foot level, the other at the 140-foot level. The temperature and humidity sensors were located in a motor-aspirated radiation-shielded housing to minimize effects of solar radiation.

Two pressure sensors were mounted on the tower, one at the 70-foot level and the other at the 140-foot level. They were used to obtain information relative to the pressures within the vortex core.

CALIBRATION AND ROUTINE CHECKS.

Single-axis hot-film anemometers were calibrated periodically by use of a laminar flow air velocity calibrator. Each hot-film anemometer was calibrated at 21 points from zero to 212 foot per second (ft/s). The square root of the velocity vs. the square of the voltage was plotted and an equation in the form of: $\sqrt{\text{Velocity}} = A_1 + B(\text{Voltage})^2$ was obtained.

At the start of each data run, reference voltages of zero and 5.00 volts were substituted for the hot-film anemometer outputs. These reference voltage were used in the computer program to properly scale the voltage outputs from the anemometers.

Due to the relationship of $(\text{voltage})^4 = K$ velocity, the error at the lower velocities was less than at full scale where it reached ± 10 percent of full scale. Calibration experience gained with the calibration of over 400 anemometers indicated that system errors were in the order of ± 5 ft/s in the velocity range of zero to 21 feet per second.

The cup anemometers were calibrated at the National Bureau of Standards in Washington, D. C., and these values were used during the test. The accuracy was within ± 0.5 miles per hour (mi/h) in the range of 2 to 30 mi/h. The sensitivity threshold was 1 mi/h with a distance constant of 5 feet. The wind direction sensors were calibrated at NAFEC and were within $\pm 6°$ of true wind direction. This large error was due primarily to the inability to accurately align the sensor in a given direction. The deadband was 3°, which was set at 357° to 360°. The distance constant of the vane was 3.5 feet.

The temperature sensors covered the range of -5°C to 45°C (23°F to 113°F) with a recorded accuracy of $\pm .25$°C(.45°F).

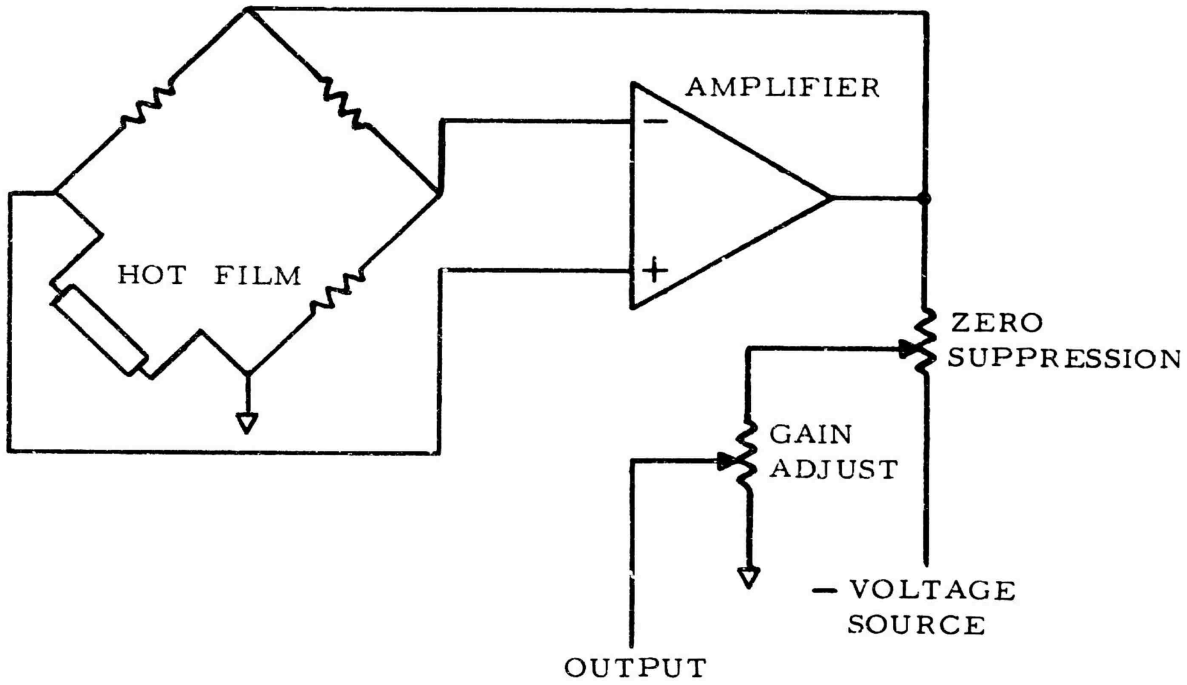

FIGURE A-4. CONSTANT RESISTANCE HOT-FILM ANEMOMETER SYSTEM

Humidity measurements were made on the 23- and 140-foot level. The error band of the sensors was ±3 percent of full scale between humidities of 10 and 90 percent.

Prior to test periods, all signals were checked for condition and the status recorded on the Daily Checkoff Sheet (figure A-5). Time would not permit the repair of malfunctioning signals prior to the test. However, every effort was made to have all signals functional for the next testing period.

During the test periods, the real time output of an oscillographic recorder was monitored to determine the functioning of the hot-film sensors and calibration voltages.

DATA COLLECTION SYSTEM.

Figure A-6 is a block diagram of the flow of signals to the data recording systems. During tests, data was recorded on three systems as follows:

1. ANALOG MAGNETIC TAPE RECORDER. This system was considered primary and all signals, as listed on the Daily Checkoff Sheet (figure A-5), were recorded on it. Referring to figure A-6 all incoming signals are routed through signal conditioners where all signals are standarized to a range of zero to 5 volts. A second function of the signal conditioner is to substitute reference voltages in place of the incoming signals. This substitution of voltages is usually referred to as calibration voltages and consists of two substitutions, zero and 5 volts direct current (d.c.).

The electrical signals are then routed to voltage controlled oscillators where the voltage is changed to a specific frequency range. Fifteen proportional band width voltage-controlled oscillators (VCO's) with center frequencies ranging from 400 Hz to 30,000 Hz are summed and the output signal is recorded on one track of the 14-track analog magnetic tape recorder. During these tests, 10 tracks were dedicated to the FM multiplex from the VCO's: one track for voice, and two tracks for central time.

2. METEOROLOGICAL RECORDING SYSTEM. In addition to the 14-track analog recorder, a 7-track analog recorder ran continuously throughout the flight tests and was used for recording meteorological data. This included the 5 temperatures, 5 wind velocities, 5 wind directions, 2 humidities, 2 pressures, event, and central time.

VCO frequency response varies directly with bandwidth. Figure A-7 tabulates the VCO's with their frequency bandwidth and their signal assignment. In order to minimize the loss of data resulting from the narrow bandwidth of the lower numbered VCO's, high-frequency and low-frequency VCO's were alternated. In this manner, the lowest frequency in any 2-foot spacing would be 45 Hz (VCO 8).

SIGNAL	REMARKS	SIGNAL	REMARKS	SIGNAL	REMARKS	SIGNAL	REMARKS
8'		62'		100'		138'	
10'		63'		101'		139'	
12'		64'		102'		140'	
14'		65'		103'		141'	
16'		66'		104'		142'	
18'		67'		105'		140V	
20'		68'		106'		T23	
22'		69'		107'		T45	
24'		70'		108'		T70	
26'		71'		109'		T100	
28'		72'		110'		T140	
30'		73'		111'		V23	
32'		74'		112'		V45	
34'		75'		113'		V70	
36'		76'		114'		V100	
38'		77'		115'		V140	
40'		78'		116'		D23	
41'		79'		117'		D45	
42'		80'		118'		D70	
43'		81'		119'		D100	
44'		82'		120'		D140	
45'		83'		121'		H23	
46'		84'		122'		H140	
47'		85'		123'		Pa	
48'		86'		124'		Pb	
49'		87'		125'		Pc	
50'		88'		126'		Pd	
51'		89'		127'		Pe	
52'		90'		128'		An-s	
53'		91'		129'		Ae-w	
54'		92'		130'		Av	
55'		93'		131'		Ah	
56'		94'		132'		Al	
57'		95'		133'		P40	
58'		96'		134'		P90	
59'		97'		135'		P140	
60'		98'		136'		Event	
61'		99'		137'		Time	

Aircraft_____ Run numbers_____ Wind direction_____

Probe direction_____ Temperature_____ Humidity_____

Barometric pressure_____

Remarks

Date_____

FIGURE A-5. WAKES AND VORTICES CHECKOFF SHEET

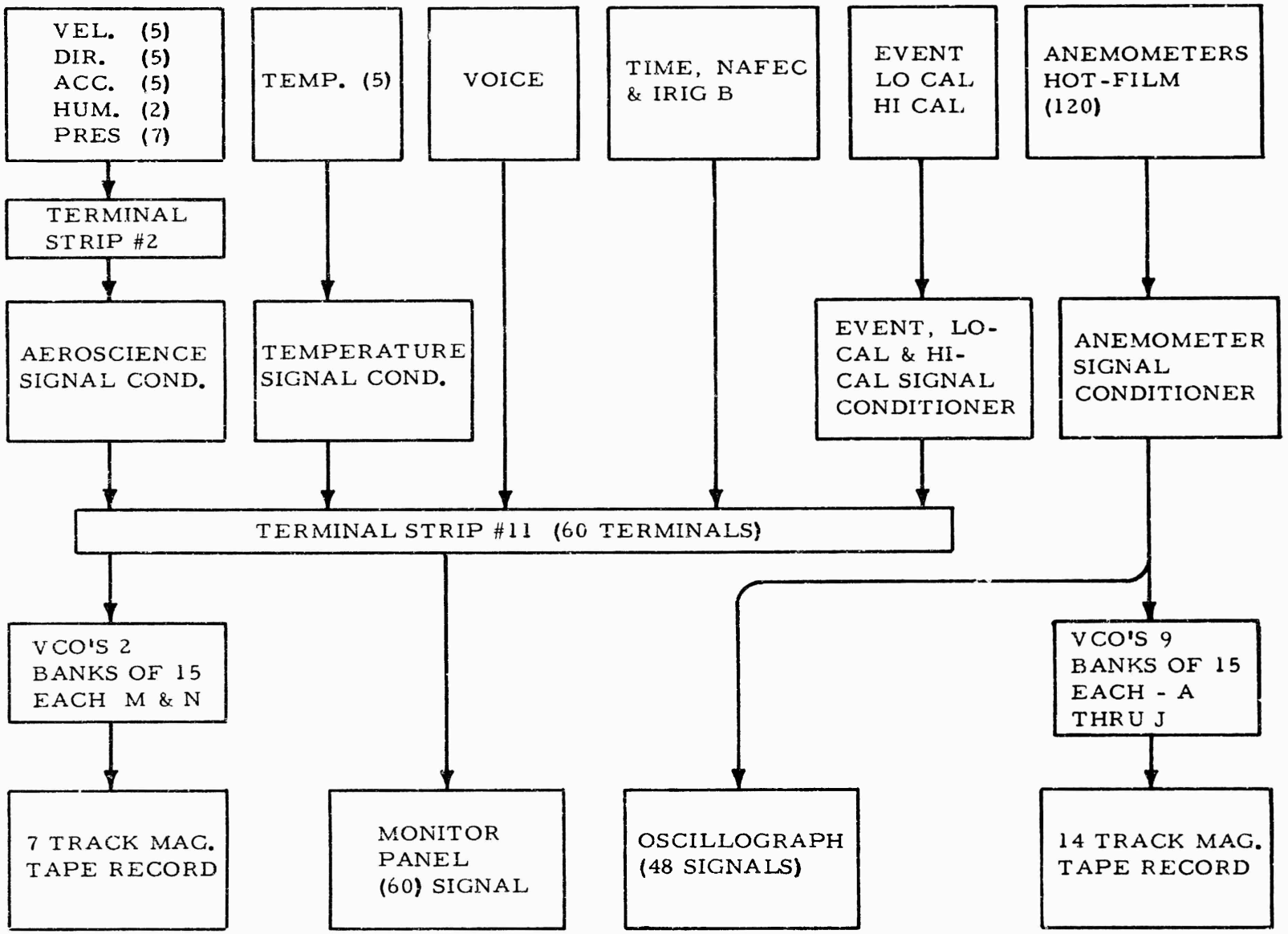

FIGURE A-6. BLOCK DIAGRAM - DATA SYSTEM WAKES AND VORTICES

VCO	FREQ	Track A	B	C	D	E	F	G	H	J	K	L	M	N	
1	6	T_{140}	56	71	86	101	Event	123	41				D_{140}	Event	
2	8	43	58	73	88	103	137	125	38				H_{23}	T_{23}	
3	11	45	60	75	90	105	138	127	34				H_{140}	T_{45}	
4	14	47	62	77	92	107	139	129	30				P_A	T_{70}	
5	20	49	64	79	94	109	140	131	26				P_B	T_{100}	
6	25	51	66	81	96	111	141	133	22				P_C	T_{140}	
7	35	53	68	83	98	113	142	135	18				P_D	V_{23}	
8	45	55	70	85	100	115	116	136	16				P_E	V_{45}	
9	59	54	69	84	99	114	118	134	20				9A1	V_{70}	
10	81	52	67	82	97	112	120	132	24	A_{ns}			9A2	V_{100}	
11	110	50	65	80	95	110	122	130	28	A_{ew}			9B1	V_{140}	
12	160	48	63	78	93	108	121	128	32	8			9B2	D23	
13	220	46	61	76	91	106	119	126	36	10			9C1	D_{45}	
14	330	44	59	74	89	104	117	124	40	12				D_{70}	
15	450	42	57	72	87	102	P140	P90	140V	14				D_{100}	
TRACK		1	2	3	4	5	8	9	10	11			12	13	5600

Numbers = level (in feet) of single axis anemometers.

A = accelerometer locations; ew = east west, ns = north south, v = vertical, h = horizontal, and l = lateral.
P40, P90 and P140 = pressure transducers to measure vertical velocities.
Event = time zero (aircraft abreast of tower).
T = temperature.
H = humidity.
V = wind velocity.
D = wind direction.

NOTE: IRIG B time is on track number 6 (Direct) on 5600 recorder and on track number 6 on VR3300 recorder.
NAFEC time is on track 7 (FM) on 5600 recorder.

FIGURE A-7. WAKES AND VORTICES VCO ASSIGNMENTS

3. OSCILLOGRAPH DATA SYSTEM. A 50-channel direct-writing oscillograph was connected to 41 of the 120 single-axis hot-film anemometers, acceleration, an event signal, and NAFEC time. The oscillographic data system was used for real time monitoring of the hot-film data and calibrate signals and vortex "hits" on the tower. By editing the oscillograph output after each flight, the location of the vortex "hits" on the tower, time between right and left vortex penetration of the tower, and time between aircraft passage by the tower, and the vortex penetration of the tower were determined. This greatly reduced the time required for subsequent data processing since only pertinent data was processed.

AIRCRAFT SPACE POSITION.

The Phototheodolite Range was used to track the aircraft in the vicinity of the vortex test tower. Three phototheodolites were normally used for tracking with the best two being used for the solution. Data obtained from the theodolite included groundspeed and track of aircraft, altitude, and horizontal distance from the aircraft to the tower. Time zero, which is defined as the time that the aircraft crossed a perpendicular line to the tower, was also obtained from the theodolite data.

CORRELATION OF ALL DATA SOURCES.

Correlation of the phototheodolite, analog magnetic tape, and the oscillograph was through a central time source synchronized to Station WWV. As the aircraft passed the tower, an operator pressed a switch that placed an event mark on the analog tape and the oscillograph. In addition, it ignited a large photo flashbulb on the tower that was within range of all data cameras and started an elapsed time clock that was also in the range of the data cameras. In this manner, all data sources were synchronized in time. A check on the accuracy of the time zero switch operation was obtained by checking that time against the time that the theodolites indicated for the shortest distance between the aircraft and the tower.

EQUIPMENT MALFUNCTION.

During this test period only a small amount of data was lost due to equipment malfunctions. An example of the rough daily checkoff sheets, used to indicate inoperative signals, is presented in figure A-8.

SIGNAL		REMARKS	SIGNAL		REMARKS	SIGNAL		REMARKS	SIGNAL		REMARKS
8'	✓	✓	62'	✓		100'	✓		138'	✓	
10'	✓		63'	✓		101'	✓		139'	✓	
12'	✓		64'	✓		102'	✓		140'	✓	
14'	✓		65'	✓		103'	✓		141'	✓	
16'	✓		66'	✓		104'	✓		142'	✓	
18'	✓		67'	✓		105'	✓		140V	✓	
20'	✓		68'	✓		106'	✓		T23	✓	2.08
22'	✓		69'	✓		107'	✓		T45	-	2.09
24'	✓		70'	✓		108'	✓		T70	✓	2.11
26'	NG	-.6V	71'	✓		109'	✓		T100	✓	2.14
28'	✓		72'	✓	Low	110'	✓		T140	✓	2.21
30'	✓		73'	✓		111'	✓		V23	✓	
32'	✓		74'	✓		112'	✓		V45	✓	
34'	✓		75'	✓		113'	✓		V70	✓	>0.7V To .5V
36'	✓		76'	✓		114'	✓		V100	✓	
38'	✓		77'	✓		115'	✓		V140	✓	
40'	✓		78'	✓		116'	✓		D23	✓	
41'	✓		79'	✓		117'	✓		D45	✓	
42'	✓		80'	✓		118'	✓	Low	D70	✓	3.40 To 3.60V
43'	✓		81'	✓		119'	✓		D100	✓	
44'	✓		82'	✓		120'	✓		D140	✓	
45'	✓		83'	✓	Low	121'	✓		H23	✓	4.80
46'	✓		84'	✓		122'	✓		H140	✓	4.75
47'	✓		85'	✓		123'	✓		Pa		
48'	✓		86'	✓		124'	✓		Pb		
49'	✓		87'	✓		125'	✓		Pc		
50'	✓		88'	✓		126'	✓		Pd		
51'	✓		89'	✓		127'	✓		Pe		
52'	✓		90'	✓		128'	✓		An-s		
53'	✓		91'	✓		129'	✓		Ae-w	✓	
54'	✓		92'	✓		130'	✓		Av	✓	
55'	✓		93'	✓		131'	✓		Ah	✓	
56'	✓		94'	✓		132'	✓		Al	✓	
57'	✓		95'	✓		133'	✓		P40	✓	
58'	✓		96'	✓		134'	✓		P90	✓	2.49
59'	✓		97'	✓		135'	✓		P140	✓	2.50
60'	✓		98'	✓		136'	✓		Event	✓	
61'	✓		99'	✓		137'	✓		Time	✓	

Aircraft 747 PanAm Run numbers 1-25 Wind direction 270°
Probe direction 220° Temperature Humidity 95%
Barometric pressure
Remarks

Date 9/14/72 0730

FIGURE A-8. WAKES AND VORTICES CHECKOFF SHEET

APPENDIX B

DATA PROCESSING

DATA FORMAT REQUIREMENTS.

The signals from the tower instrumentation (figure A-2) were properly conditioned to voltage-controlled oscillators in the FM Multiplex System.

DATA SCHEMATIC FLOW.

A schematic of information flow is shown in figure B-1. Data was demultiplexed, unpacked, calibrated, and floated by the 7090 computer program. The output consists of calibrated velocity curves grouped by individual sensors along with the associated meteorological information. Data for each sensor appears in chronological order in floating point format. The data retrieval program including calibration, conversion, format plot subroutine, and selected variable time history output is shown in figure B-2.

DATA RETRIEVAL.

The multiplexed CENDAR data is checked for validity by investigating such items as "0" bit error, time word error, tape redundancy, data channel malfunctions, and record word count error. During demultiplexing, data were grouped according to each sensor and then outputted. During unpacking and floating, data words were broken down into bytes and decoded into floating point format. The history of data retrieval was then outputted for future reference.

Physical high- and low-calibration values with accompanying sensor voltages are obtained at the probe calibrated to standard conditions (70°F, 29.92" mercury (Hg)). To compensate for atmospheric conditions, all versions of the CII Program multiply these values by the following factor:

$$\left[\frac{(29.92)(T+460)}{530(P)}\right]$$

Where T = ambient temperature in degrees fahrenheit
P = ambient pressure in inches Hg

The hot-film sensors operate at a steady temperature of 450° at standard conditions. To compensate for nonstandard operating conditions, the CII M7 program multiplies M and B of Y = MX + B by the following factor:

$$\left[\frac{380}{450-T} = \frac{450 - 70}{450 - T}\right]$$

This equation is used to relate velocity (Y) to sensor voltage (X).

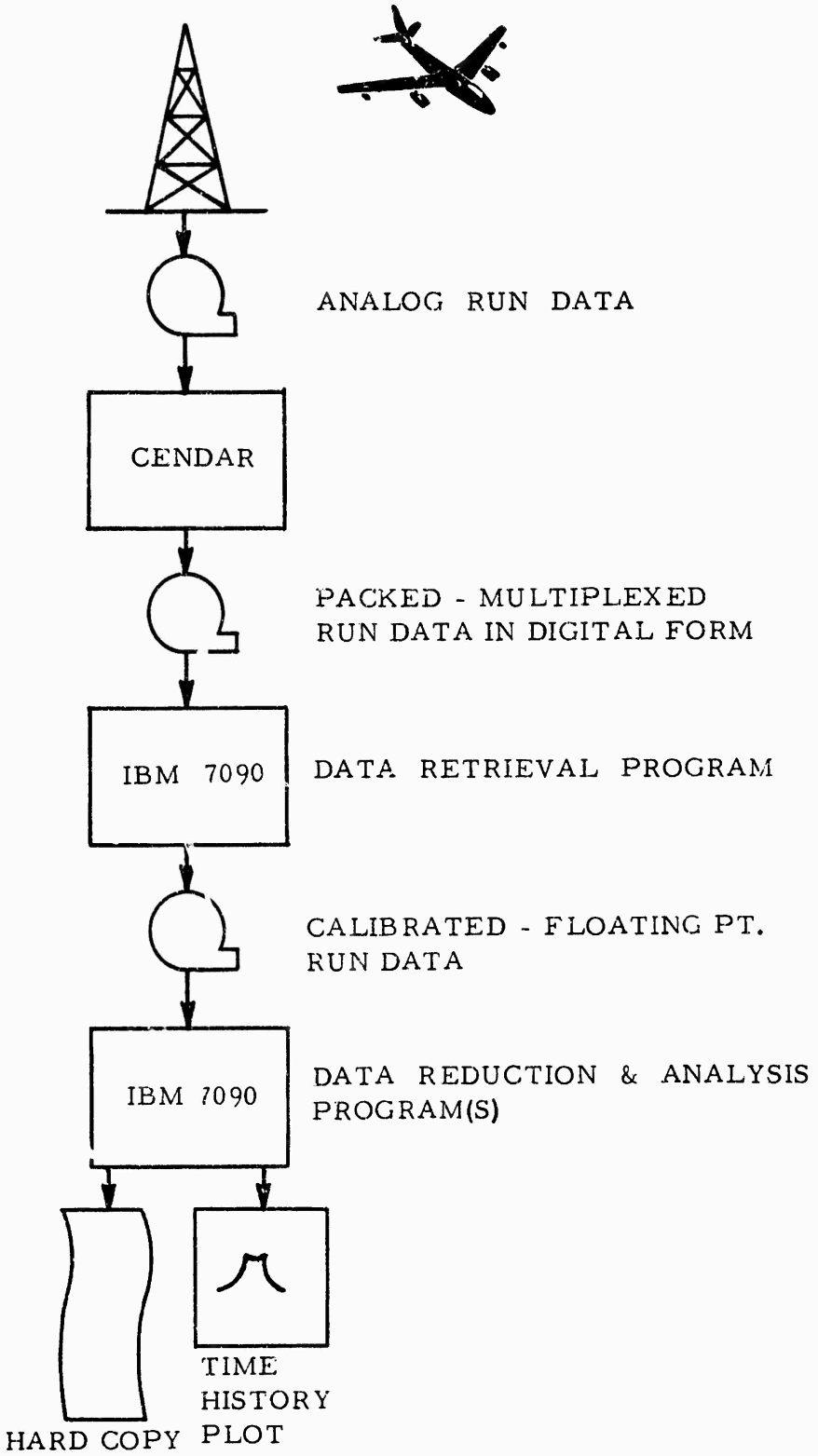

SCHEMATIC OF INFORMATION FLOW

FIGURE B-1. SCHEMATIC OF INFORMATION FLOW

DATA RETRIEVAL PROGRAM

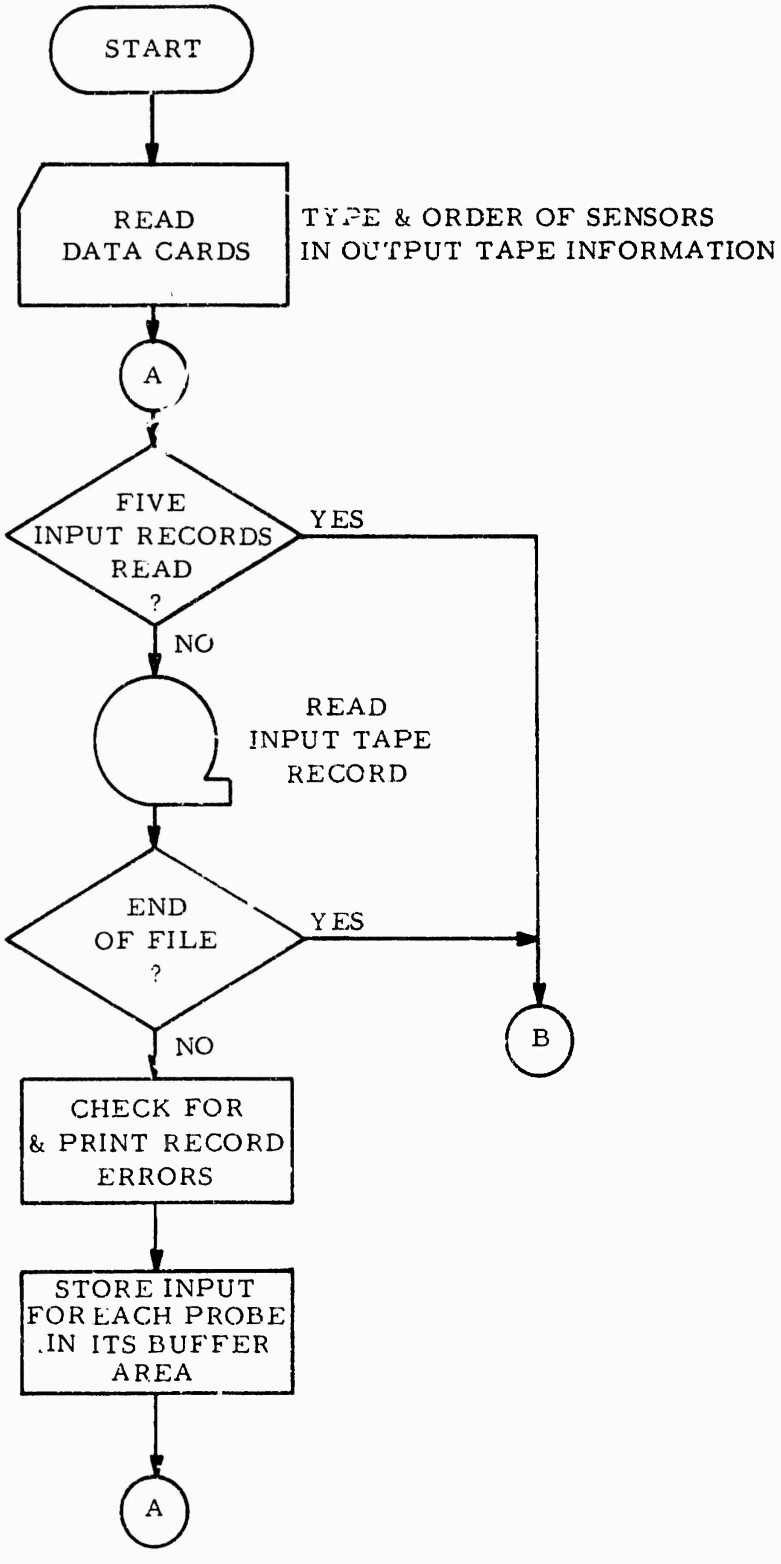

FIGURE B-2. DATA RETRIEVAL PROGRAM (Sheet 1 of 3)

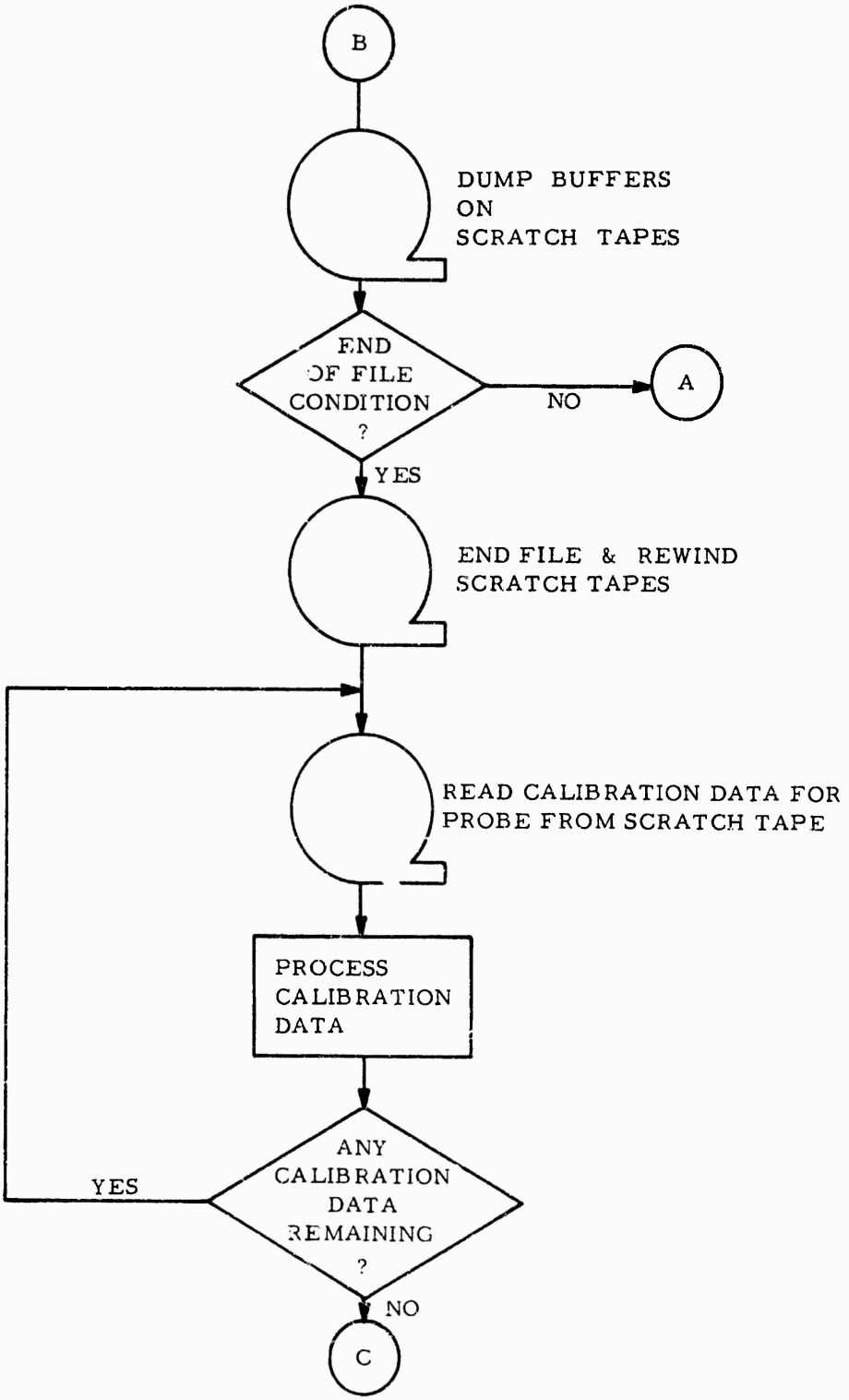

FIGURE B-2. DATA RETRIEVAL PROGRAM (Sheet 2 of 3)

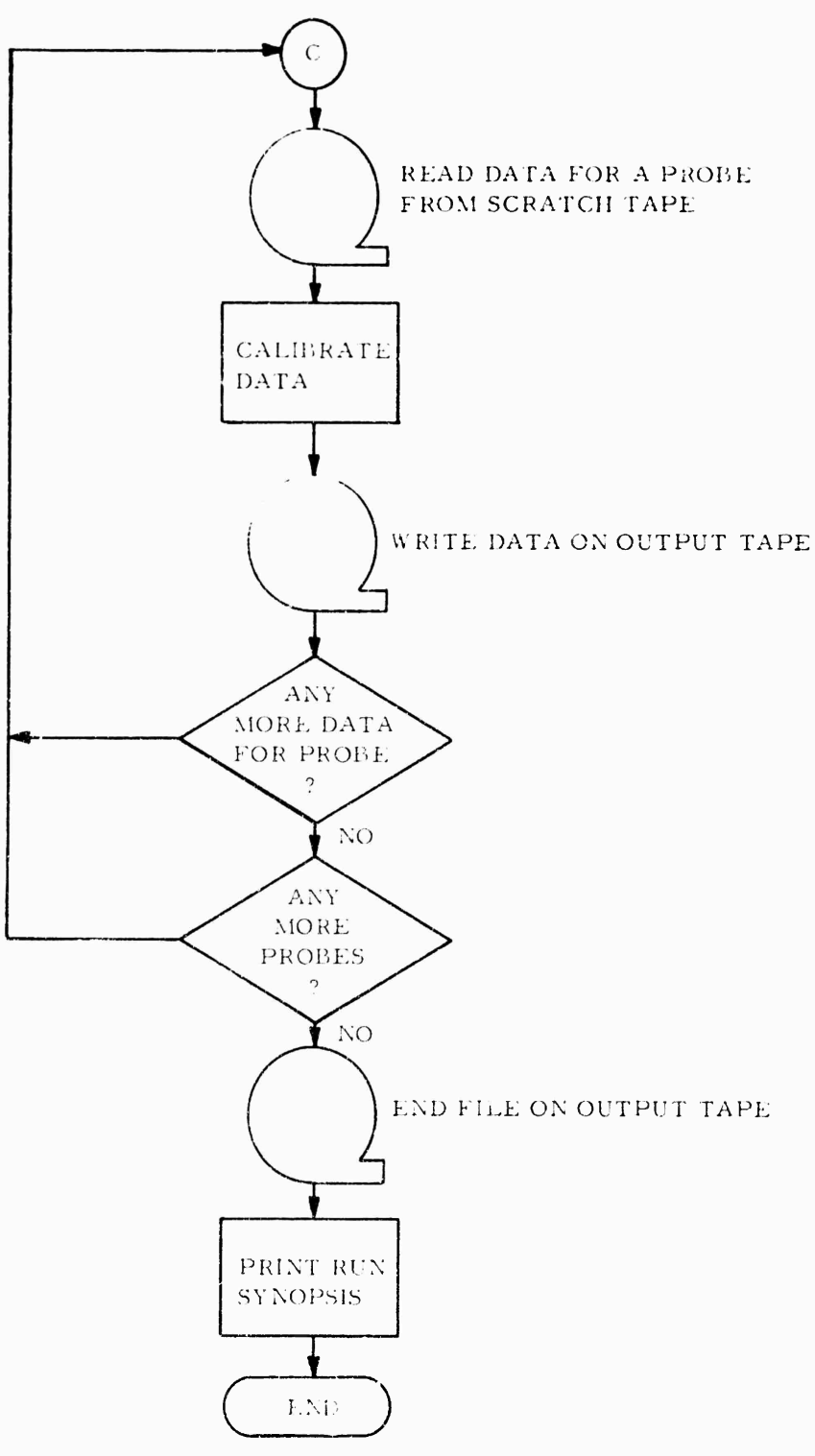

FIGURE B-2. DATA RETRIEVAL PROGRAM (Sheet 3 of 3)

COMPUTER PROGRAMS.

There are two basic data collection computer programs being used by this project. The first is entitled CENDAR II, Modification 7 (CII M7). It operates upon digitized raw data yielding calibrated data and a processing history. The second program is entitled Plot II (PII). It accepts calibrated data as input and yields a tape formatted for use on a data plotter.

The plot programs yield a time history of tangential velocity versus elapsed time. Each normal plotted point is the average of 50 data values (0.050 sec). The averaging has a low-pass filtering effect and also reduces the number of plotted points to a manageable size. Expanded plots have an variable time scale i.e., fewer than 50 data values per plot point, and, consequently, the low-pass filter characteristics will also vary. A schematic of the sensor plot program is shown in figure B-3.

CII M7 PROGRAM SERIES LOGIC. This FORTRAN IV and MAP Program is intended to be run on the IBM 7090 Computer. It requires two data channels with seven tape drives per channel.

There are three types of internal program table:

Type 1. Tables remain more or less constant. These tables contain values related to particular sensors and need only be updated when a sensor's calibration changes or a sensor is replaced. Updating is accomplished by NAME LIST Cards.

Type 2. Tables remain constant for the duration of a single run. Atmospheric conditions, sensors to process, header information, etc., fall into this category. These tables are updated using data cards.

Type 3. Tables are updated for each run, but this is done automatically by the program using input data and values from tables Type 1 and 2 above. CENDAR calibration values, maximum tangential velocity tables, etc., appear in this class. When the program goes into execution, it reads the NAME LIST Cards, if any, and data cards. Appropriate tables are updated. The input file contains 20 records of low-calibration values and then 20 records of high-calibration values followed by data values. All input on tape is multiplexed. The program reads the low-calibration values and finds the mean ($\bar{X}$) and standard deviation σ for each sensor. A second look is taken at this data and all values outside the limits $\bar{X} - \sigma$, $\bar{X} + \sigma$ are discarded. A new mean $\bar{\bar{X}}$ and standard deviation $\bar{\sigma}$ are found and outputted as part of the processing history. The $\bar{\bar{X}}$ value is stored in a table of low-calibration tape values. This same algorithm is followed for obtaining the high-calibration values.

There are actually three sets of calibration values for low and also for high-calibration of each sensor. The sensor voltage value related to a particular physical parameter, the physical parameter itself, and the

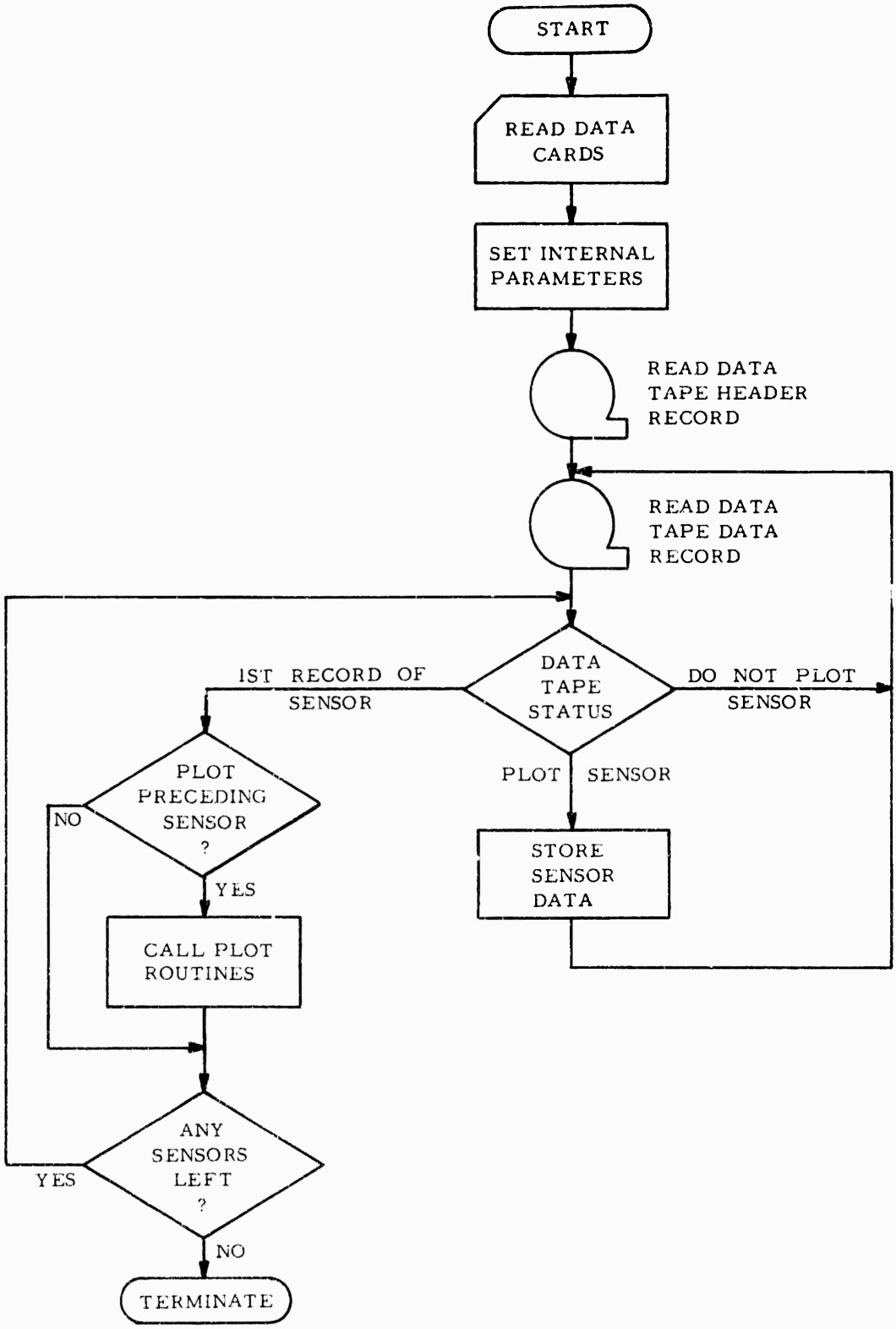

FIGURE B-3. SCHEMATIC OF PLOT II PROGRAM SERIES

CENDAR tape calibration values. It is necessary to relate the CENDAR values, which are in units of volts, to the sensor calibration values in units of volts and then obtain the physical value represented by a particular sensor output.

Once the sensors have been calibrated, the data is read into the core in blocks of five physical records. Only the first sensor in use for the current file is calibrated and outputted. The other sensors are demultiplexed and written on scratch tapes. When an "end of file" is sensed on the input tape, the scratch tapes are rewound and their contents processed and outputted one sensor at a time. Just before a sensor's data is written on the output tape, it is calibrated and checked for maximum value and related time. The program continues processing data until all desired sensors are processed. Routines are incorporated to skip files which contain no useful data. Extensive quality control procedures are observed to monitor the input data, scratch tape data, and time.

The program prints out quality control tables which form part of the processing history and are retained; it is therefore possible to check on the data of any given run, in case of questionable output. A table of maximum values is also outputted. Caution is necessary when using this table because of the possibility of the vortex magnitude associated with the far wing tip exceeding the normally greater magnitude of the near wing tip vortex. Times associated with vortex hits are outputted to resolve this difficulty.

PII PROGRAM SERIES LOGIC. This FORTRAN IV Program is intended to be run on the IBM 7090 computer. It requires two data channels with one tape unit per channel. Data cards are used to describe various parameters such as sensors to plot scale factors for abscissas and ordinates, number of data points to average per plot point, etc. CII output is inputted to this program. The calibrated data for the various sensors processed appears in serial fashion on this input tape. PII processes up to 3,000 plot point data values for any requested sensor. It then outputs on the plot tape using standard CalComp subroutines. When all required sensors for a given run are processed, the data plotter accepts the plot tape and plots a time history for each sensor.

Programming efficiency dictated a variation in algorithms used to determine maximum tangential velocities in the CII Series and the PII Series of programs. The CII Series operates upon 50 consecutive legal data values while the PII series operates upon legal values contained within 50 consecutive data values. The operation of either program consists of finding the mean data value and checking it against the existing maximum mean data value. When the maximum mean is redefined, its associated time is declared as the median time value associated with the group of data values related to the new maximum mean. If there are no illegal data values, the results of these two algorithms are identical. However, divergence occurs in proportion to the degradation of quality of input data. The quality of input data so far has been high, so this has posed no real problem.

CII PROGRAM MATHEMATICS.

In order to remove spurious values from calibration data, the program performs the following computations on the first 40 records of each file. The first 20 records contain low-calibration values, the next 20 high-calibration values. An indication of the quality of calibration values, and quite probably, test data values also, can be obtained by noting the number of calibration points, N^1, used in the final calculations of $\bar{\bar{X}}_H$ and $\bar{\bar{X}}_L$.

$$\bar{X} = \frac{\Sigma Xc}{N} \qquad \text{Raw mean}$$

$$\bar{\sigma} = \left[\frac{\Sigma X^2c-(\Sigma Xc)^2/N}{N-1}\right]^{1/2} \qquad \text{Raw standard deviation}$$

Where Xc = input tape calibration value (-10V Xc +10V)
N = number of x values (840) - number values in the absence of "0-Bit" errors.

Let the set X^1c values consist of all X values satisfying the criterion

$$\bar{X} - 1\sigma < X_c^1 < \bar{X} + 1\sigma$$

$$\bar{\bar{X}} = \frac{\Sigma X_c^1}{N^1}$$

$$\bar{\bar{\sigma}} = \left[\frac{\Sigma(X^1)^2-(\Sigma X^1)^2/N^1}{N^1-1}\right]^{1/2}$$

$\bar{X}$, $\bar{\sigma}$, $\bar{\bar{X}}$, and $\bar{\bar{\sigma}}$ are calculated separately for both low and high-calibrations. X is used in calibration of data. N^1 and $\bar{\bar{\sigma}}$ are outputted along with $\bar{\bar{X}}$ in processing history.

This routine remains unchanged in all versions of the CII Program.

Test data is calibrated by using a linearized calibration curve. The CII M7 Program uses a segmented curve obtained by reference to 4 point values. This yields three linear sections to approximate the true calibration curve.

Sensor data is calibrated using the following expression:

$$Y = MX + B$$

$$M = (P_H 1/2 - P_L 1/2) / (\bar{\bar{X}}_H^2 - \bar{\bar{X}}_L^2)$$

$$B = P_H 1/2 - M\bar{\bar{X}}_H 1/2$$

Where P_H = Physical value (ft/s) equivalent to high-calibration sensor voltage.

P_L = Physical value (ft/s) equivalent to low-calibration sensor voltage.

$\bar{\bar{X}}_H$ = CENDAR voltage representation (volts) of high-calibration sensor voltage.

$\bar{\bar{X}}_L$ = CENDAR voltage representation of low-calibration sensor voltage.

APPENDIX C

TANGENTIAL VELOCITY DISTRIBUTIONS

NOTE: Ambient wind speeds quoted are the 100 foot mean values from appendix F, except when parenthesized - these values are from backup instrumentation located on tower at 140 feet AGL. They are "spot" readings taken approximately at the time the airplane passed the tower.

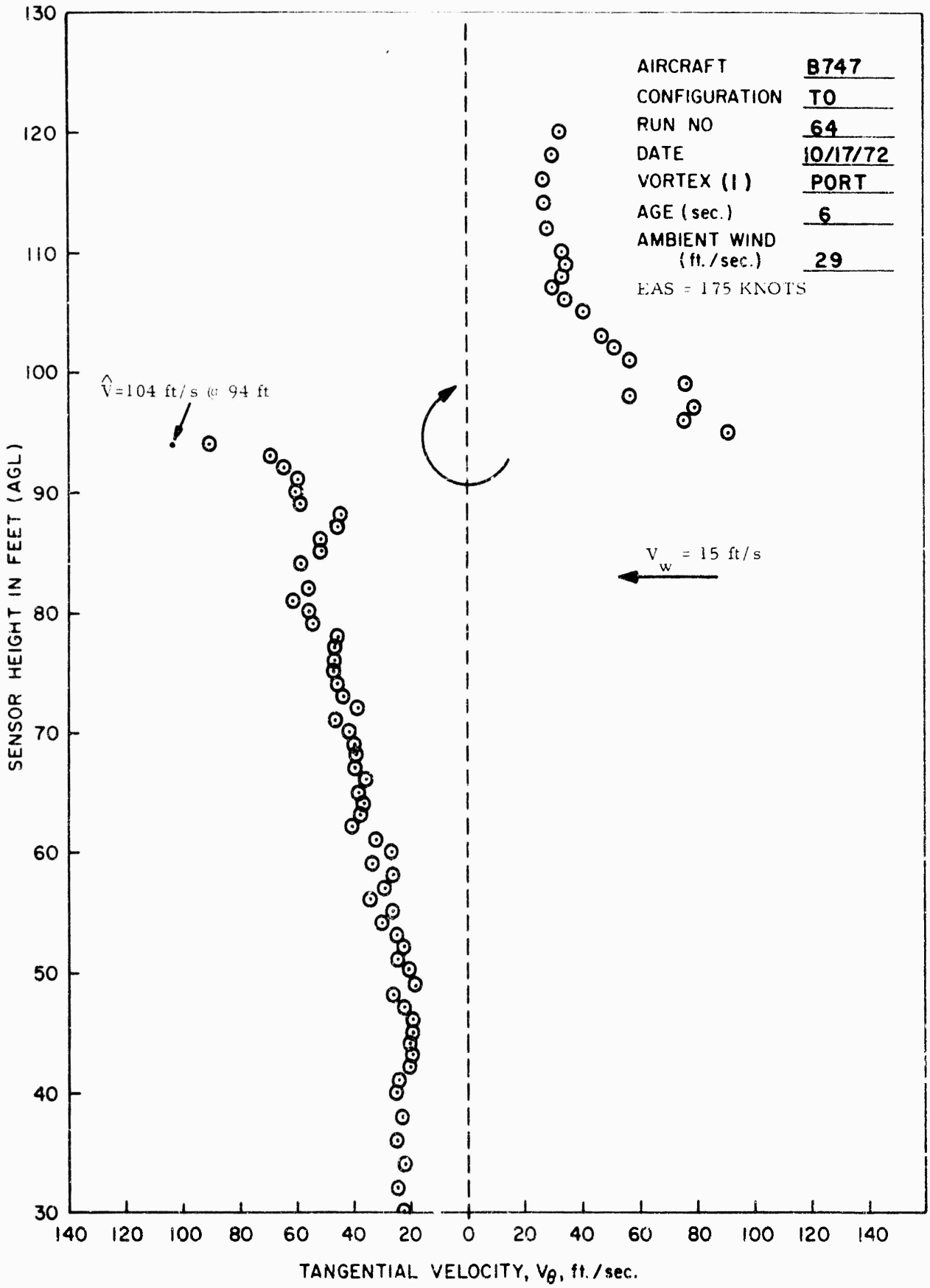
AIRCRAFT B747
CONFIGURATION TO
RUN NO 64
DATE 10/17/72
VORTEX (1) PORT
AGE (sec.) 6
AMBIENT WIND (ft./sec.) 29
EAS = 175 KNOTS
$\hat{V}$=104 ft/s @ 94 ft
V_w = 15 ft/s
SENSOR HEIGHT IN FEET (AGL)
130
120
110
100
90
80
70
60
50
40
30
140 120 100 80 60 40 20 0 20 40 60 80 100 120 140
TANGENTIAL VELOCITY, V_θ, ft./sec.

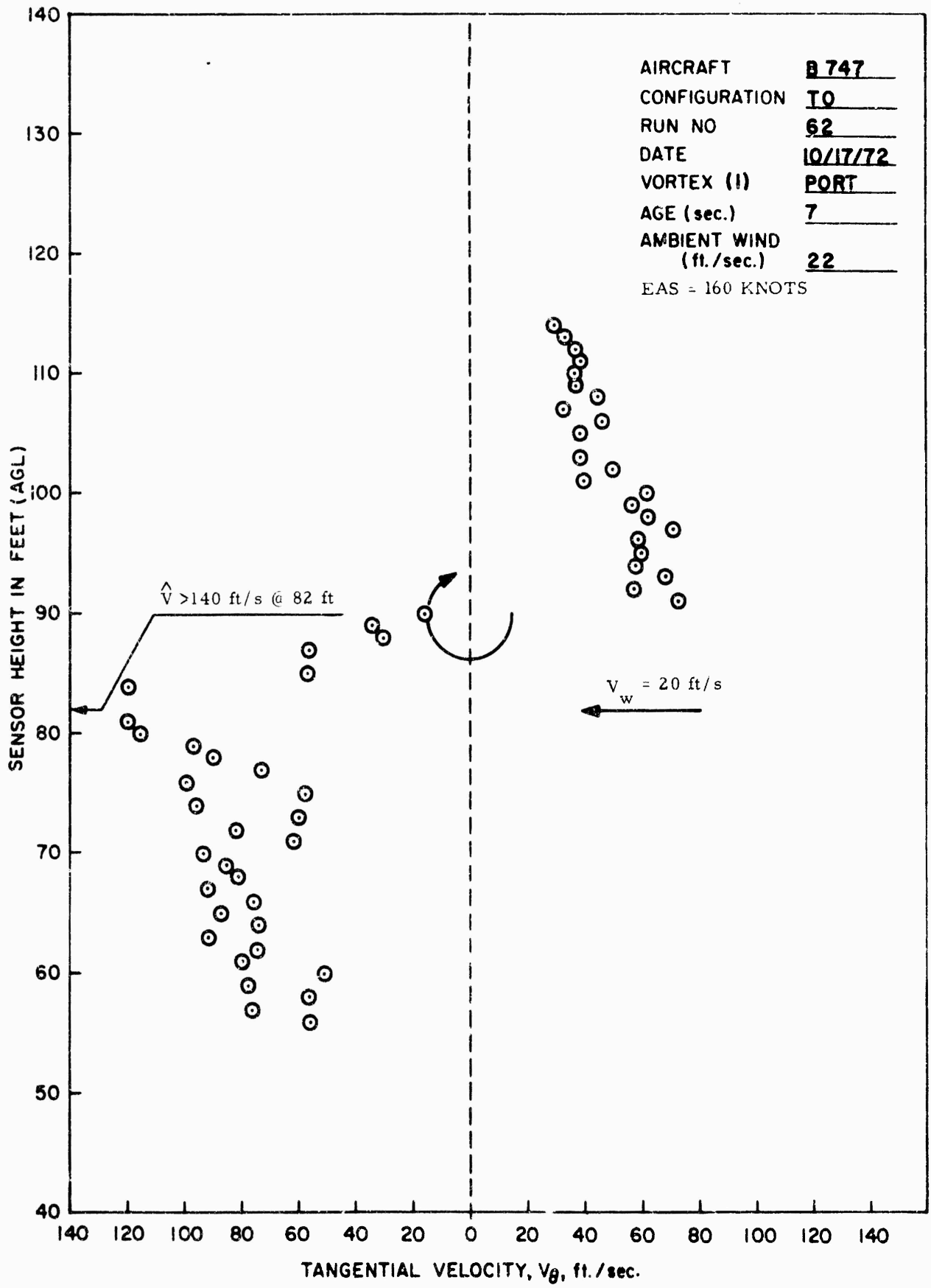
AIRCRAFT B 747
CONFIGURATION TO
RUN NO 62
DATE 10/17/72
VORTEX (1) PORT
AGE (sec.) 7
AMBIENT WIND (ft./sec.) 22
EAS = 160 KNOTS
$\hat{V}$ >140 ft/s @ 82 ft
V_w = 20 ft/s
SENSOR HEIGHT IN FEET (AGL)
TANGENTIAL VELOCITY, V_θ, ft./sec.
140
130
120
110
100
90
80
70
60
50
40
140 120 100 80 60 40 20 0 20 40 60 80 100 120 140

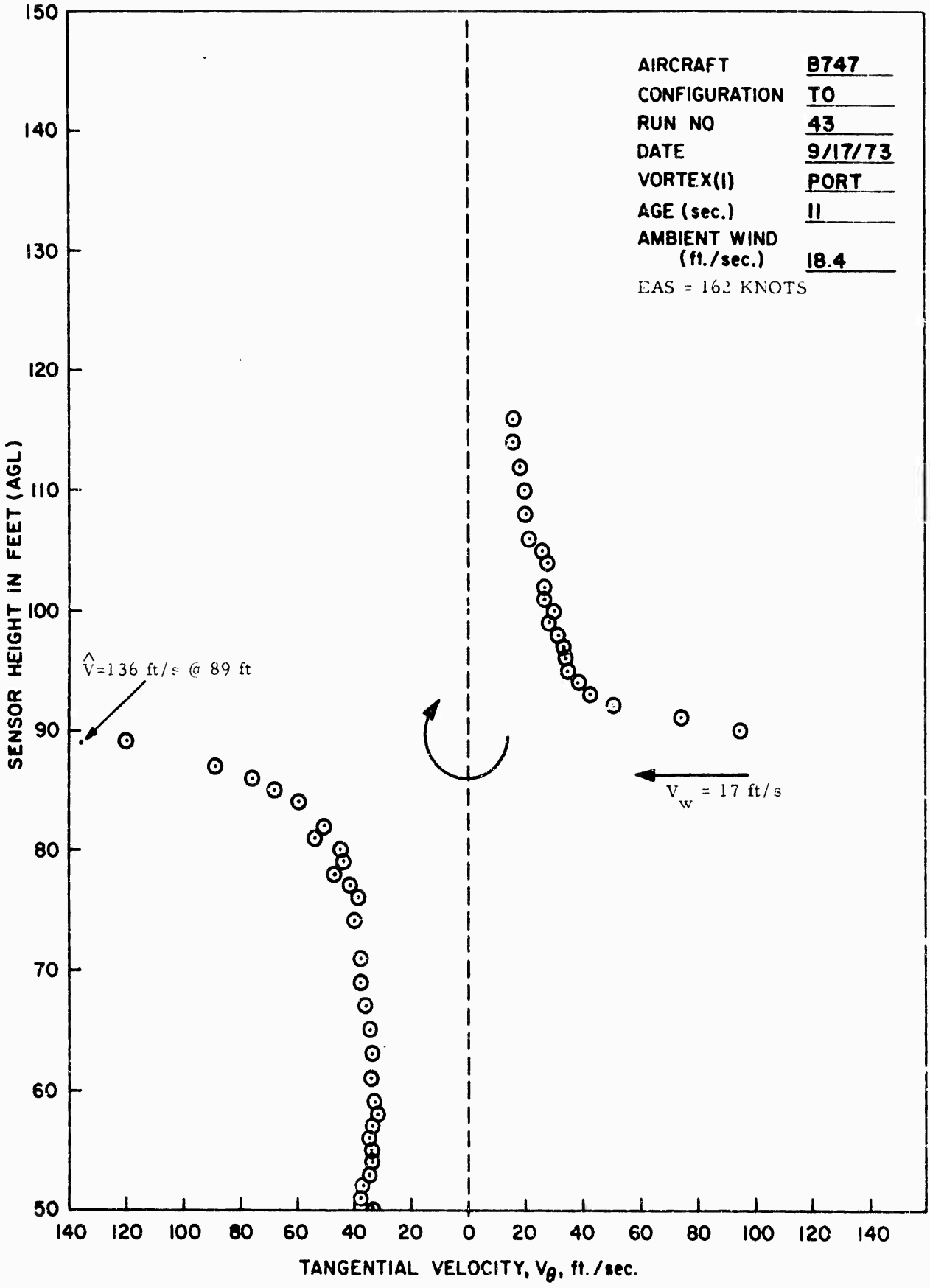
AIRCRAFT B747
CONFIGURATION TO
RUN NO 43
DATE 9/17/73
VORTEX(I) PORT
AGE (sec.) 11
AMBIENT WIND (ft./sec.) 18.4
EAS = 162 KNOTS
$\hat{V}$=136 ft/s @ 89 ft
V_w = 17 ft/s
SENSOR HEIGHT IN FEET (AGL)
150
140
130
120
110
100
90
80
70
60
50
140 120 100 80 60 40 20 0 20 40 60 80 100 120 140
TANGENTIAL VELOCITY, V_θ, ft./sec.

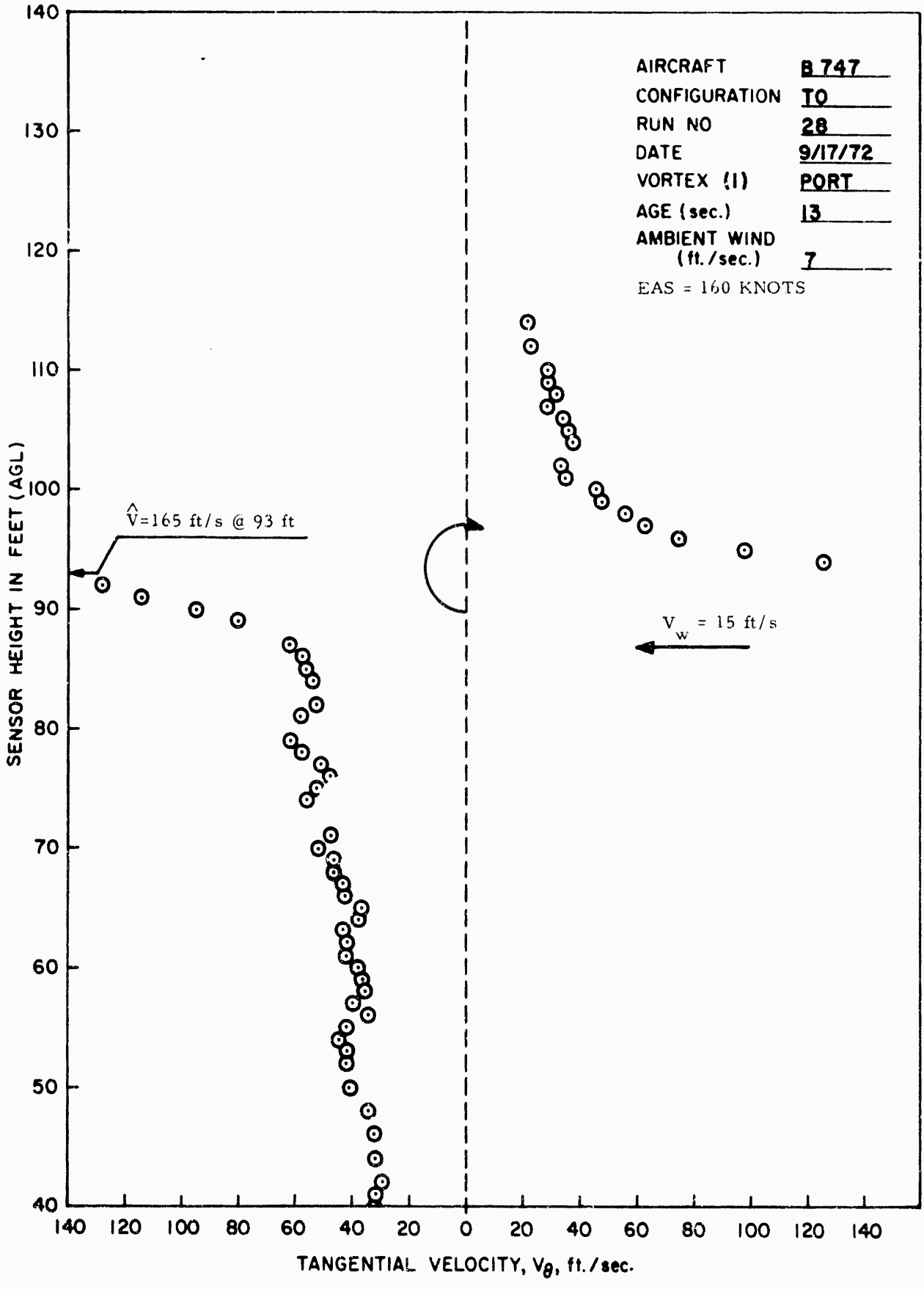
AIRCRAFT B 747
CONFIGURATION TO
RUN NO 28
DATE 9/17/72
VORTEX (1) PORT
AGE (sec.) 13
AMBIENT WIND (ft./sec.) 7
EAS = 160 KNOTS
$\hat{V}$=165 ft/s @ 93 ft
V_w = 15 ft/s
SENSOR HEIGHT IN FEET (AGL)
140
130
120
110
100
90
80
70
60
50
40
140 120 100 80 60 40 20 0 20 40 60 80 100 120 140
TANGENTIAL VELOCITY, V_θ, ft./sec.

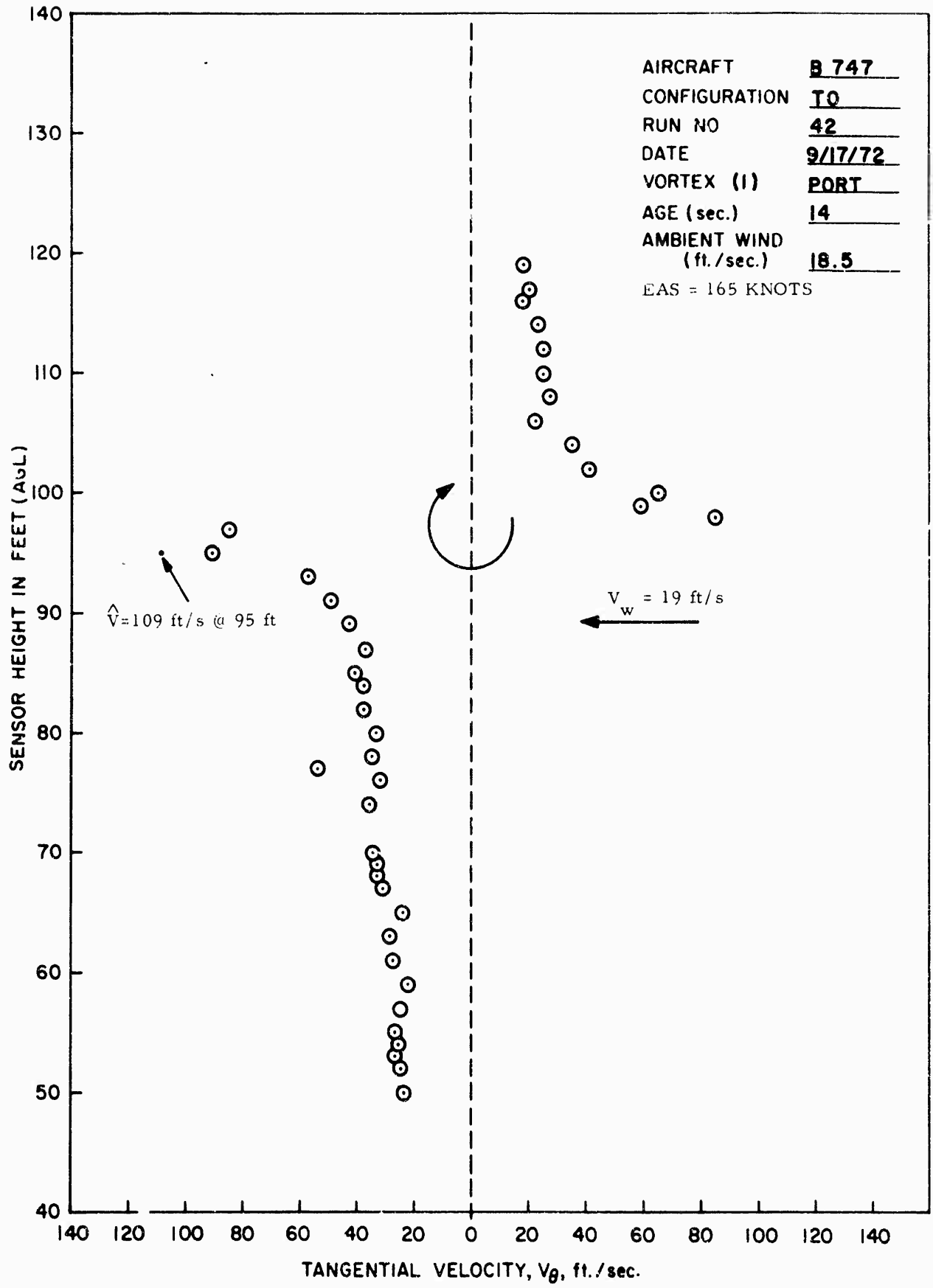
AIRCRAFT B 747
CONFIGURATION TO
RUN NO 42
DATE 9/17/72
VORTEX (1) PORT
AGE (sec.) 14
AMBIENT WIND (ft./sec.) 18.5
EAS = 165 KNOTS
$\hat{V}$=109 ft/s @ 95 ft
V_w = 19 ft/s
SENSOR HEIGHT IN FEET (AGL)
TANGENTIAL VELOCITY, V_θ, ft./sec.
140
130
120
110
100
90
80
70
60
50
40
140 120 100 80 60 40 20 0 20 40 60 80 100 120 140

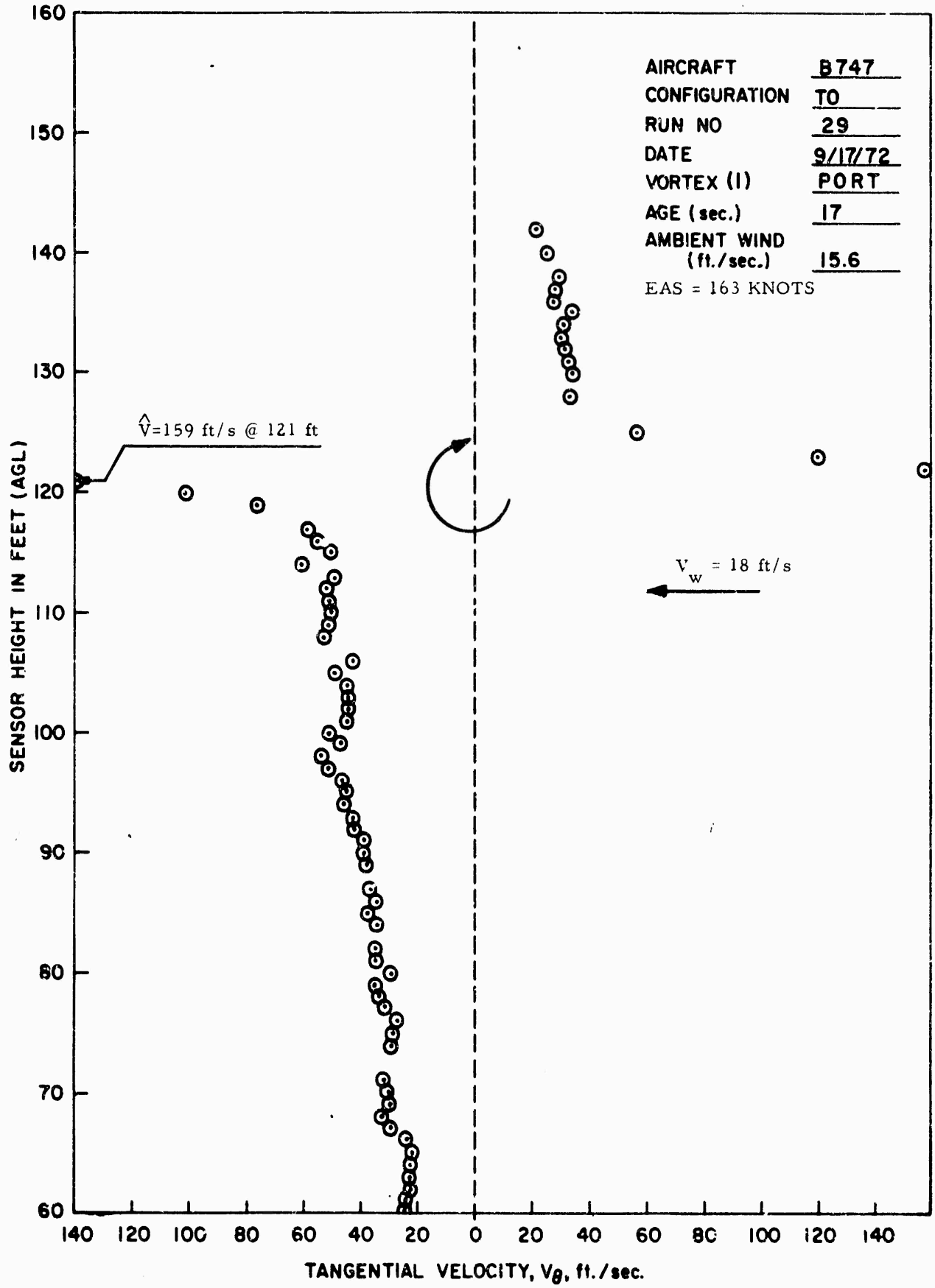
AIRCRAFT B747
CONFIGURATION TO
RUN NO 29
DATE 9/17/72
VORTEX (1) PORT
AGE (sec.) 17
AMBIENT WIND (ft./sec.) 15.6
EAS = 163 KNOTS
$\hat{V}$=159 ft/s @ 121 ft
V_w = 18 ft/s
SENSOR HEIGHT IN FEET (AGL)
160
150
140
130
120
110
100
90
80
70
60
140 120 100 80 60 40 20 0 20 40 60 80 100 120 140
TANGENTIAL VELOCITY, V_θ, ft./sec.

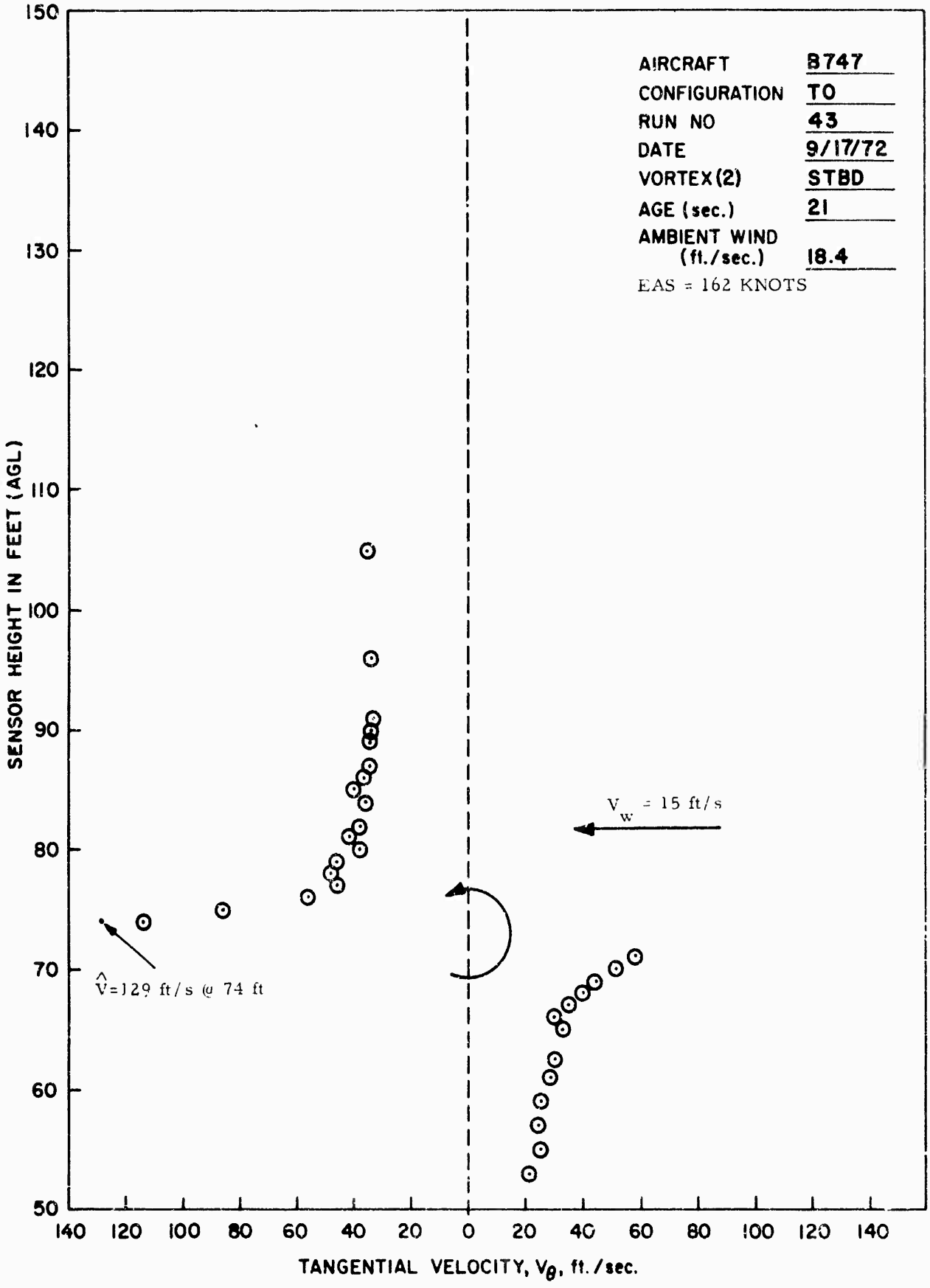
AIRCRAFT B747
CONFIGURATION TO
RUN NO 43
DATE 9/17/72
VORTEX(2) STBD
AGE (sec.) 21
AMBIENT WIND (ft./sec.) 18.4
EAS = 162 KNOTS
V_w = 15 ft/s
$\hat{V}$=129 ft/s @ 74 ft
SENSOR HEIGHT IN FEET (AGL)
150
140
130
120
110
100
90
80
70
60
50
140 120 100 80 60 40 20 0 20 40 60 80 100 120 140
TANGENTIAL VELOCITY, V_θ, ft./sec.

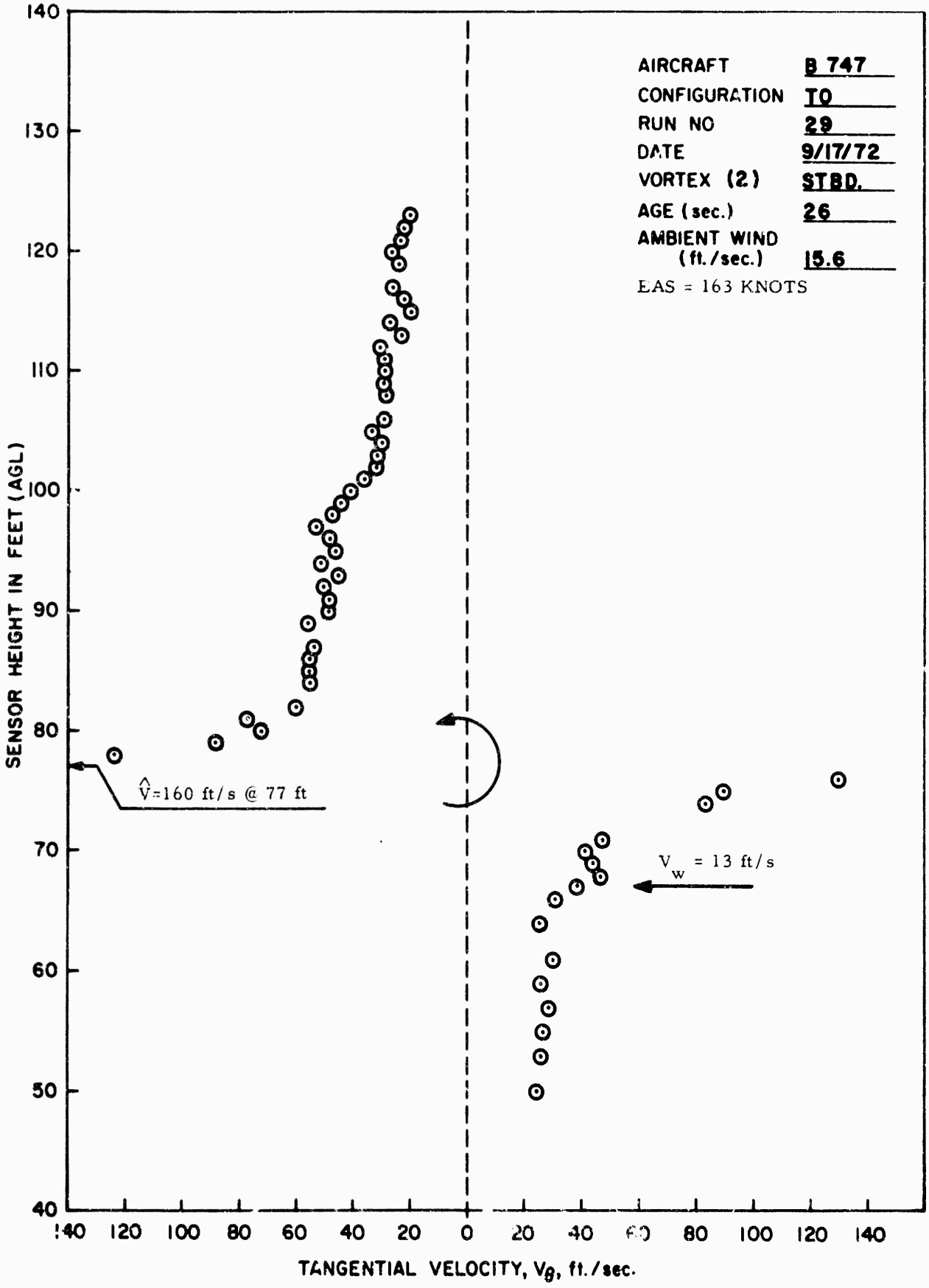
AIRCRAFT B 747
CONFIGURATION TO
RUN NO 29
DATE 9/17/72
VORTEX (2) STBD.
AGE (sec.) 26
AMBIENT WIND (ft./sec.) 15.6
EAS = 163 KNOTS
SENSOR HEIGHT IN FEET (AGL)
140
130
120
110
100
90
80
70
60
50
40
V̂=160 ft/s @ 77 ft
V_w = 13 ft/s
140 120 100 80 60 40 20 0 20 40 60 80 100 120 140
TANGENTIAL VELOCITY, V_θ, ft./sec.

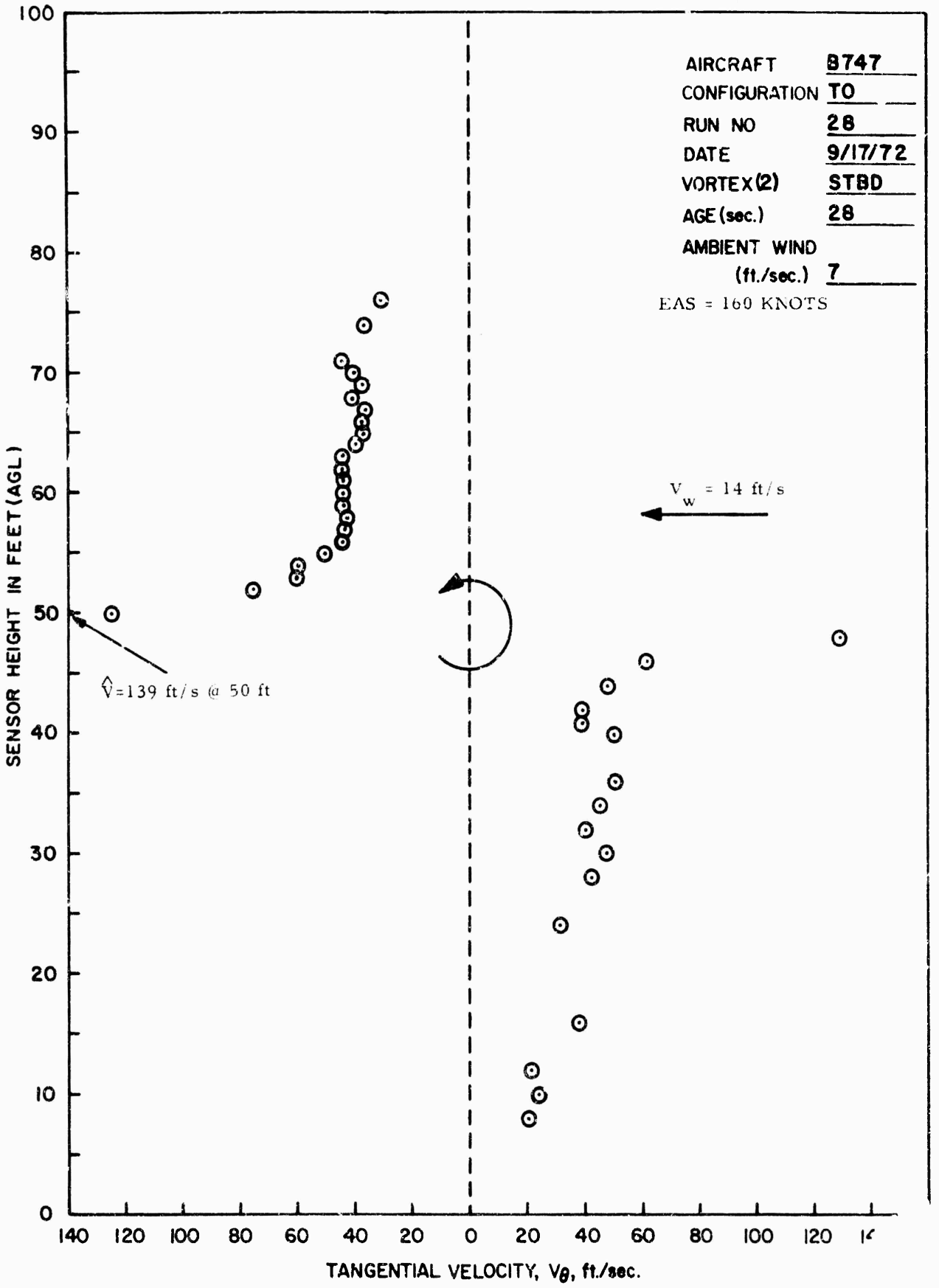
AIRCRAFT B747
CONFIGURATION TO
RUN NO 28
DATE 9/17/72
VORTEX(2) STBD
AGE(sec.) 28
AMBIENT WIND (ft./sec.) 7
EAS = 160 KNOTS
V_w = 14 ft/s
$\hat{V}$=139 ft/s @ 50 ft
SENSOR HEIGHT IN FEET(AGL)
TANGENTIAL VELOCITY, V_θ, ft./sec.
100
90
80
70
60
50
40
30
20
10
0
140
120
100
80
60
40
20
0
20
40
60
80
100
120

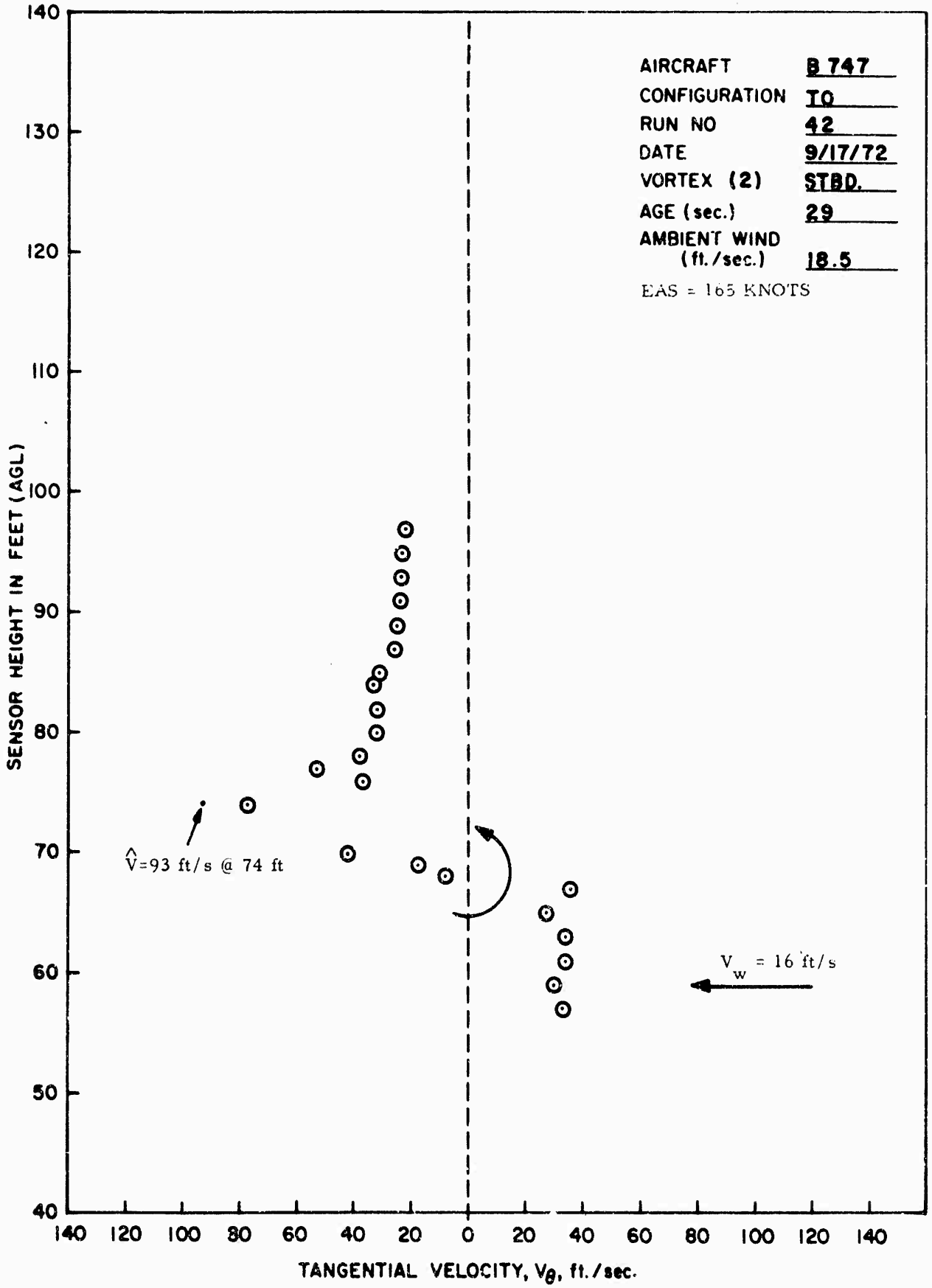
AIRCRAFT B 747
CONFIGURATION TO
RUN NO 42
DATE 9/17/72
VORTEX (2) STBD.
AGE (sec.) 29
AMBIENT WIND (ft./sec.) 18.5
EAS = 165 KNOTS
SENSOR HEIGHT IN FEET (AGL)
140
130
120
110
100
90
80
70
60
50
40
$\hat{V}$=93 ft/s @ 74 ft
V_w = 16 ft/s
140 120 100 80 60 40 20 0 20 40 60 80 100 120 140
TANGENTIAL VELOCITY, V_θ, ft./sec.

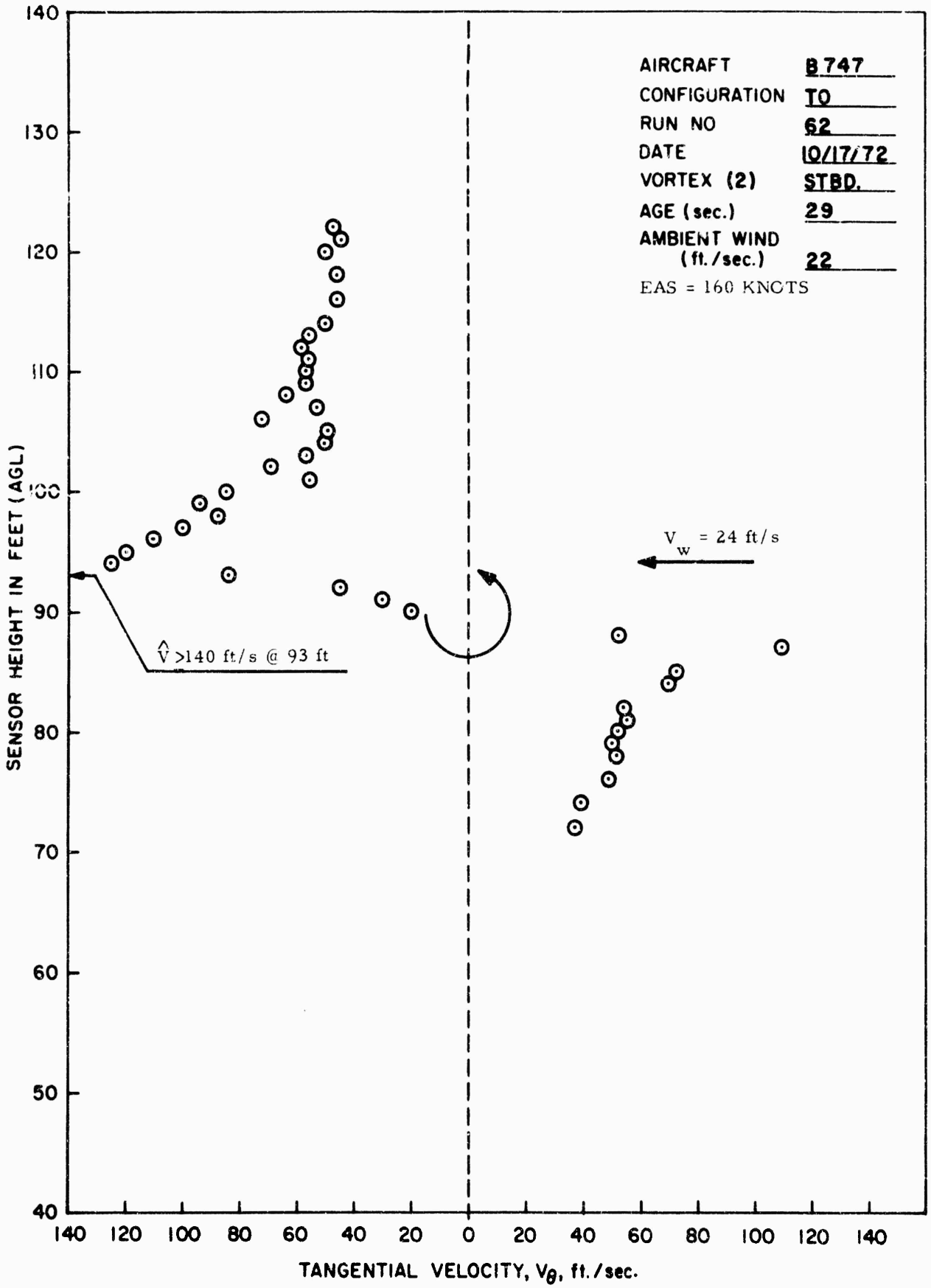
AIRCRAFT B 747
CONFIGURATION TO
RUN NO 62
DATE 10/17/72
VORTEX (2) STBD.
AGE (sec.) 29
AMBIENT WIND (ft./sec.) 22
EAS = 160 KNOTS
V_w = 24 ft/s
$\hat{V}$ >140 ft/s @ 93 ft
SENSOR HEIGHT IN FEET (AGL)
140
130
120
110
100
90
80
70
60
50
40
140 120 100 80 60 40 20 0 20 40 60 80 100 120 140
TANGENTIAL VELOCITY, V_θ, ft./sec.

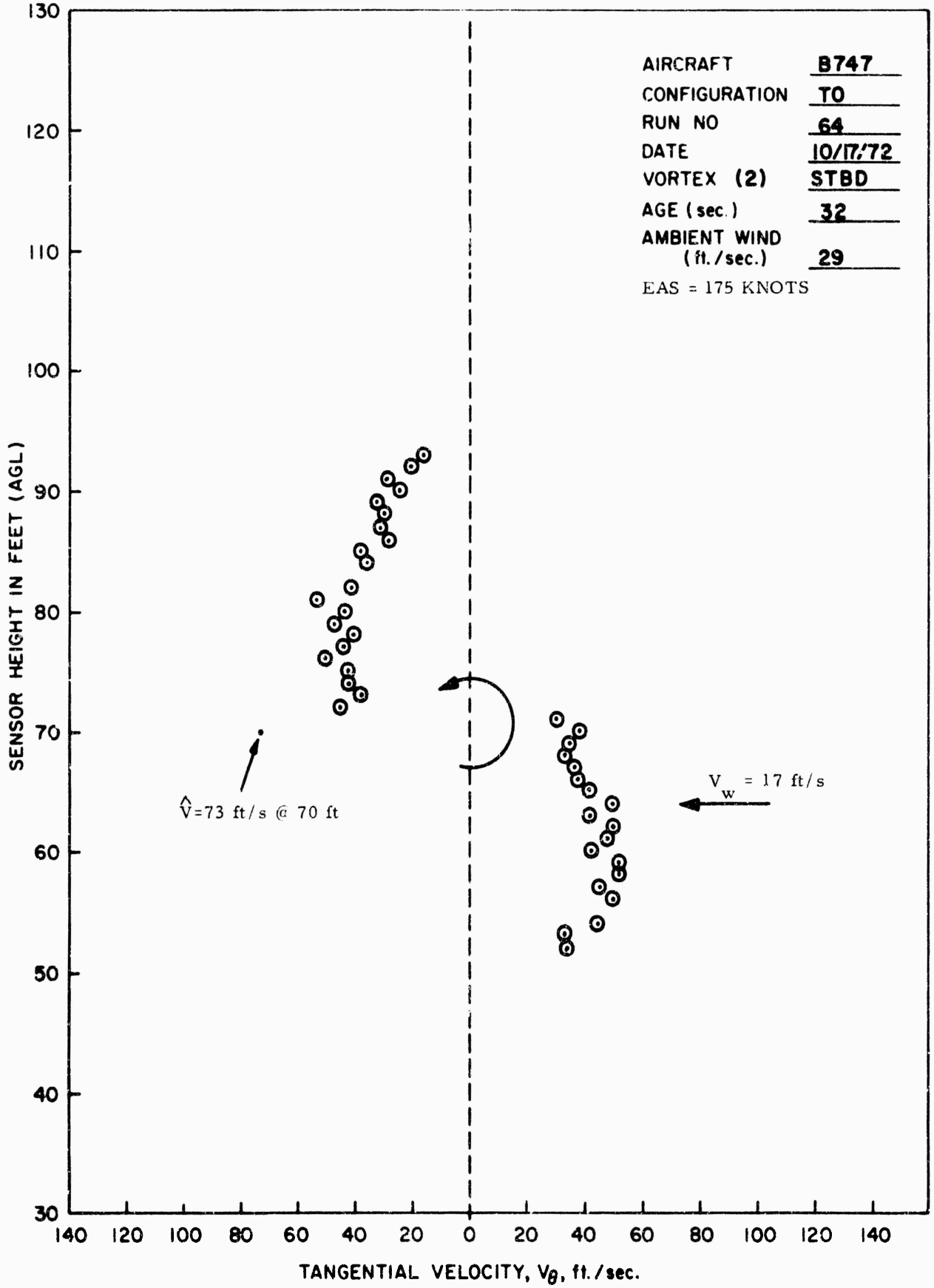
AIRCRAFT B747
CONFIGURATION TO
RUN NO 64
DATE 10/17/72
VORTEX (2) STBD
AGE (sec.) 32
AMBIENT WIND (ft./sec.) 29
EAS = 175 KNOTS
SENSOR HEIGHT IN FEET (AGL)
130
120
110
100
90
80
70
60
50
40
30
140 120 100 80 60 40 20 0 20 40 60 80 100 120 140
TANGENTIAL VELOCITY, V_θ, ft./sec.
$\hat{V}$=73 ft/s @ 70 ft
V_w = 17 ft/s

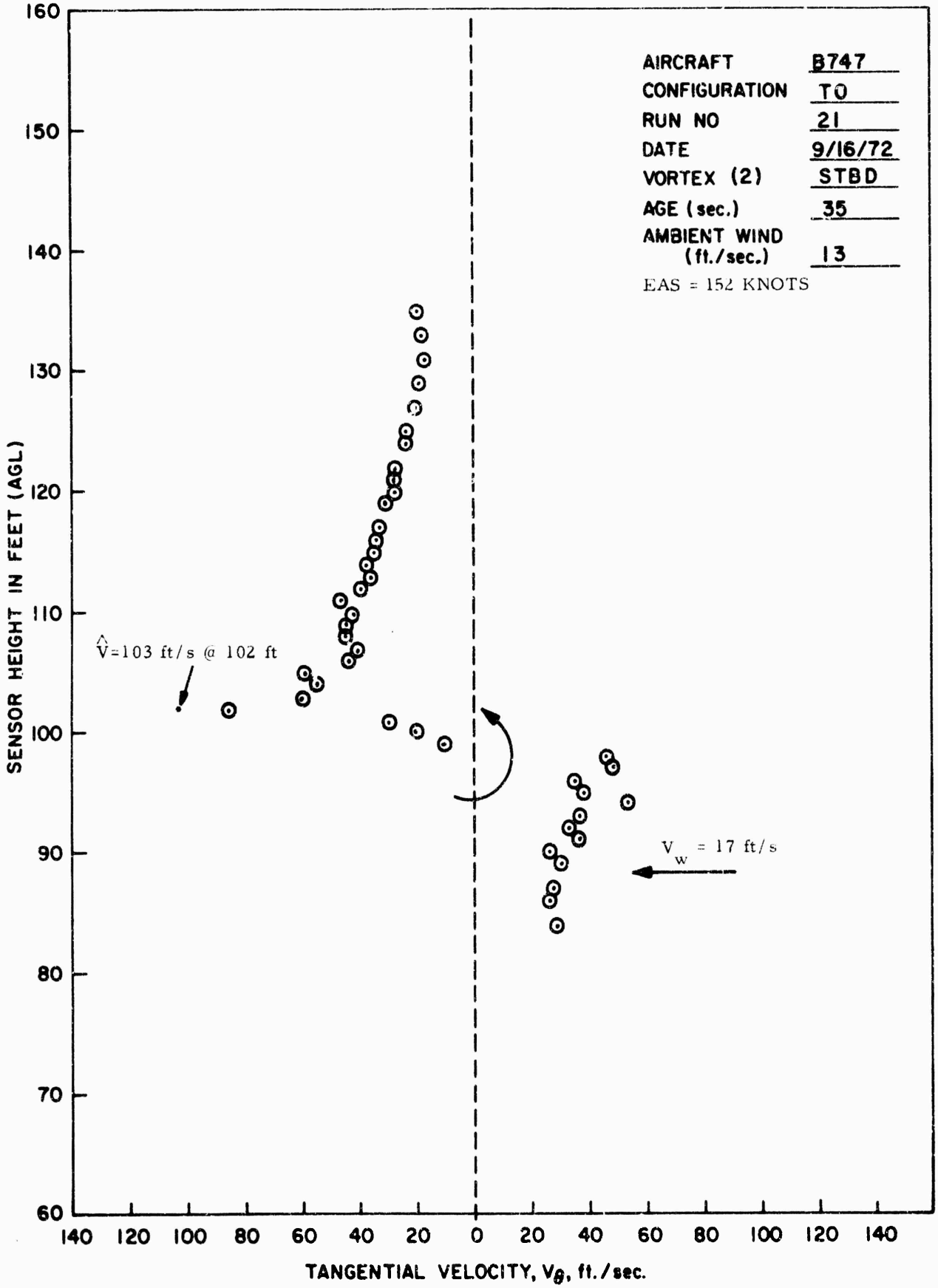
AIRCRAFT B747
CONFIGURATION TO
RUN NO 21
DATE 9/16/72
VORTEX (2) STBD
AGE (sec.) 35
AMBIENT WIND (ft./sec.) 13
EAS = 152 KNOTS
$\hat{V}$=103 ft/s @ 102 ft
V_w = 17 ft/s
SENSOR HEIGHT IN FEET (AGL)
TANGENTIAL VELOCITY, V_θ, ft./sec.
160
150
140
130
120
110
100
90
80
70
60
140 120 100 80 60 40 20 0 20 40 60 80 100 120 140

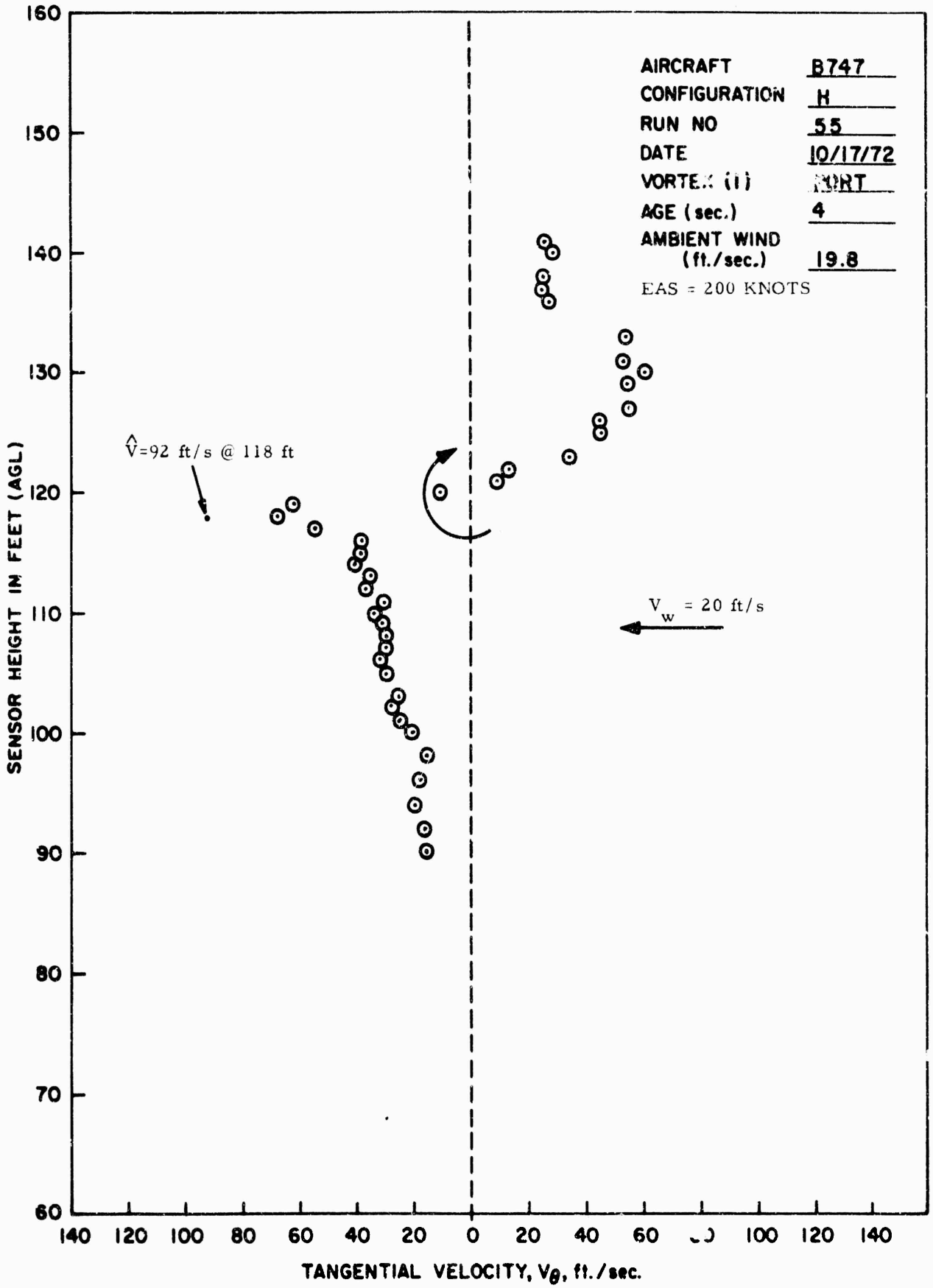
AIRCRAFT B747
CONFIGURATION H
RUN NO 55
DATE 10/17/72
VORTEX (1) PORT
AGE (sec.) 4
AMBIENT WIND (ft./sec.) 19.8
EAS = 200 KNOTS
$\hat{V}$=92 ft/s @ 118 ft
V_w = 20 ft/s
SENSOR HEIGHT IN FEET (AGL)
160
150
140
130
120
110
100
90
80
70
60
140 120 100 80 60 40 20 0 20 40 60 80 100 120 140
TANGENTIAL VELOCITY, V_θ, ft./sec.

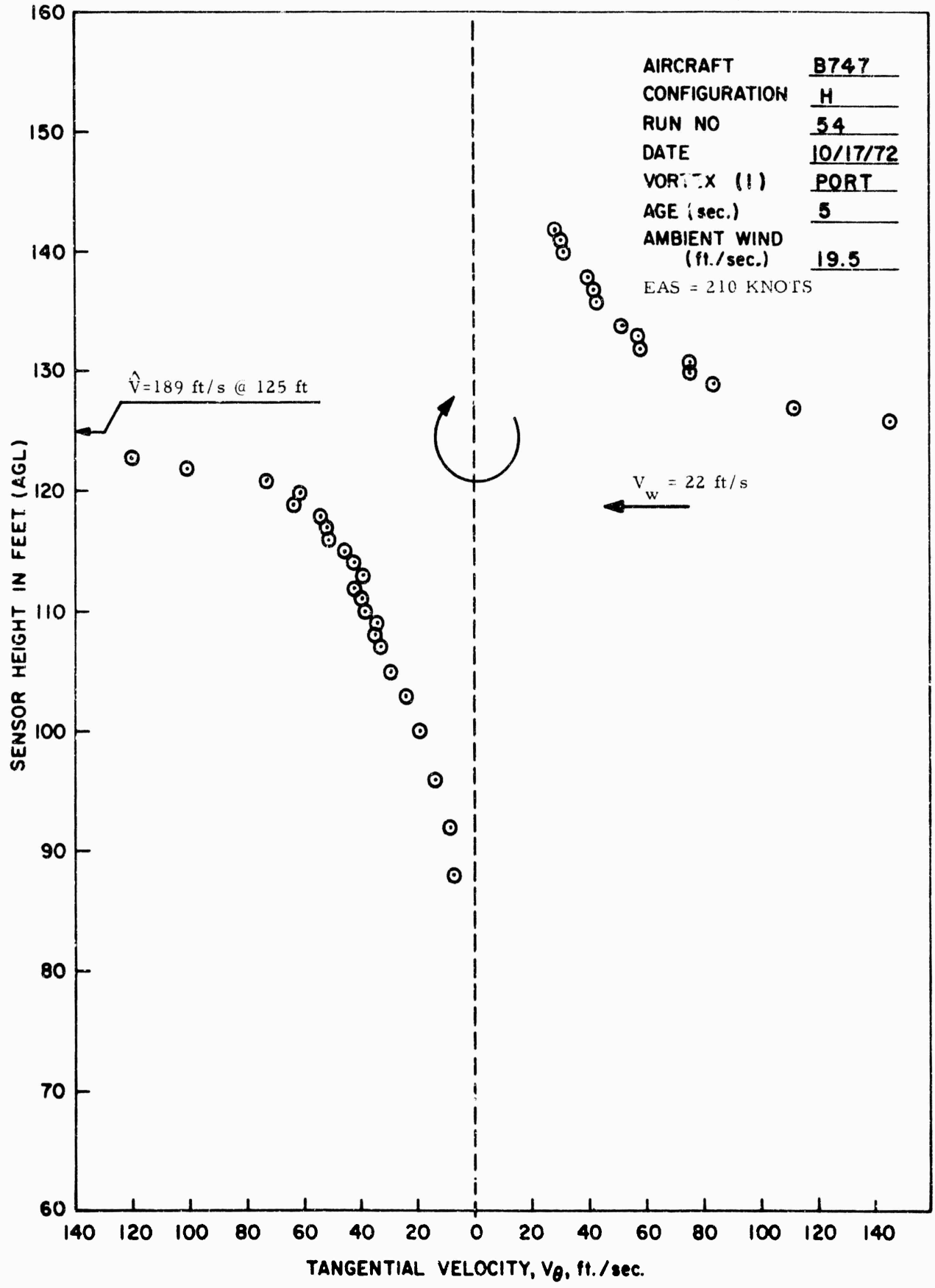
AIRCRAFT B747
CONFIGURATION H
RUN NO 54
DATE 10/17/72
VORTEX (1) PORT
AGE (sec.) 5
AMBIENT WIND (ft./sec.) 19.5
EAS = 210 KNOTS
$\hat{V}$=189 ft/s @ 125 ft
V_w = 22 ft/s
SENSOR HEIGHT IN FEET (AGL)
160
150
140
130
120
110
100
90
80
70
60
140 120 100 80 60 40 20 0 20 40 60 80 100 120 140
TANGENTIAL VELOCITY, V_θ, ft./sec.

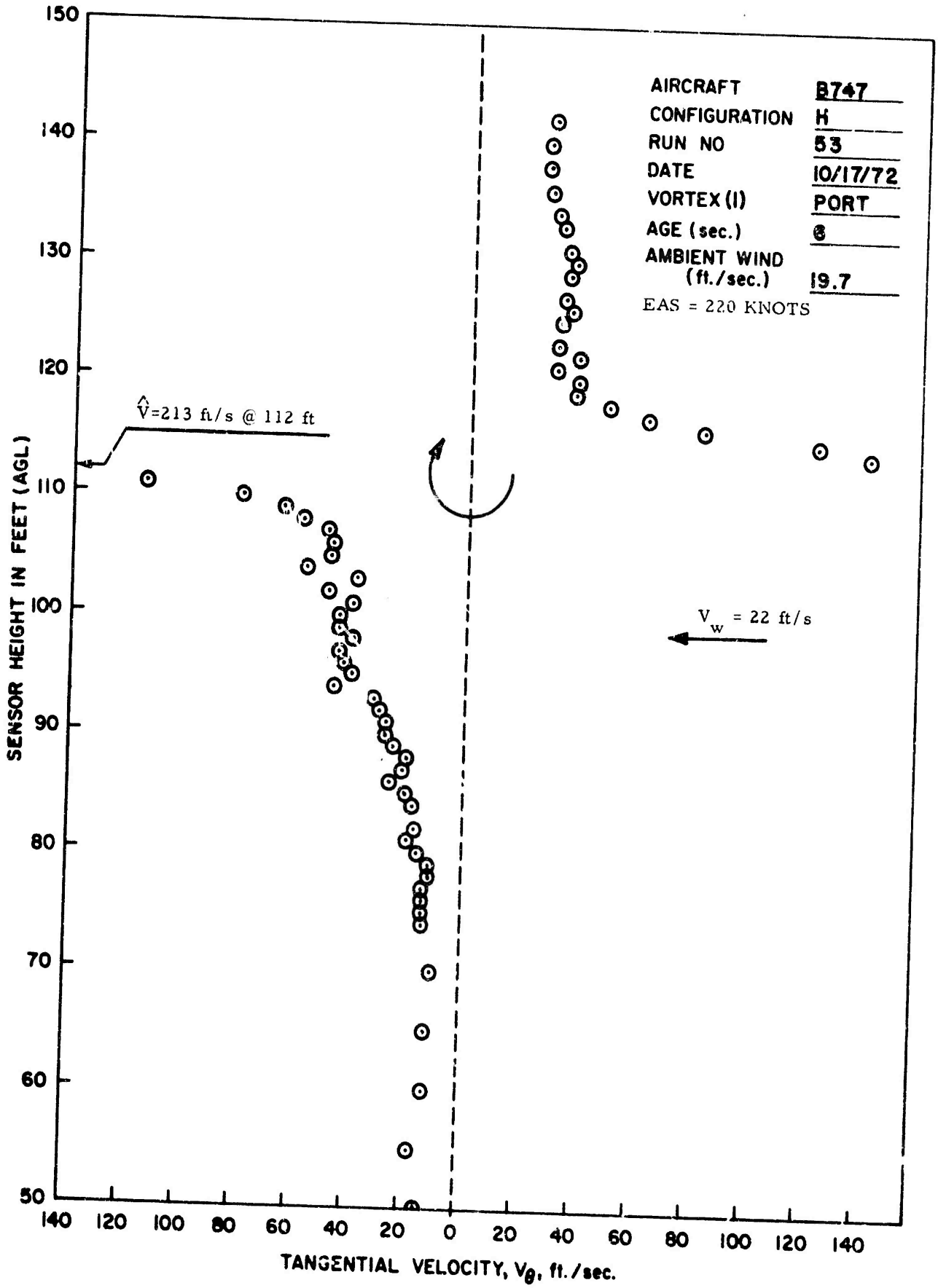
AIRCRAFT B747
CONFIGURATION H
RUN NO 53
DATE 10/17/72
VORTEX (I) PORT
AGE (sec.) 8
AMBIENT WIND (ft./sec.) 19.7
EAS = 220 KNOTS
$\hat{V}$=213 ft/s @ 112 ft
V_w = 22 ft/s
SENSOR HEIGHT IN FEET (AGL)
150
140
130
120
110
100
90
80
70
60
50
140 120 100 80 60 40 20 0 20 40 60 80 100 120 140
TANGENTIAL VELOCITY, V_θ, ft./sec.

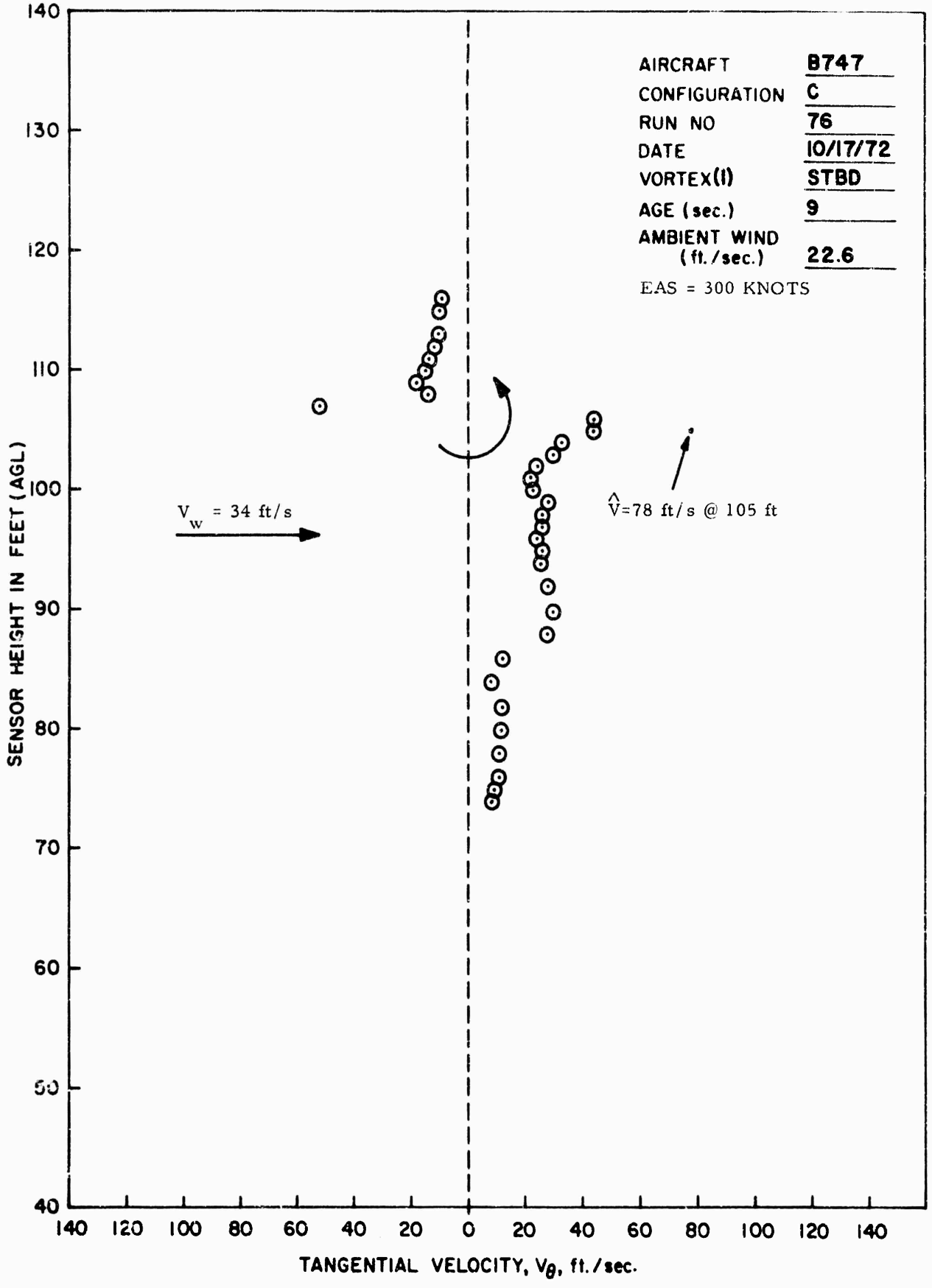
AIRCRAFT B747
CONFIGURATION C
RUN NO 76
DATE 10/17/72
VORTEX(1) STBD
AGE (sec.) 9
AMBIENT WIND (ft./sec.) 22.6
EAS = 300 KNOTS
V_w = 34 ft/s
$\hat{V}$=78 ft/s @ 105 ft
SENSOR HEIGHT IN FEET (AGL)
140
130
120
110
100
90
80
70
60
50
40
140 120 100 80 60 40 20 0 20 40 60 80 100 120 140
TANGENTIAL VELOCITY, V_θ, ft./sec.

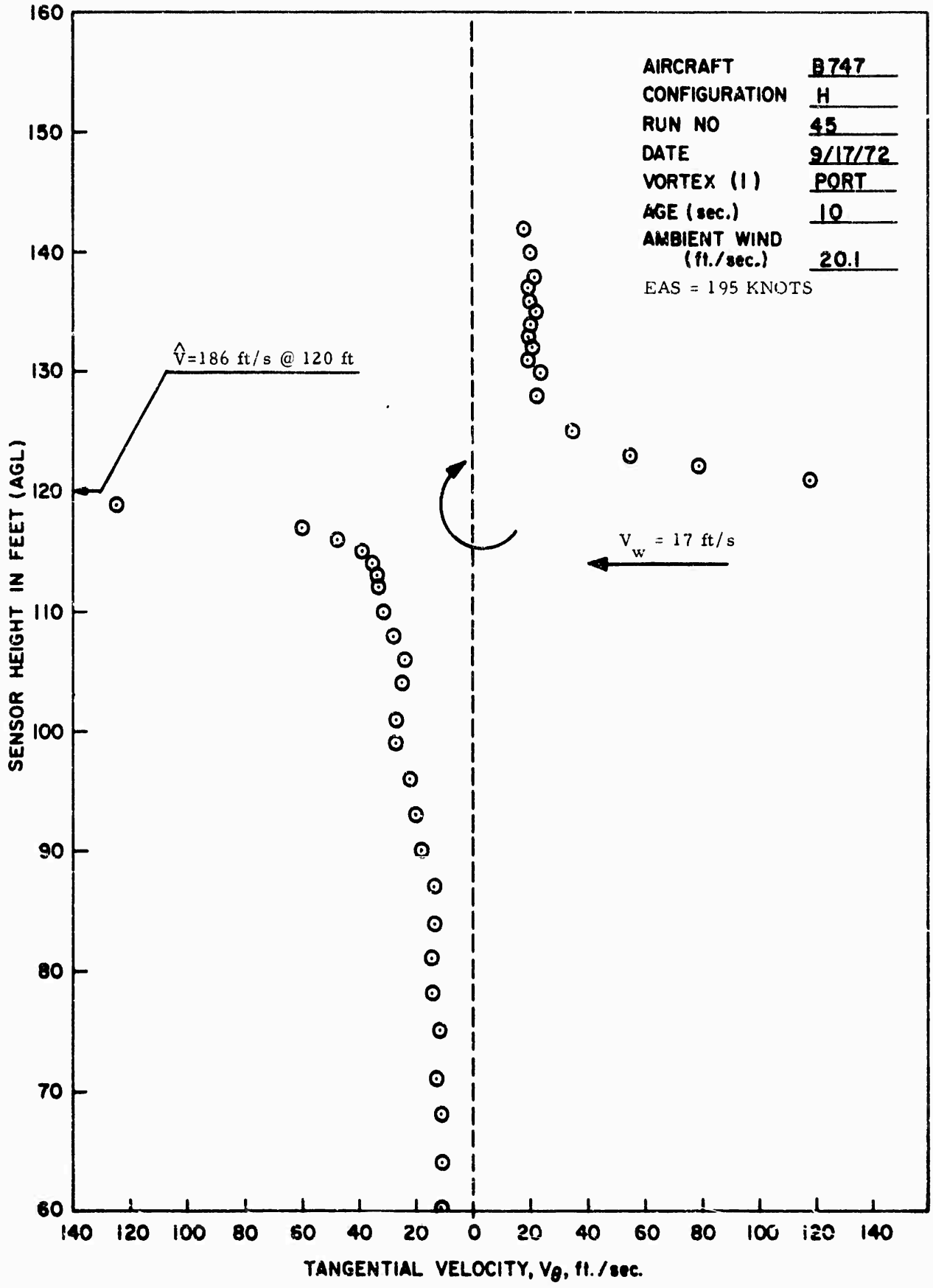
AIRCRAFT B747
CONFIGURATION H
RUN NO 45
DATE 9/17/72
VORTEX (1) PORT
AGE (sec.) 10
AMBIENT WIND (ft./sec.) 20.1
EAS = 195 KNOTS
$\hat{V}$=186 ft/s @ 120 ft
V_w = 17 ft/s
SENSOR HEIGHT IN FEET (AGL)
160
150
140
130
120
110
100
90
80
70
60
140 120 100 80 60 40 20 0 20 40 60 80 100 120 140
TANGENTIAL VELOCITY, V_θ, ft./sec.

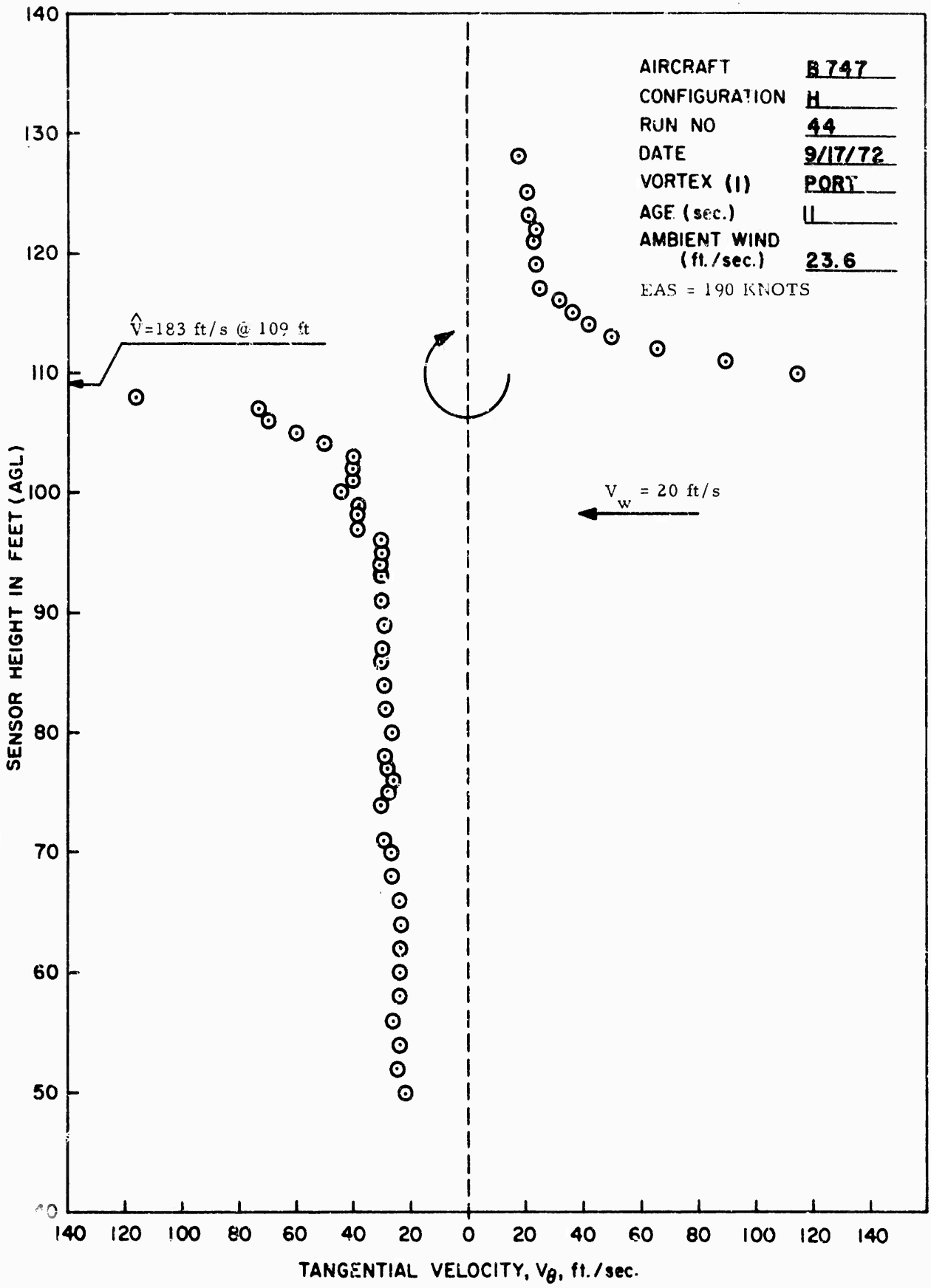
AIRCRAFT B 747
CONFIGURATION H
RUN NO 44
DATE 9/17/72
VORTEX (1) PORT
AGE (sec.) 11
AMBIENT WIND (ft./sec.) 23.6
EAS = 190 KNOTS
$\hat{V}$=183 ft/s @ 109 ft
V_w = 20 ft/s
SENSOR HEIGHT IN FEET (AGL)
TANGENTIAL VELOCITY, V_θ, ft./sec.
140
130
120
110
100
90
80
70
60
50
40
140 120 100 80 60 40 20 0 20 40 60 80 100 120 140

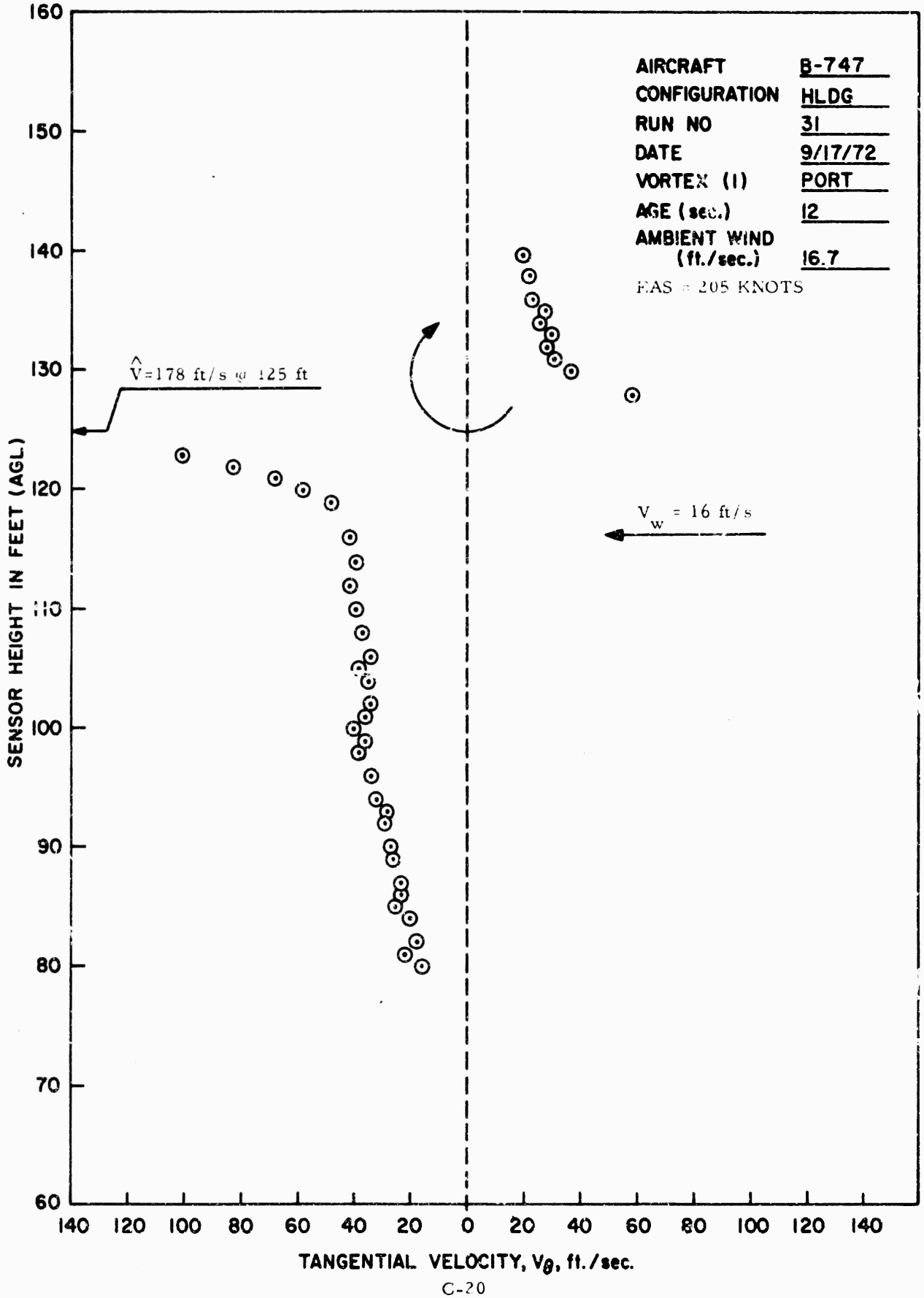
AIRCRAFT B-747
CONFIGURATION HLDG
RUN NO 31
DATE 9/17/72
VORTEX (1) PORT
AGE (sec.) 12
AMBIENT WIND (ft./sec.) 16.7
EAS = 205 KNOTS
$\hat{V}$=178 ft/s @ 125 ft
V_w = 16 ft/s
SENSOR HEIGHT IN FEET (AGL)
160
150
140
130
120
110
100
90
80
70
60
140 120 100 80 60 40 20 0 20 40 60 80 100 120 140
TANGENTIAL VELOCITY, V_θ, ft./sec.

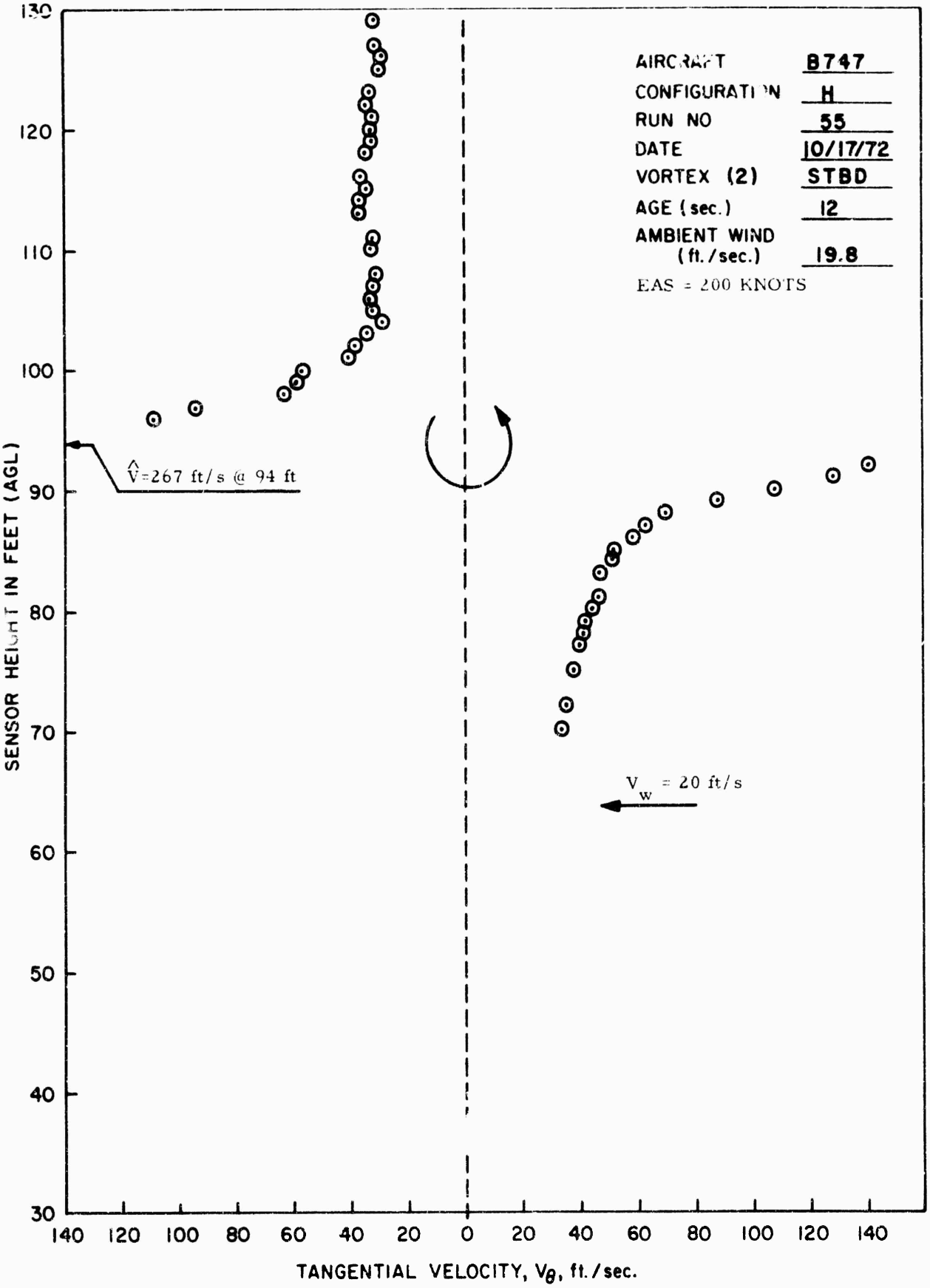
AIRCRAFT B747
CONFIGURATION H
RUN NO 55
DATE 10/17/72
VORTEX (2) STBD
AGE (sec.) 12
AMBIENT WIND (ft./sec.) 19.8
EAS = 200 KNOTS
$\hat{V}$=267 ft/s @ 94 ft
V_w = 20 ft/s
SENSOR HEIGHT IN FEET (AGL)
TANGENTIAL VELOCITY, V_θ, ft./sec.
130
120
110
100
90
80
70
60
50
40
30
140 120 100 80 60 40 20 0 20 40 60 80 100 120 140

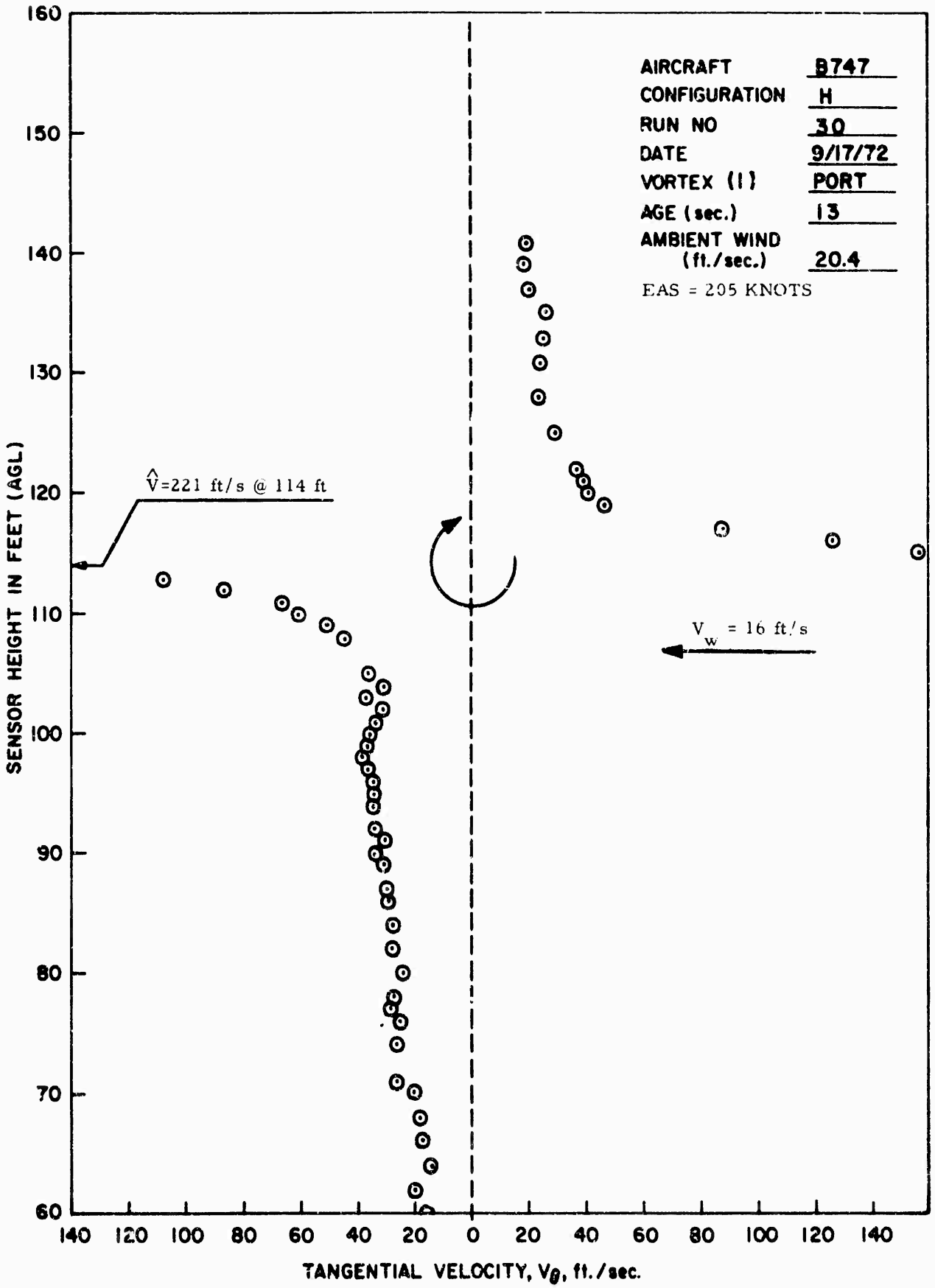
AIRCRAFT B747
CONFIGURATION H
RUN NO 30
DATE 9/17/72
VORTEX (1) PORT
AGE (sec.) 13
AMBIENT WIND (ft./sec.) 20.4
EAS = 205 KNOTS
$\hat{V}$=221 ft/s @ 114 ft
V_w = 16 ft/s
SENSOR HEIGHT IN FEET (AGL)
160
150
140
130
120
110
100
90
80
70
60
140 120 100 80 60 40 20 0 20 40 60 80 100 120 140
TANGENTIAL VELOCITY, V_θ, ft./sec.

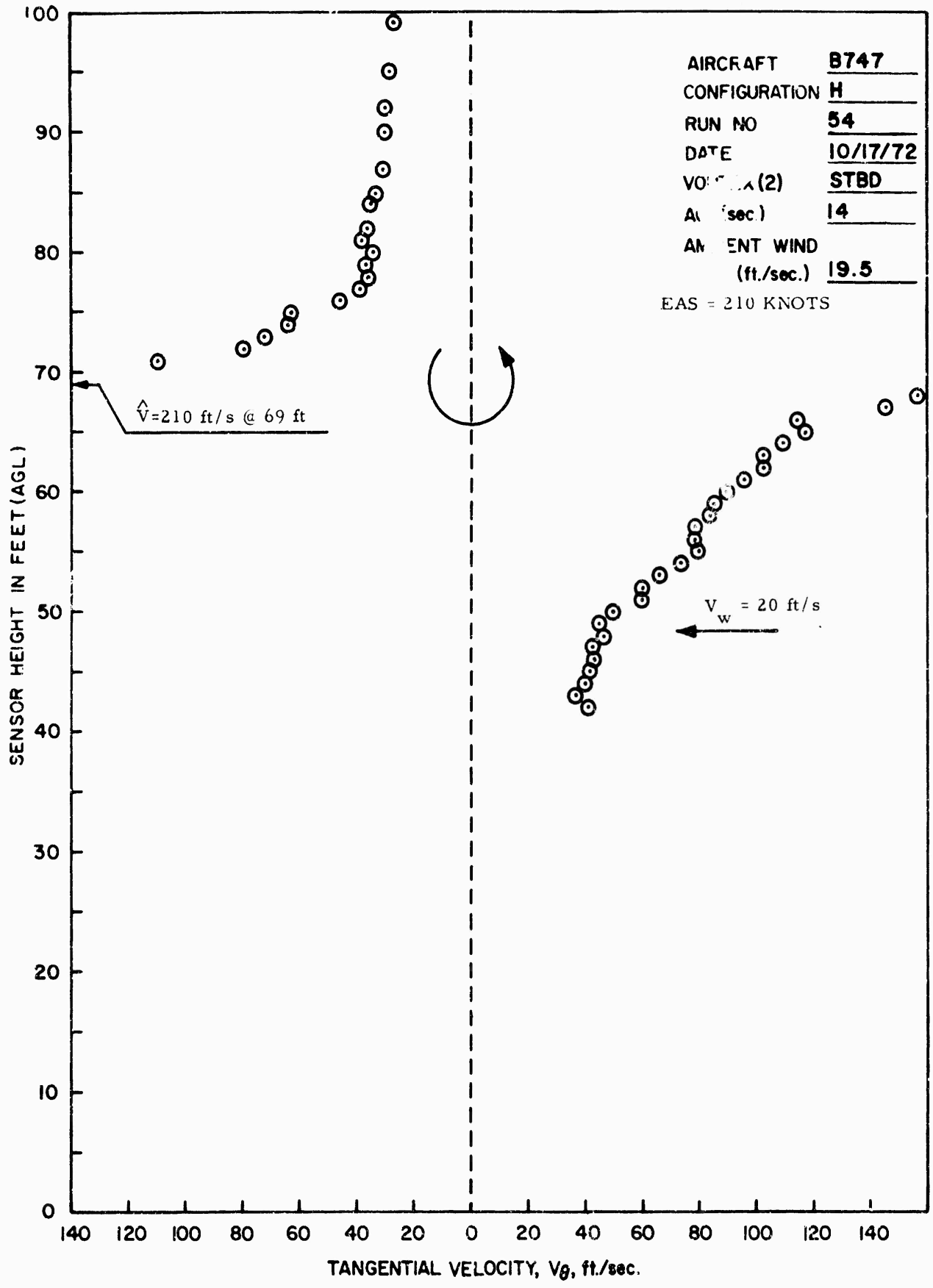
AIRCRAFT B747
CONFIGURATION H
RUN NO 54
DATE 10/17/72
VO[illegible](2) STBD
A[illegible](sec.) 14
AM[illegible]ENT WIND (ft./sec.) 19.5
EAS = 210 KNOTS
$\hat{V}$=210 ft/s @ 69 ft
V_w = 20 ft/s
SENSOR HEIGHT IN FEET (AGL)
TANGENTIAL VELOCITY, Vg, ft./sec.
0
10
20
30
40
50
60
70
80
90
100
140 120 100 80 60 40 20 0 20 40 60 80 100 120 140

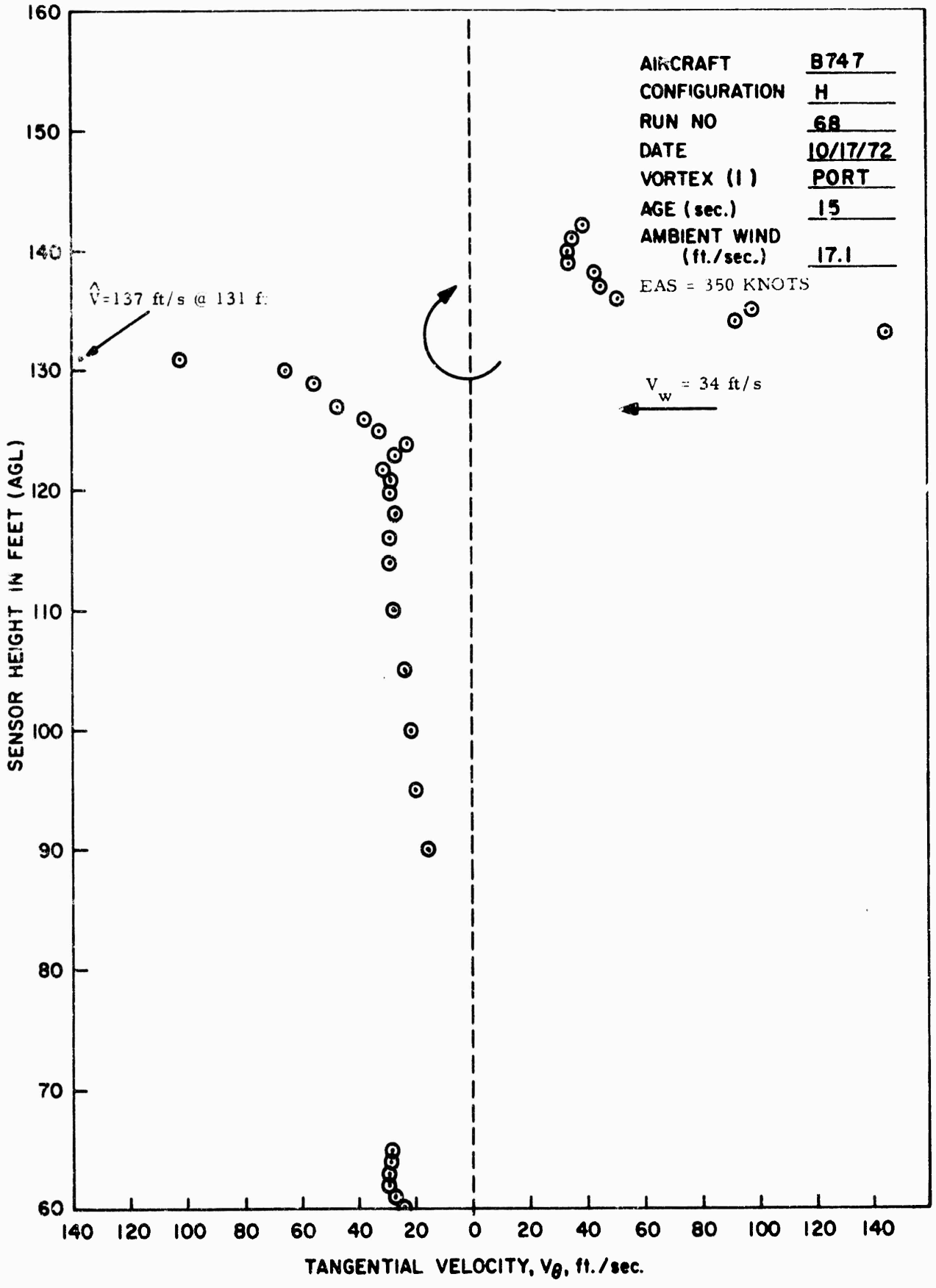
AIRCRAFT B747
CONFIGURATION H
RUN NO 68
DATE 10/17/72
VORTEX (1) PORT
AGE (sec.) 15
AMBIENT WIND (ft./sec.) 17.1
EAS = 350 KNOTS
$\hat{V}$=137 ft/s @ 131 f
V_w = 34 ft/s
SENSOR HEIGHT IN FEET (AGL)
160
150
140
130
120
110
100
90
80
70
60
140 120 100 80 60 40 20 0 20 40 60 80 100 120 140
TANGENTIAL VELOCITY, V_θ, ft./sec.

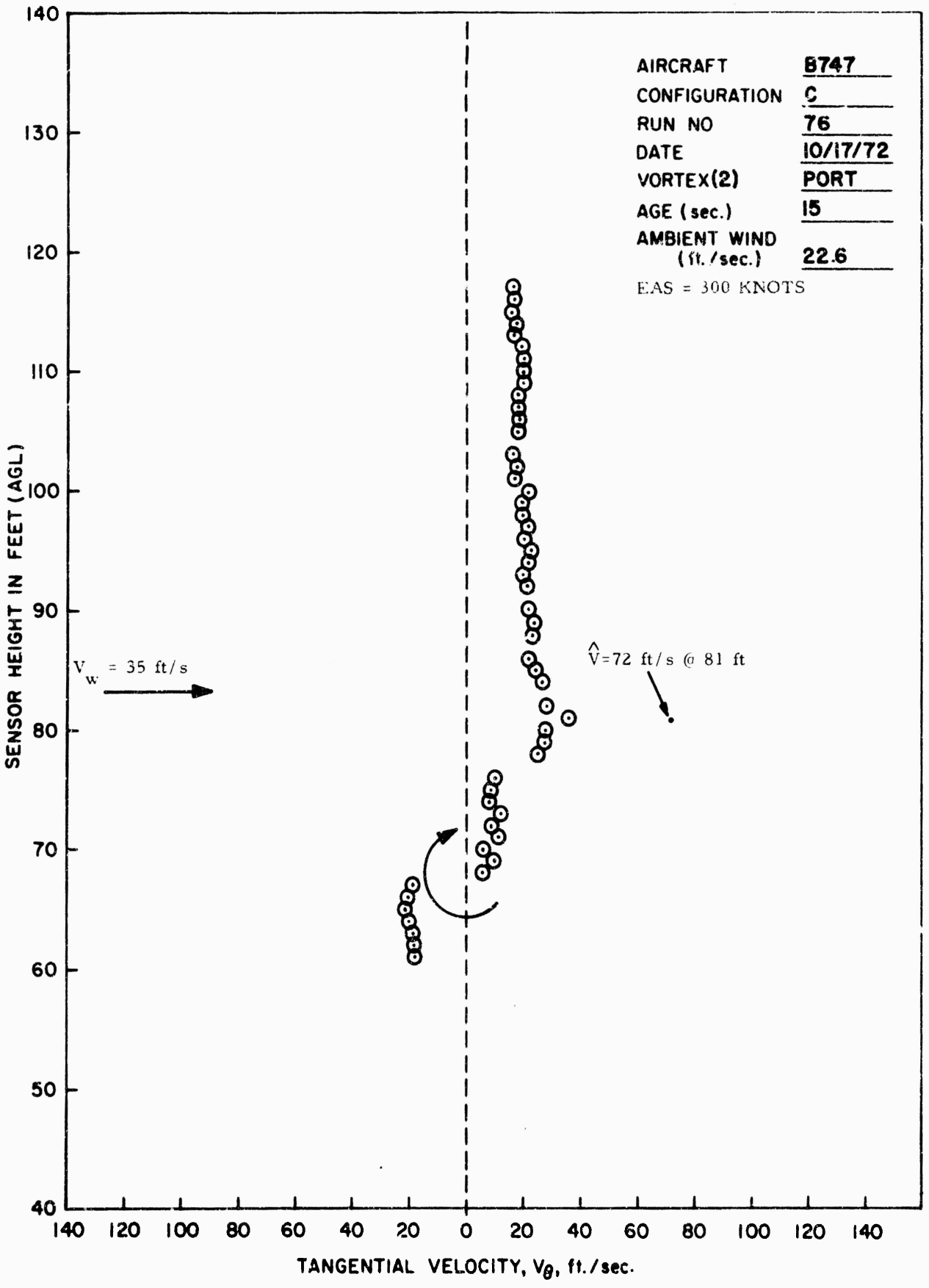
AIRCRAFT B747
CONFIGURATION C
RUN NO 76
DATE 10/17/72
VORTEX(2) PORT
AGE (sec.) 15
AMBIENT WIND (ft./sec.) 22.6
EAS = 300 KNOTS
V_w = 35 ft/s
$\hat{V}$=72 ft/s @ 81 ft
SENSOR HEIGHT IN FEET (AGL)
140
130
120
110
100
90
80
70
60
50
40
140 120 100 80 60 40 20 0 20 40 60 80 100 120 140
TANGENTIAL VELOCITY, V_θ, ft./sec.

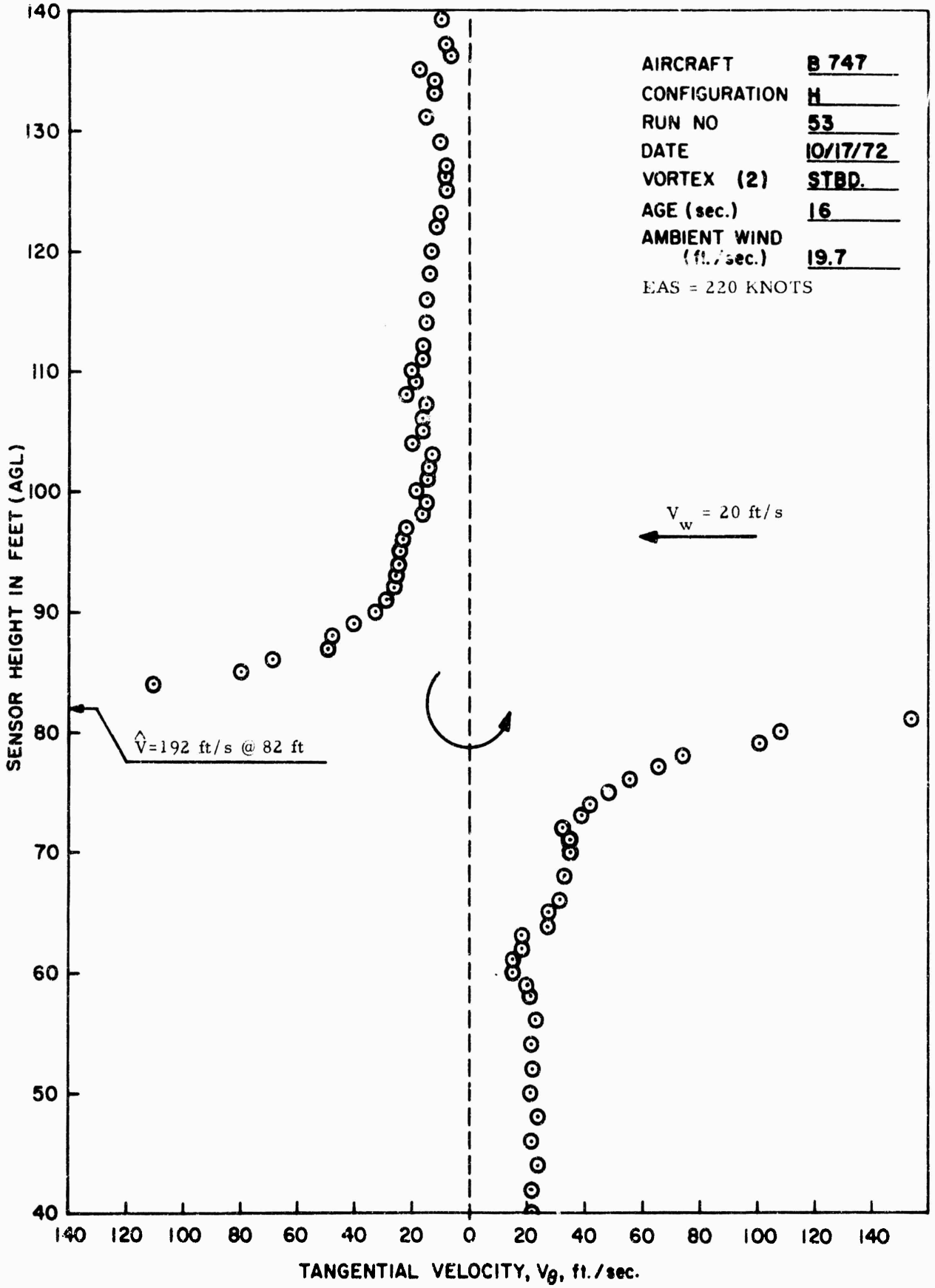
AIRCRAFT B 747
CONFIGURATION H
RUN NO 53
DATE 10/17/72
VORTEX (2) STBD.
AGE (sec.) 16
AMBIENT WIND (ft./sec.) 19.7
EAS = 220 KNOTS
V_w = 20 ft/s
$\hat{V}$=192 ft/s @ 82 ft
SENSOR HEIGHT IN FEET (AGL)
140
130
120
110
100
90
80
70
60
50
40
140 120 100 80 60 40 20 0 20 40 60 80 100 120 140
TANGENTIAL VELOCITY, V_θ, ft./sec.

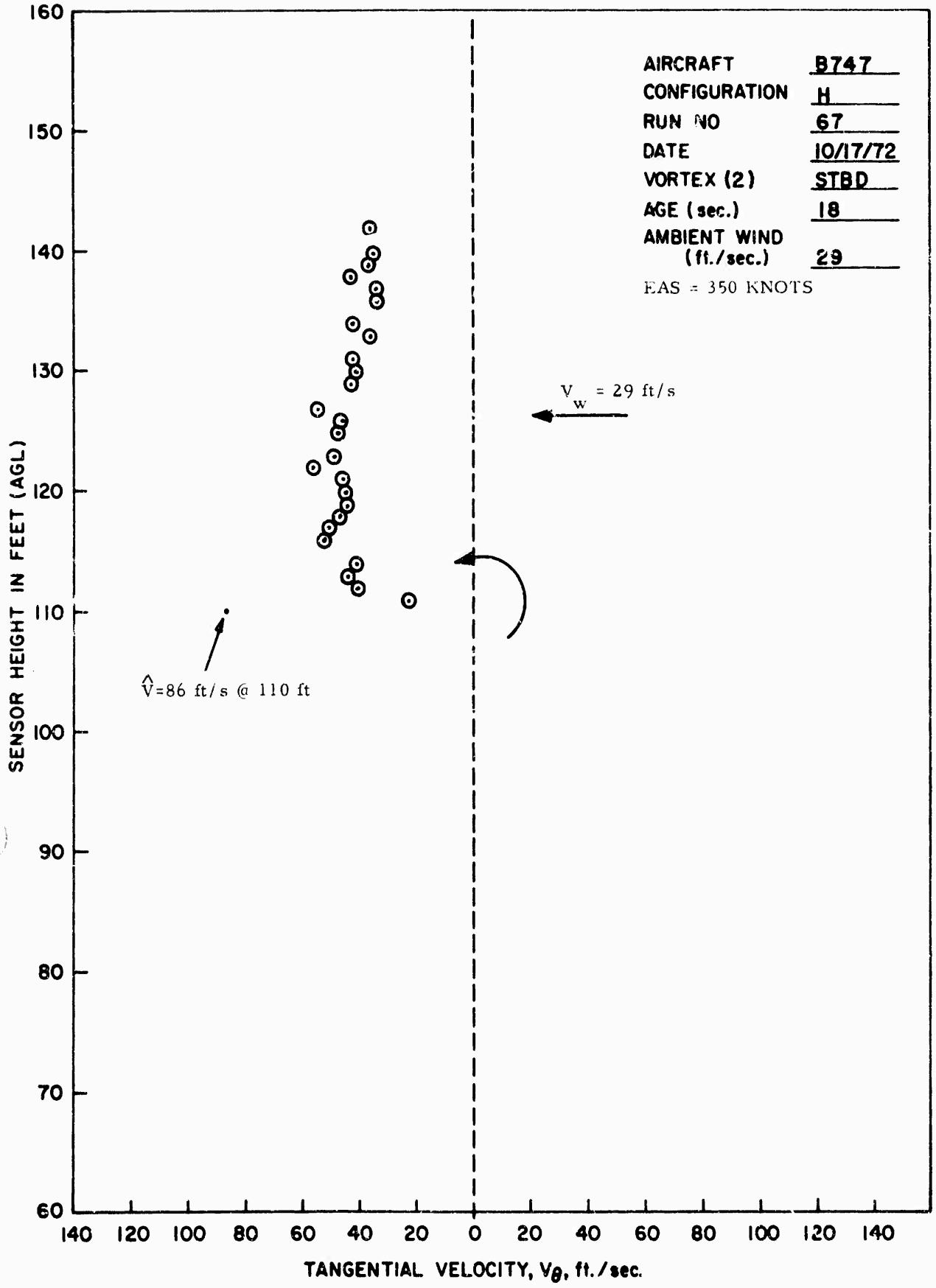
AIRCRAFT B747
CONFIGURATION H
RUN NO 67
DATE 10/17/72
VORTEX (2) STBD
AGE (sec.) 18
AMBIENT WIND (ft./sec.) 29
EAS = 350 KNOTS
V_w = 29 ft/s
$\hat{V}$=86 ft/s @ 110 ft
SENSOR HEIGHT IN FEET (AGL)
160
150
140
130
120
110
100
90
80
70
60
140 120 100 80 60 40 20 0 20 40 60 80 100 120 140
TANGENTIAL VELOCITY, V_θ, ft./sec.

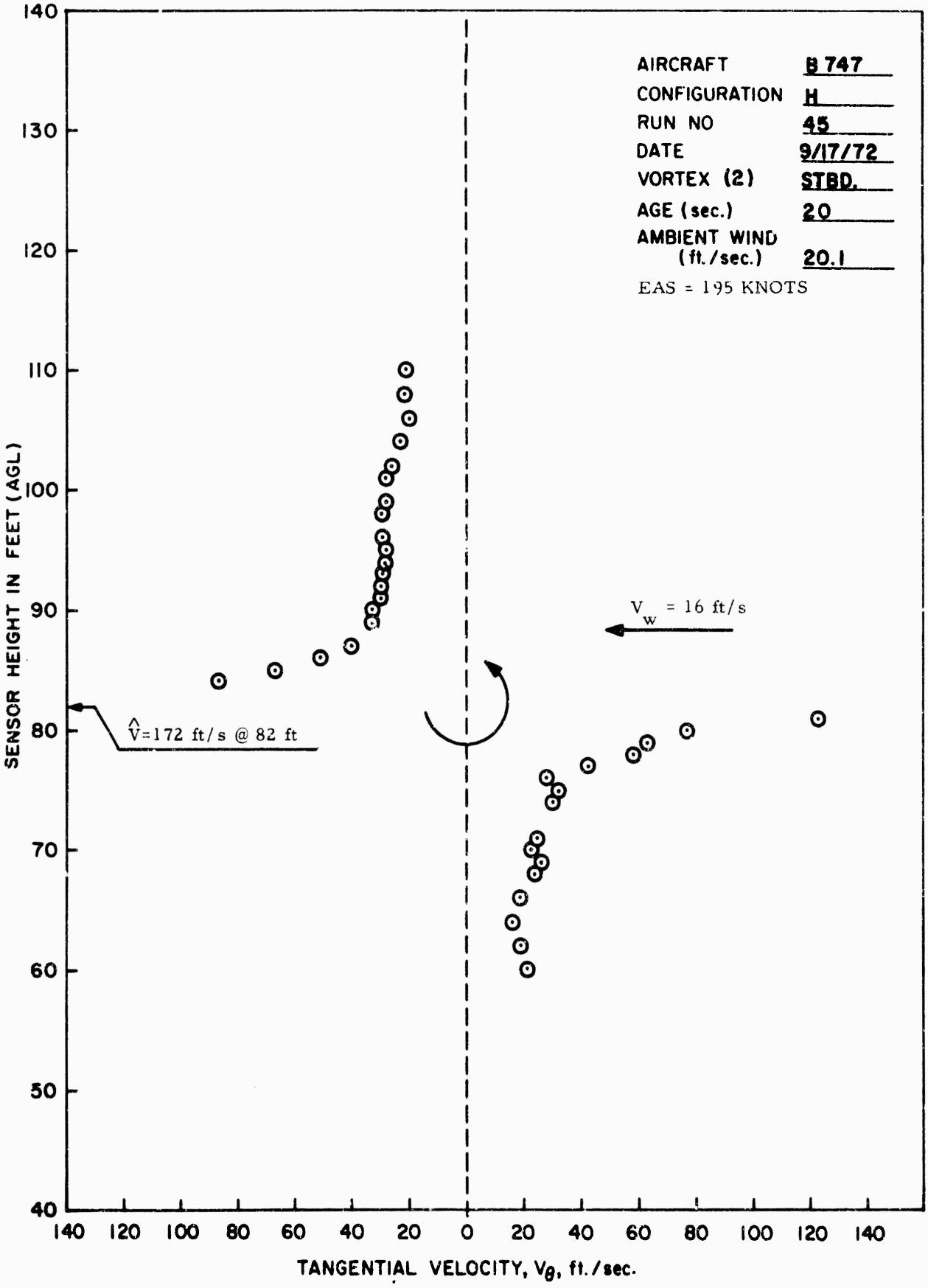
AIRCRAFT B 747
CONFIGURATION H
RUN NO 45
DATE 9/17/72
VORTEX (2) STBD.
AGE (sec.) 20
AMBIENT WIND (ft./sec.) 20.1
EAS = 195 KNOTS
V_w = 16 ft/s
$\hat{V}$=172 ft/s @ 82 ft
SENSOR HEIGHT IN FEET (AGL)
140
130
120
110
100
90
80
70
60
50
40
140 120 100 80 60 40 20 0 20 40 60 80 100 120 140
TANGENTIAL VELOCITY, V_θ, ft./sec.

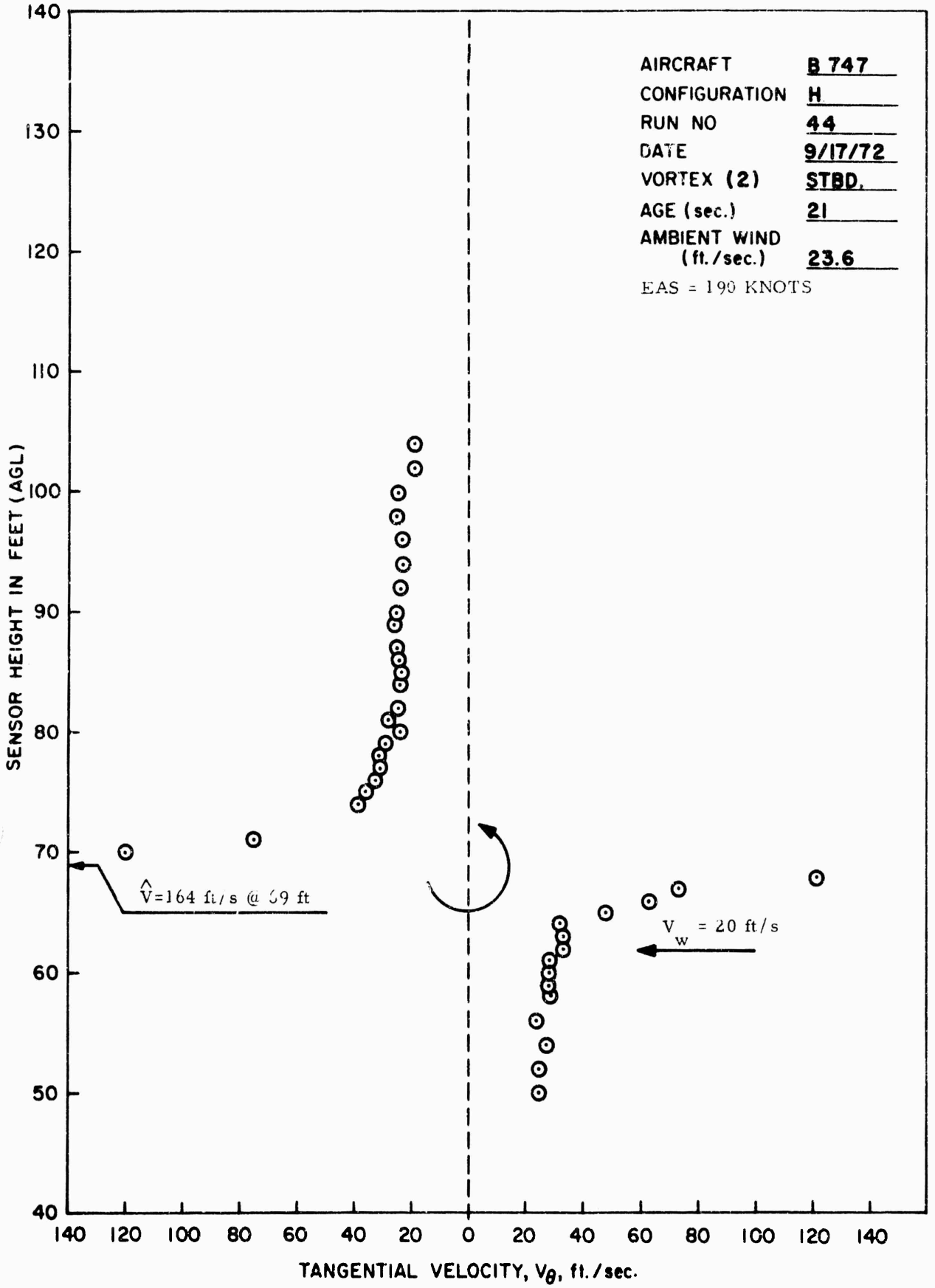
AIRCRAFT B 747
CONFIGURATION H
RUN NO 44
DATE 9/17/72
VORTEX (2) STBD.
AGE (sec.) 21
AMBIENT WIND (ft./sec.) 23.6
EAS = 190 KNOTS
SENSOR HEIGHT IN FEET (AGL)
140
130
120
110
100
90
80
70
60
50
40
$\hat{V}$=164 ft/s @ 69 ft
V_w = 20 ft/s
140 120 100 80 60 40 20 0 20 40 60 80 100 120 140
TANGENTIAL VELOCITY, V_θ, ft./sec.

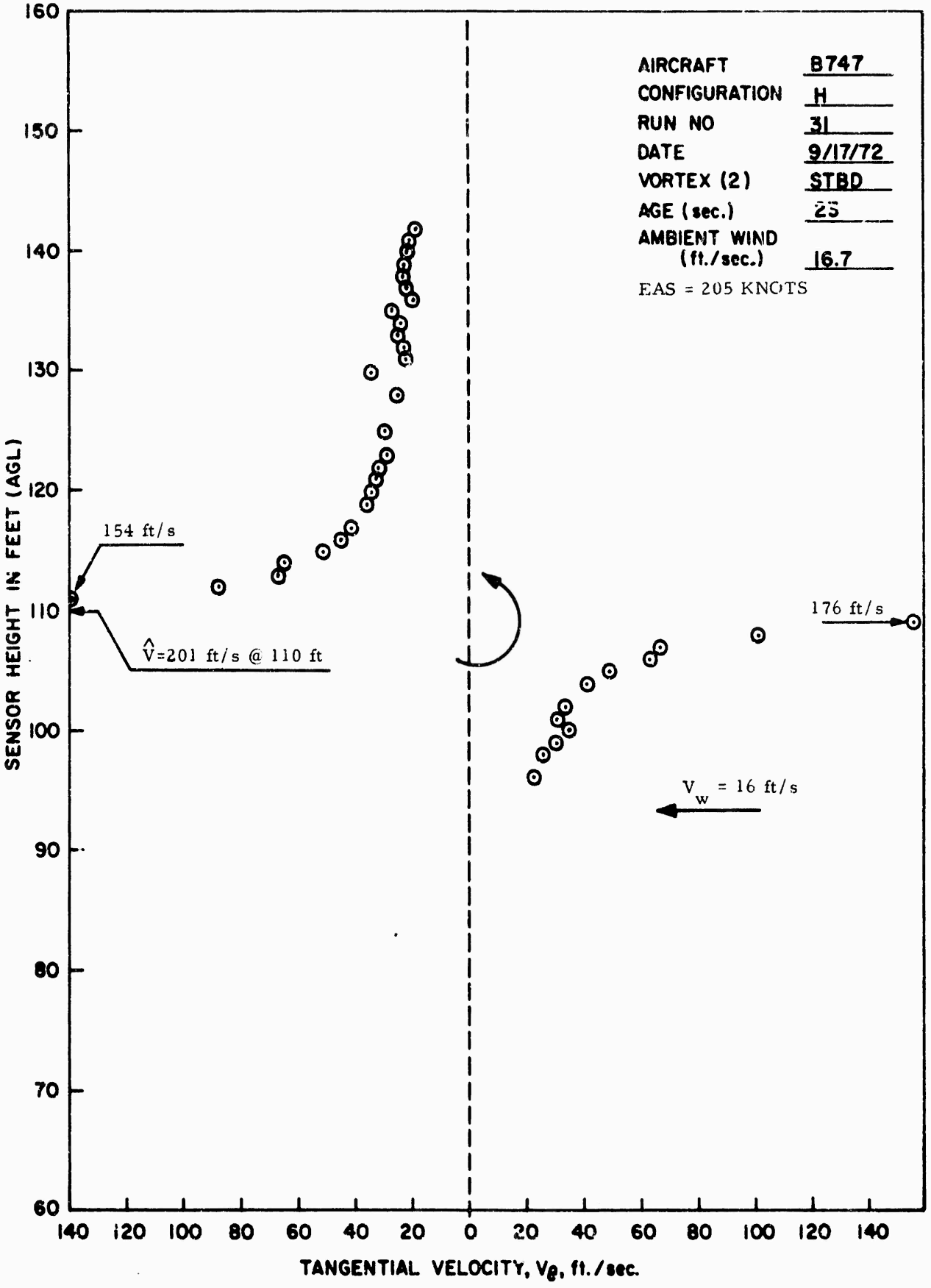
AIRCRAFT B747
CONFIGURATION H
RUN NO 31
DATE 9/17/72
VORTEX (2) STBD
AGE (sec.) 25
AMBIENT WIND (ft./sec.) 16.7
EAS = 205 KNOTS
154 ft/s
$\hat{V}$=201 ft/s @ 110 ft
176 ft/s
V_w = 16 ft/s
SENSOR HEIGHT IN FEET (AGL)
160
150
140
130
120
110
100
90
80
70
60
140 120 100 80 60 40 20 0 20 40 60 80 100 120 140
TANGENTIAL VELOCITY, V_θ, ft./sec.

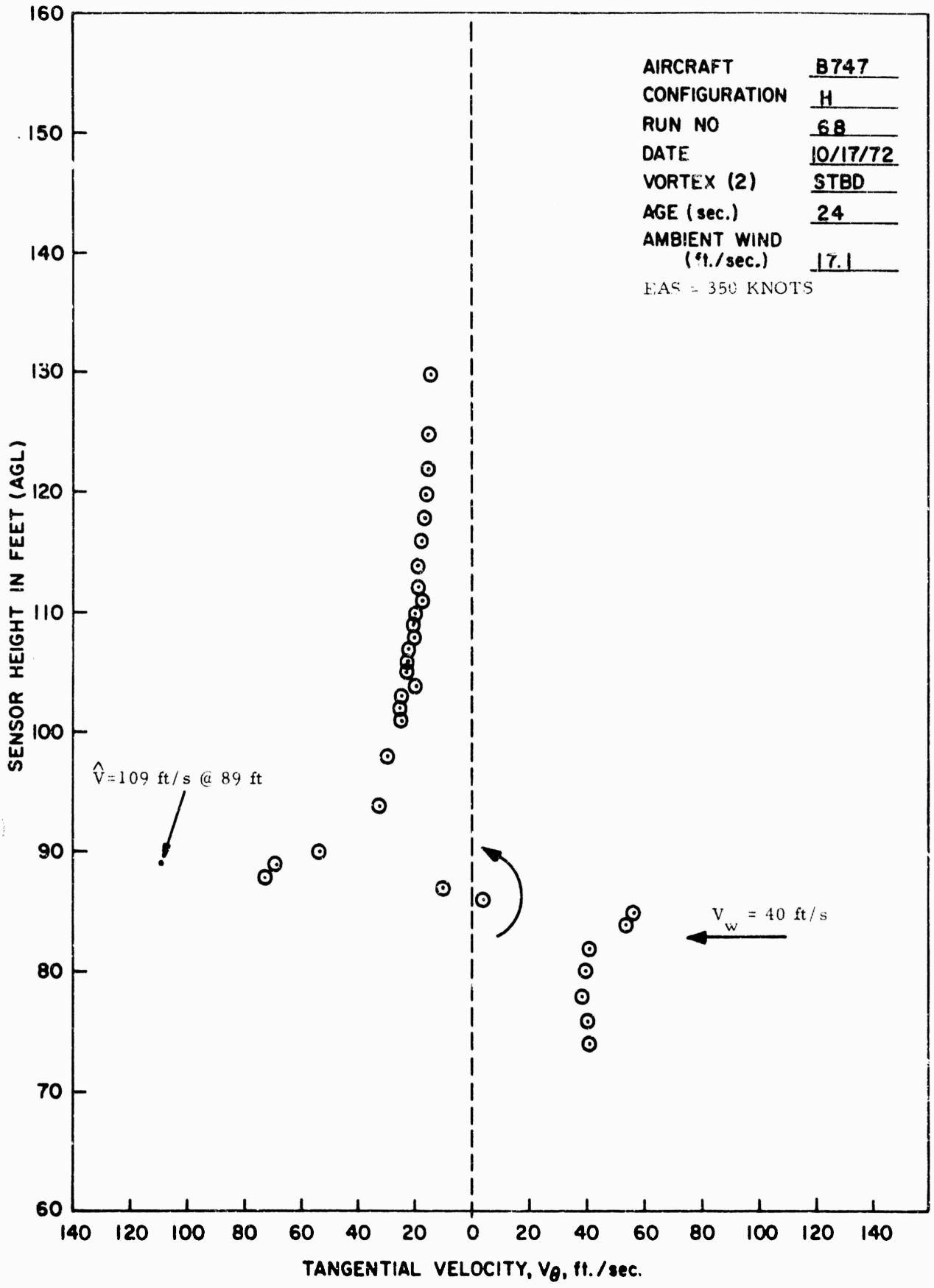
AIRCRAFT B747
CONFIGURATION H
RUN NO 68
DATE 10/17/72
VORTEX (2) STBD
AGE (sec.) 24
AMBIENT WIND (ft./sec.) 17.1
EAS = 350 KNOTS
SENSOR HEIGHT IN FEET (AGL)
160
150
140
130
120
110
100
90
80
70
60
$\hat{V}$=109 ft/s @ 89 ft
V_w = 40 ft/s
140 120 100 80 60 40 20 0 20 40 60 80 100 120 140
TANGENTIAL VELOCITY, V_θ, ft./sec.

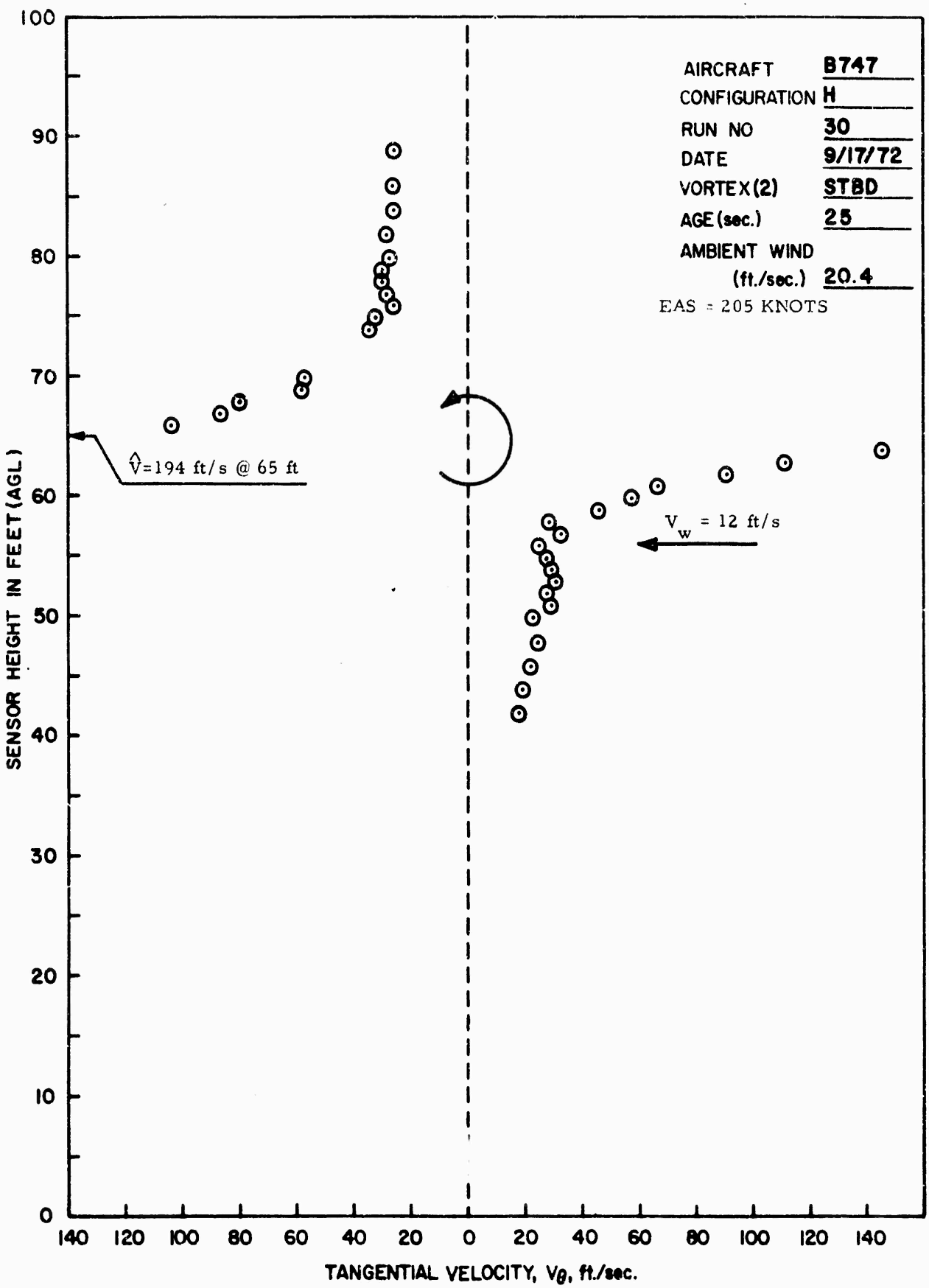
AIRCRAFT B747
CONFIGURATION H
RUN NO 30
DATE 9/17/72
VORTEX(2) STBD
AGE(sec.) 25
AMBIENT WIND
(ft./sec.) 20.4
EAS = 205 KNOTS
V̂=194 ft/s @ 65 ft
V_w = 12 ft/s
SENSOR HEIGHT IN FEET(AGL)
TANGENTIAL VELOCITY, Vθ, ft./sec.
100
90
80
70
60
50
40
30
20
10
0
140 120 100 80 60 40 20 0 20 40 60 80 100 120 140

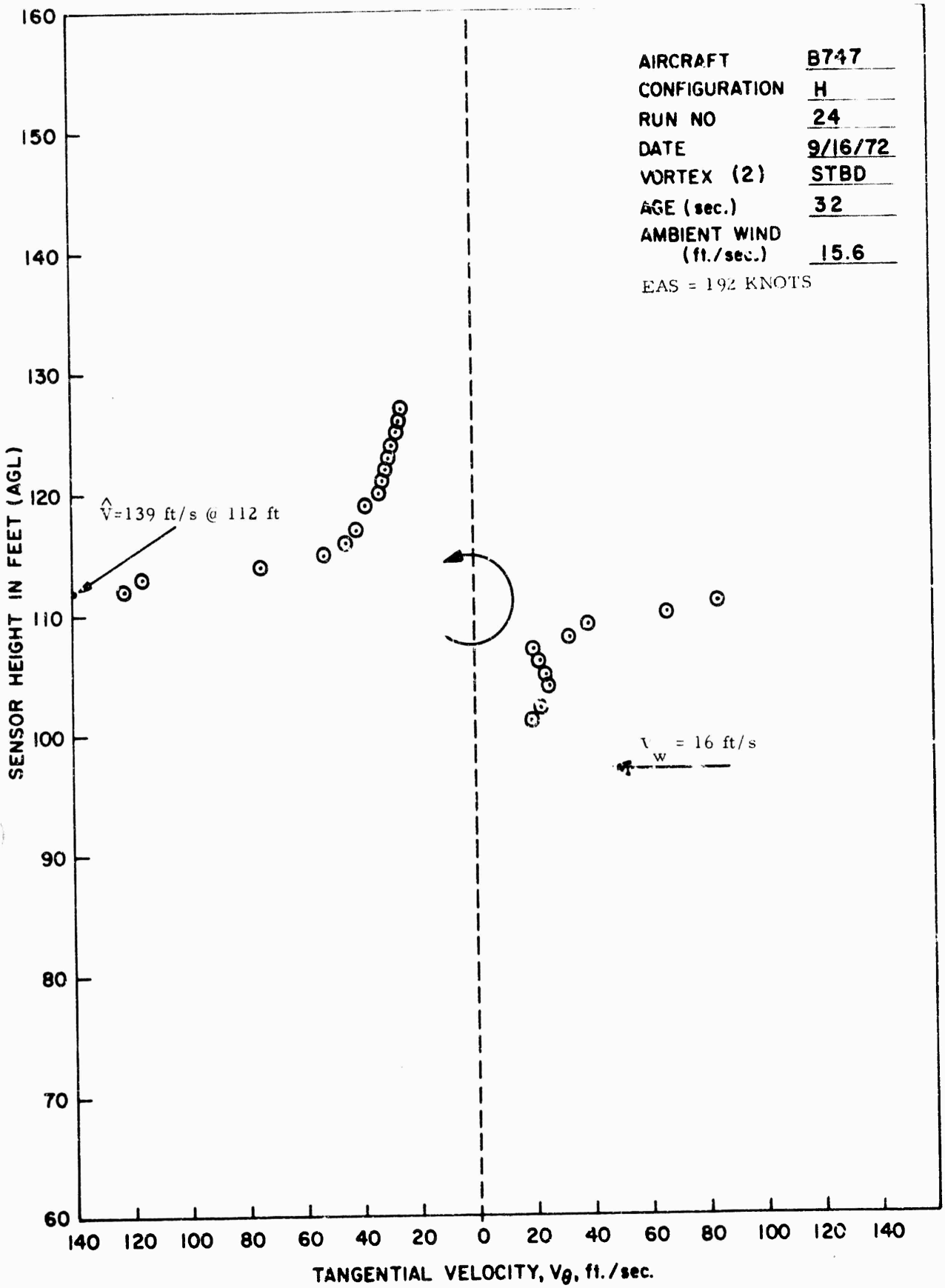
AIRCRAFT B747
CONFIGURATION H
RUN NO 24
DATE 9/16/72
VORTEX (2) STBD
AGE (sec.) 32
AMBIENT WIND (ft./sec.) 15.6
EAS = 192 KNOTS
$\hat{V}$=139 ft/s @ 112 ft
V_w = 16 ft/s
SENSOR HEIGHT IN FEET (AGL)
160
150
140
130
120
110
100
90
80
70
60
140 120 100 80 60 40 20 0 20 40 60 80 100 120 140
TANGENTIAL VELOCITY, V_θ, ft./sec.

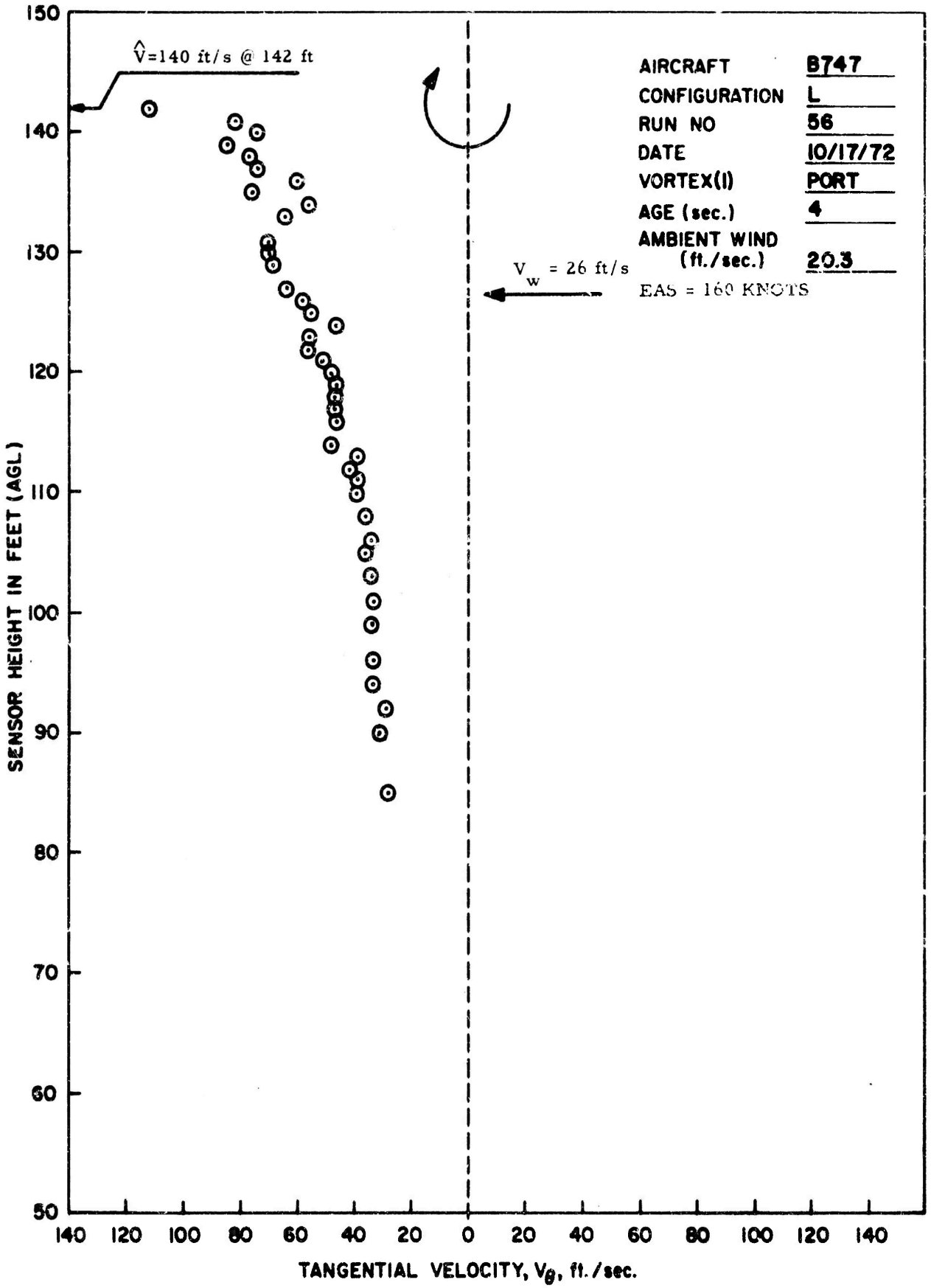
$\hat{V}$=140 ft/s @ 142 ft
AIRCRAFT B747
CONFIGURATION L
RUN NO 56
DATE 10/17/72
VORTEX(I) PORT
AGE (sec.) 4
AMBIENT WIND (ft./sec.) 20.3
V_w = 26 ft/s
EAS = 160 KNOTS
SENSOR HEIGHT IN FEET (AGL)
150
140
130
120
110
100
90
80
70
60
50
140 120 100 80 60 40 20 0 20 40 60 80 100 120 140
TANGENTIAL VELOCITY, V_θ, ft./sec.

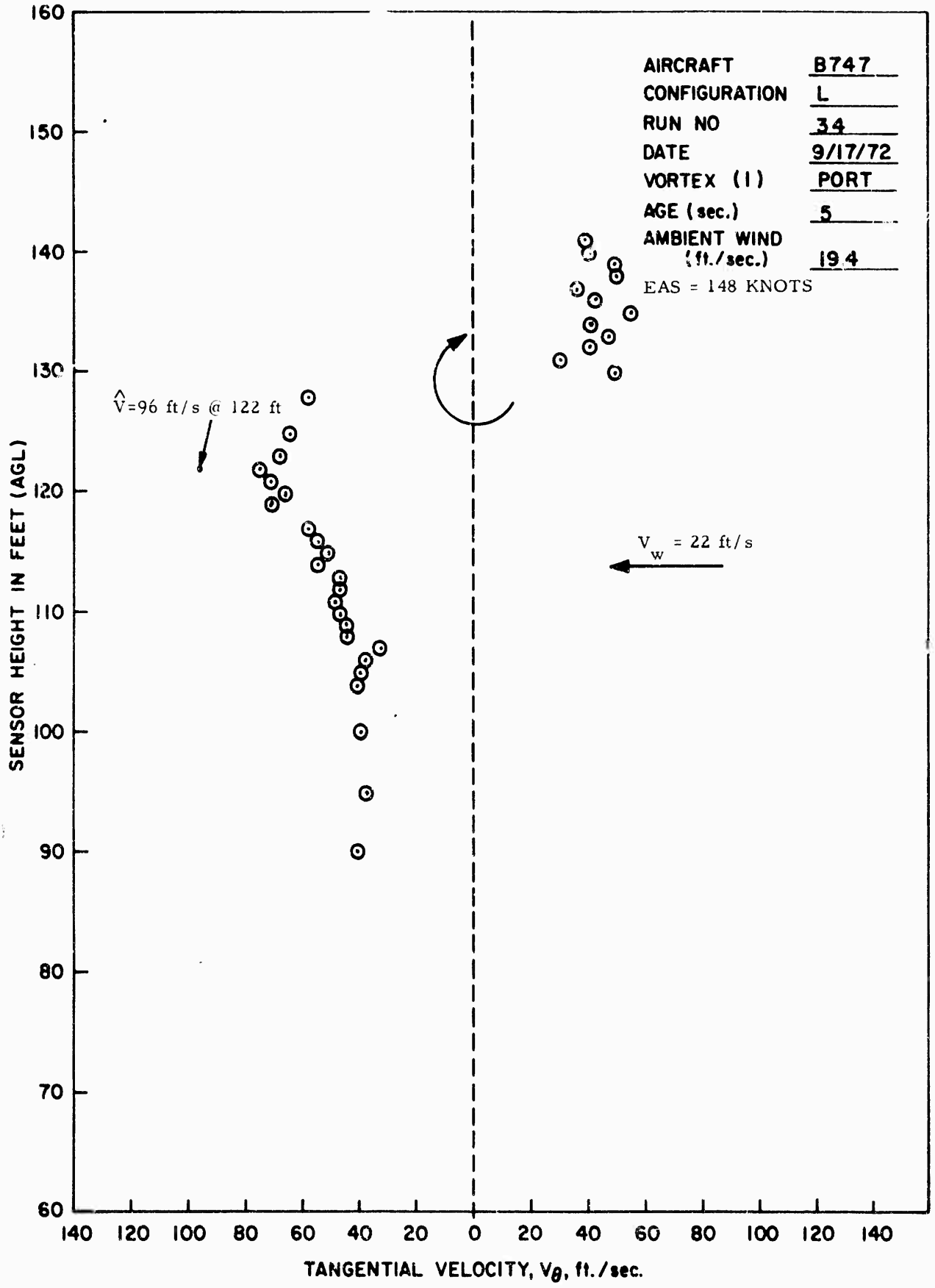
AIRCRAFT B747
CONFIGURATION L
RUN NO 34
DATE 9/17/72
VORTEX (1) PORT
AGE (sec.) 5
AMBIENT WIND (ft./sec.) 19.4
EAS = 148 KNOTS
$\hat{V}$=96 ft/s @ 122 ft
V_w = 22 ft/s
SENSOR HEIGHT IN FEET (AGL)
160
150
140
130
120
110
100
90
80
70
60
140 120 100 80 60 40 20 0 20 40 60 80 100 120 140
TANGENTIAL VELOCITY, V_θ, ft./sec.

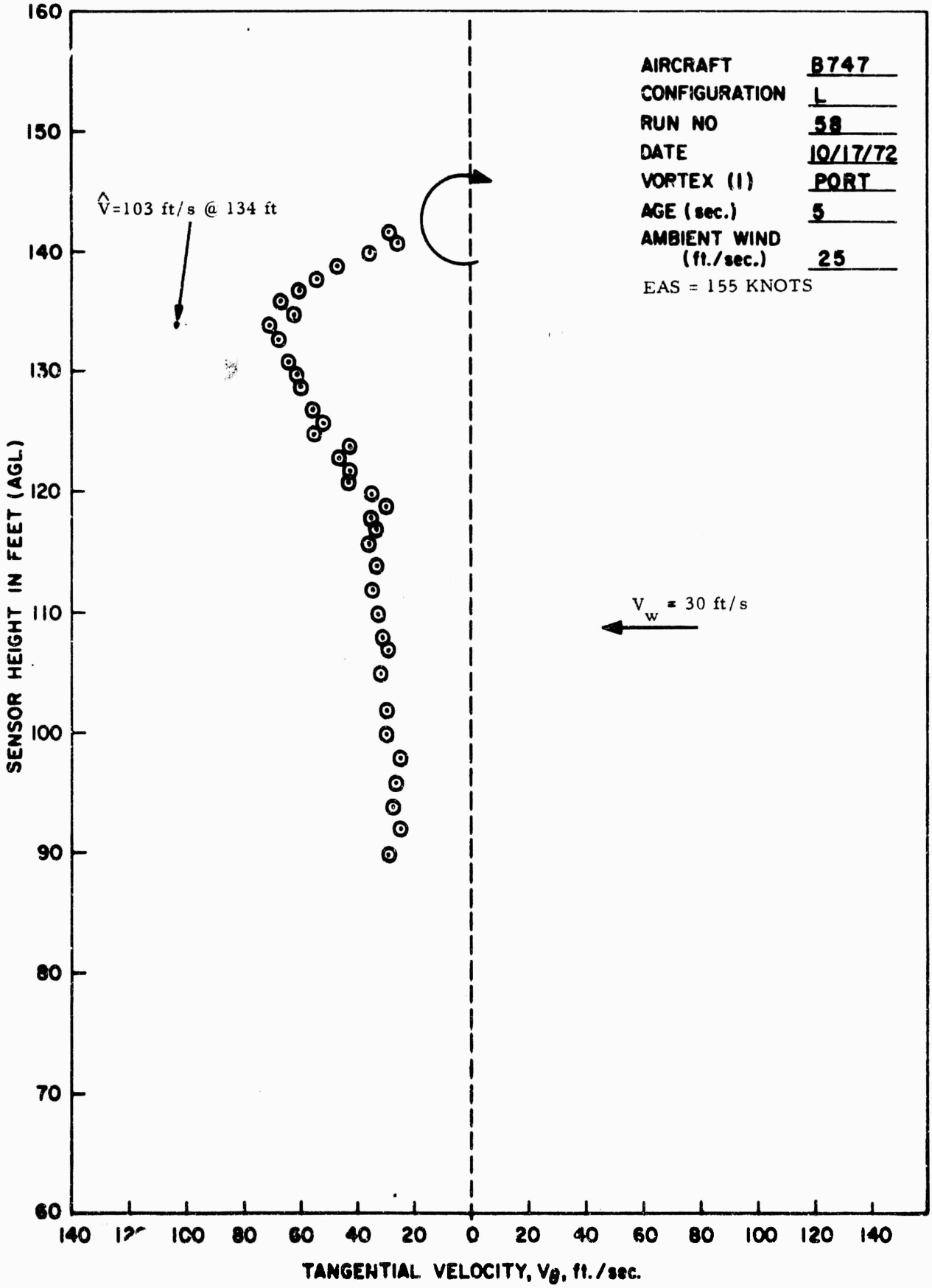
AIRCRAFT B747
CONFIGURATION L
RUN NO 58
DATE 10/17/72
VORTEX (1) PORT
AGE (sec.) 5
AMBIENT WIND (ft./sec.) 25
EAS = 155 KNOTS
$\hat{V}$=103 ft/s @ 134 ft
V_w = 30 ft/s
SENSOR HEIGHT IN FEET (AGL.)
160
150
140
130
120
110
100
90
80
70
60
140
120
100
80
60
40
20
0
20
40
60
80
100
120
140
TANGENTIAL VELOCITY, V_θ, ft./sec.

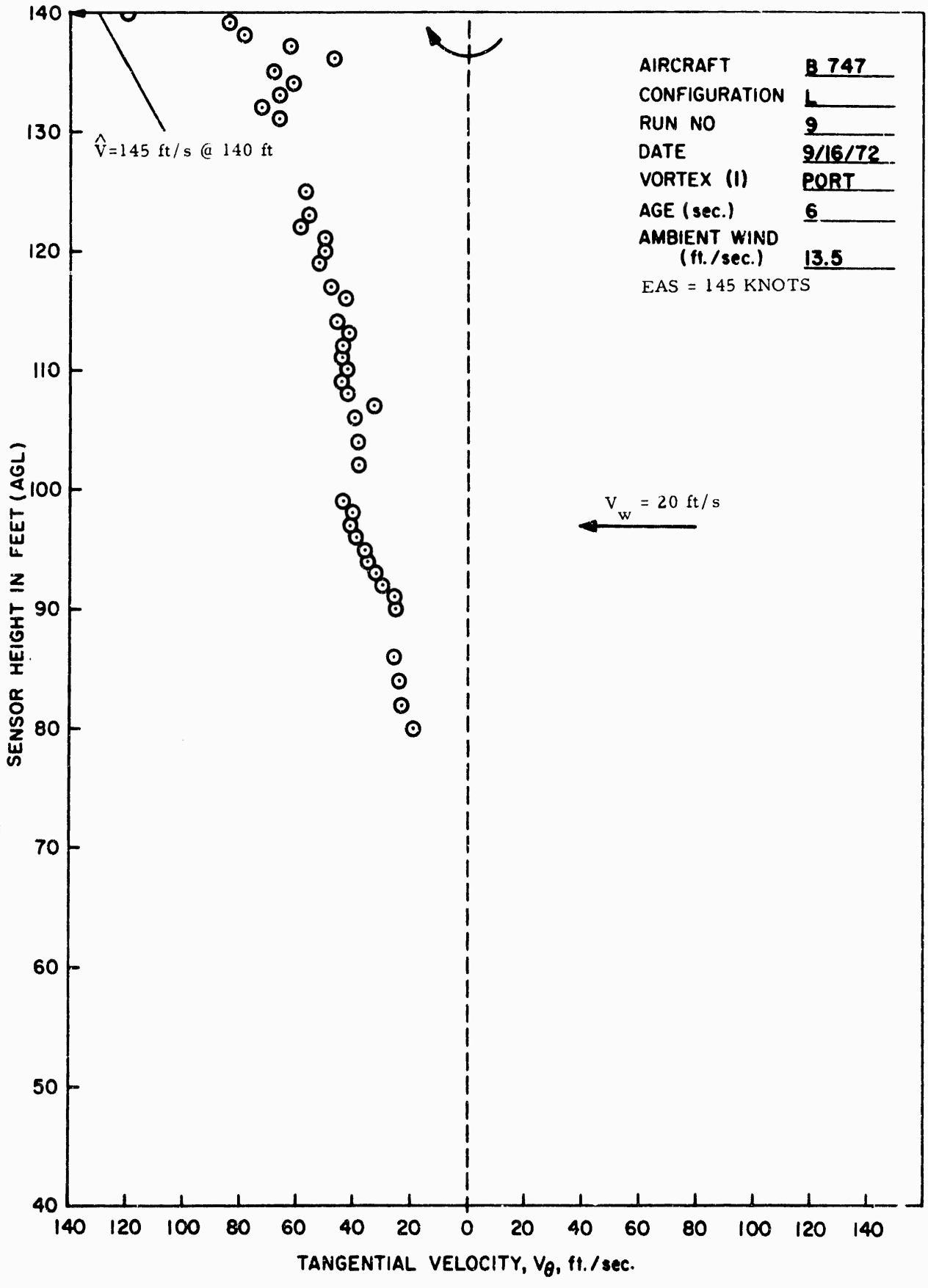
AIRCRAFT B 747
CONFIGURATION L
RUN NO 9
DATE 9/16/72
VORTEX (1) PORT
AGE (sec.) 6
AMBIENT WIND (ft./sec.) 13.5
EAS = 145 KNOTS
$\hat{V}$=145 ft/s @ 140 ft
V_w = 20 ft/s
SENSOR HEIGHT IN FEET (AGL)
140
130
120
110
100
90
80
70
60
50
40
140 120 100 80 60 40 20 0 20 40 60 80 100 120 140
TANGENTIAL VELOCITY, V_θ, ft./sec.

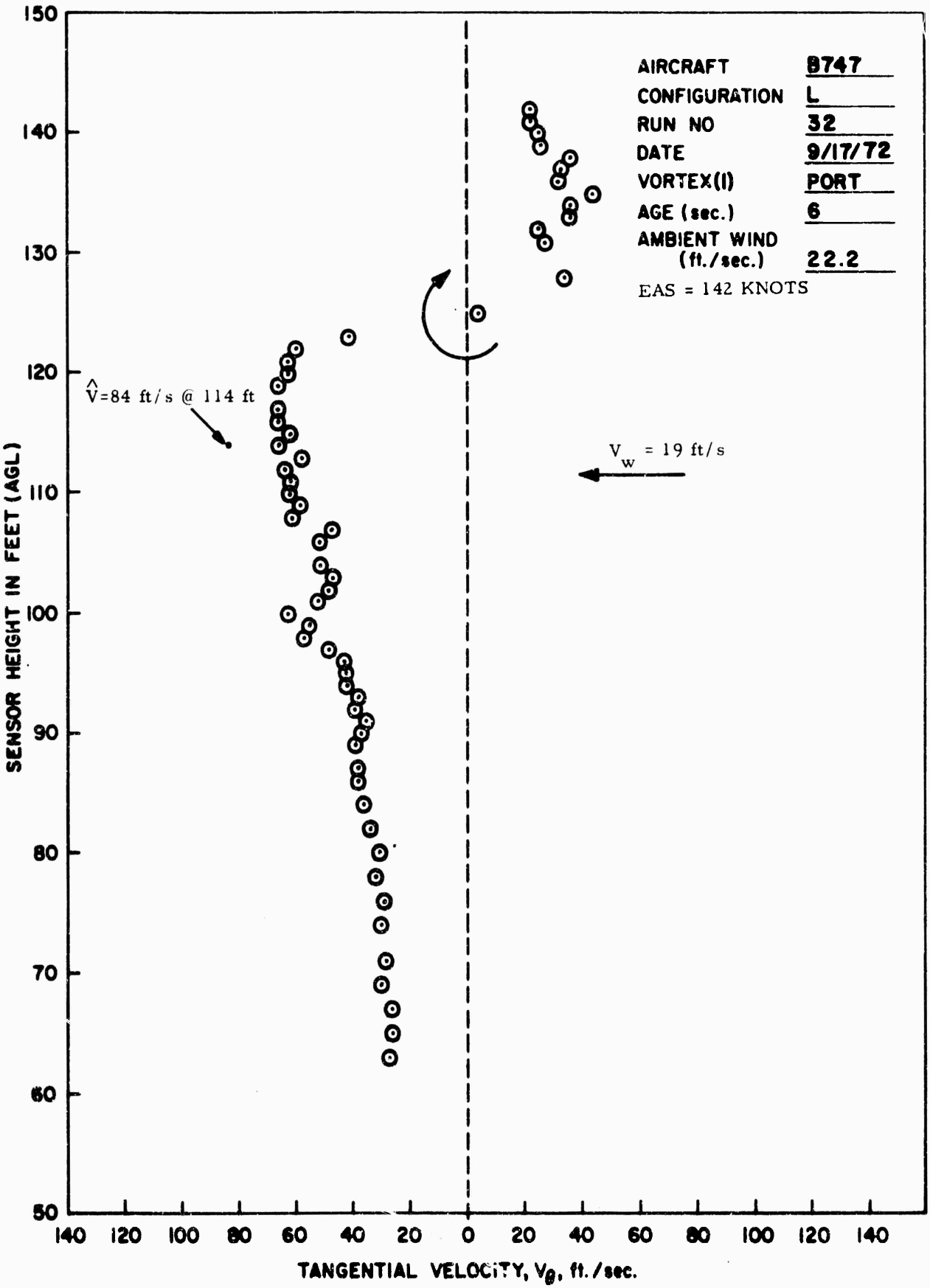
AIRCRAFT B747
CONFIGURATION L
RUN NO 32
DATE 9/17/72
VORTEX(1) PORT
AGE (sec.) 6
AMBIENT WIND (ft./sec.) 22.2
EAS = 142 KNOTS
$\hat{V}$=84 ft/s @ 114 ft
V_w = 19 ft/s
SENSOR HEIGHT IN FEET (AGL)
150
140
130
120
110
100
90
80
70
60
50
140 120 100 80 60 40 20 0 20 40 60 80 100 120 140
TANGENTIAL VELOCITY, V_θ, ft./sec.

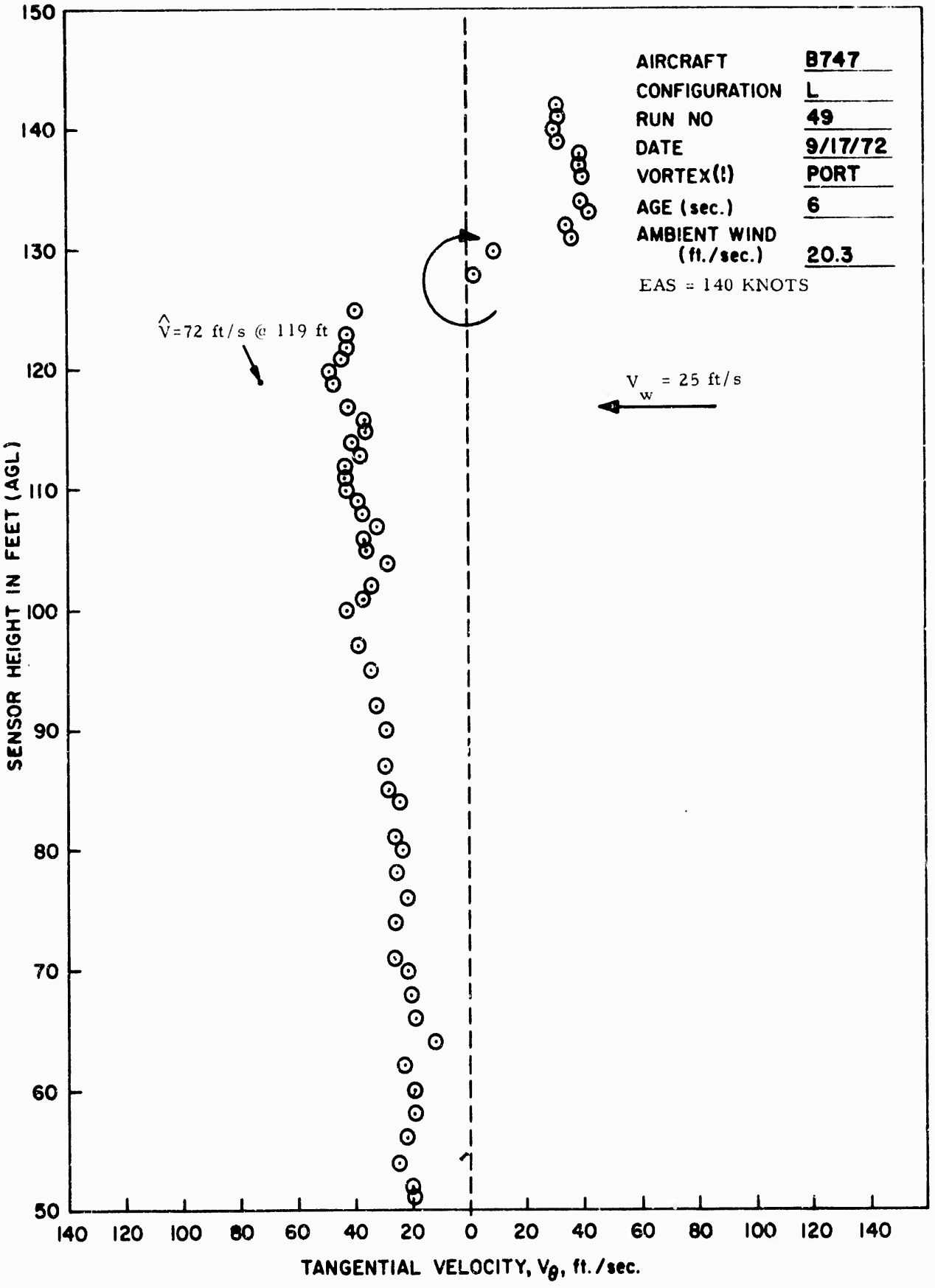
AIRCRAFT B747
CONFIGURATION L
RUN NO 49
DATE 9/17/72
VORTEX(!) PORT
AGE (sec.) 6
AMBIENT WIND (ft./sec.) 20.3
EAS = 140 KNOTS
$\hat{V}$=72 ft/s @ 119 ft
V_w = 25 ft/s
SENSOR HEIGHT IN FEET (AGL)
150
140
130
120
110
100
90
80
70
60
50
140 120 100 80 60 40 20 0 20 40 60 80 100 120 140
TANGENTIAL VELOCITY, V_θ, ft./sec.

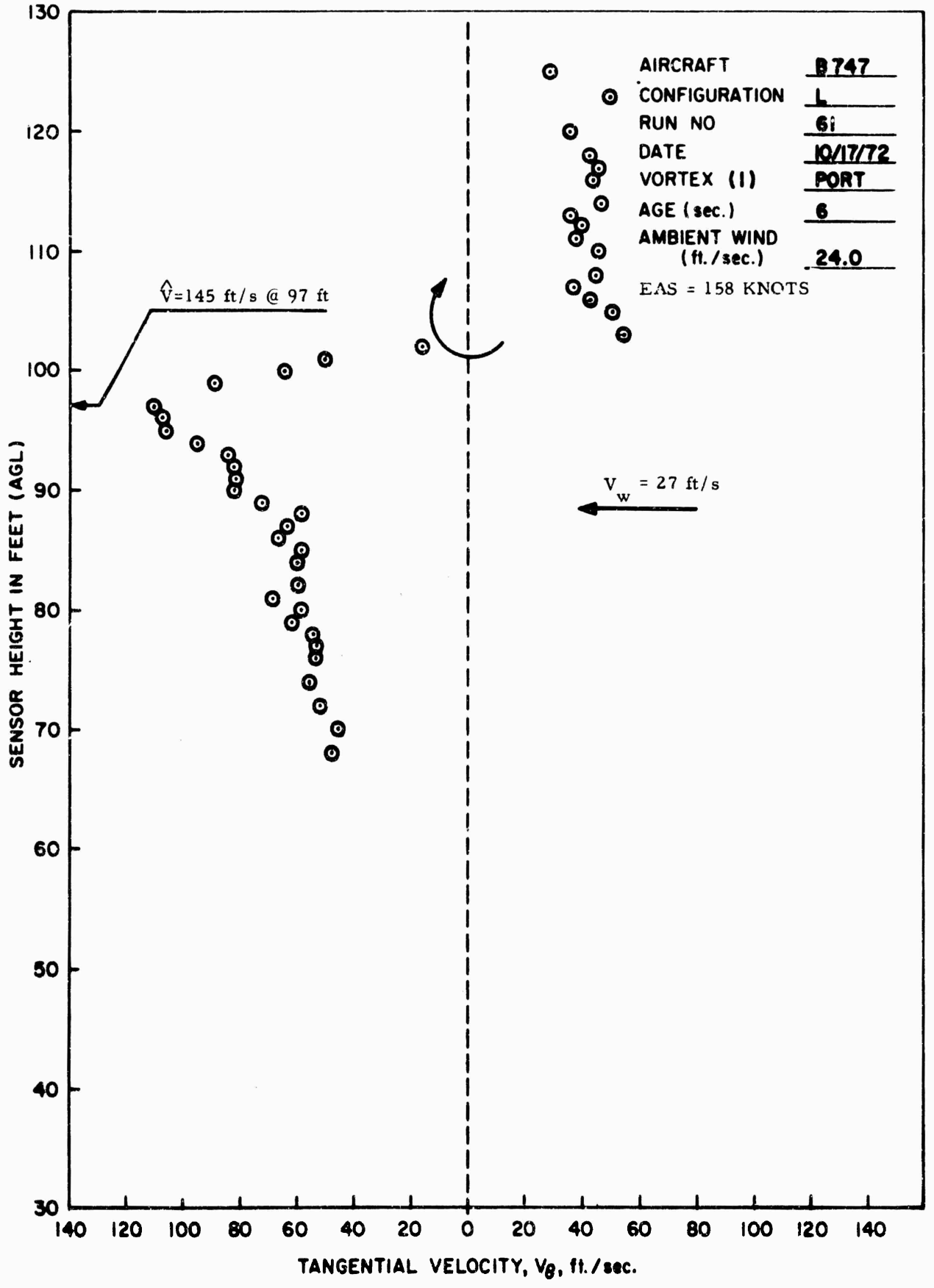
AIRCRAFT B747
CONFIGURATION L
RUN NO 6i
DATE 10/17/72
VORTEX (1) PORT
AGE (sec.) 6
AMBIENT WIND (ft./sec.) 24.0
EAS = 158 KNOTS
V=145 ft/s @ 97 ft
V_w = 27 ft/s
SENSOR HEIGHT IN FEET (AGL)
130
120
110
100
90
80
70
60
50
40
30
140 120 100 80 60 40 20 0 20 40 60 80 100 120 140
TANGENTIAL VELOCITY, Vθ, ft./sec.

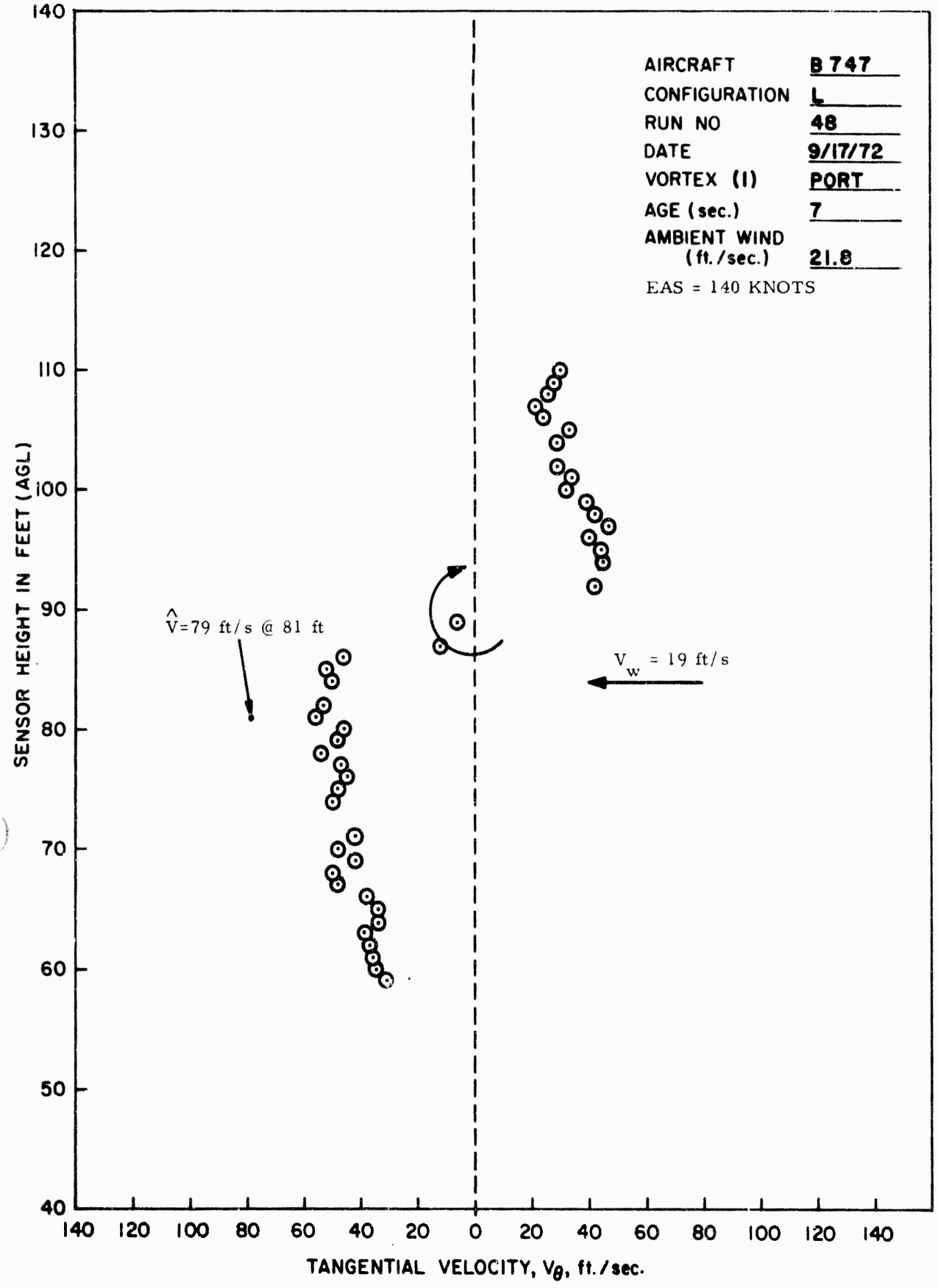
AIRCRAFT B 747
CONFIGURATION L
RUN NO 48
DATE 9/17/72
VORTEX (1) PORT
AGE (sec.) 7
AMBIENT WIND (ft./sec.) 21.8
EAS = 140 KNOTS
$\hat{V}$=79 ft/s @ 81 ft
V_w = 19 ft/s
SENSOR HEIGHT IN FEET (AGL)
140
130
120
110
100
90
80
70
60
50
40
140 120 100 80 60 40 20 0 20 40 60 80 100 120 140
TANGENTIAL VELOCITY, V_θ, ft./sec.

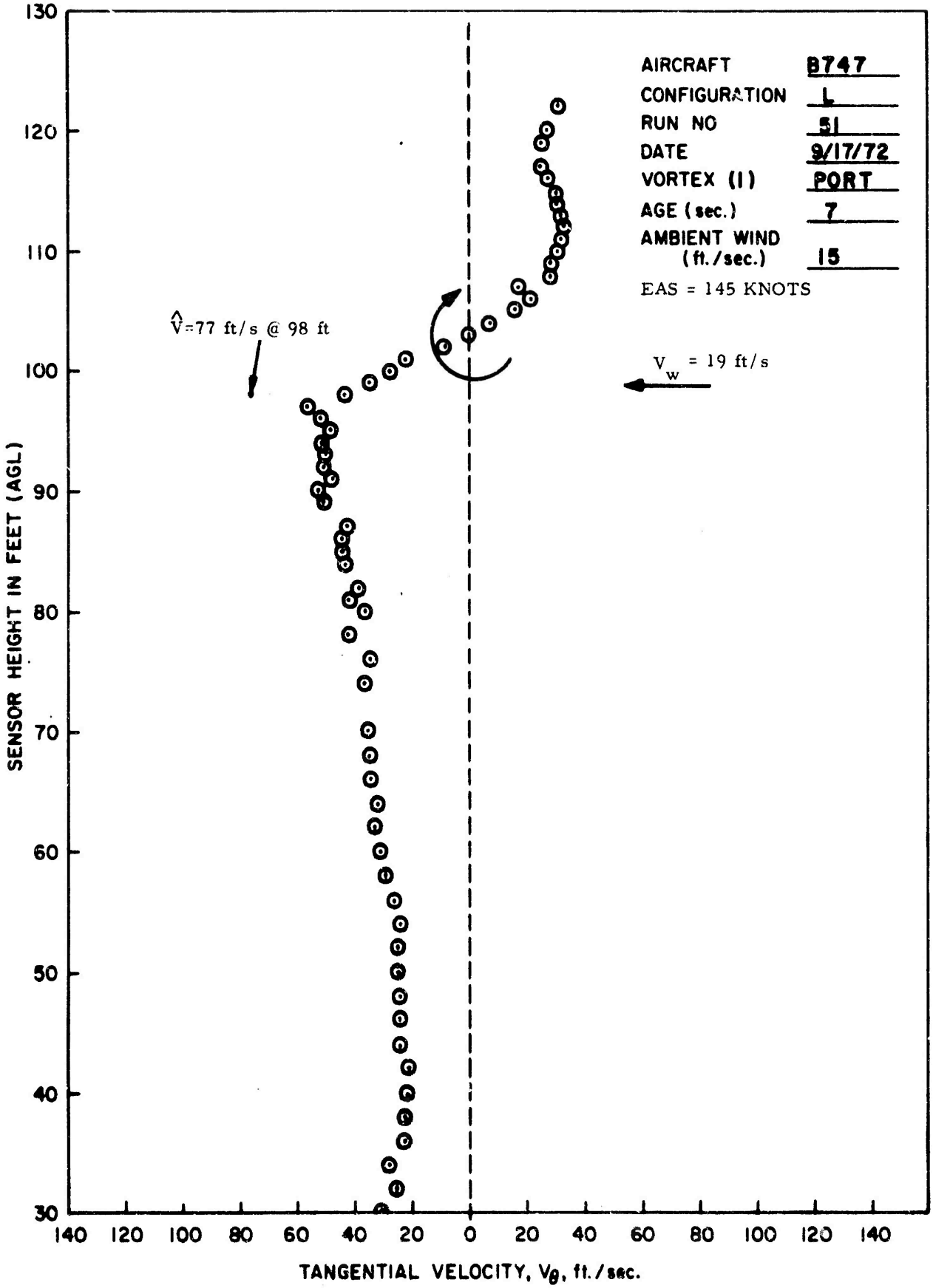
AIRCRAFT B747
CONFIGURATION L
RUN NO 51
DATE 9/17/72
VORTEX (1) PORT
AGE (sec.) 7
AMBIENT WIND (ft./sec.) 15
EAS = 145 KNOTS
$\hat{V}$=77 ft/s @ 98 ft
V_w = 19 ft/s
SENSOR HEIGHT IN FEET (AGL)
130
120
110
100
90
80
70
60
50
40
30
140 120 100 80 60 40 20 0 20 40 60 80 100 120 140
TANGENTIAL VELOCITY, V_θ, ft./sec.

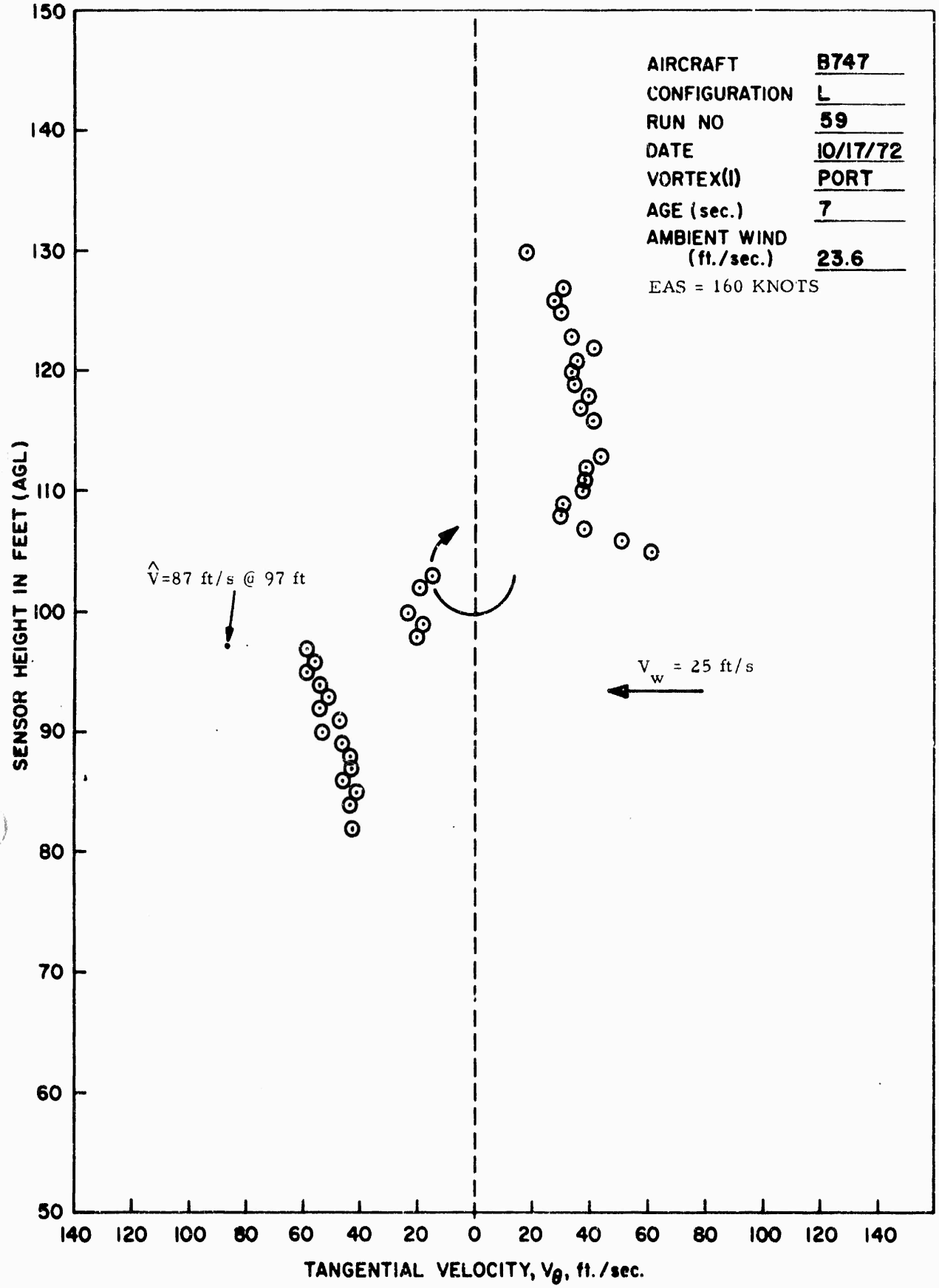
AIRCRAFT B747
CONFIGURATION L
RUN NO 59
DATE 10/17/72
VORTEX(I) PORT
AGE (sec.) 7
AMBIENT WIND (ft./sec.) 23.6
EAS = 160 KNOTS
$\hat{V}$=87 ft/s @ 97 ft
V_w = 25 ft/s
SENSOR HEIGHT IN FEET (AGL)
150
140
130
120
110
100
90
80
70
60
50
140 120 100 80 60 40 20 0 20 40 60 80 100 120 140
TANGENTIAL VELOCITY, V_θ, ft./sec.

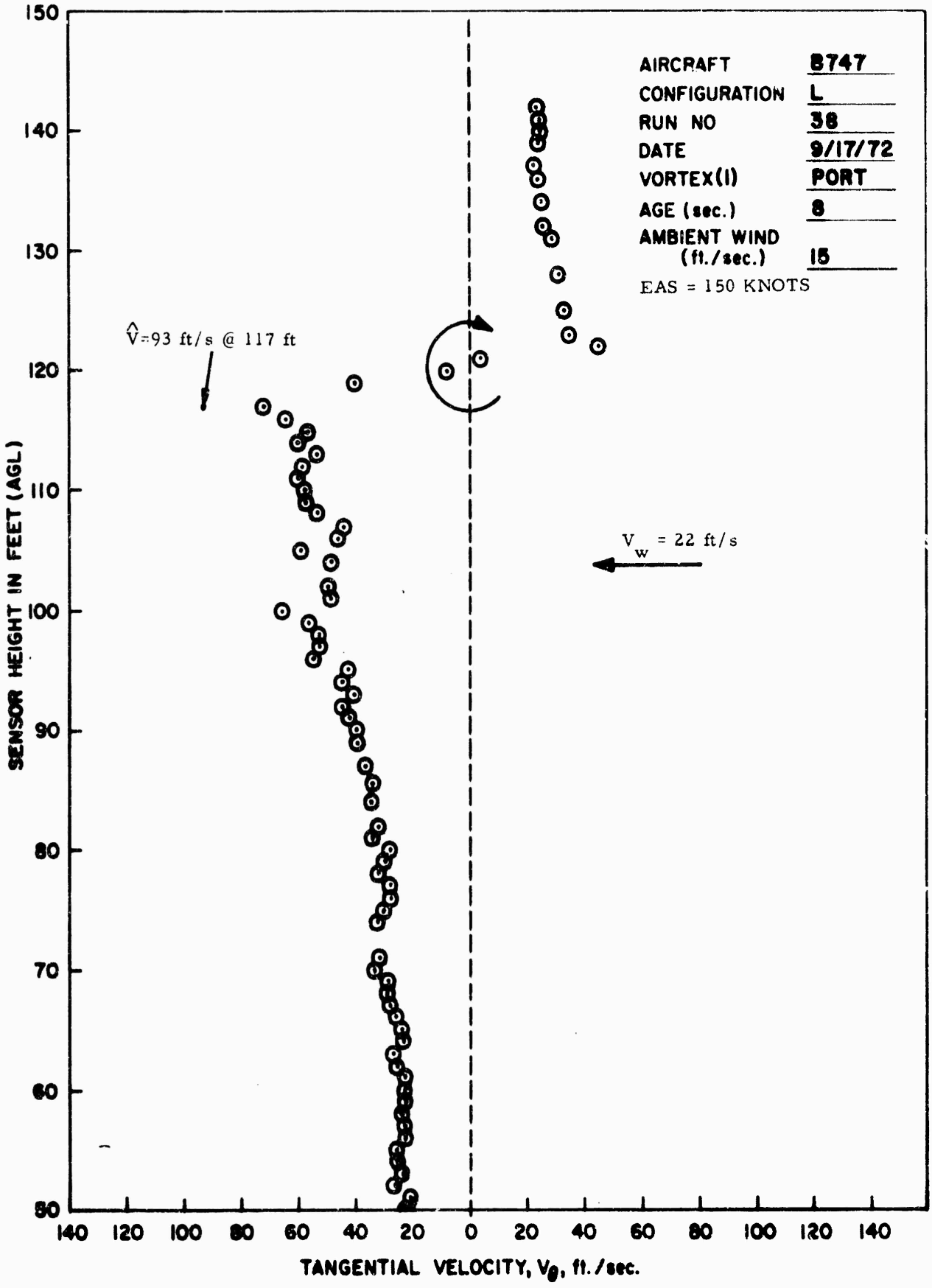
AIRCRAFT B747
CONFIGURATION L
RUN NO 38
DATE 9/17/72
VORTEX(I) PORT
AGE (sec.) 8
AMBIENT WIND (ft./sec.) 15
EAS = 150 KNOTS
$\hat{V}$=93 ft/s @ 117 ft
V_w = 22 ft/s
SENSOR HEIGHT IN FEET (AGL)
150
140
130
120
110
100
90
80
70
60
50
140 120 100 80 60 40 20 0 20 40 60 80 100 120 140
TANGENTIAL VELOCITY, V_θ, ft./sec.

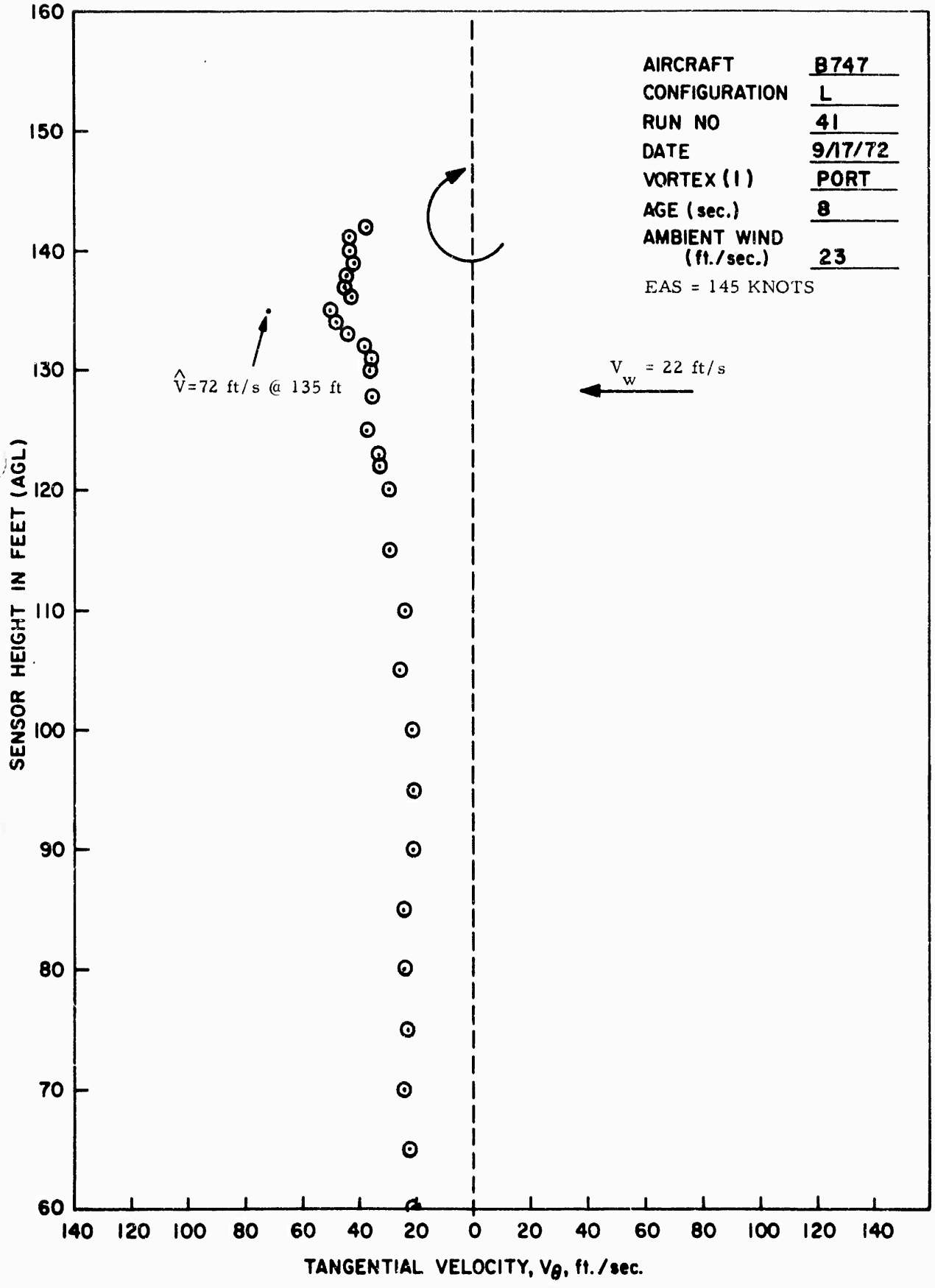
AIRCRAFT B747
CONFIGURATION L
RUN NO 41
DATE 9/17/72
VORTEX (1) PORT
AGE (sec.) 8
AMBIENT WIND (ft./sec.) 23
EAS = 145 KNOTS
V̂=72 ft/s @ 135 ft
V_w = 22 ft/s
SENSOR HEIGHT IN FEET (AGL)
160
150
140
130
120
110
100
90
80
70
60
140 120 100 80 60 40 20 0 20 40 60 80 100 120 140
TANGENTIAL VELOCITY, Vθ, ft./sec.

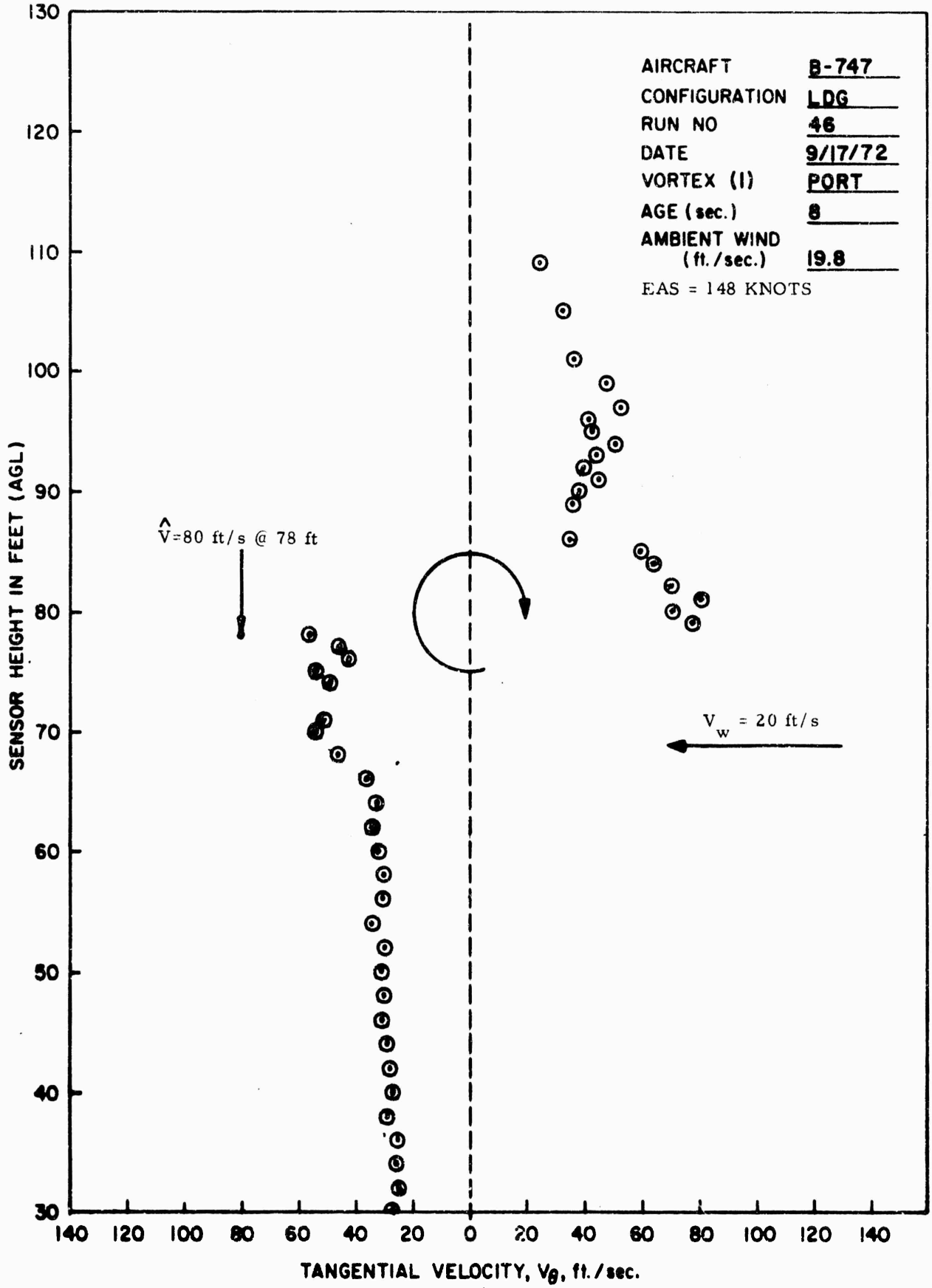
AIRCRAFT B-747
CONFIGURATION LDG
RUN NO 46
DATE 9/17/72
VORTEX (1) PORT
AGE (sec.) 8
AMBIENT WIND (ft./sec.) 19.8
EAS = 148 KNOTS
$\hat{V}$=80 ft/s @ 78 ft
V_w = 20 ft/s
SENSOR HEIGHT IN FEET (AGL)
130
120
110
100
90
80
70
60
50
40
30
140 120 100 80 60 40 20 0 20 40 60 80 100 120 140
TANGENTIAL VELOCITY, V_θ, ft./sec.

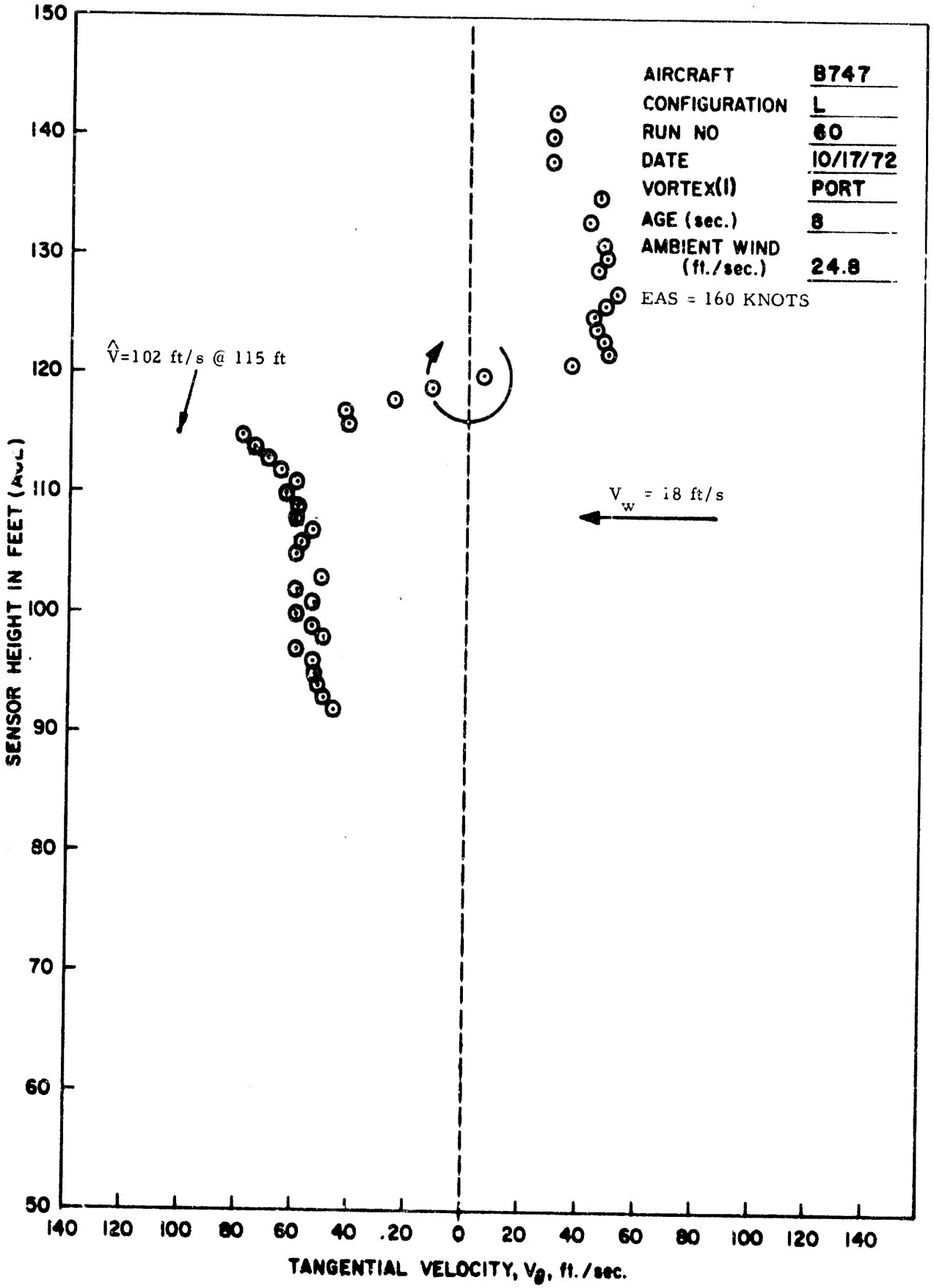
AIRCRAFT B747
CONFIGURATION L
RUN NO 60
DATE 10/17/72
VORTEX(1) PORT
AGE (sec.) 8
AMBIENT WIND (ft./sec.) 24.8
EAS = 160 KNOTS
$\hat{V}$=102 ft/s @ 115 ft
V_w = 18 ft/s
SENSOR HEIGHT IN FEET (AGL)
150
140
130
120
110
100
90
80
70
60
50
140 120 100 80 60 40 20 0 20 40 60 80 100 120 140
TANGENTIAL VELOCITY, V_θ, ft./sec.

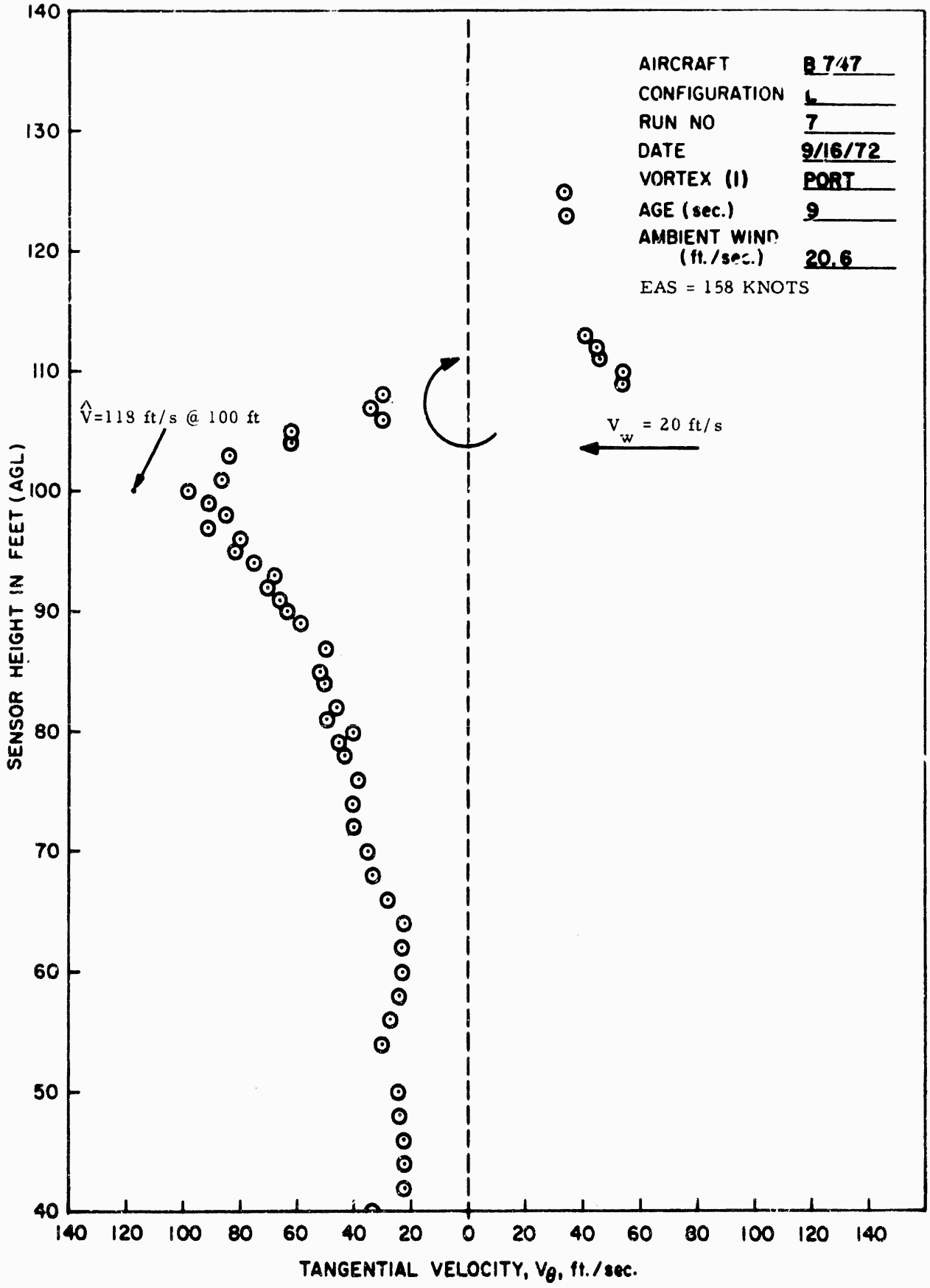
AIRCRAFT B 747
CONFIGURATION L
RUN NO 7
DATE 9/16/72
VORTEX (1) PORT
AGE (sec.) 9
AMBIENT WIND (ft./sec.) 20.6
EAS = 158 KNOTS
$\hat{V}$=118 ft/s @ 100 ft
V_w = 20 ft/s
SENSOR HEIGHT IN FEET (AGL)
140
130
120
110
100
90
80
70
60
50
40
140 120 100 80 60 40 20 0 20 40 60 80 100 120 140
TANGENTIAL VELOCITY, V_θ, ft./sec.

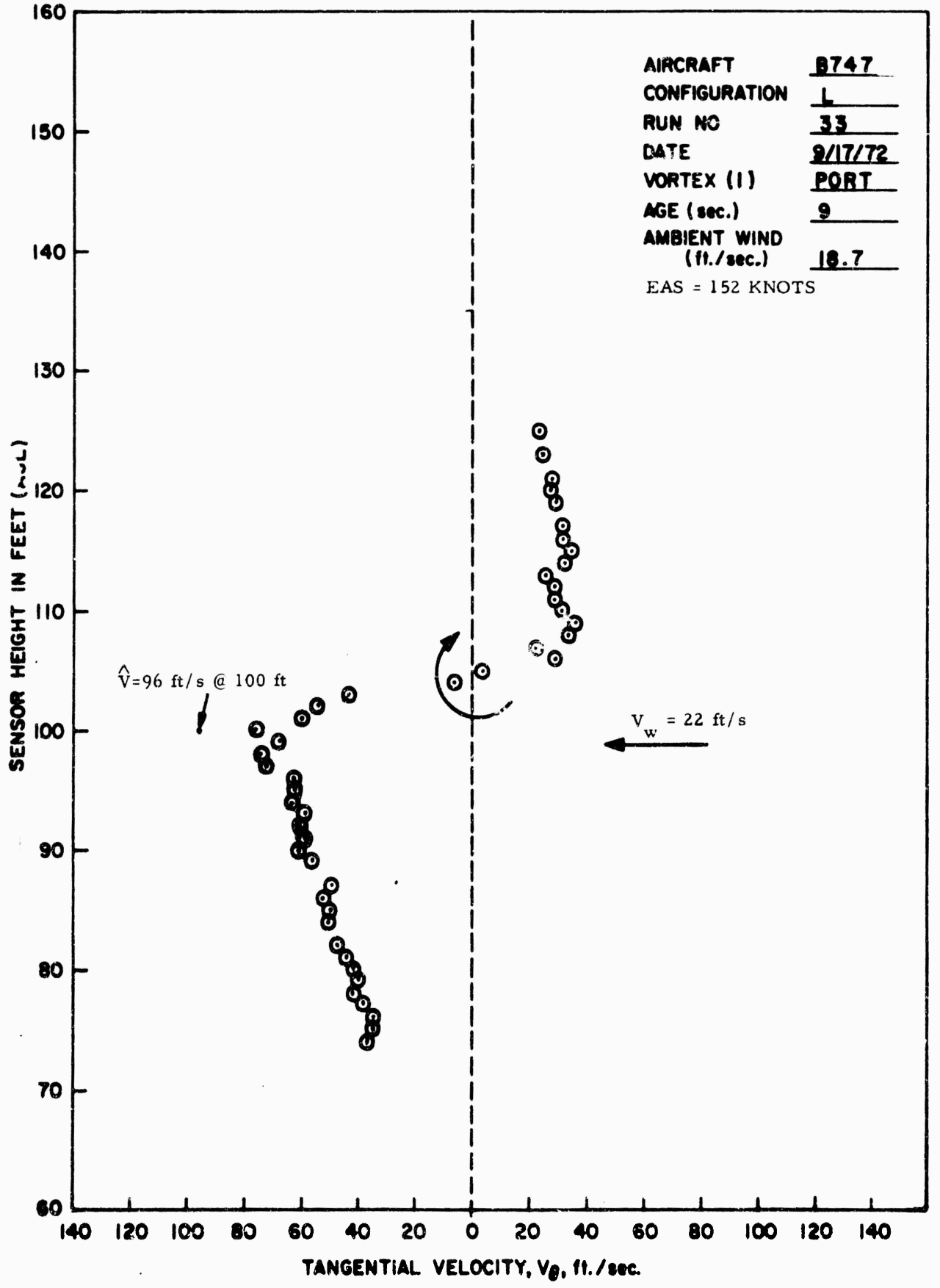
AIRCRAFT B747
CONFIGURATION L
RUN NO 33
DATE 9/17/72
VORTEX (1) PORT
AGE (sec.) 9
AMBIENT WIND (ft./sec.) 18.7
EAS = 152 KNOTS
$\hat{V}$=96 ft/s @ 100 ft
V_w = 22 ft/s
SENSOR HEIGHT IN FEET (AGL)
TANGENTIAL VELOCITY, V_θ, ft./sec.
160
150
140
130
120
110
100
90
80
70
60
140 120 100 80 60 40 20 0 20 40 60 80 100 120 140

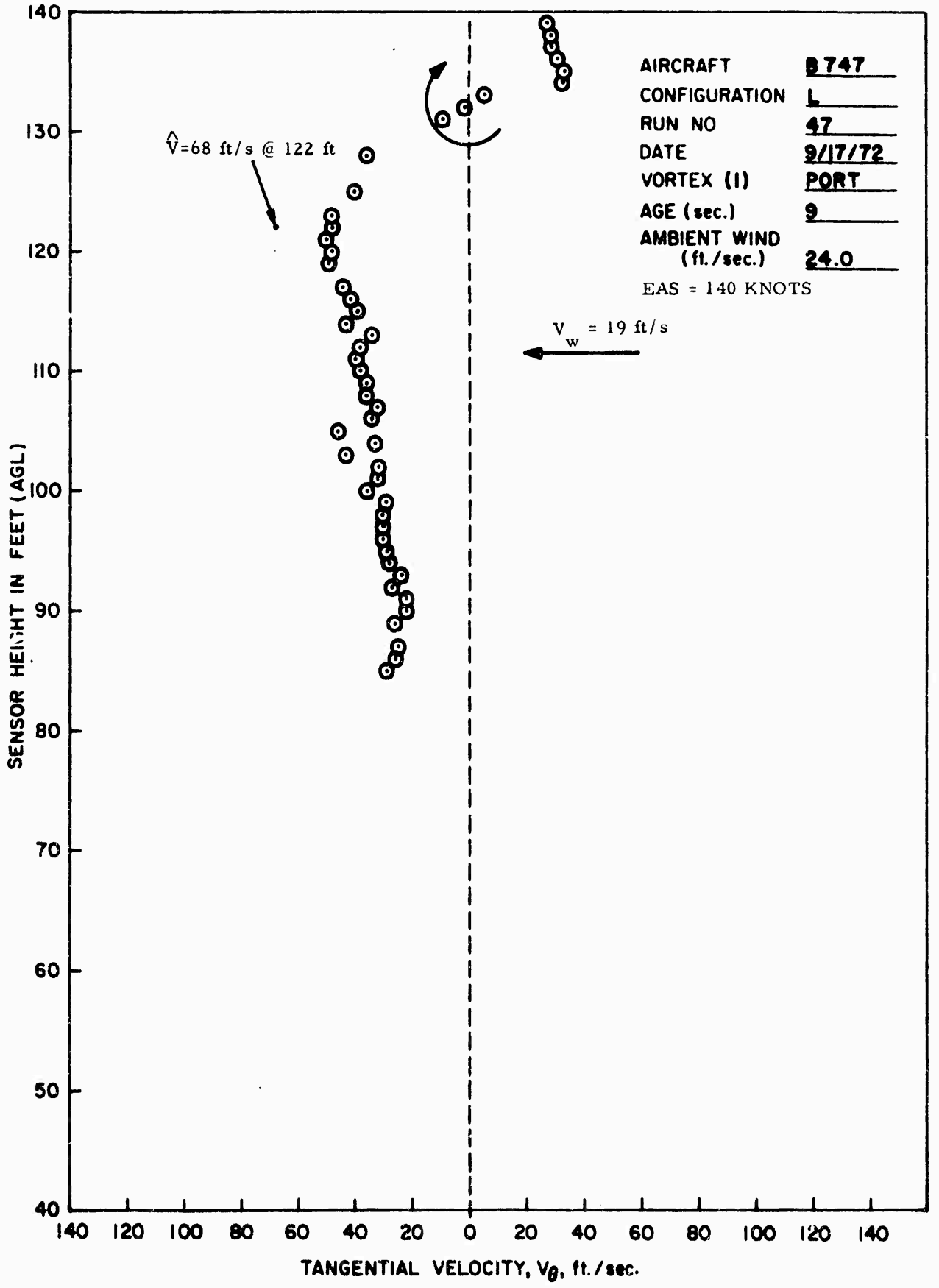
AIRCRAFT B 747
CONFIGURATION L
RUN NO 47
DATE 9/17/72
VORTEX (1) PORT
AGE (sec.) 9
AMBIENT WIND (ft./sec.) 24.0
EAS = 140 KNOTS
$\hat{V}$=68 ft/s @ 122 ft
V_w = 19 ft/s
SENSOR HEIGHT IN FEET (AGL)
140
130
120
110
100
90
80
70
60
50
40
140 120 100 80 60 40 20 0 20 40 60 80 100 120 140
TANGENTIAL VELOCITY, V_θ, ft./sec.

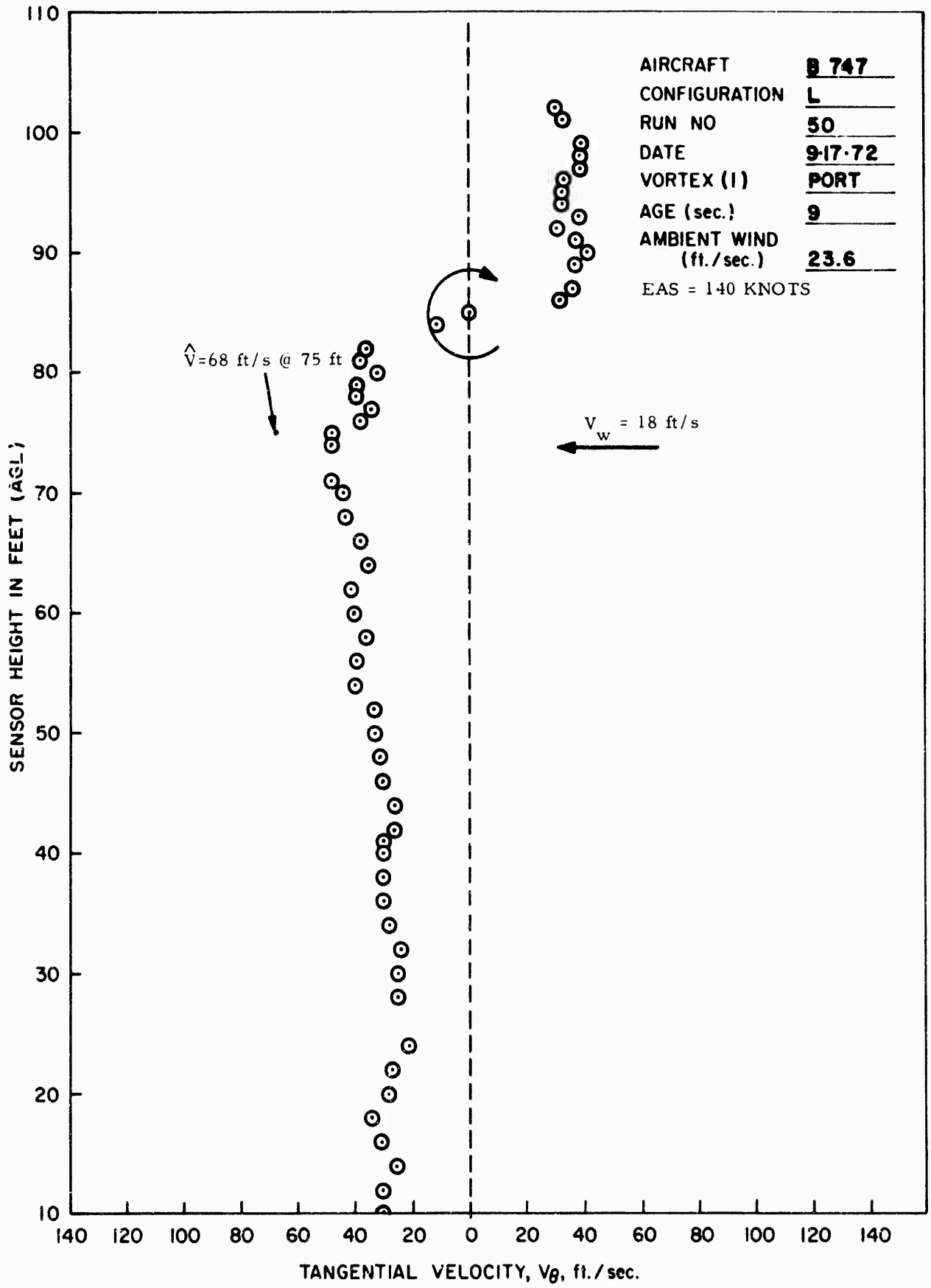
AIRCRAFT B 747
CONFIGURATION L
RUN NO 50
DATE 9-17-72
VORTEX (1) PORT
AGE (sec.) 9
AMBIENT WIND (ft./sec.) 23.6
EAS = 140 KNOTS
V̂=68 ft/s @ 75 ft
V_w = 18 ft/s
SENSOR HEIGHT IN FEET (AGL)
110
100
90
80
70
60
50
40
30
20
10
140 120 100 80 60 40 20 0 20 40 60 80 100 120 140
TANGENTIAL VELOCITY, Vθ, ft./sec.

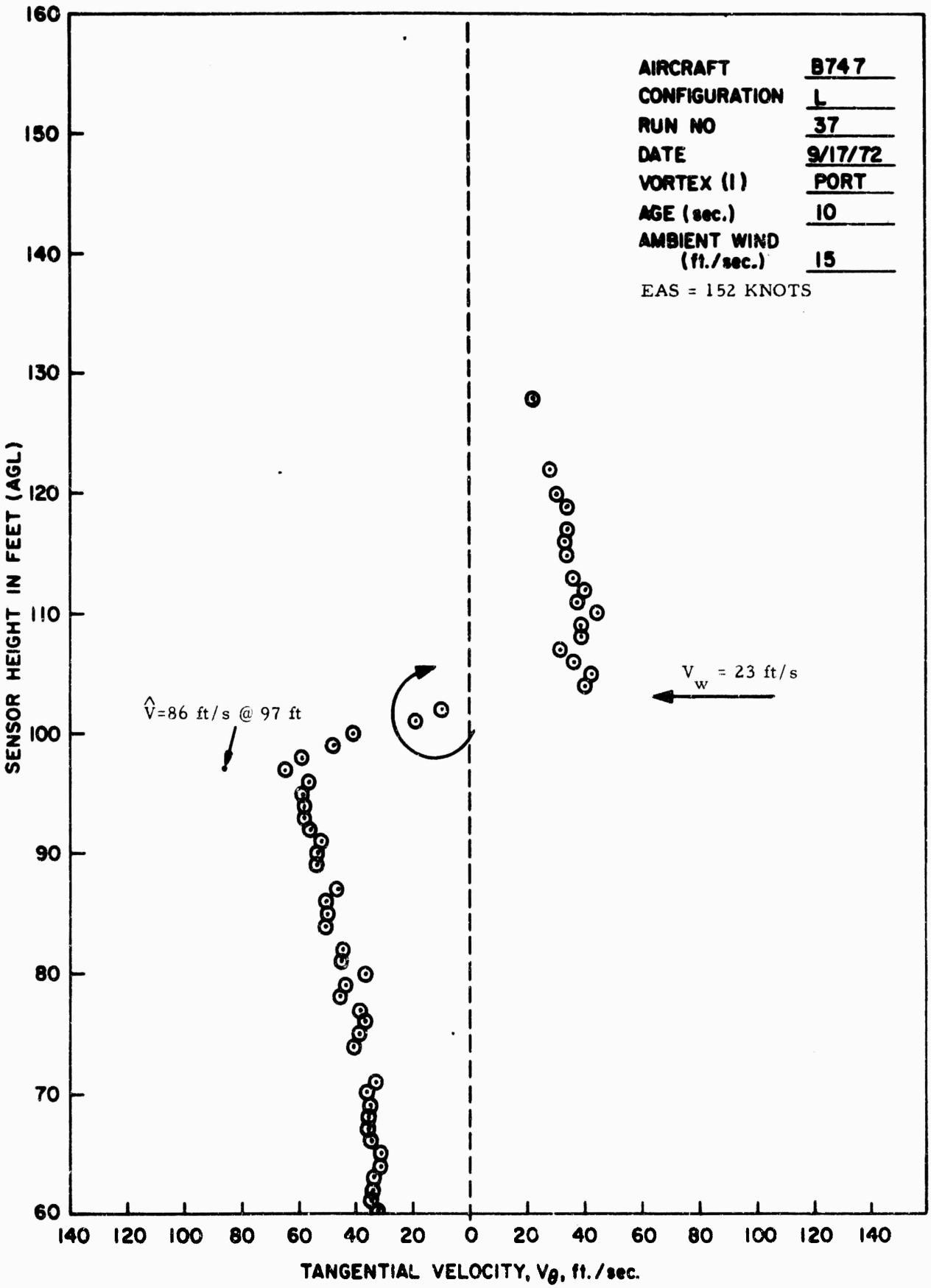
AIRCRAFT B747
CONFIGURATION L
RUN NO 37
DATE 9/17/72
VORTEX (1) PORT
AGE (sec.) 10
AMBIENT WIND (ft./sec.) 15
EAS = 152 KNOTS
$\hat{V}$=86 ft/s @ 97 ft
V_w = 23 ft/s
SENSOR HEIGHT IN FEET (AGL)
160
150
140
130
120
110
100
90
80
70
60
140 120 100 80 60 40 20 0 20 40 60 80 100 120 140
TANGENTIAL VELOCITY, V_θ, ft./sec.

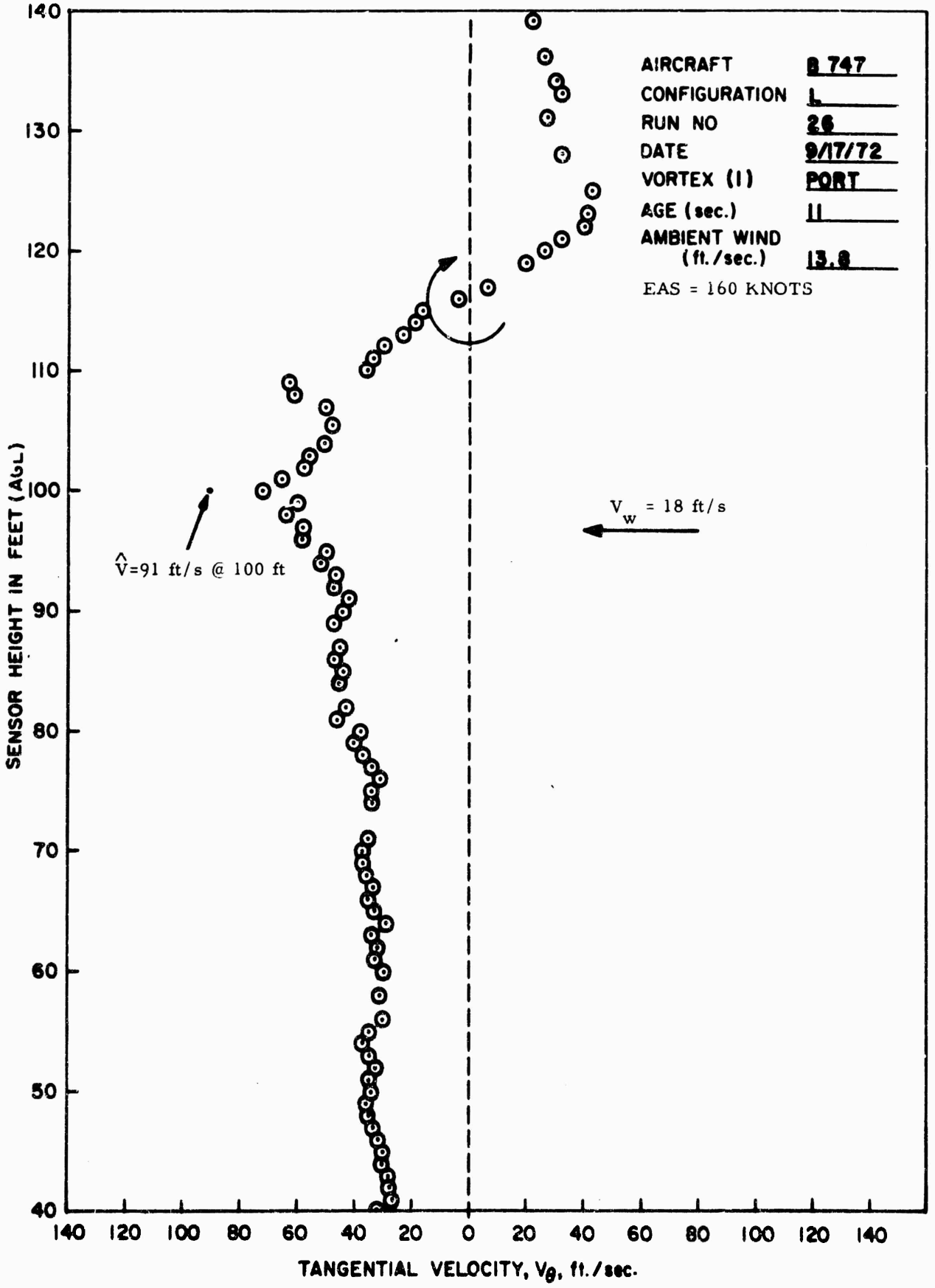
AIRCRAFT B 747
CONFIGURATION L
RUN NO 26
DATE 9/17/72
VORTEX (1) PORT
AGE (sec.) 11
AMBIENT WIND (ft./sec.) 13.8
EAS = 160 KNOTS
V_w = 18 ft/s
$\hat{V}$=91 ft/s @ 100 ft
SENSOR HEIGHT IN FEET (AGL)
TANGENTIAL VELOCITY, V_θ, ft./sec.
140
130
120
110
100
90
80
70
60
50
40
140 120 100 80 60 40 20 0 20 40 60 80 100 120 140

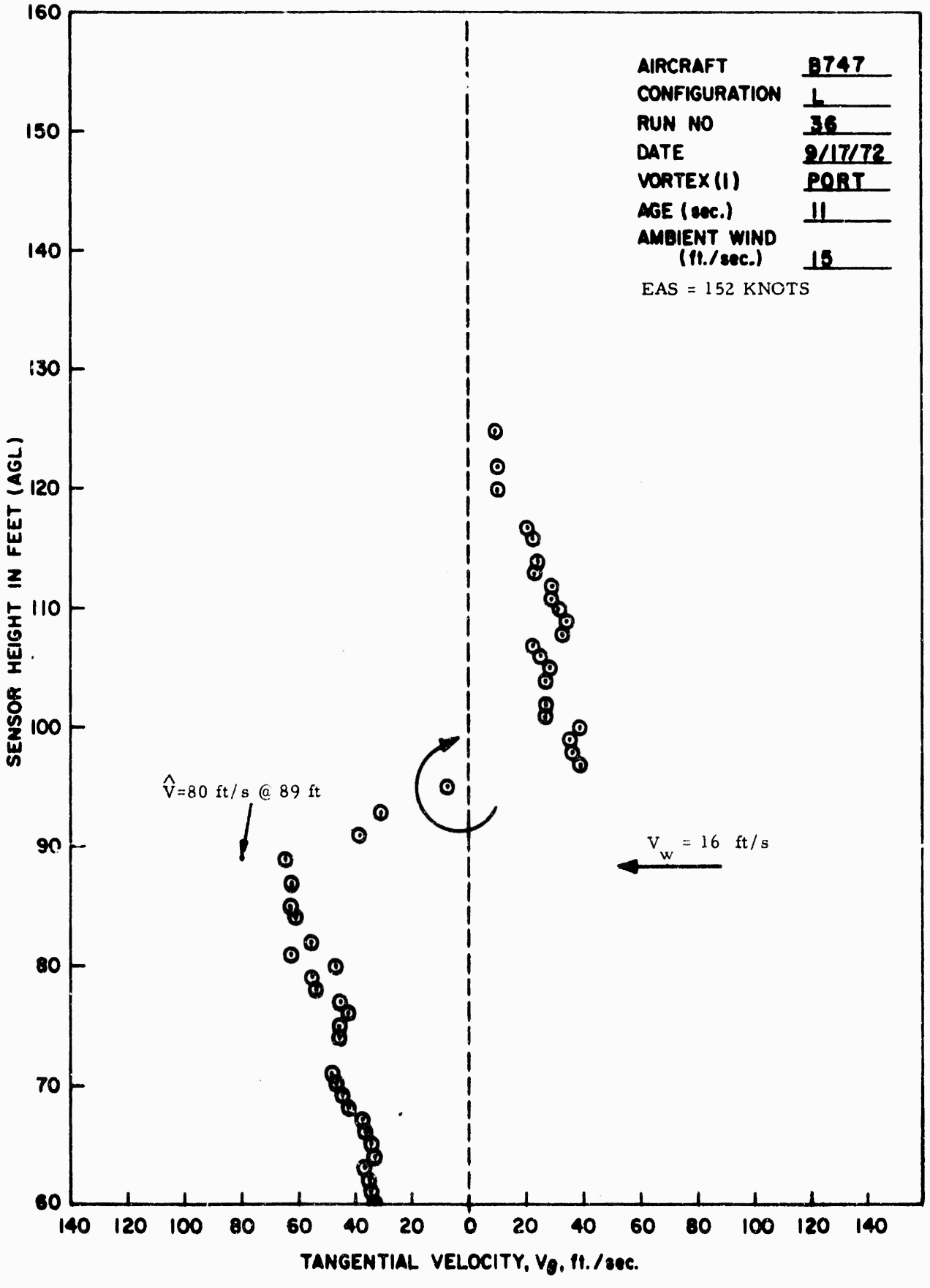
AIRCRAFT B747
CONFIGURATION L
RUN NO 36
DATE 9/17/72
VORTEX (1) PORT
AGE (sec.) 11
AMBIENT WIND (ft./sec.) 15
EAS = 152 KNOTS
$\hat{V}$=80 ft/s @ 89 ft
V_w = 16 ft/s
SENSOR HEIGHT IN FEET (AGL)
TANGENTIAL VELOCITY, V_θ, ft./sec.
160
150
140
130
120
110
100
90
80
70
60
140 120 100 80 60 40 20 0 20 40 60 80 100 120 140

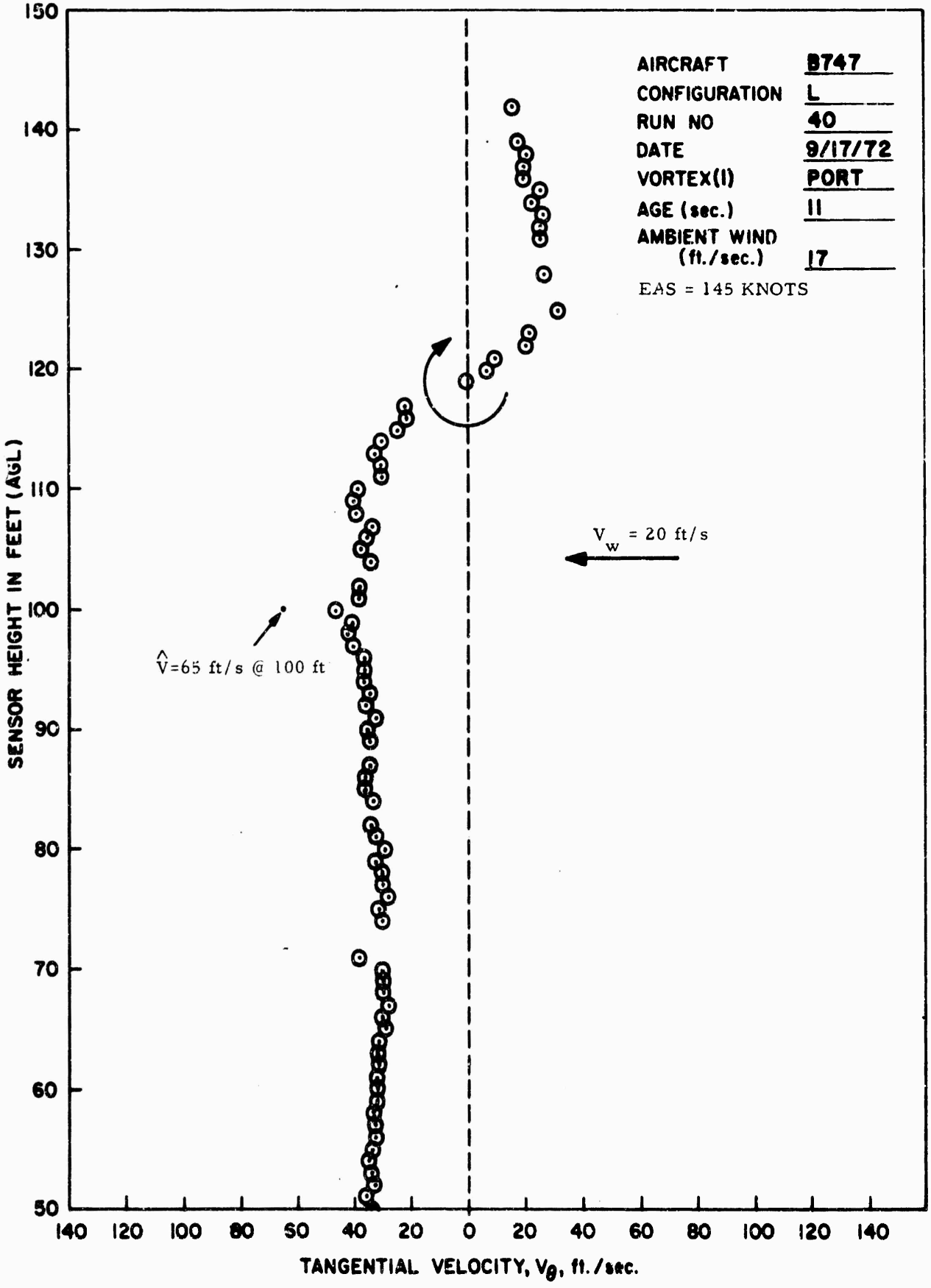
AIRCRAFT B747
CONFIGURATION L
RUN NO 40
DATE 9/17/72
VORTEX(1) PORT
AGE (sec.) 11
AMBIENT WIND (ft./sec.) 17
EAS = 145 KNOTS
V_w = 20 ft/s
$\hat{V}$=65 ft/s @ 100 ft
SENSOR HEIGHT IN FEET (AGL)
150
140
130
120
110
100
90
80
70
60
50
140 120 100 80 50 40 20 0 20 40 60 80 100 120 140
TANGENTIAL VELOCITY, V_θ, ft./sec.

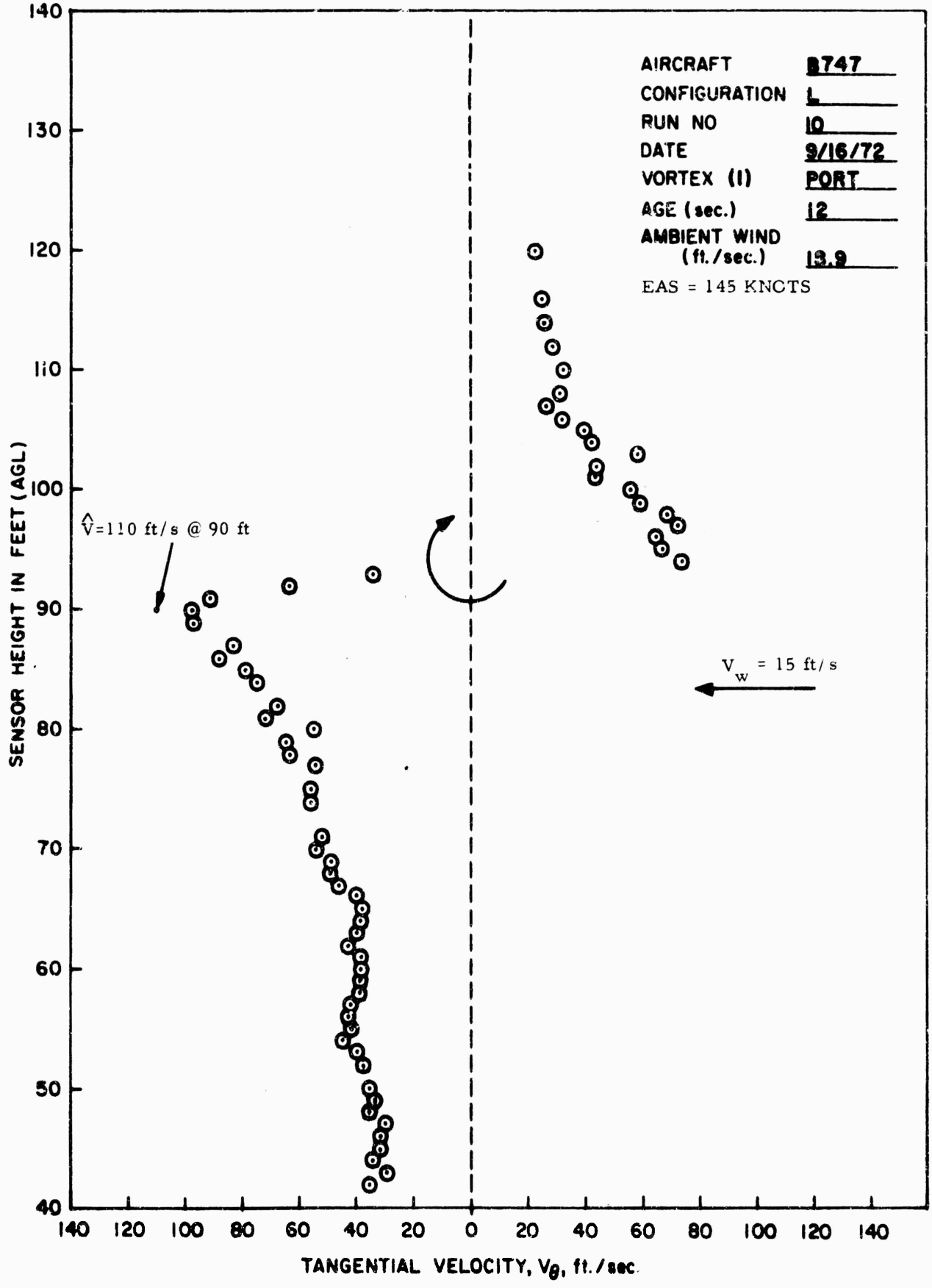
AIRCRAFT B747
CONFIGURATION L
RUN NO 10
DATE 9/16/72
VORTEX (1) PORT
AGE (sec.) 12
AMBIENT WIND (ft./sec.) 13.9
EAS = 145 KNOTS
$\hat{V}$=110 ft/s @ 90 ft
V_w = 15 ft/s
SENSOR HEIGHT IN FEET (AGL)
TANGENTIAL VELOCITY, V_θ, ft./sec.
140
130
120
110
100
90
80
70
60
50
40
140 120 100 80 60 40 20 0 20 40 60 80 100 120 140

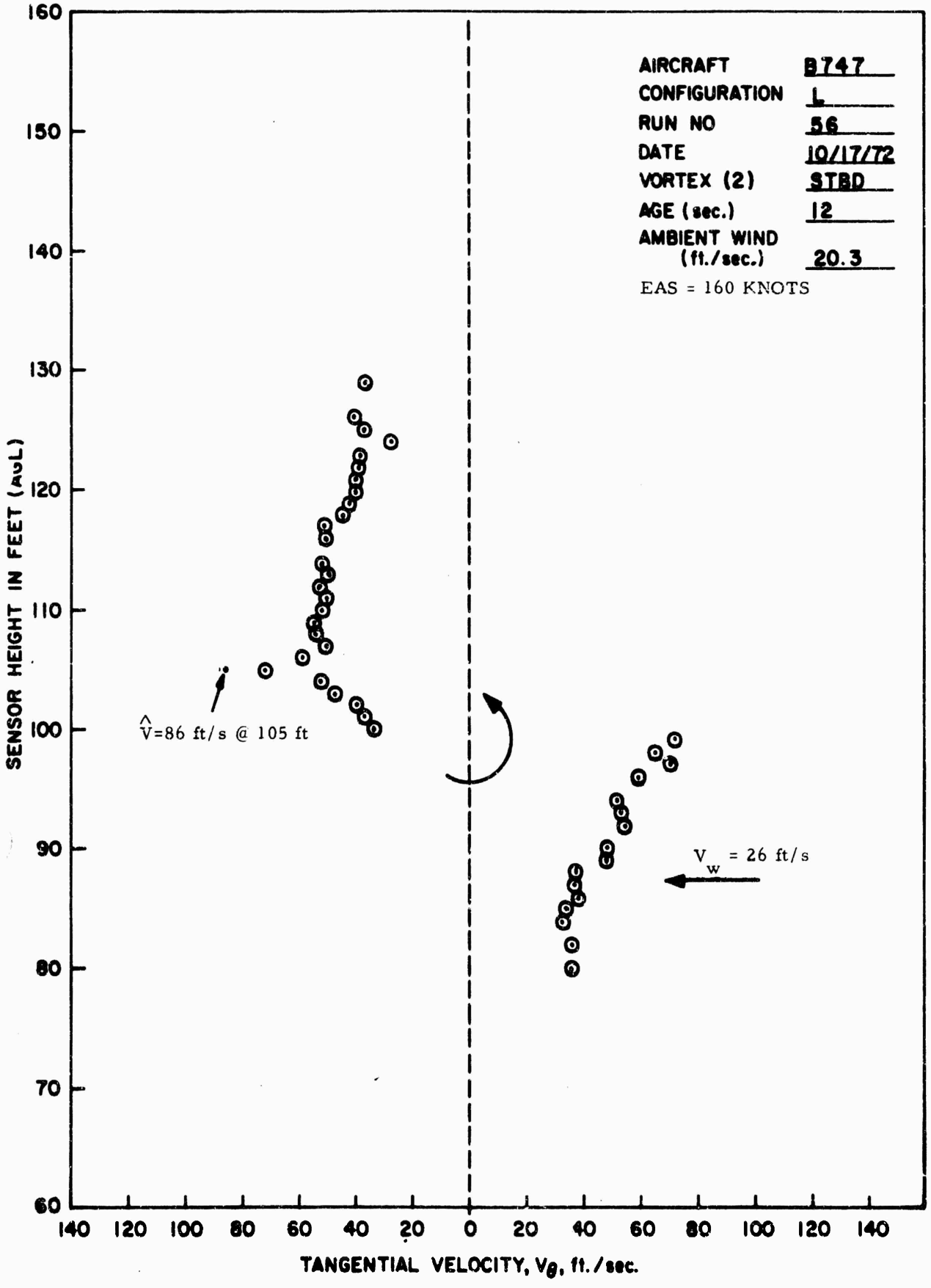
AIRCRAFT B747
CONFIGURATION L
RUN NO 56
DATE 10/17/72
VORTEX (2) STBD
AGE (sec.) 12
AMBIENT WIND (ft./sec.) 20.3
EAS = 160 KNOTS
SENSOR HEIGHT IN FEET (AGL)
160
150
140
130
120
110
100
90
80
70
60
$\hat{V}$=86 ft/s @ 105 ft
V_w = 26 ft/s
140 120 100 80 60 40 20 0 20 40 60 80 100 120 140
TANGENTIAL VELOCITY, V_θ, ft./sec.

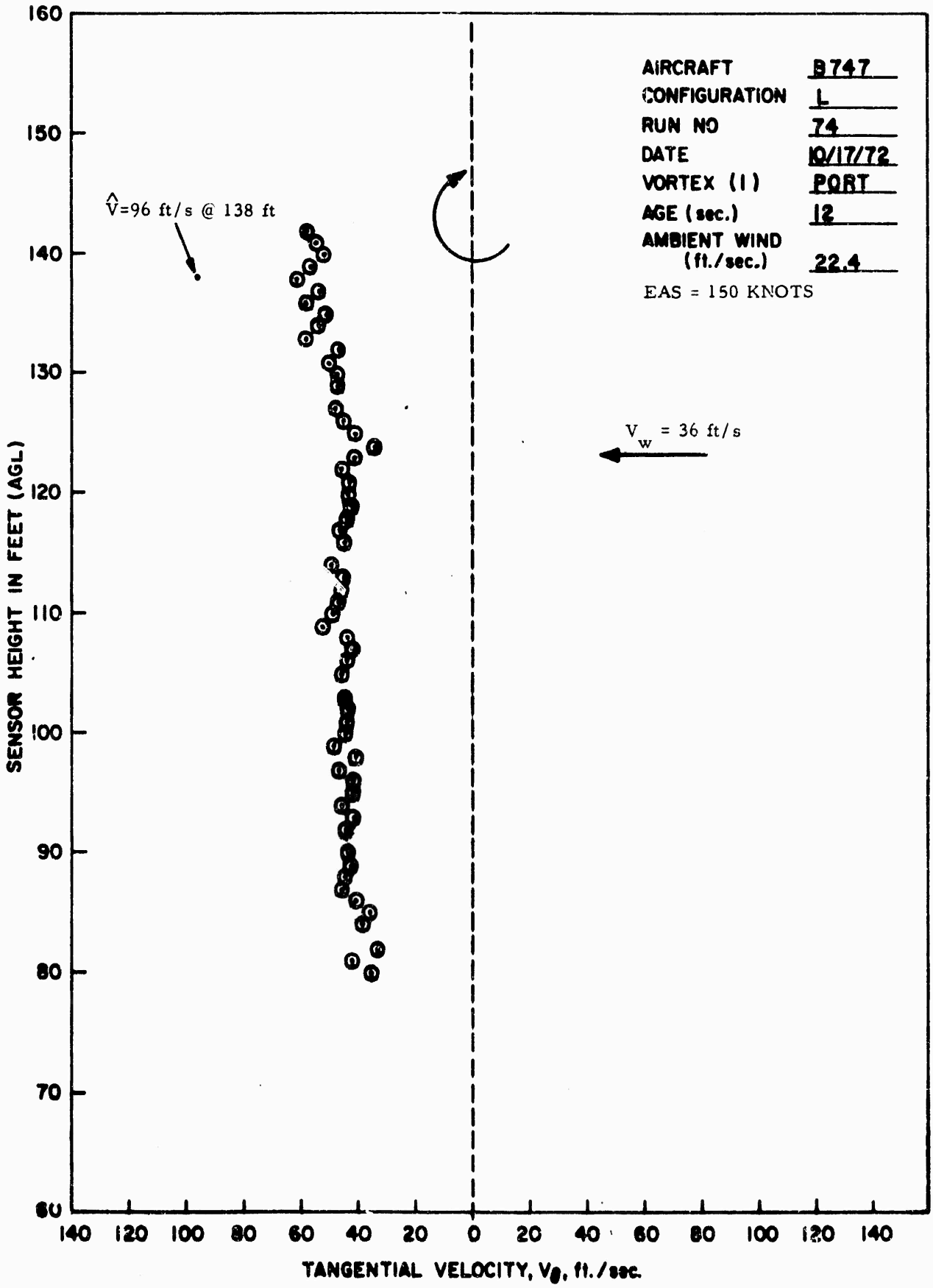
AIRCRAFT B747
CONFIGURATION L
RUN NO 74
DATE 10/17/72
VORTEX (1) PORT
AGE (sec.) 12
AMBIENT WIND (ft./sec.) 22.4
EAS = 150 KNOTS
$\hat{V}$=96 ft/s @ 138 ft
V_w = 36 ft/s
SENSOR HEIGHT IN FEET (AGL)
160
150
140
130
120
110
100
90
80
70
60
140 120 100 80 60 40 20 0 20 40 60 80 100 120 140
TANGENTIAL VELOCITY, V_θ, ft./sec.

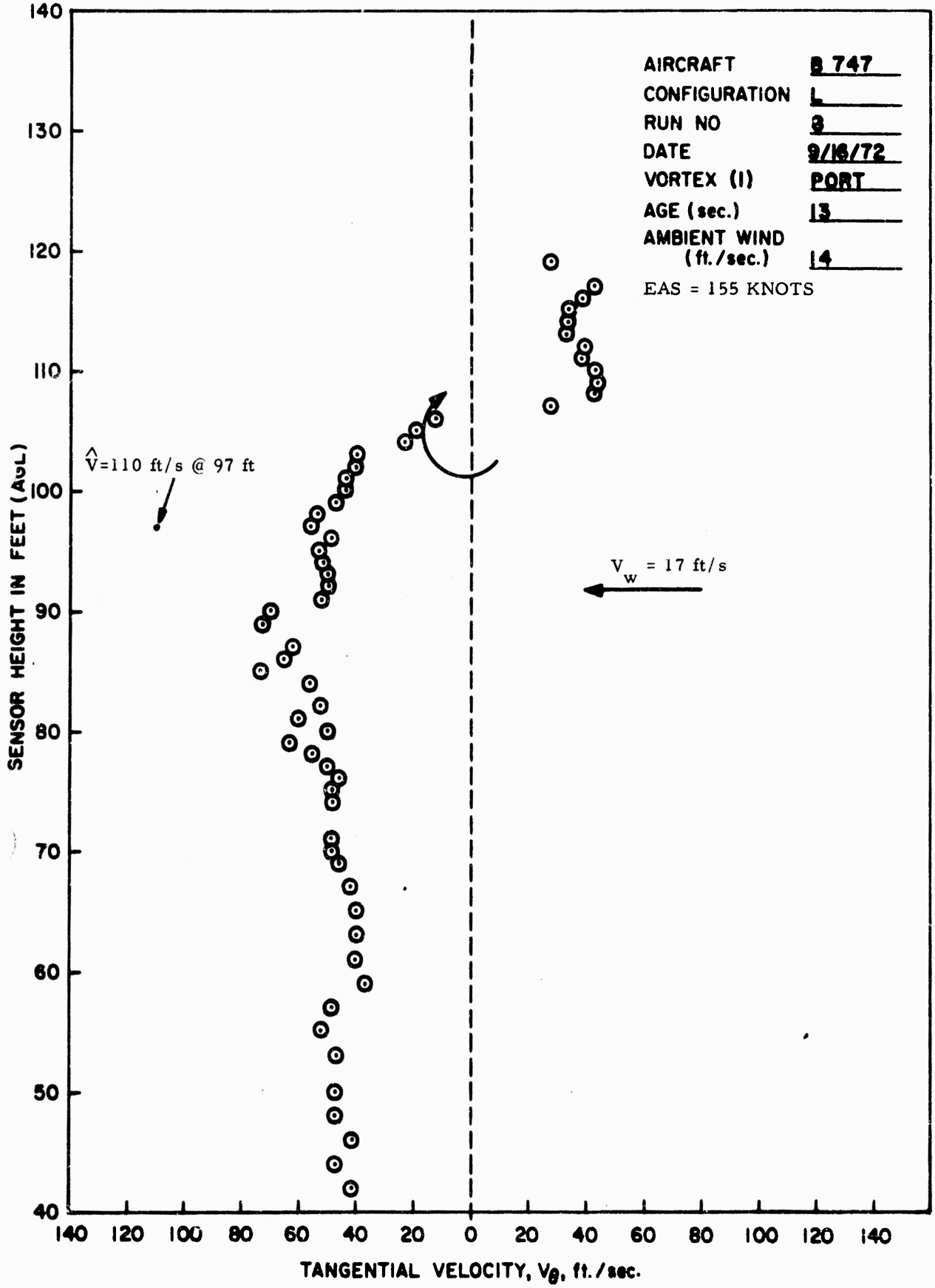
AIRCRAFT B 747
CONFIGURATION L
RUN NO 8
DATE 9/16/72
VORTEX (1) PORT
AGE (sec.) 13
AMBIENT WIND (ft./sec.) 14
EAS = 155 KNOTS
$\hat{V}$=110 ft/s @ 97 ft
V_w = 17 ft/s
SENSOR HEIGHT IN FEET (AGL)
140
130
120
110
100
90
80
70
60
50
40
140 120 100 80 60 40 20 0 20 40 60 80 100 120 140
TANGENTIAL VELOCITY, V_θ, ft./sec.

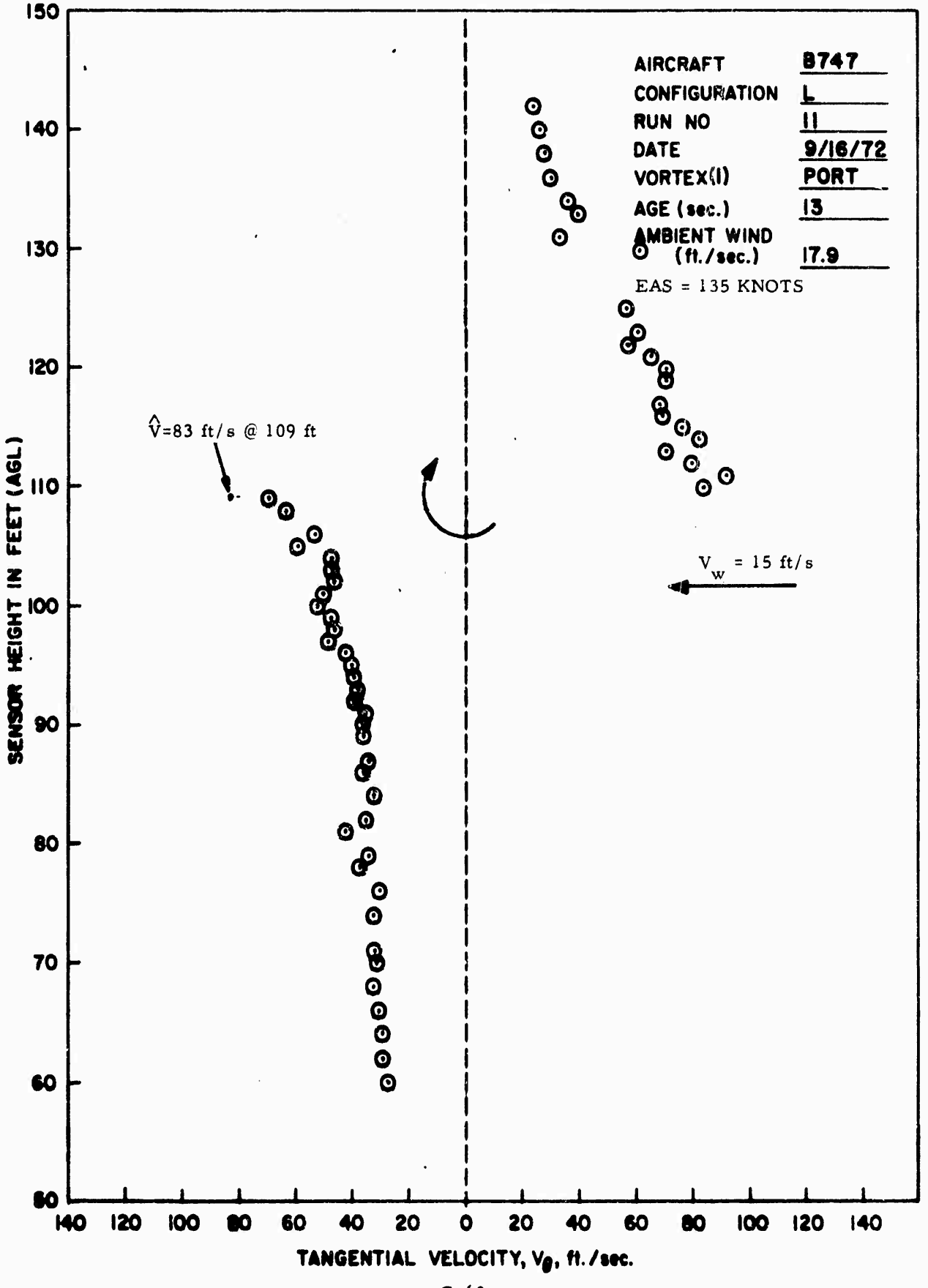
AIRCRAFT 8747
CONFIGURATION L
RUN NO 11
DATE 9/16/72
VORTEX(1) PORT
AGE (sec.) 13
AMBIENT WIND (ft./sec.) 17.9
EAS = 135 KNOTS
$\hat{V}$=83 ft/s @ 109 ft
V_w = 15 ft/s
SENSOR HEIGHT IN FEET (AGL)
150
140
130
120
110
100
90
80
70
60
50
140 120 100 80 60 40 20 0 20 40 60 80 100 120 140
TANGENTIAL VELOCITY, V_θ, ft./sec.

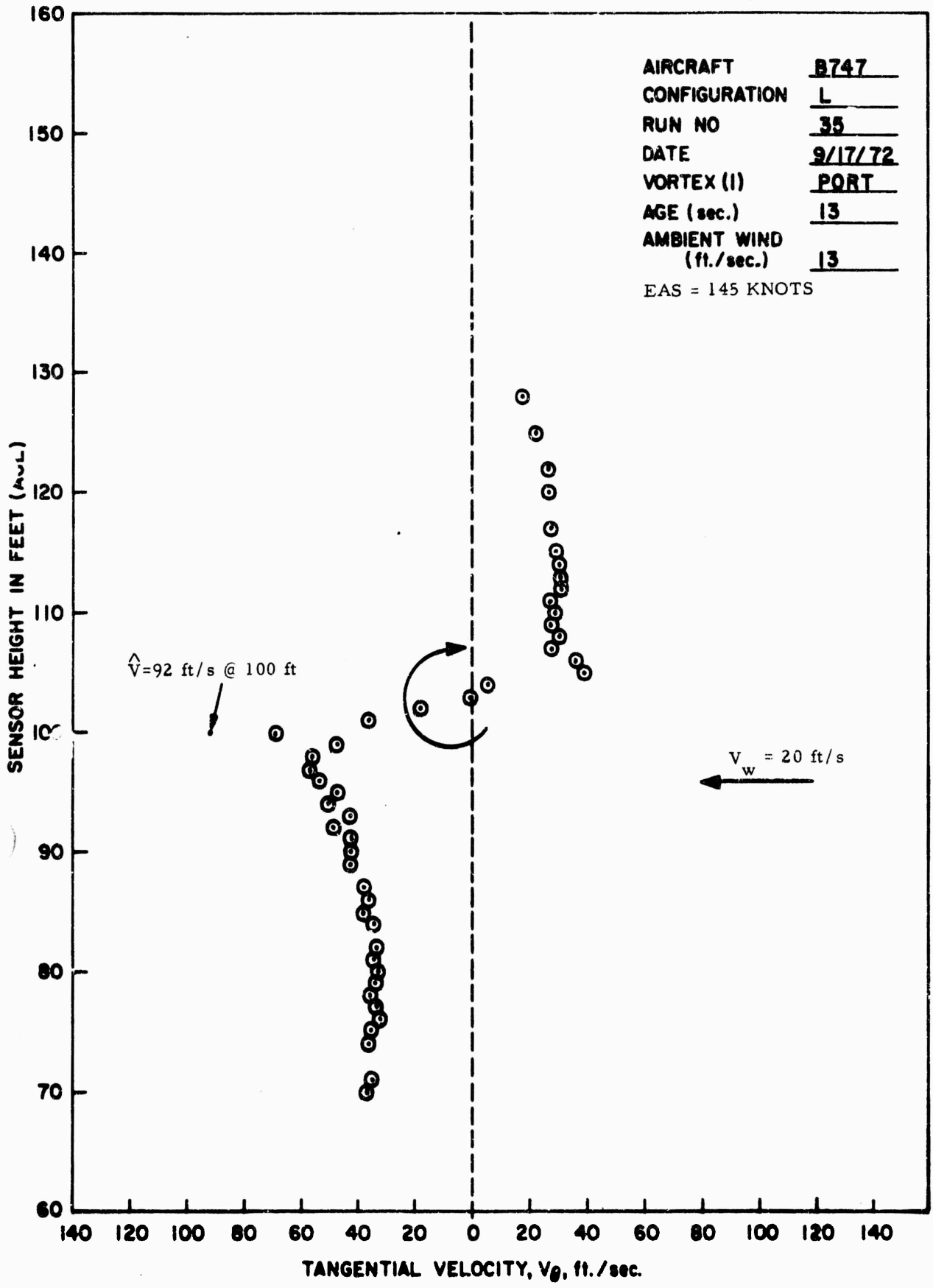
AIRCRAFT B747
CONFIGURATION L
RUN NO 35
DATE 9/17/72
VORTEX (I) PORT
AGE (sec.) 13
AMBIENT WIND (ft./sec.) 13
EAS = 145 KNOTS
$\hat{V}$=92 ft/s @ 100 ft
V_w = 20 ft/s
SENSOR HEIGHT IN FEET (AGL)
TANGENTIAL VELOCITY, V_θ, ft./sec.
160
150
140
130
120
110
100
90
80
70
60
140 120 100 80 60 40 20 0 20 40 60 80 100 120 140

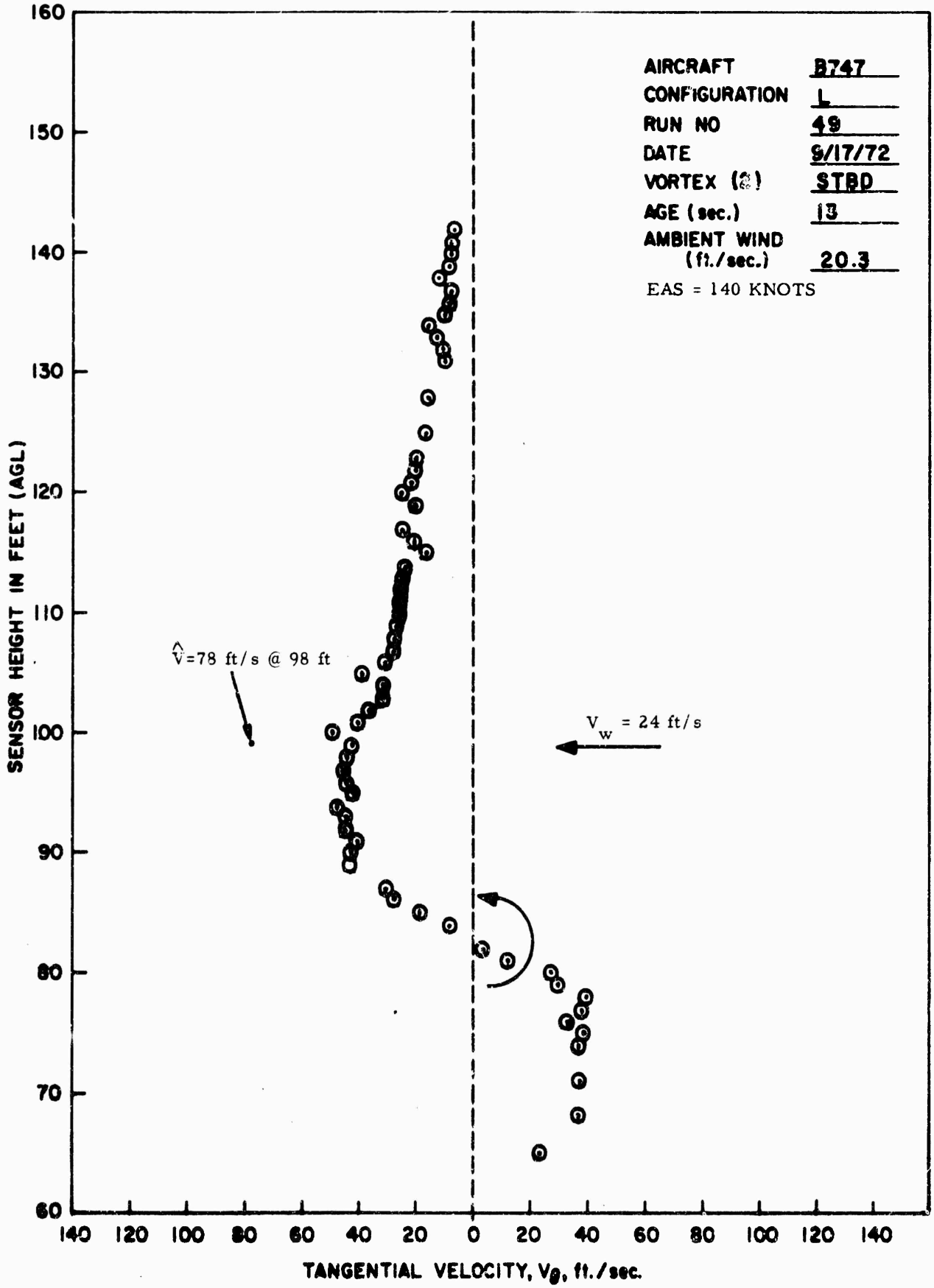
AIRCRAFT B747
CONFIGURATION L
RUN NO 49
DATE 9/17/72
VORTEX (2) STBD
AGE (sec.) 13
AMBIENT WIND (ft./sec.) 20.3
EAS = 140 KNOTS
$\hat{V}$=78 ft/s @ 98 ft
V_w = 24 ft/s
SENSOR HEIGHT IN FEET (AGL)
160
150
140
130
120
110
100
90
80
70
60
140 120 100 80 60 40 20 0 20 40 60 80 100 120 140
TANGENTIAL VELOCITY, V_θ, ft./sec.

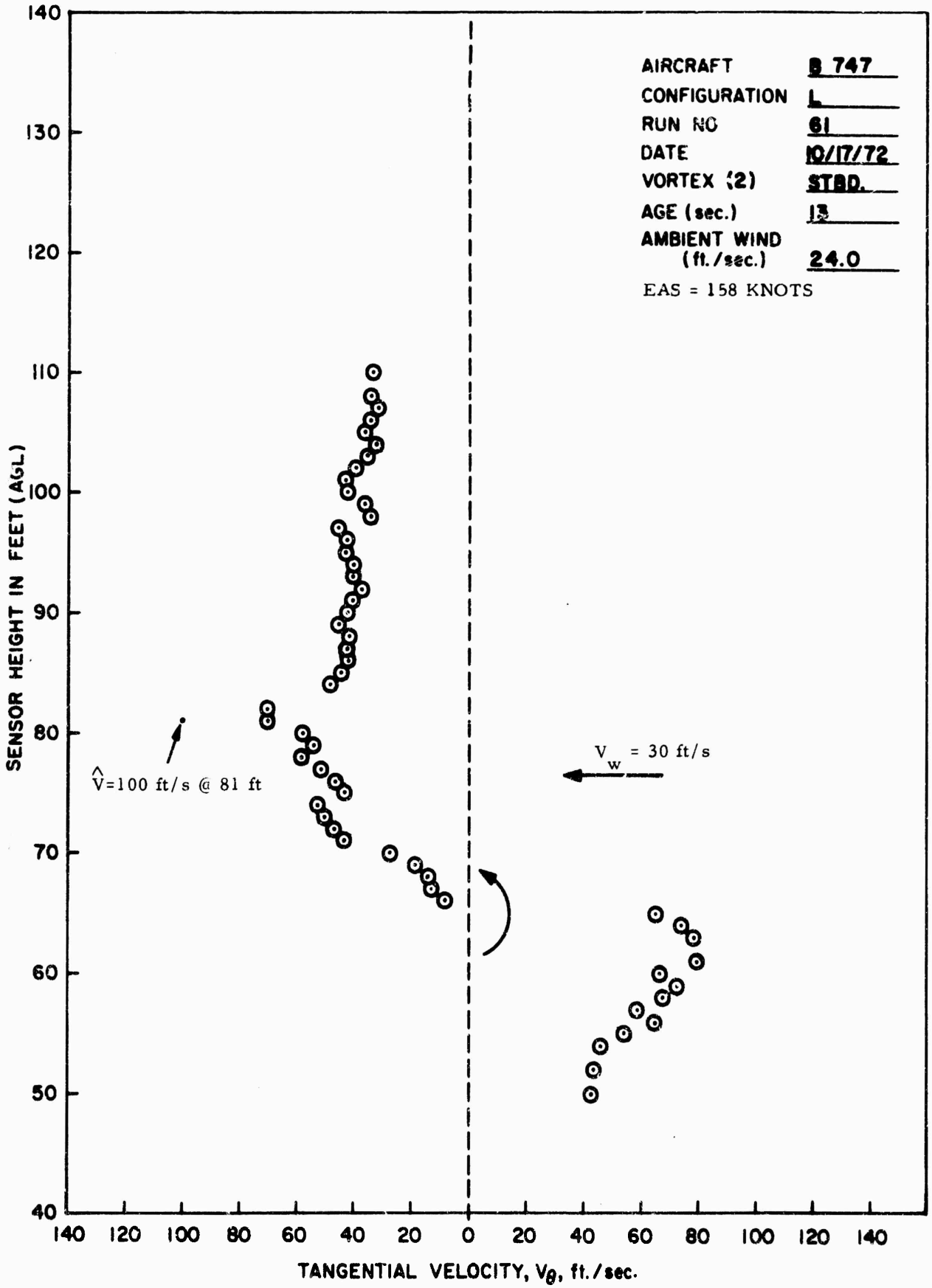
AIRCRAFT B 747
CONFIGURATION L
RUN NO 61
DATE 10/17/72
VORTEX (2) STBD.
AGE (sec.) 13
AMBIENT WIND (ft./sec.) 24.0
EAS = 158 KNOTS
$\hat{V}$=100 ft/s @ 81 ft
V_w = 30 ft/s
SENSOR HEIGHT IN FEET (AGL)
TANGENTIAL VELOCITY, V_θ, ft./sec.
140
130
120
110
100
90
80
70
60
50
40
140 120 100 80 60 40 20 0 20 40 60 80 100 120 140

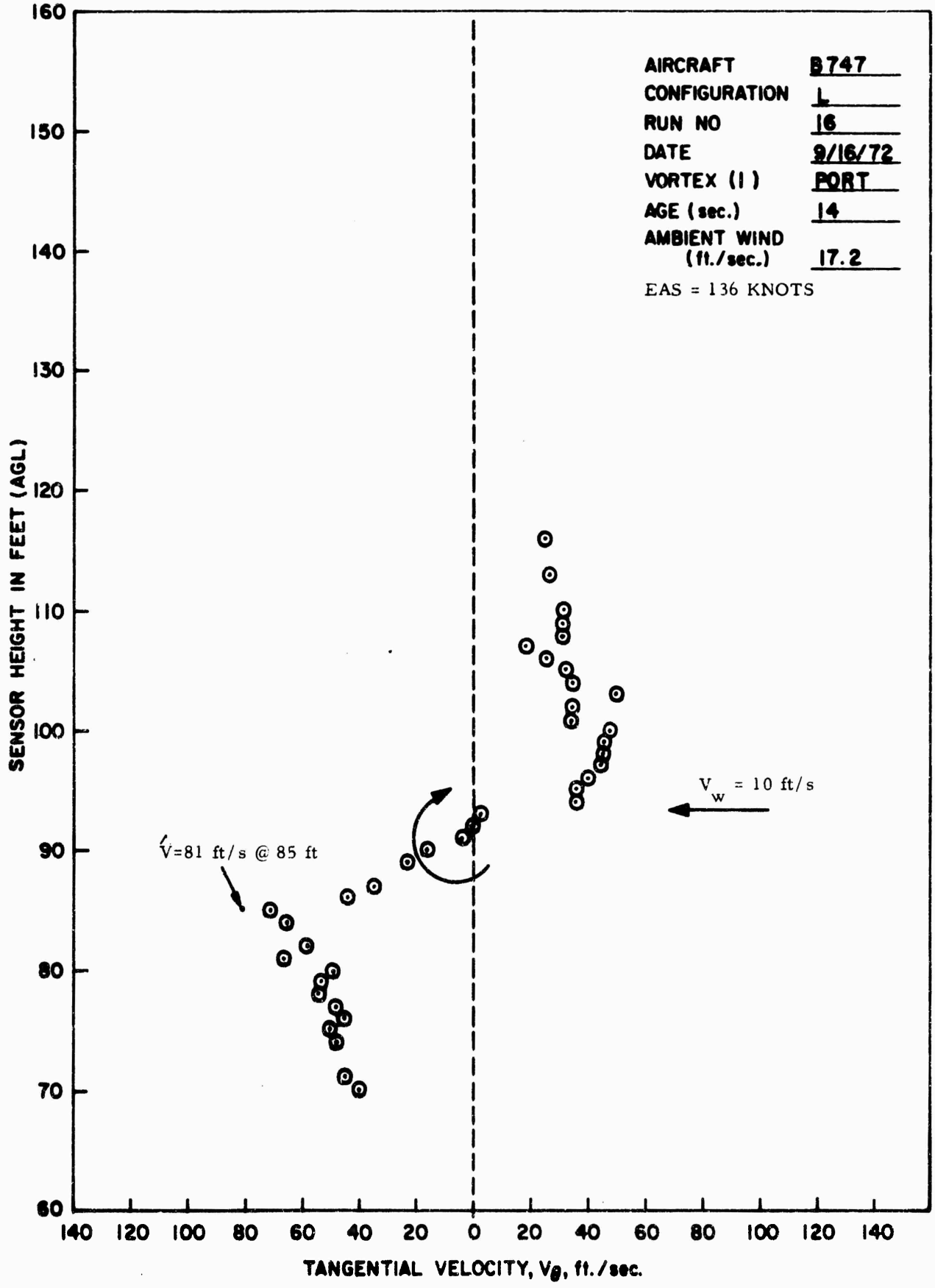
AIRCRAFT B747
CONFIGURATION L
RUN NO 16
DATE 9/16/72
VORTEX (1) PORT
AGE (sec.) 14
AMBIENT WIND (ft./sec.) 17.2
EAS = 136 KNOTS
SENSOR HEIGHT IN FEET (AGL)
160
150
140
130
120
110
100
90
80
70
60
V=81 ft/s @ 85 ft
V_w = 10 ft/s
140 120 100 80 60 40 20 0 20 40 60 80 100 120 140
TANGENTIAL VELOCITY, V_θ, ft./sec.

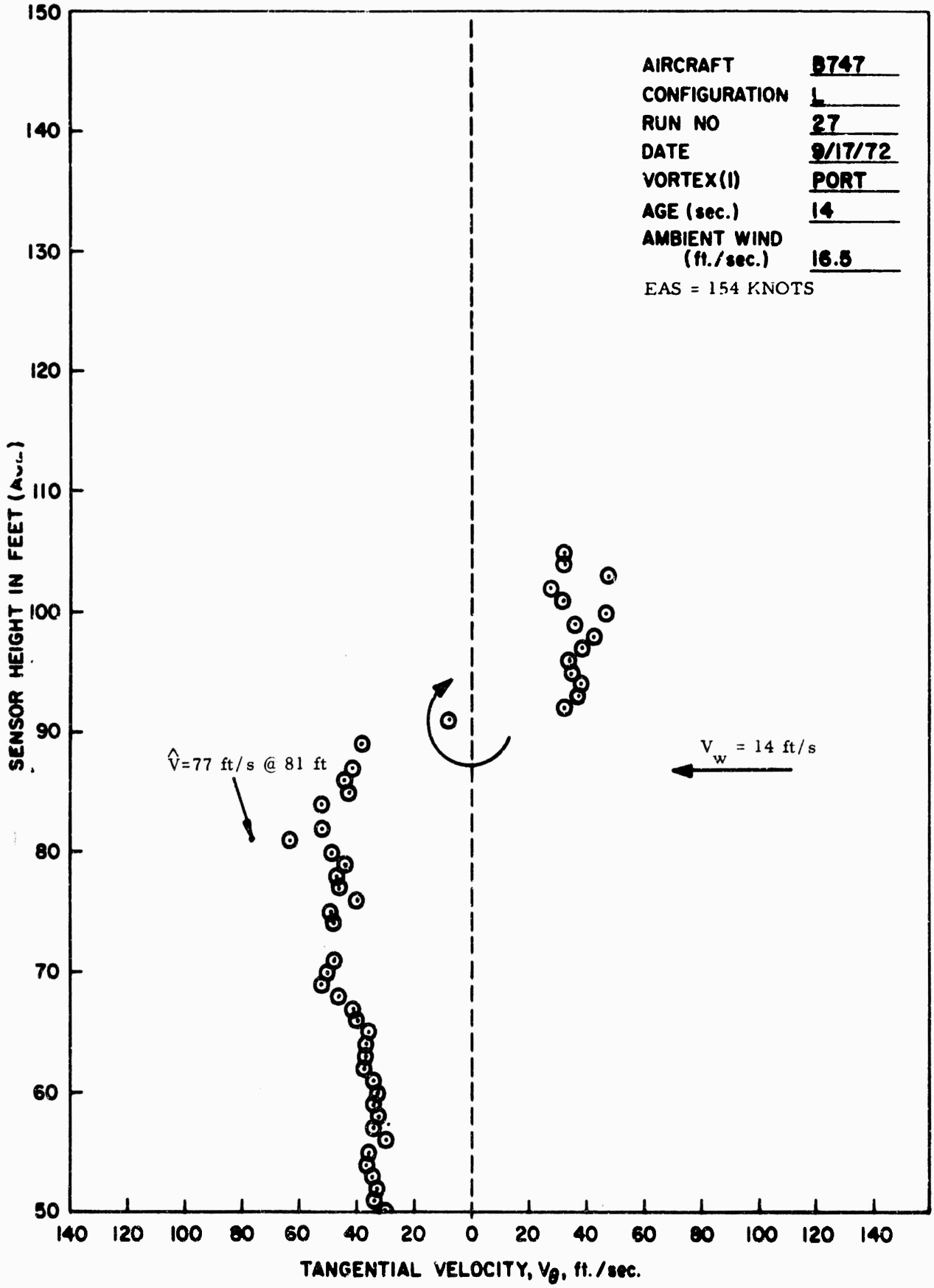
AIRCRAFT B747
CONFIGURATION L
RUN NO 27
DATE 9/17/72
VORTEX(1) PORT
AGE (sec.) 14
AMBIENT WIND (ft./sec.) 16.5
EAS = 154 KNOTS
$\hat{V}$=77 ft/s @ 81 ft
V_w = 14 ft/s
SENSOR HEIGHT IN FEET (AGL)
TANGENTIAL VELOCITY, V_θ, ft./sec.
150
140
130
120
110
100
90
80
70
60
50
140 120 100 80 60 40 20 0 20 40 60 80 100 120 140

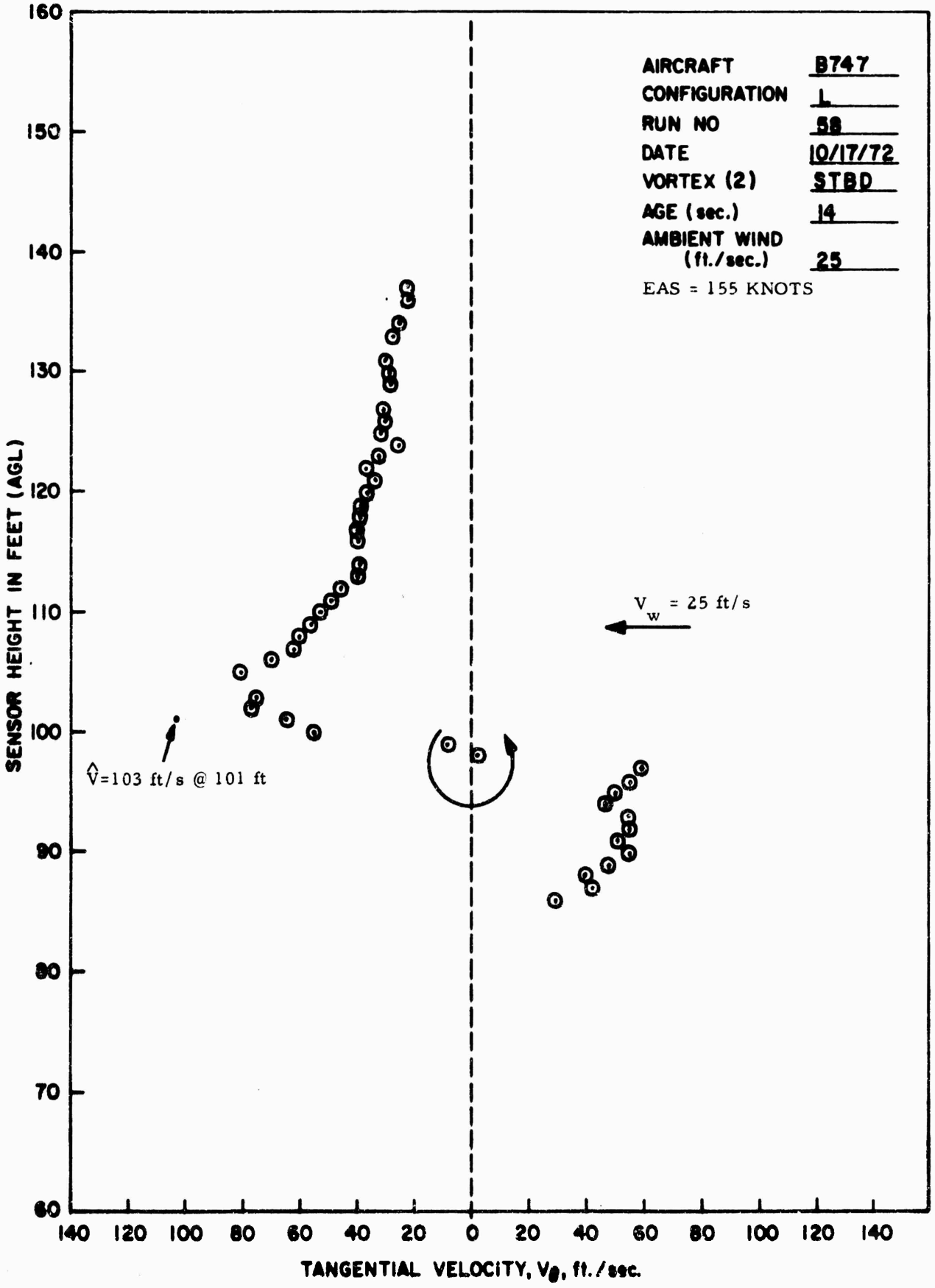
AIRCRAFT B747
CONFIGURATION L
RUN NO 58
DATE 10/17/72
VORTEX (2) STBD
AGE (sec.) 14
AMBIENT WIND (ft./sec.) 25
EAS = 155 KNOTS
V_w = 25 ft/s
$\hat{V}$=103 ft/s @ 101 ft
SENSOR HEIGHT IN FEET (AGL)
160
150
140
130
120
110
100
90
80
70
60
140 120 100 80 60 40 20 0 20 40 60 80 100 120 140
TANGENTIAL VELOCITY, V_θ, ft./sec.

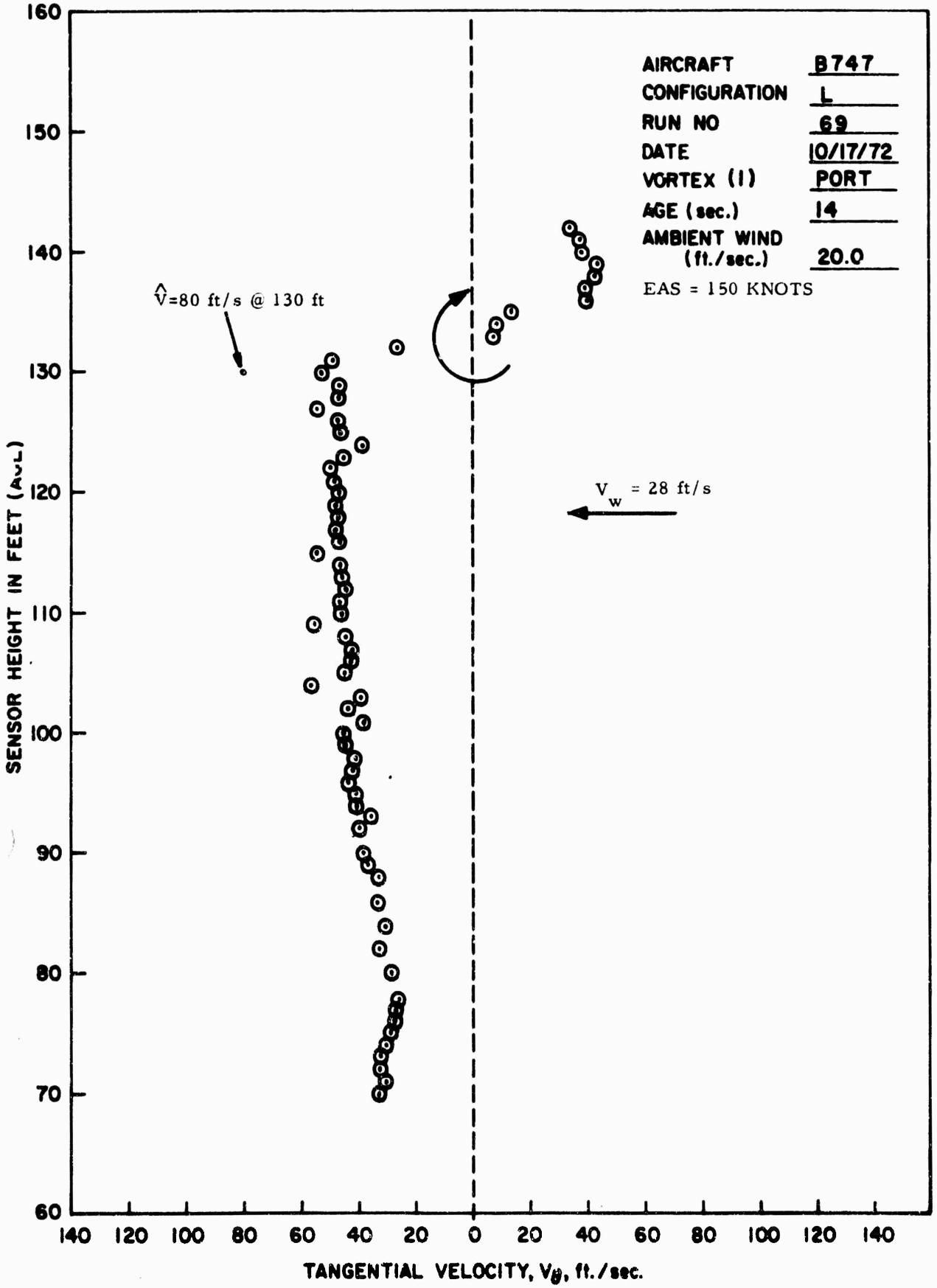
AIRCRAFT B747
CONFIGURATION L
RUN NO 69
DATE 10/17/72
VORTEX (1) PORT
AGE (sec.) 14
AMBIENT WIND (ft./sec.) 20.0
EAS = 150 KNOTS
$\hat{V}$=80 ft/s @ 130 ft
V_w = 28 ft/s
SENSOR HEIGHT IN FEET (AGL)
160
150
140
130
120
110
100
90
80
70
60
140 120 100 80 60 40 20 0 20 40 60 80 100 120 140
TANGENTIAL VELOCITY, V_θ, ft./sec.

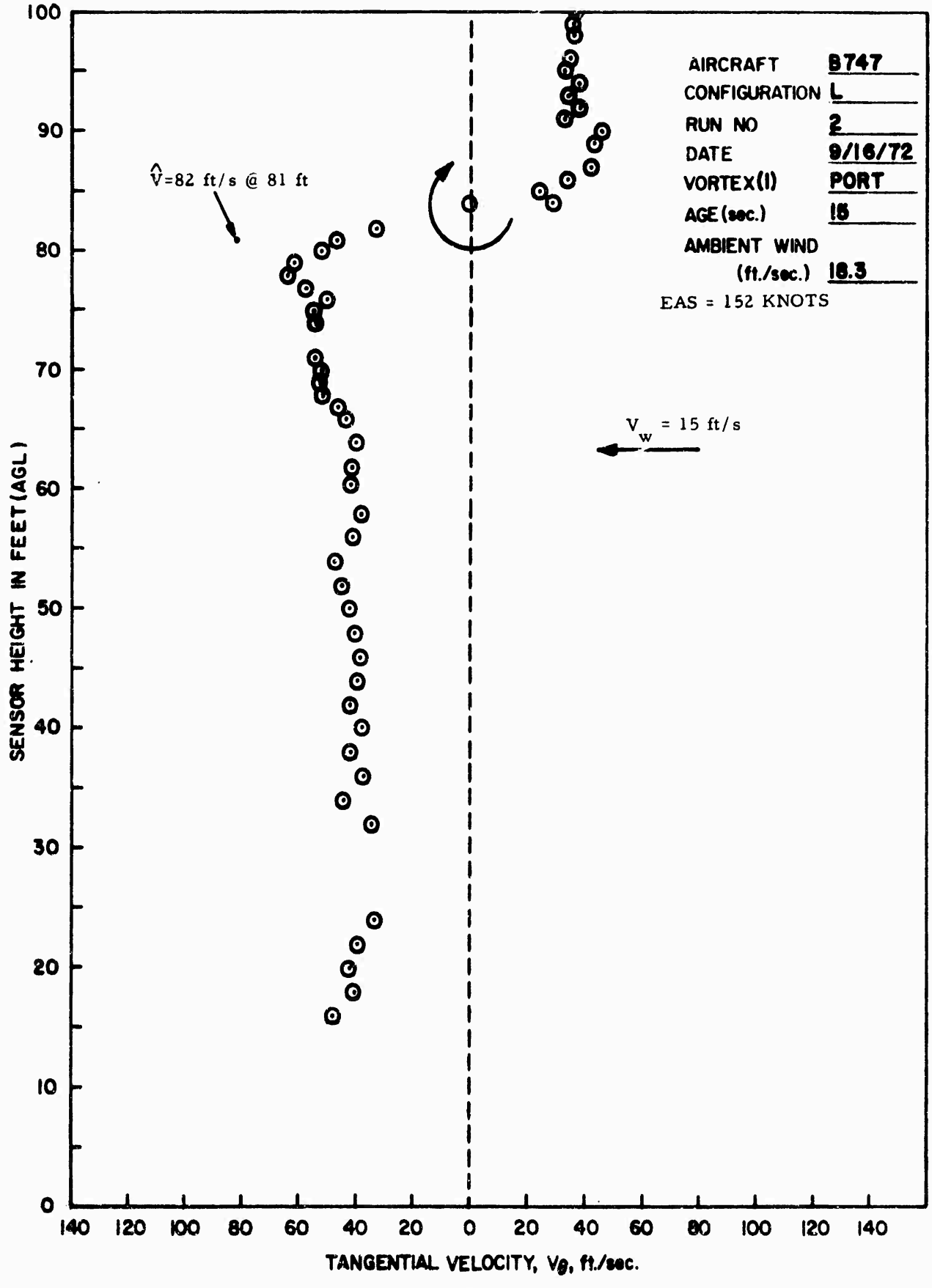
AIRCRAFT B747
CONFIGURATION L
RUN NO 2
DATE 9/16/72
VORTEX(1) PORT
AGE(sec.) 15
AMBIENT WIND (ft./sec.) 18.3
EAS = 152 KNOTS
$\hat{V}$=82 ft/s @ 81 ft
V_w = 15 ft/s
SENSOR HEIGHT IN FEET(AGL)
TANGENTIAL VELOCITY, Vθ, ft./sec.
0
10
20
30
40
50
60
70
80
90
100
140 120 100 80 60 40 20 0 20 40 60 80 100 120 140

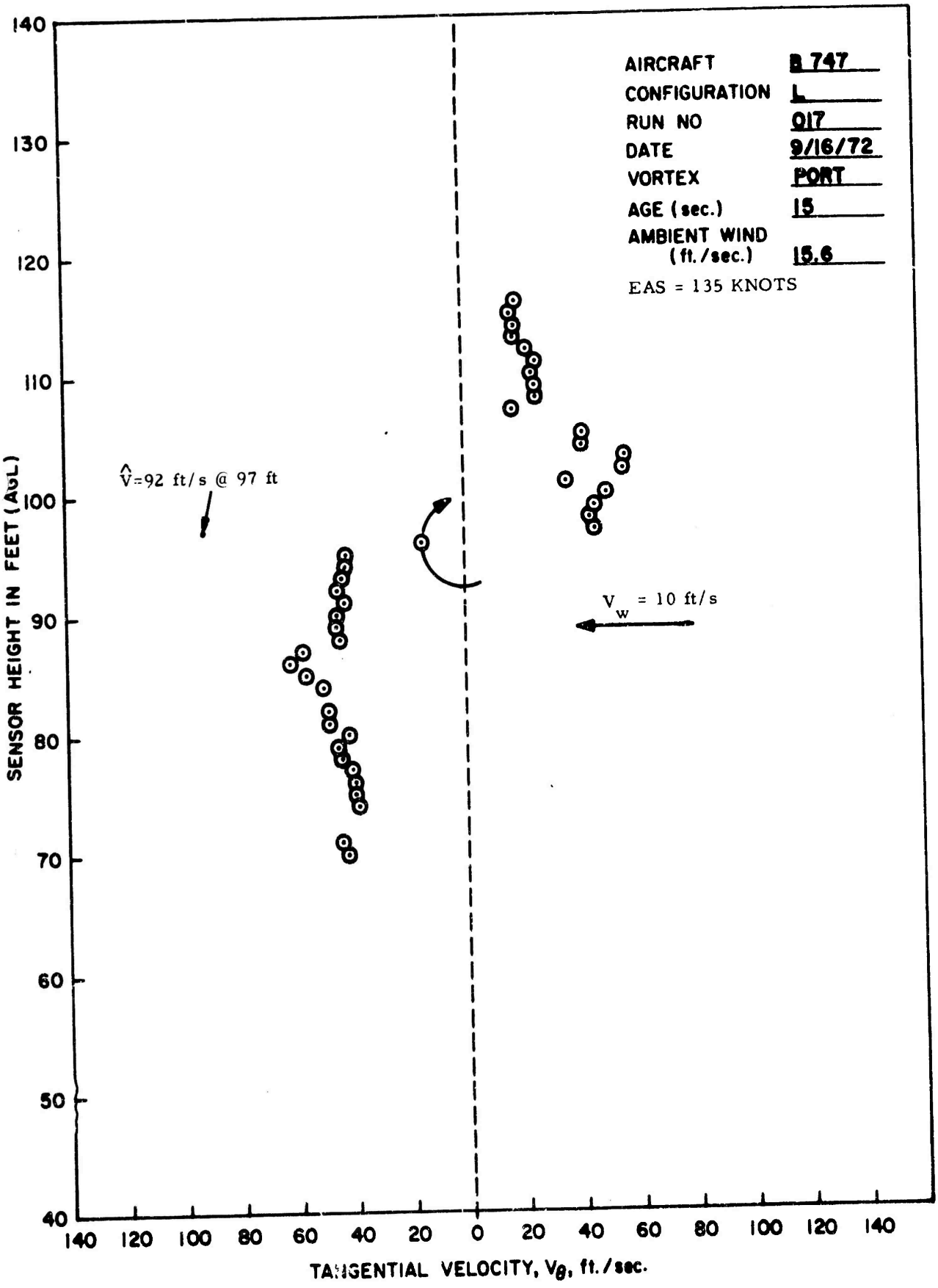
AIRCRAFT B 747
CONFIGURATION L
RUN NO 017
DATE 9/16/72
VORTEX PORT
AGE (sec.) 15
AMBIENT WIND (ft./sec.) 15.6
EAS = 135 KNOTS
$\hat{V}$=92 ft/s @ 97 ft
V_w = 10 ft/s
SENSOR HEIGHT IN FEET (AGL)
140
130
120
110
100
90
80
70
60
50
40
140 120 100 80 60 40 20 0 20 40 60 80 100 120 140
TANGENTIAL VELOCITY, V_θ, ft./sec.

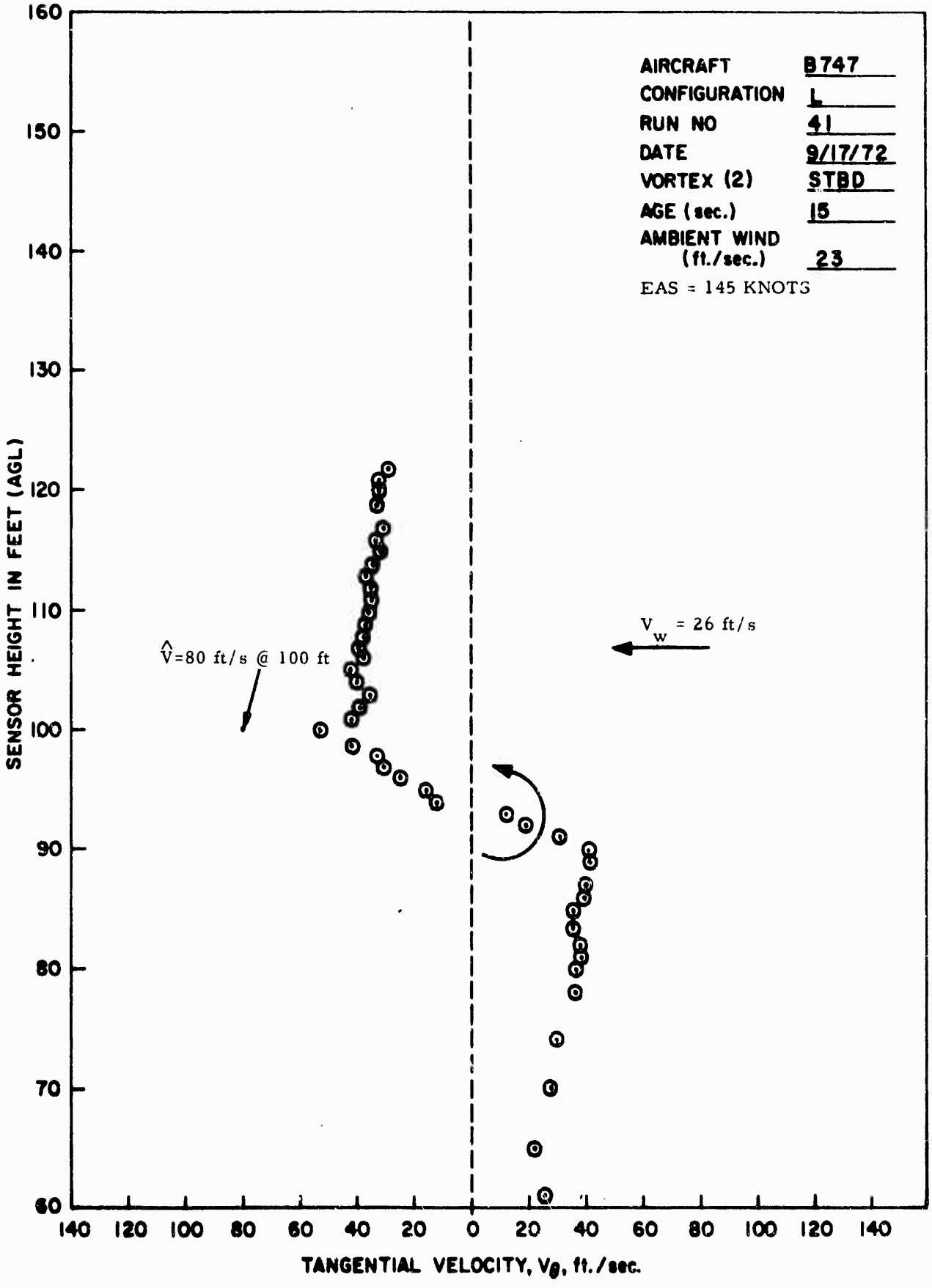
AIRCRAFT B747
CONFIGURATION L
RUN NO 41
DATE 9/17/72
VORTEX (2) STBD
AGE (sec.) 15
AMBIENT WIND (ft./sec.) 23
EAS = 145 KNOTS
$\hat{V}$=80 ft/s @ 100 ft
V_w = 26 ft/s
SENSOR HEIGHT IN FEET (AGL)
160
150
140
130
120
110
100
90
80
70
60
140 120 100 80 60 40 20 0 20 40 60 80 100 120 140
TANGENTIAL VELOCITY, V_θ, ft./sec.

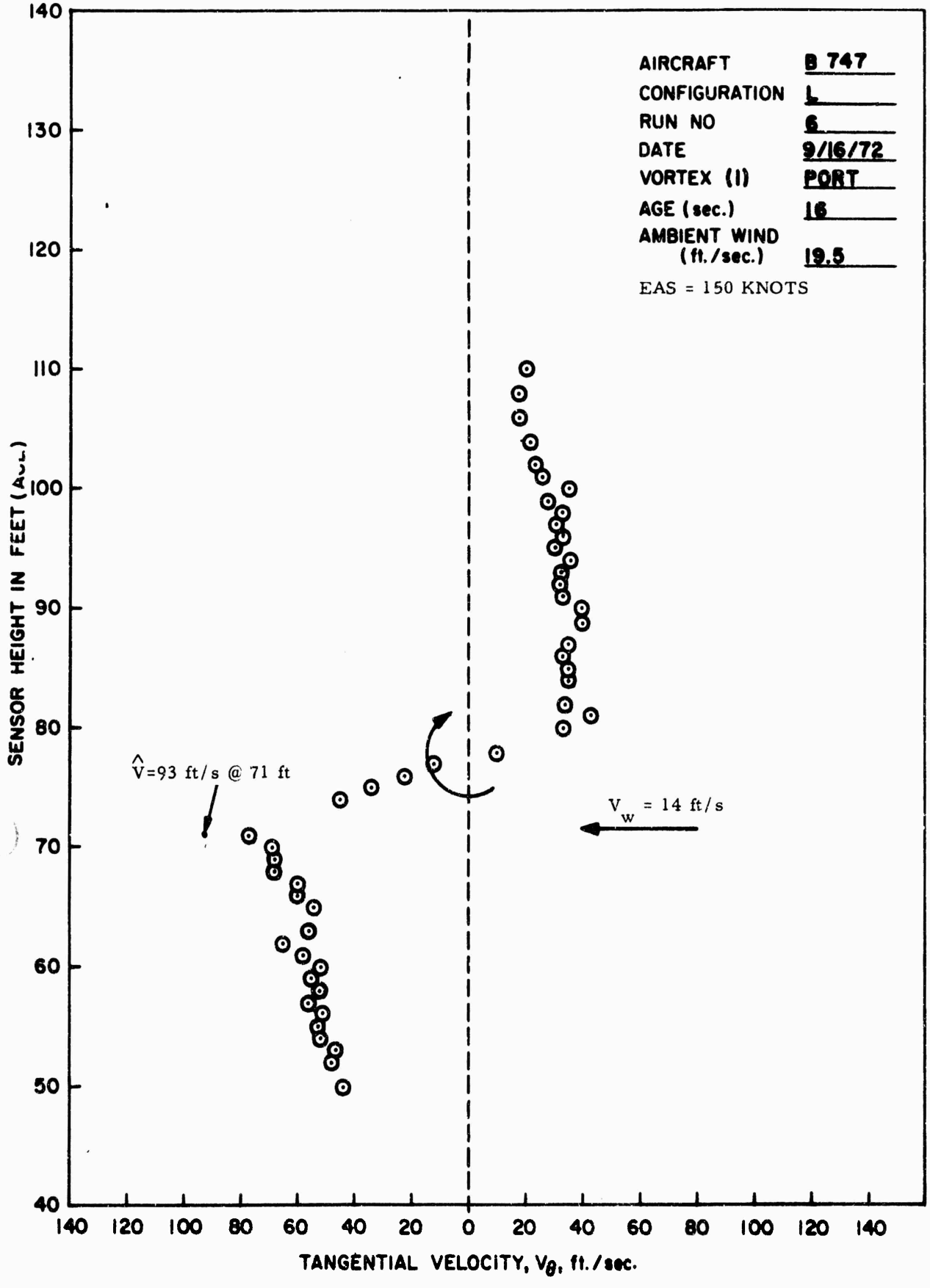
AIRCRAFT B 747
CONFIGURATION L
RUN NO 6
DATE 9/16/72
VORTEX (1) PORT
AGE (sec.) 16
AMBIENT WIND (ft./sec.) 19.5
EAS = 150 KNOTS
$\hat{V}$=93 ft/s @ 71 ft
V_w = 14 ft/s
SENSOR HEIGHT IN FEET (AGL)
TANGENTIAL VELOCITY, V_θ, ft./sec.
140
130
120
110
100
90
80
70
60
50
40
140 120 100 80 60 40 20 0 20 40 60 80 100 120 140

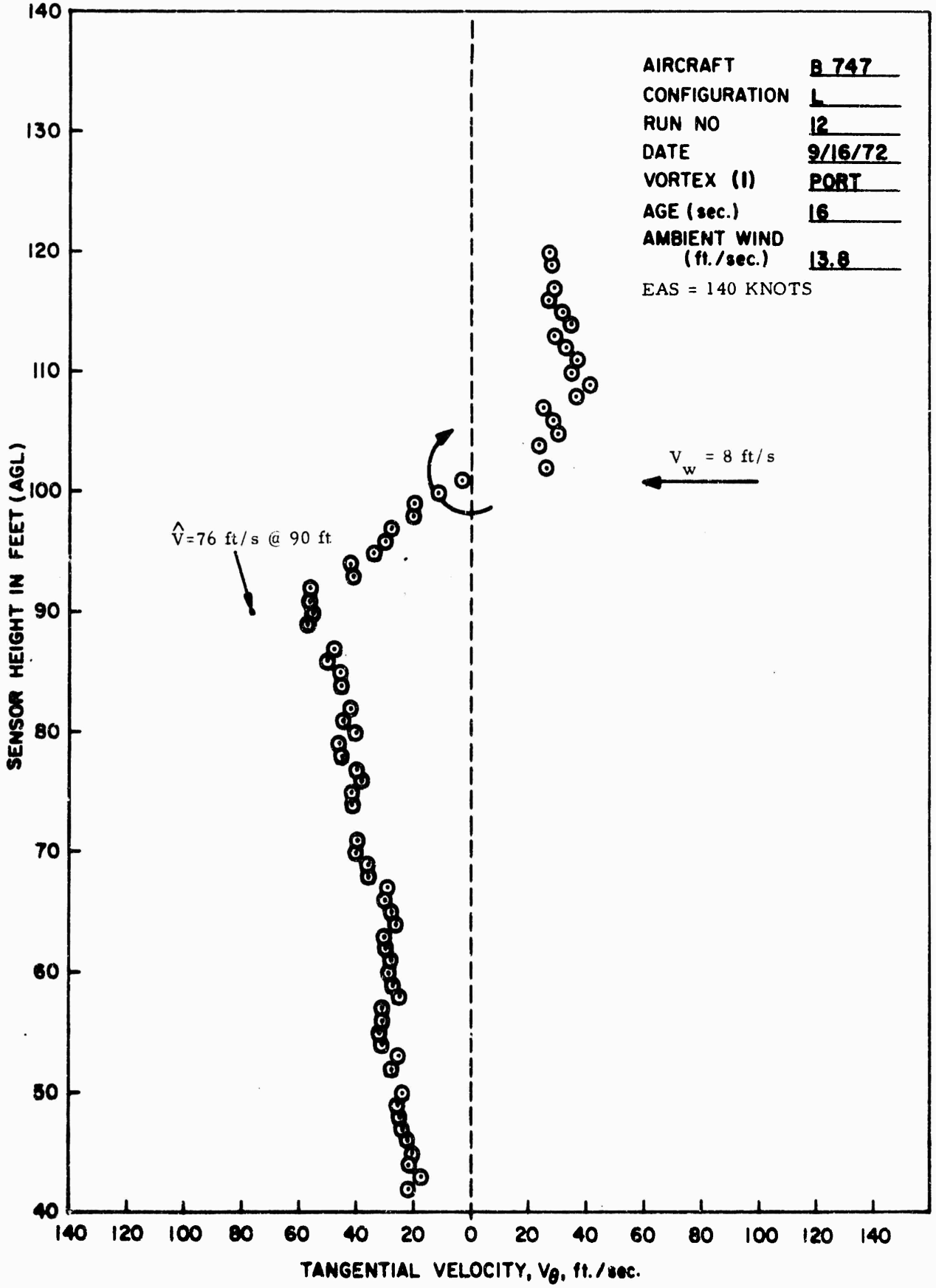
AIRCRAFT B 747
CONFIGURATION L
RUN NO 12
DATE 9/16/72
VORTEX (1) PORT
AGE (sec.) 16
AMBIENT WIND (ft./sec.) 13.8
EAS = 140 KNOTS
V_w = 8 ft/s
$\hat{V}$=76 ft/s @ 90 ft
SENSOR HEIGHT IN FEET (AGL)
140
130
120
110
100
90
80
70
60
50
40
140 120 100 80 60 40 20 0 20 40 60 80 100 120 140
TANGENTIAL VELOCITY, V_θ, ft./sec.

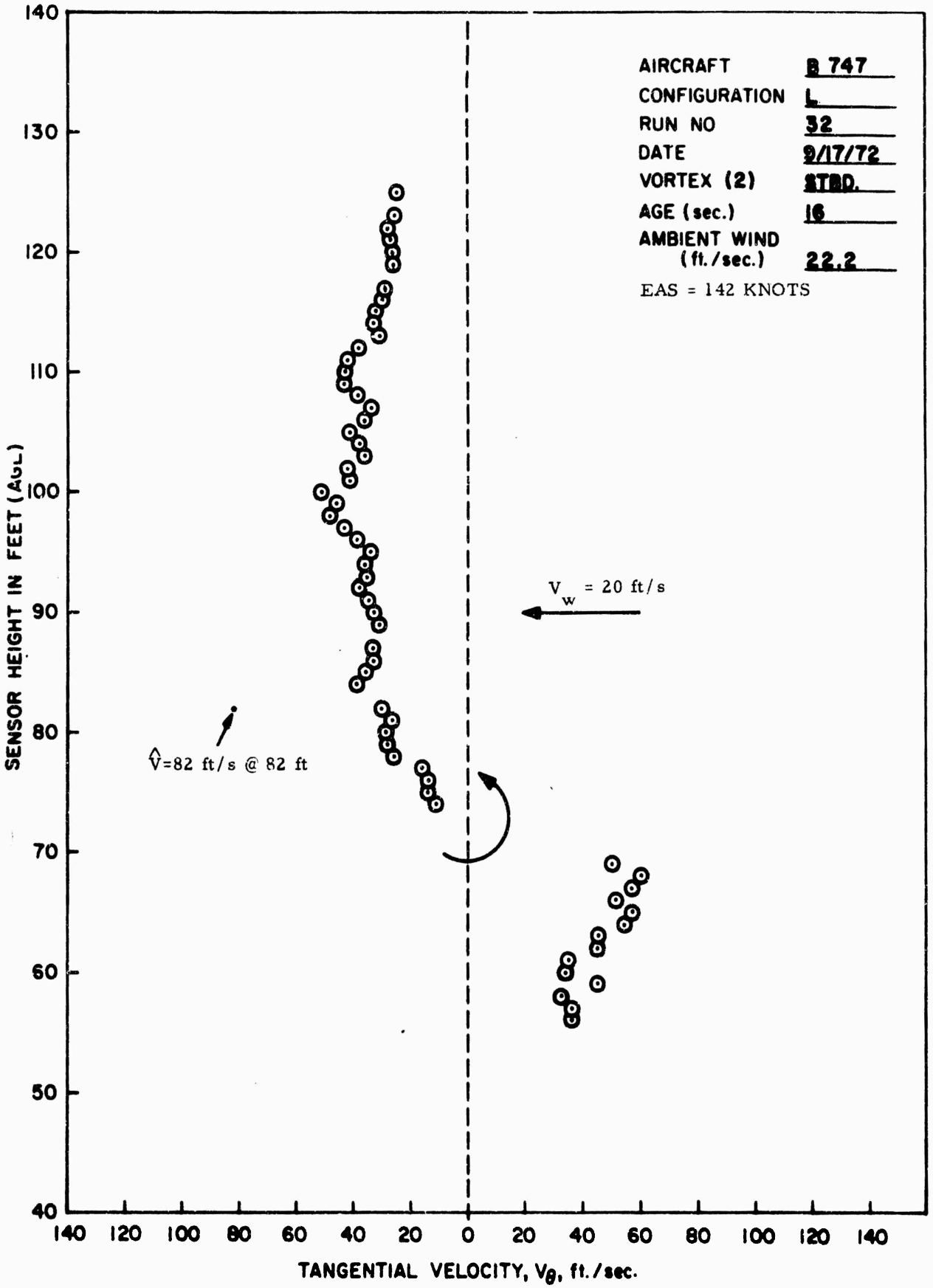
AIRCRAFT B 747
CONFIGURATION L
RUN NO 32
DATE 9/17/72
VORTEX (2) STBD.
AGE (sec.) 16
AMBIENT WIND (ft./sec.) 22.2
EAS = 142 KNOTS
V_w = 20 ft/s
$\hat{V}$=82 ft/s @ 82 ft
SENSOR HEIGHT IN FEET (AGL)
TANGENTIAL VELOCITY, V_θ, ft./sec.
140
130
120
110
100
90
80
70
60
50
40
140 120 100 80 60 40 20 0 20 40 60 80 100 120 140

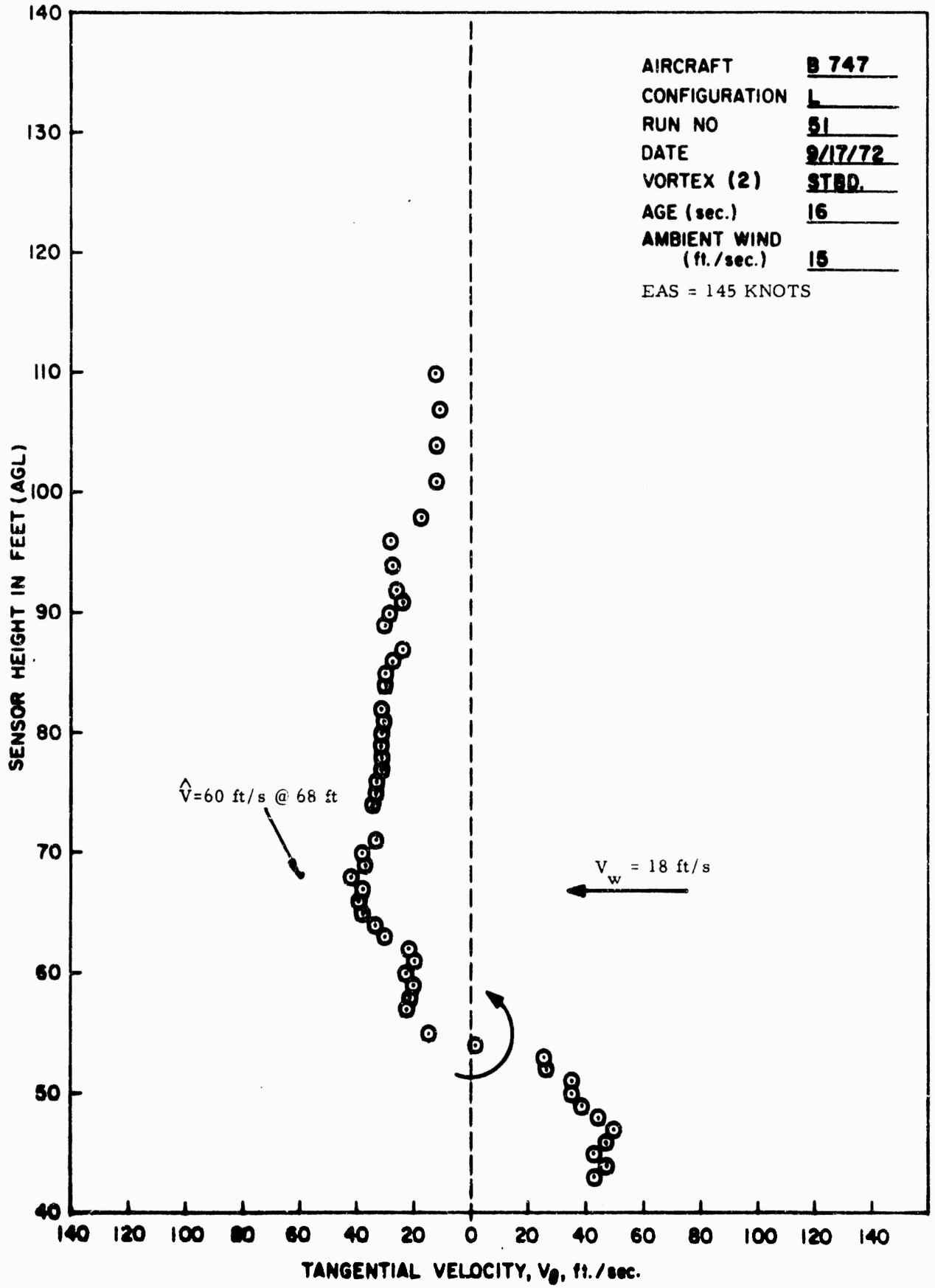
AIRCRAFT B 747
CONFIGURATION L
RUN NO 51
DATE 9/17/72
VORTEX (2) STBD.
AGE (sec.) 16
AMBIENT WIND (ft./sec.) 15
EAS = 145 KNOTS
SENSOR HEIGHT IN FEET (AGL)
140
130
120
110
100
90
80
70
60
50
40
$\hat{V}$=60 ft/s @ 68 ft
V_w = 18 ft/s
140 120 100 80 60 40 20 0 20 40 60 80 100 120 140
TANGENTIAL VELOCITY, V_θ, ft./sec.

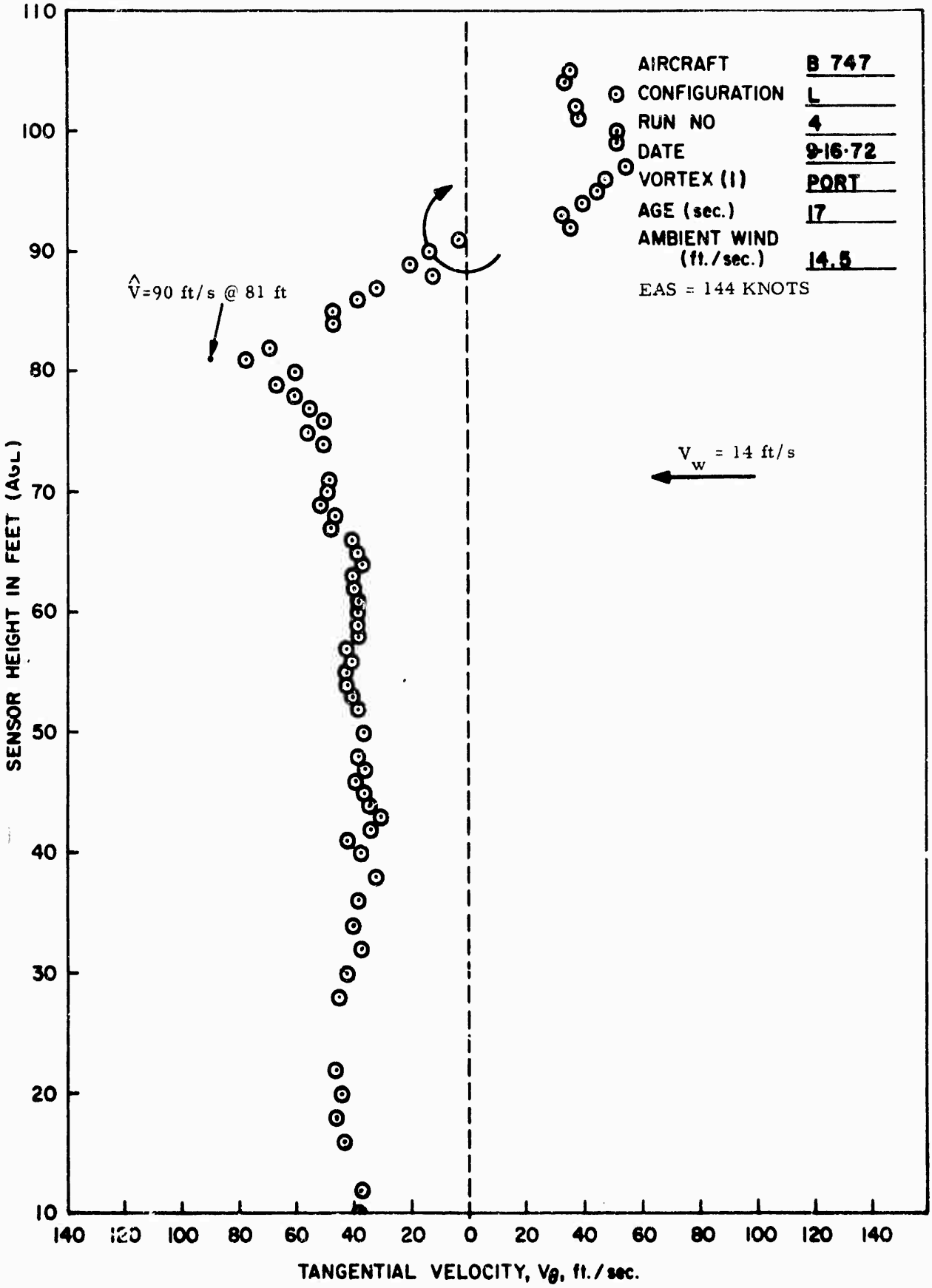
AIRCRAFT B 747
CONFIGURATION L
RUN NO 4
DATE 9-16-72
VORTEX (1) PORT
AGE (sec.) 17
AMBIENT WIND (ft./sec.) 14.5
EAS = 144 KNOTS
$\hat{V}$=90 ft/s @ 81 ft
V_w = 14 ft/s
SENSOR HEIGHT IN FEET (AGL)
TANGENTIAL VELOCITY, V_θ, ft./sec.
110
100
90
80
70
60
50
40
30
20
10
140 120 100 80 60 40 20 0 20 40 60 80 100 120 140

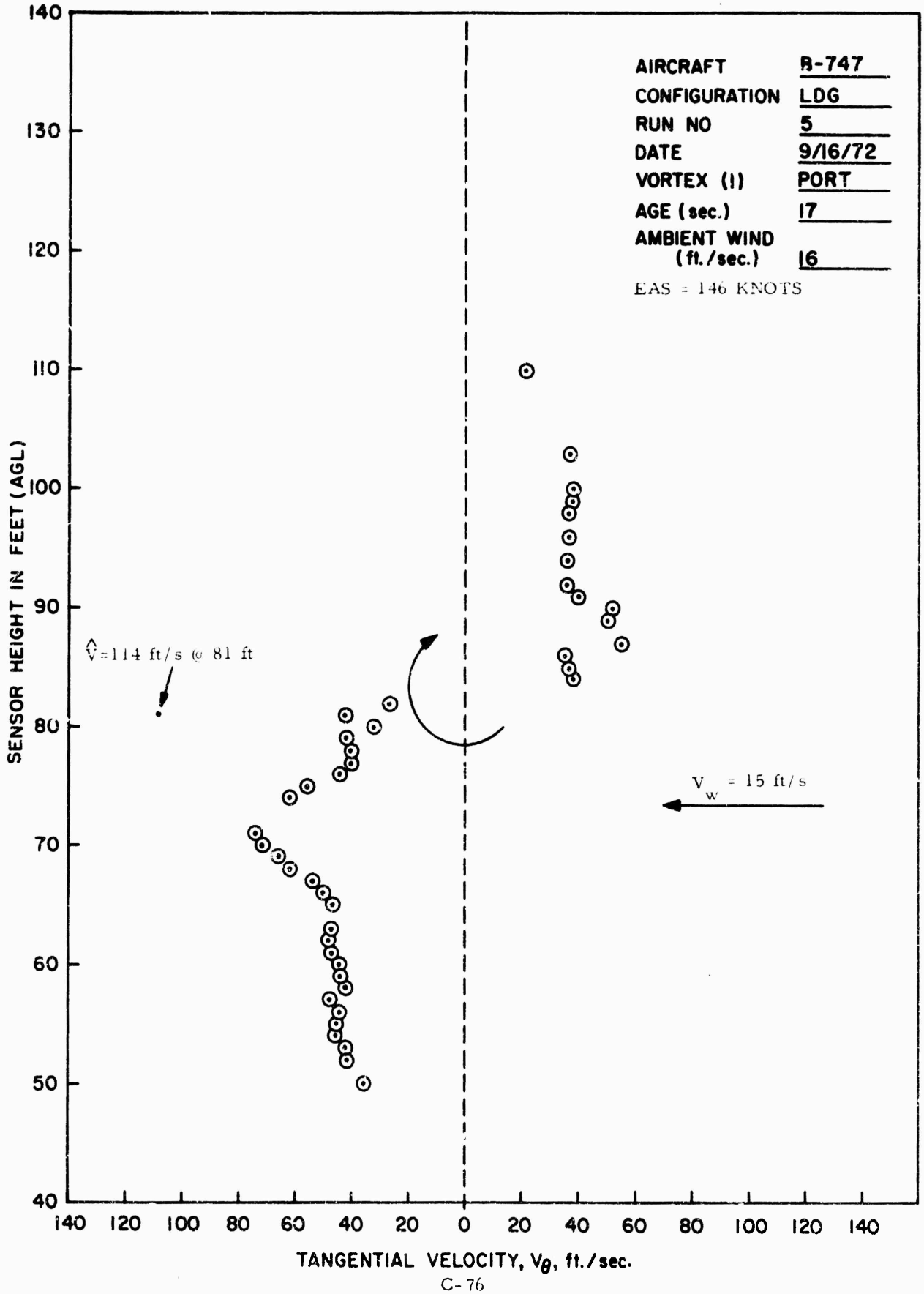
AIRCRAFT B-747
CONFIGURATION LDG
RUN NO 5
DATE 9/16/72
VORTEX (1) PORT
AGE (sec.) 17
AMBIENT WIND (ft./sec.) 16
EAS = 146 KNOTS
$\hat{V}$=114 ft/s @ 81 ft
V_w = 15 ft/s
SENSOR HEIGHT IN FEET (AGL)
TANGENTIAL VELOCITY, V_θ, ft./sec.
140
130
120
110
100
90
80
70
60
50
40
140 120 100 80 60 40 20 0 20 40 60 80 100 120 140

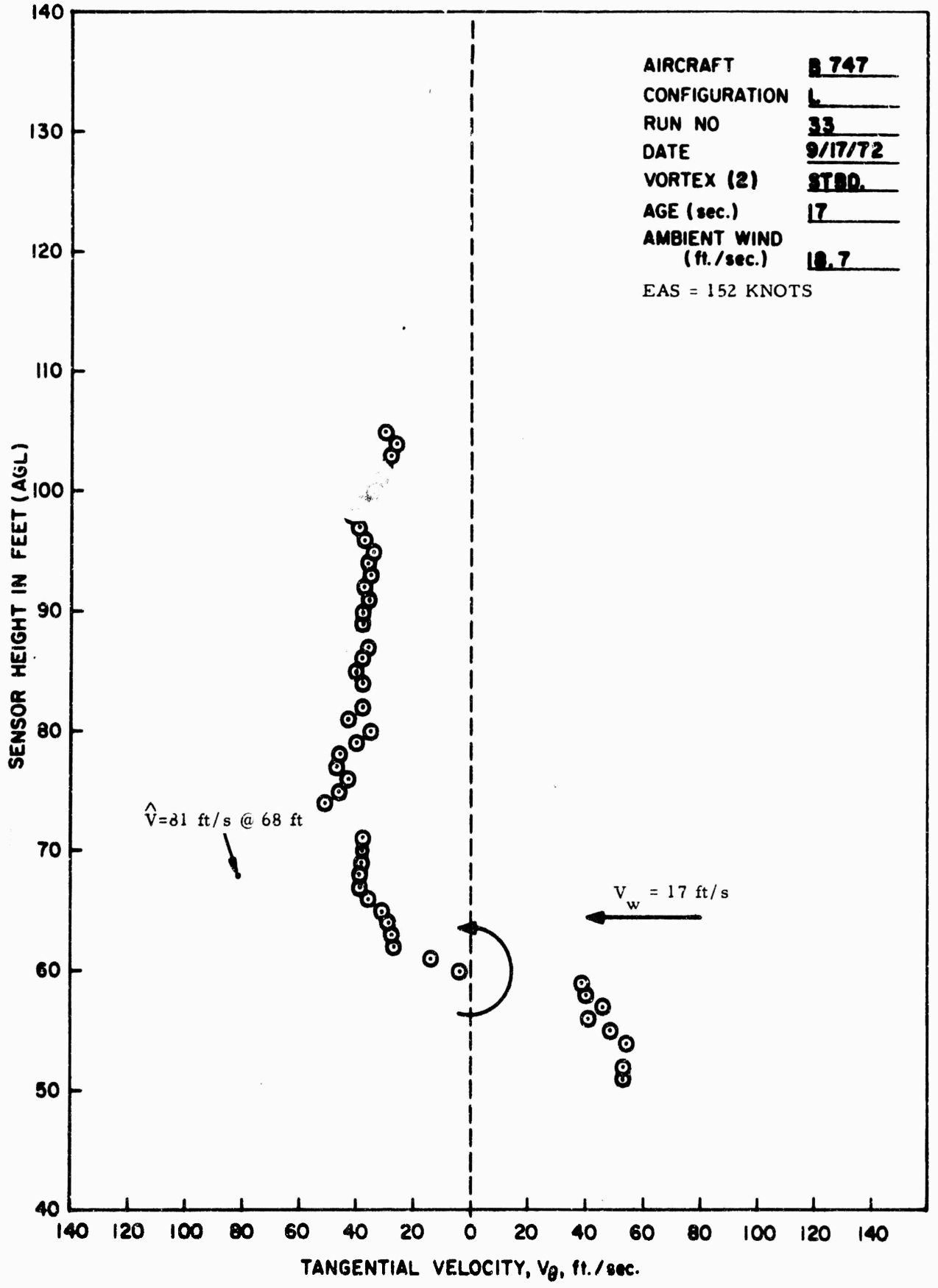
AIRCRAFT B 747
CONFIGURATION L
RUN NO 33
DATE 9/17/72
VORTEX (2) STBD.
AGE (sec.) 17
AMBIENT WIND (ft./sec.) 18.7
EAS = 152 KNOTS
$\hat{V}$=81 ft/s @ 68 ft
V_w = 17 ft/s
SENSOR HEIGHT IN FEET (AGL)
TANGENTIAL VELOCITY, V_θ, ft./sec.
140
130
120
110
100
90
80
70
60
50
40
140 120 100 80 60 40 20 0 20 40 60 80 100 120 140

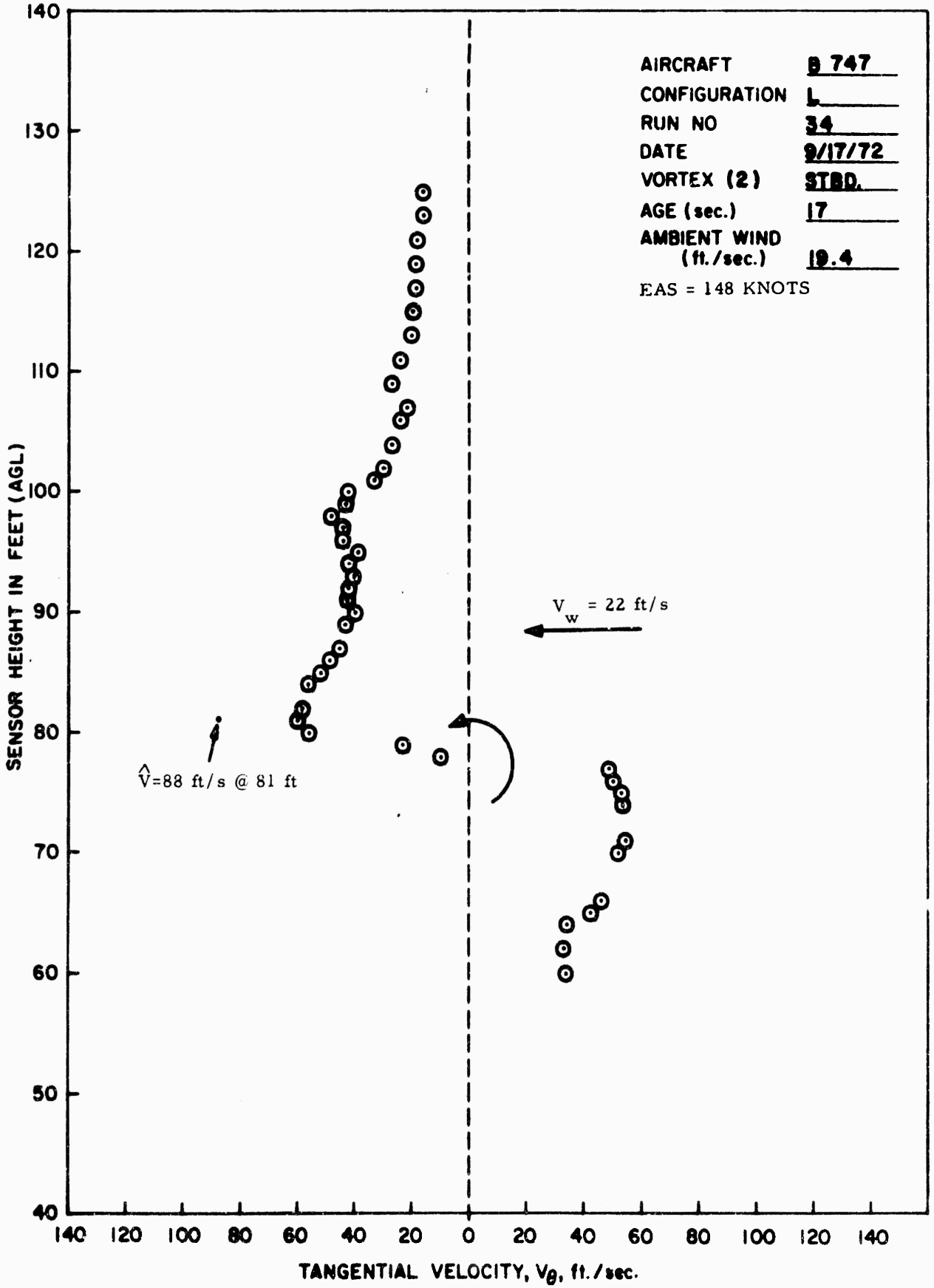
AIRCRAFT B 747
CONFIGURATION L
RUN NO 34
DATE 9/17/72
VORTEX (2) STBD.
AGE (sec.) 17
AMBIENT WIND (ft./sec.) 19.4
EAS = 148 KNOTS
V_w = 22 ft/s
$\hat{V}$=88 ft/s @ 81 ft
SENSOR HEIGHT IN FEET (AGL)
TANGENTIAL VELOCITY, V_θ, ft./sec.
140
130
120
110
100
90
80
70
60
50
40
140 120 100 80 60 40 20 0 20 40 60 80 100 120 140

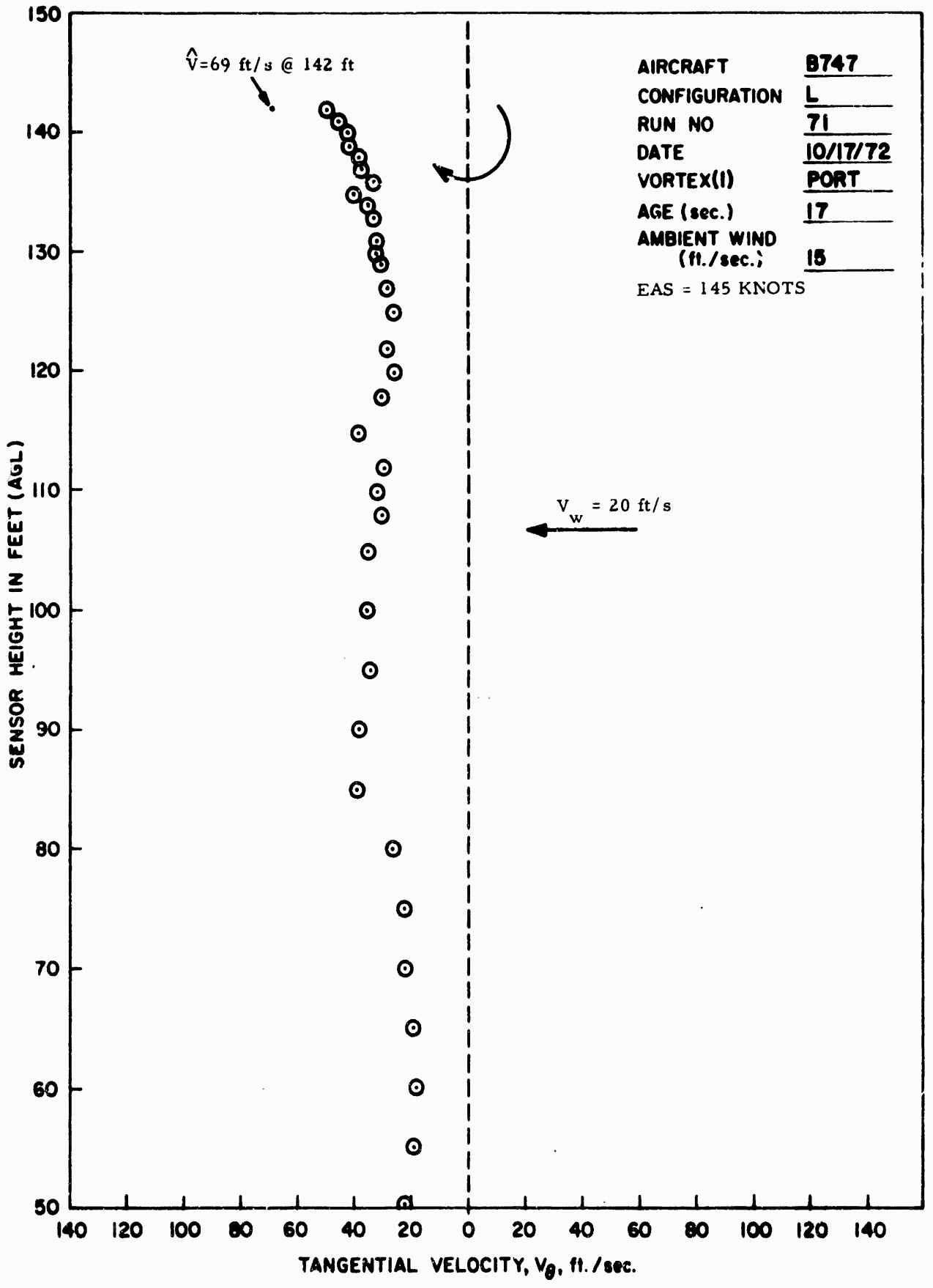
$\hat{V}$=69 ft/s @ 142 ft
AIRCRAFT B747
CONFIGURATION L
RUN NO 71
DATE 10/17/72
VORTEX(1) PORT
AGE (sec.) 17
AMBIENT WIND (ft./sec.) 15
EAS = 145 KNOTS
V_w = 20 ft/s
SENSOR HEIGHT IN FEET (AGL)
150
140
130
120
110
100
90
80
70
60
50
140 120 100 80 60 40 20 0 20 40 60 80 100 120 140
TANGENTIAL VELOCITY, V_θ, ft./sec.

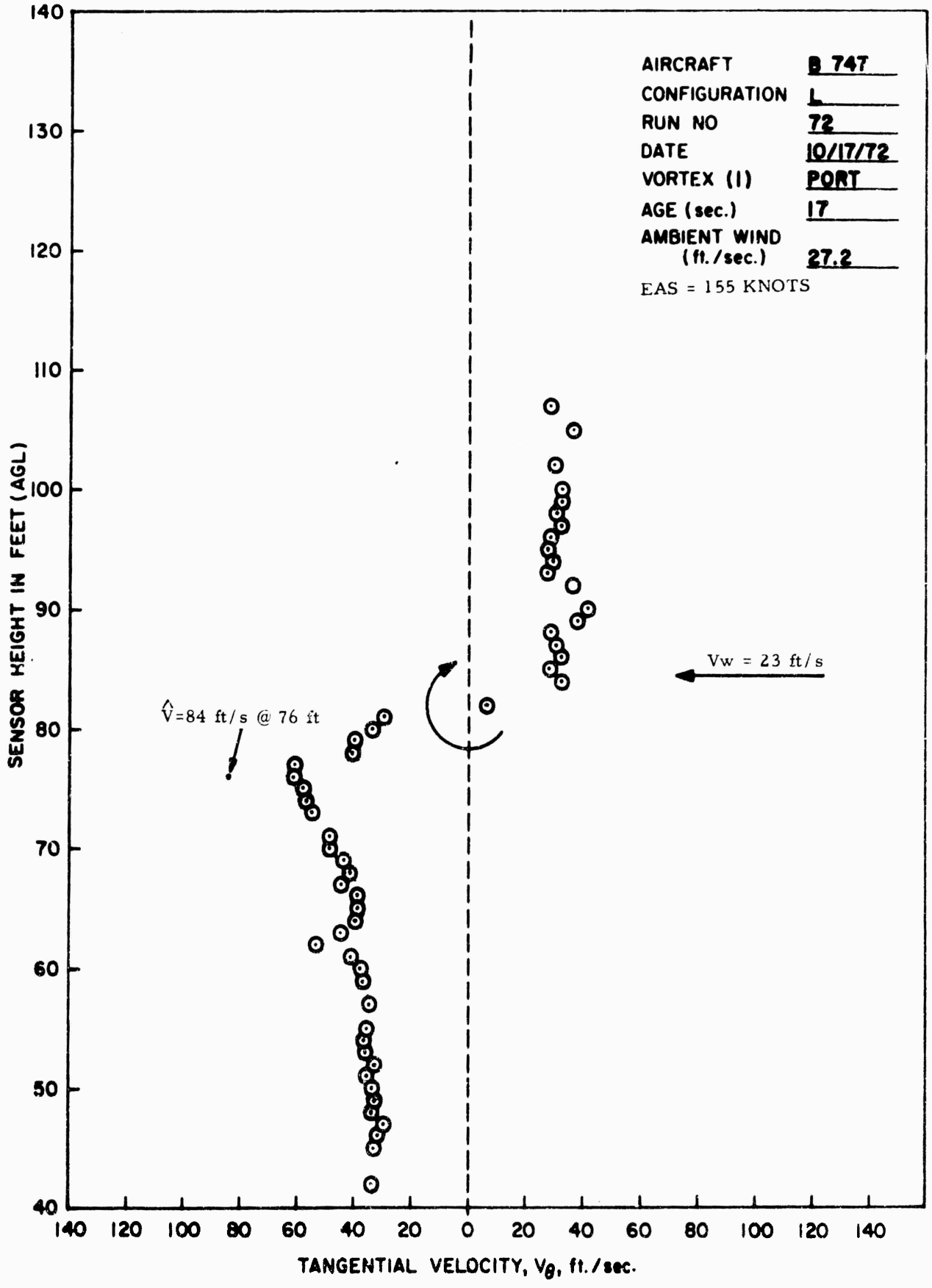
AIRCRAFT B 747
CONFIGURATION L
RUN NO 72
DATE 10/17/72
VORTEX (1) PORT
AGE (sec.) 17
AMBIENT WIND (ft./sec.) 27.2
EAS = 155 KNOTS
Vw = 23 ft/s
V̂=84 ft/s @ 76 ft
SENSOR HEIGHT IN FEET (AGL)
TANGENTIAL VELOCITY, Vθ, ft./sec.
140
130
120
110
100
90
80
70
60
50
40
140 120 100 80 60 40 20 0 20 40 60 80 100 120 140

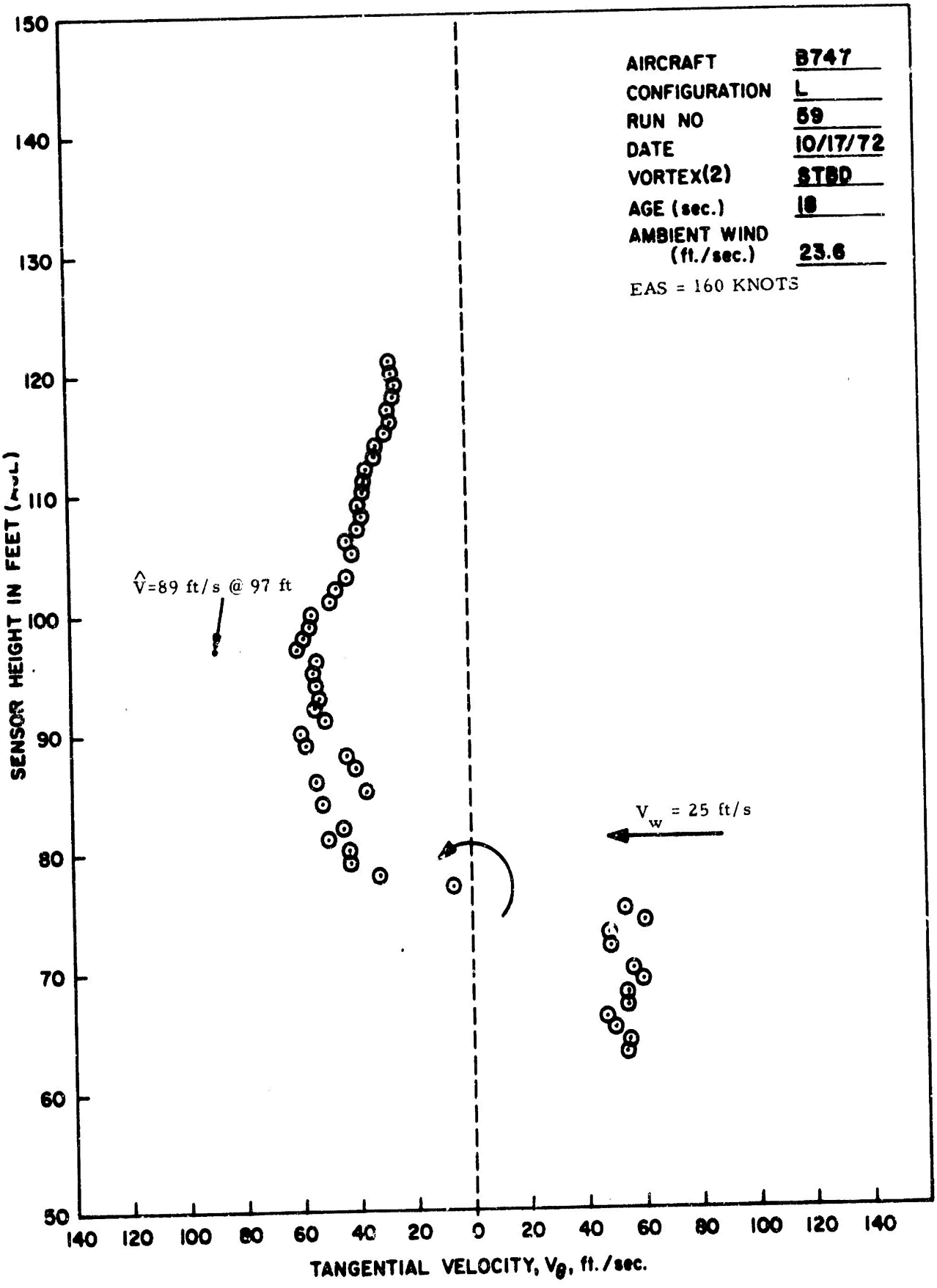
AIRCRAFT B747
CONFIGURATION L
RUN NO 59
DATE 10/17/72
VORTEX(2) STBD
AGE (sec.) 18
AMBIENT WIND (ft./sec.) 23.6
EAS = 160 KNOTS
$\hat{V}$=89 ft/s @ 97 ft
V_w = 25 ft/s
SENSOR HEIGHT IN FEET (AGL)
TANGENTIAL VELOCITY, V_θ, ft./sec.
150
140
130
120
110
100
90
80
70
60
50
140 120 100 80 60 40 20 0 20 40 60 80 100 120 140

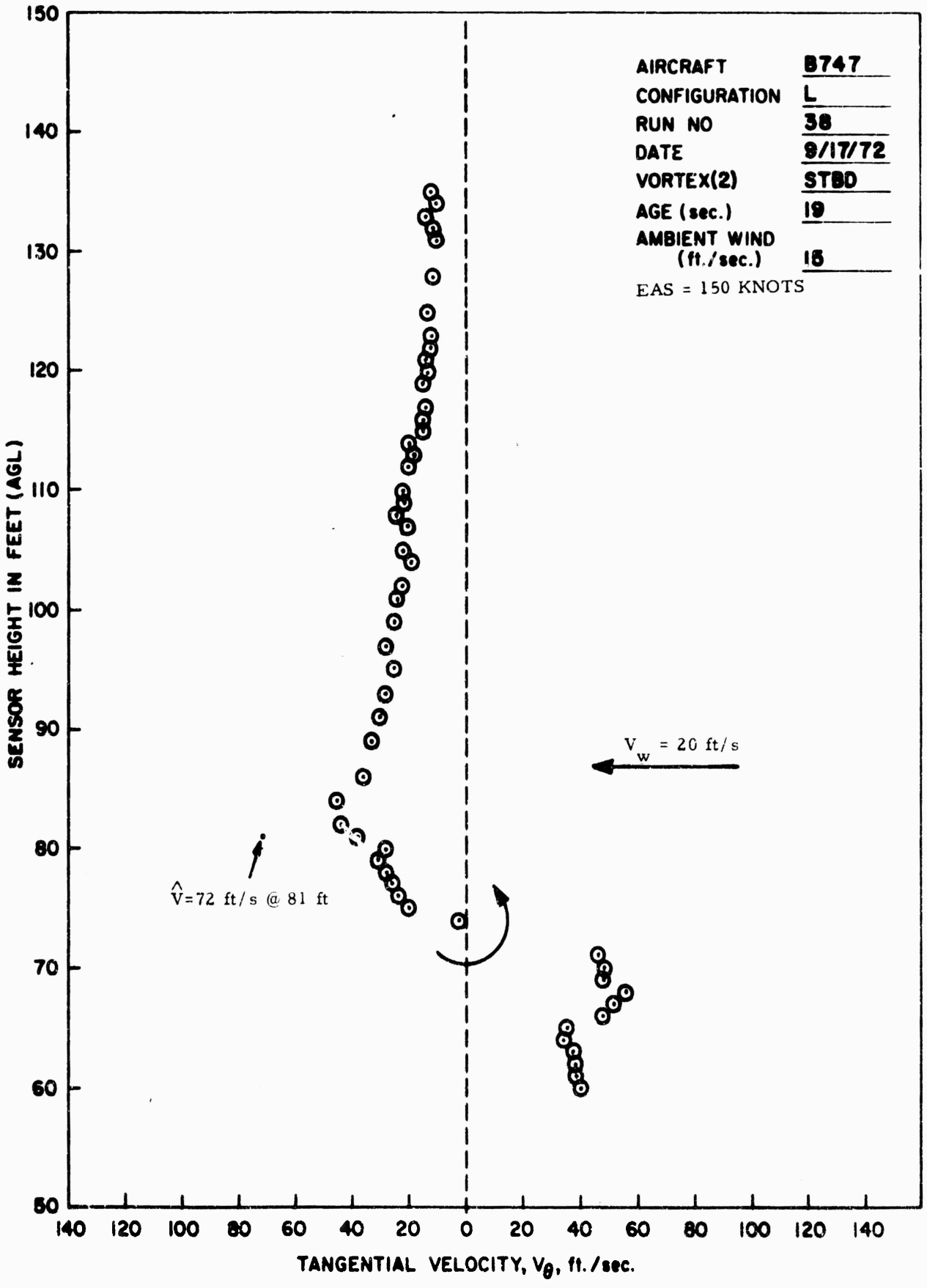
AIRCRAFT B747
CONFIGURATION L
RUN NO 38
DATE 9/17/72
VORTEX(2) STBD
AGE (sec.) 19
AMBIENT WIND (ft./sec.) 15
EAS = 150 KNOTS
V_w = 20 ft/s
$\hat{V}$=72 ft/s @ 81 ft
SENSOR HEIGHT IN FEET (AGL)
150
140
130
120
110
100
90
80
70
60
50
140 120 100 80 60 40 20 0 20 40 60 80 100 120 140
TANGENTIAL VELOCITY, V_θ, ft./sec.

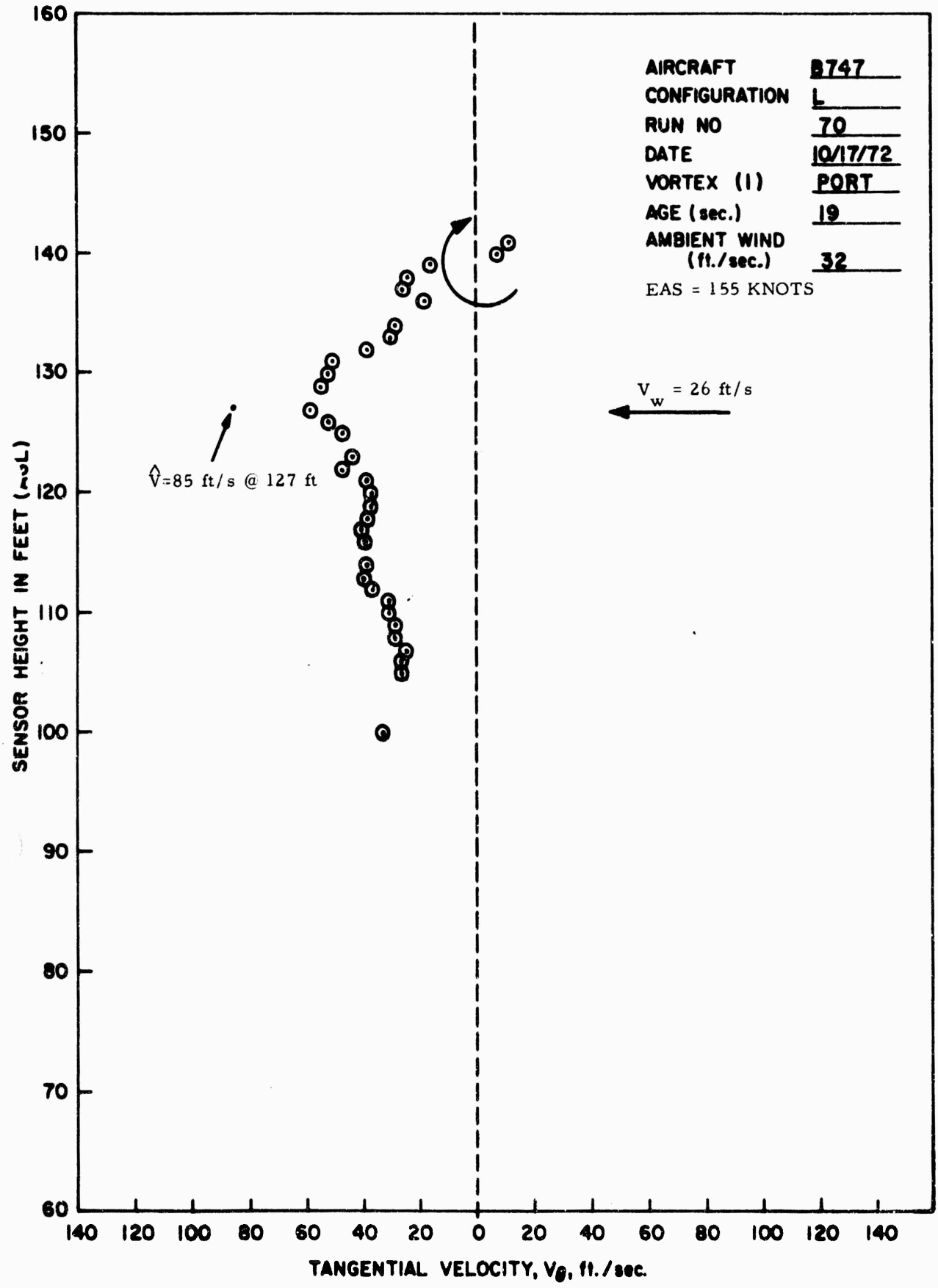
AIRCRAFT B747
CONFIGURATION L
RUN NO 70
DATE 10/17/72
VORTEX (1) PORT
AGE (sec.) 19
AMBIENT WIND (ft./sec.) 32
EAS = 155 KNOTS
V_w = 26 ft/s
V=85 ft/s @ 127 ft
SENSOR HEIGHT IN FEET (AGL)
TANGENTIAL VELOCITY, V_θ, ft./sec.
160
150
140
130
120
110
100
90
80
70
60
140 120 100 80 60 40 20 0 20 40 60 80 100 120 140

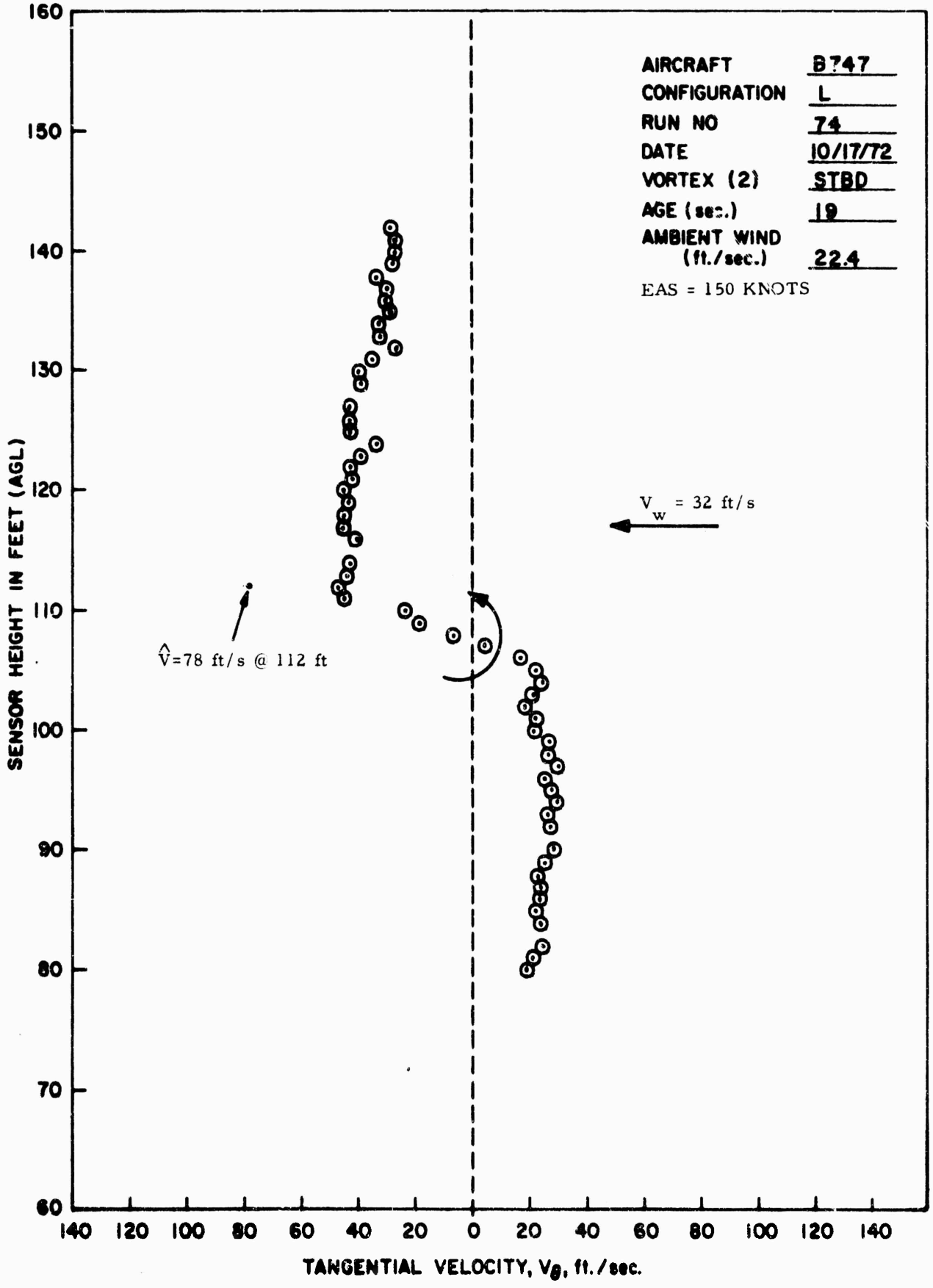
AIRCRAFT B747
CONFIGURATION L
RUN NO 74
DATE 10/17/72
VORTEX (2) STBD
AGE (sec.) 19
AMBIENT WIND (ft./sec.) 22.4
EAS = 150 KNOTS
V_w = 32 ft/s
$\hat{V}$=78 ft/s @ 112 ft
SENSOR HEIGHT IN FEET (AGL)
160
150
140
130
120
110
100
90
80
70
60
140 120 100 80 60 40 20 0 20 40 60 80 100 120 140
TANGENTIAL VELOCITY, V_θ, ft./sec.

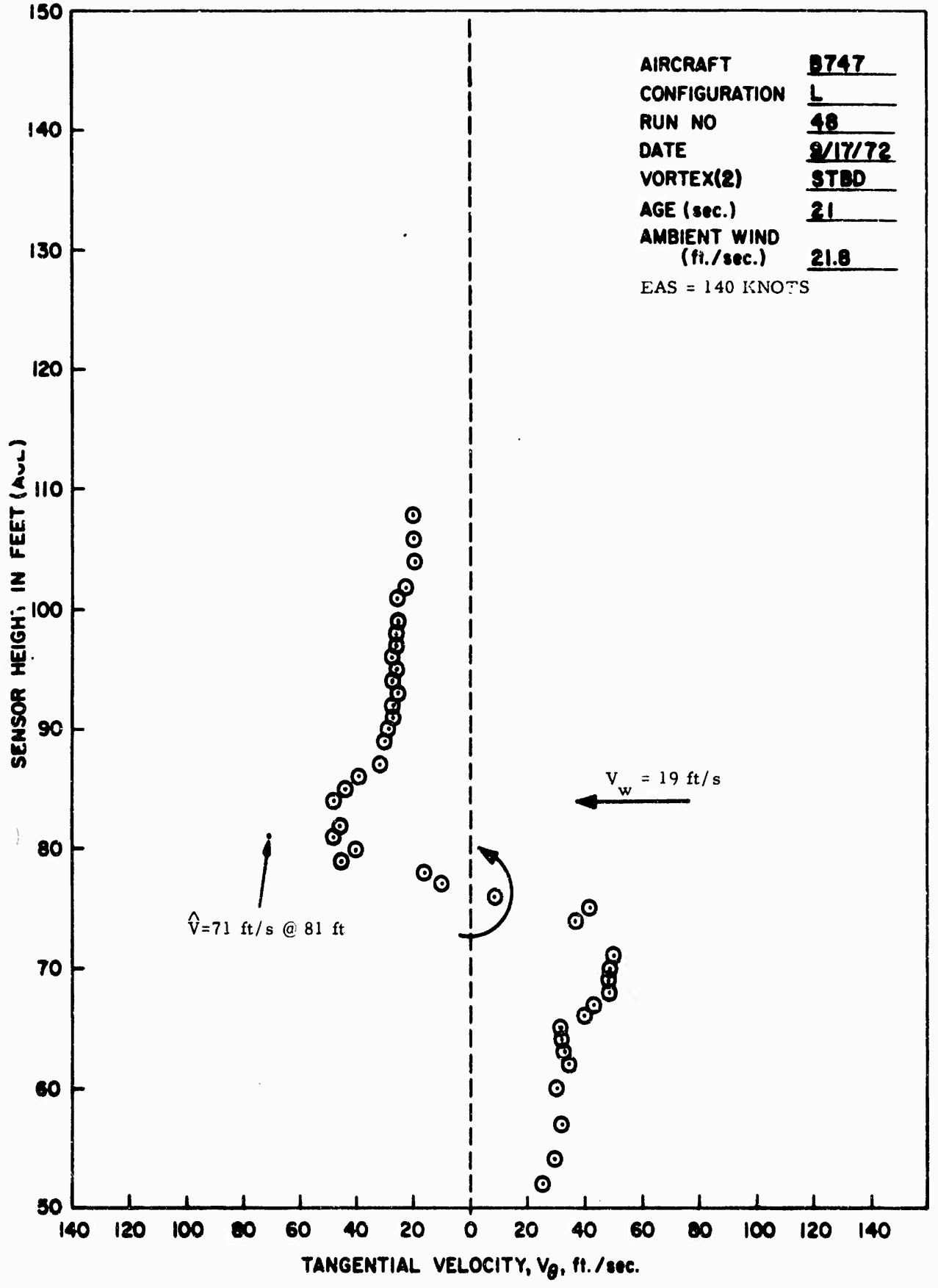
AIRCRAFT B747
CONFIGURATION L
RUN NO 48
DATE 9/17/72
VORTEX(2) STBD
AGE (sec.) 21
AMBIENT WIND (ft./sec.) 21.8
EAS = 140 KNOTS
V_w = 19 ft/s
$\hat{V}$=71 ft/s @ 81 ft
SENSOR HEIGHT IN FEET (AGL)
150
140
130
120
110
100
90
80
70
60
50
140 120 100 80 60 40 20 0 20 40 60 80 100 120 140
TANGENTIAL VELOCITY, V_θ, ft./sec.

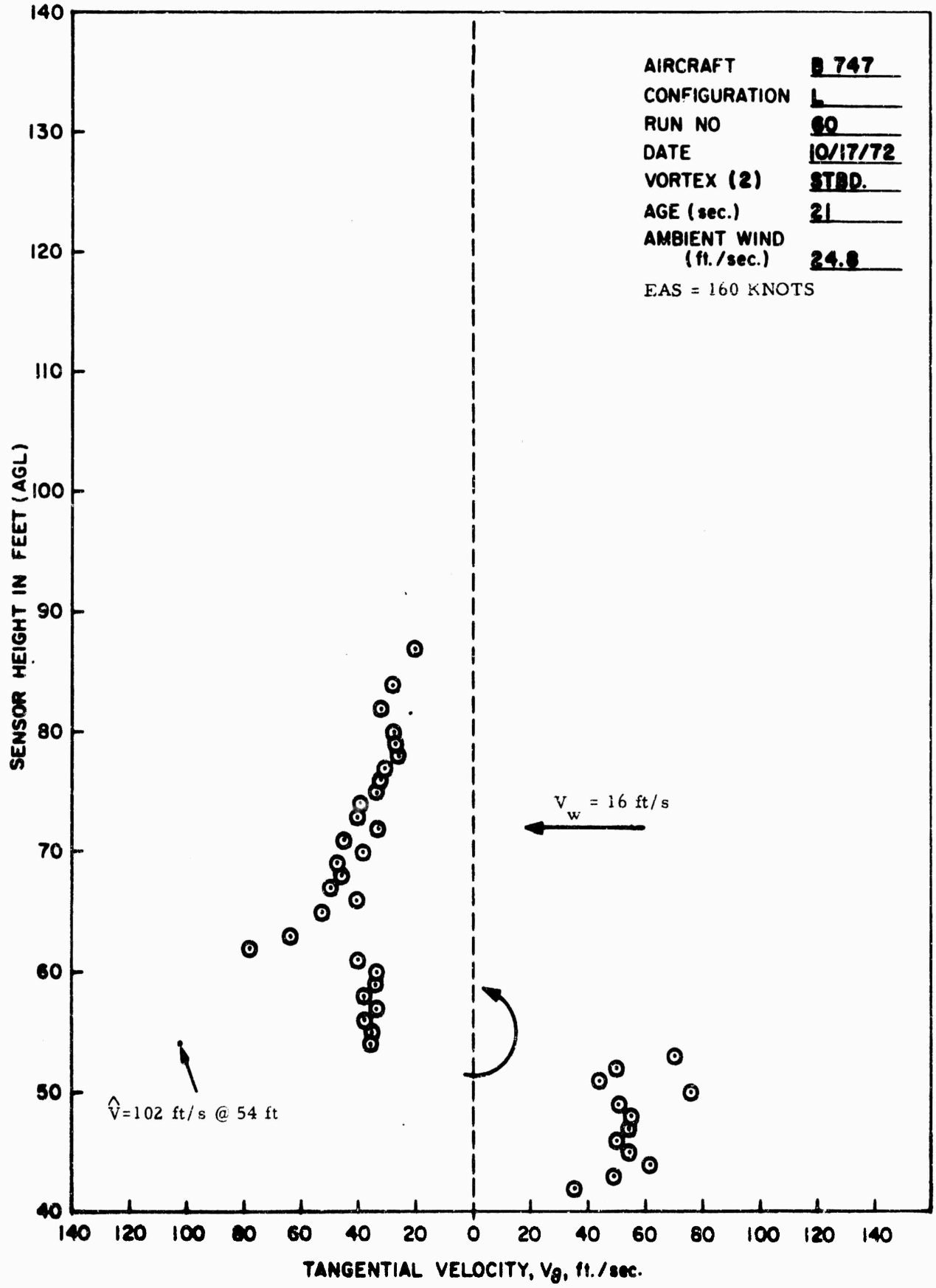
AIRCRAFT B 747
CONFIGURATION L
RUN NO 60
DATE 10/17/72
VORTEX (2) STBD.
AGE (sec.) 21
AMBIENT WIND (ft./sec.) 24.8
EAS = 160 KNOTS
V_w = 16 ft/s
$\hat{V}$=102 ft/s @ 54 ft
SENSOR HEIGHT IN FEET (AGL)
TANGENTIAL VELOCITY, V_θ, ft./sec.
140
130
120
110
100
90
80
70
60
50
40
140 120 100 80 60 40 20 0 20 40 60 80 100 120 140

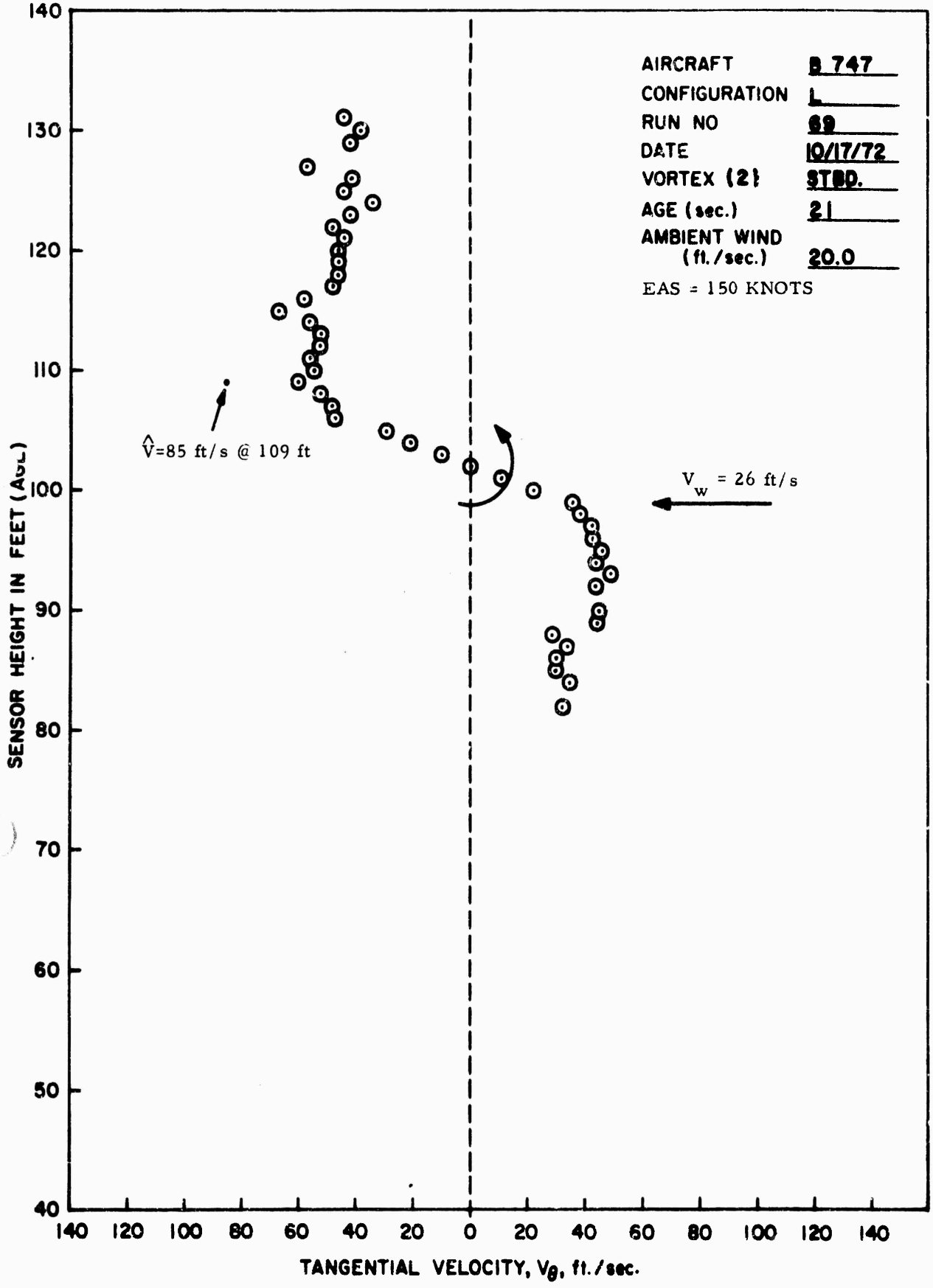
AIRCRAFT B 747
CONFIGURATION L
RUN NO 69
DATE 10/17/72
VORTEX (2) STBD.
AGE (sec.) 21
AMBIENT WIND (ft./sec.) 20.0
EAS = 150 KNOTS
V̂=85 ft/s @ 109 ft
V_w = 26 ft/s
SENSOR HEIGHT IN FEET (AGL)
TANGENTIAL VELOCITY, V_θ, ft./sec.
140
130
120
110
100
90
80
70
60
50
40
140 120 100 80 60 40 20 0 20 40 60 80 100 120 140

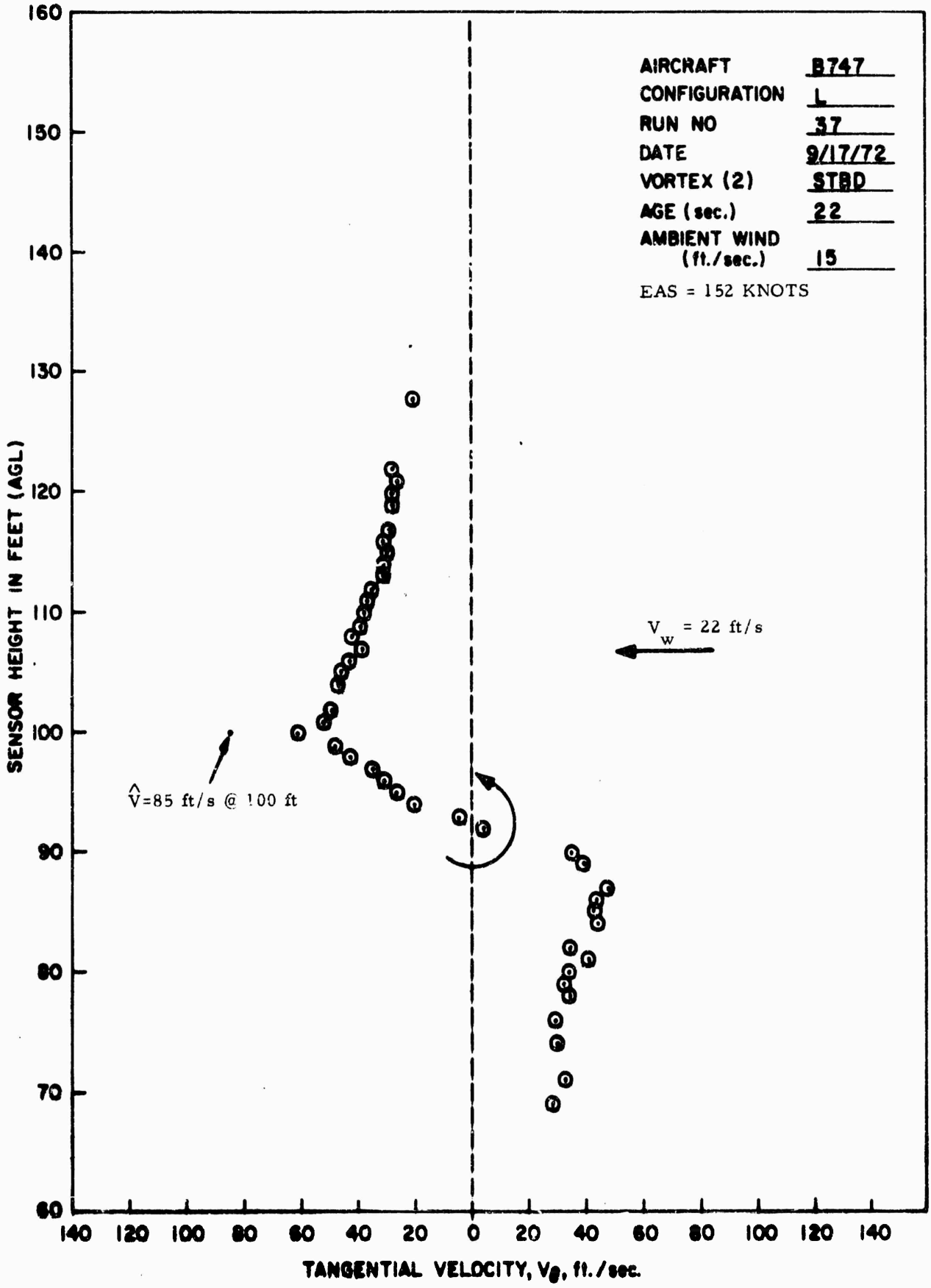
AIRCRAFT B747
CONFIGURATION L
RUN NO 37
DATE 9/17/72
VORTEX (2) STBD
AGE (sec.) 22
AMBIENT WIND (ft./sec.) 15
EAS = 152 KNOTS
V_w = 22 ft/s
$\hat{V}$=85 ft/s @ 100 ft
SENSOR HEIGHT IN FEET (AGL)
160
150
140
130
120
110
100
90
80
70
60
140 120 100 80 60 40 20 0 20 40 60 80 100 120 140
TANGENTIAL VELOCITY, V_θ, ft./sec.

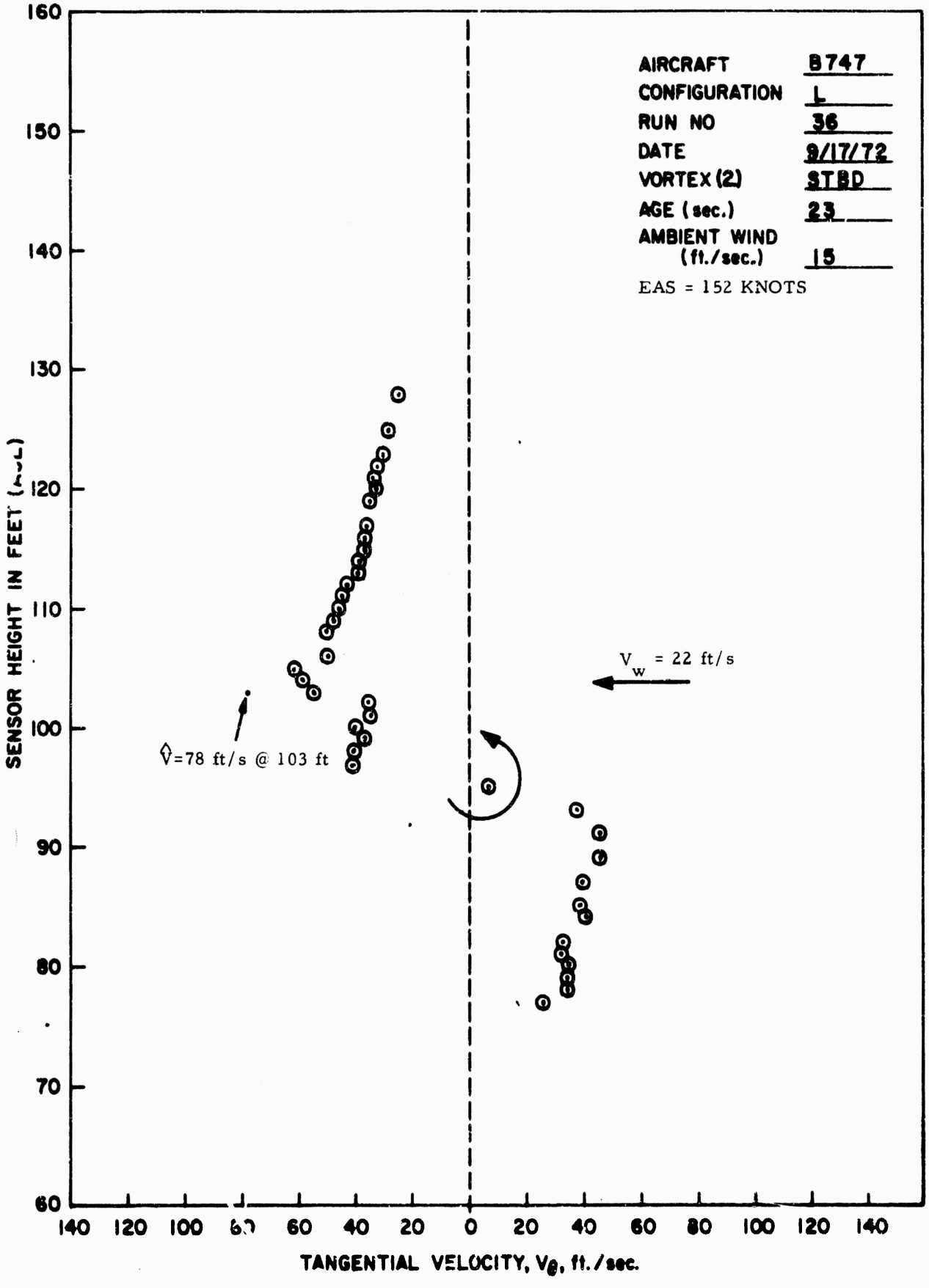
AIRCRAFT B747
CONFIGURATION L
RUN NO 36
DATE 9/17/72
VORTEX (2) STBD
AGE (sec.) 23
AMBIENT WIND (ft./sec.) 15
EAS = 152 KNOTS
V_w = 22 ft/s
◊=78 ft/s @ 103 ft
SENSOR HEIGHT IN FEET (AGL)
TANGENTIAL VELOCITY, V_θ, ft./sec.
160
150
140
130
120
110
100
90
80
70
60
140 120 100 60 60 40 20 0 20 40 60 80 100 120 140

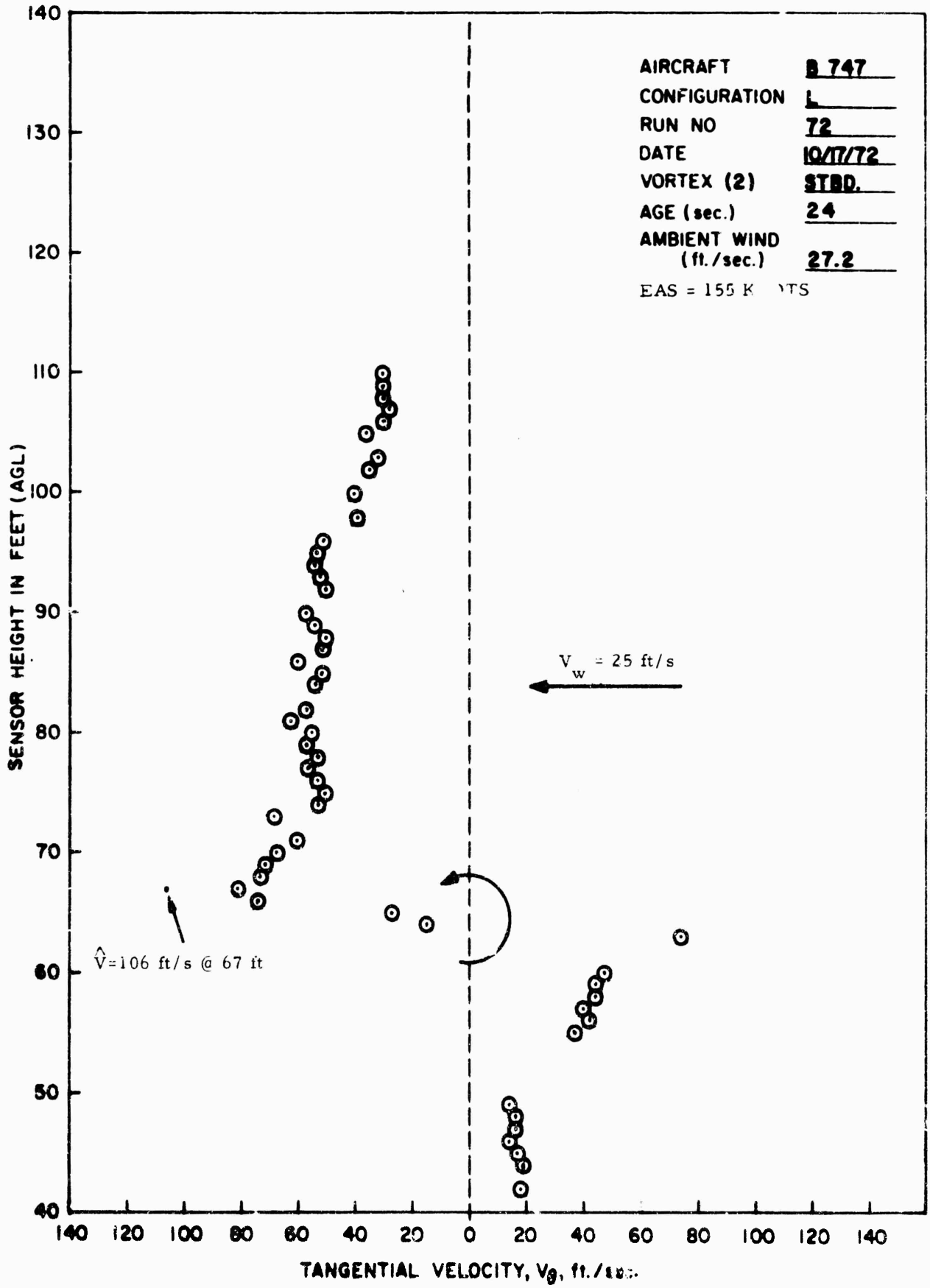
AIRCRAFT B 747
CONFIGURATION L
RUN NO 72
DATE 10/17/72
VORTEX (2) STBD.
AGE (sec.) 24
AMBIENT WIND (ft./sec.) 27.2
EAS = 155 K TS
V_w = 25 ft/s
$\hat{V}$=106 ft/s @ 67 ft
SENSOR HEIGHT IN FEET (AGL)
TANGENTIAL VELOCITY, V_θ, ft./sec.
140
130
120
110
100
90
80
70
60
50
40
140 120 100 80 60 40 20 0 20 40 60 80 100 120 140

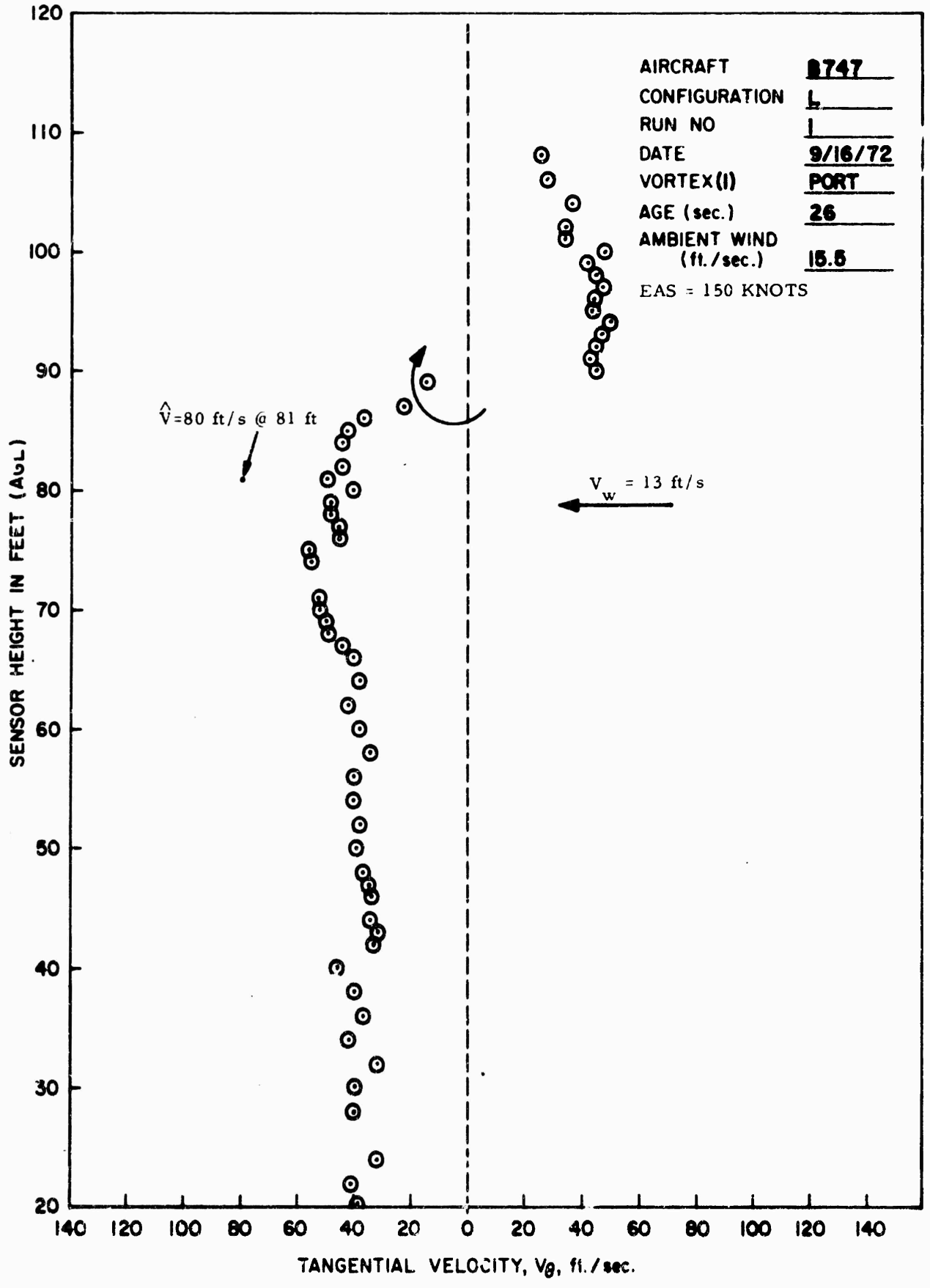
AIRCRAFT B747
CONFIGURATION L
RUN NO 1
DATE 9/16/72
VORTEX(1) PORT
AGE (sec.) 26
AMBIENT WIND (ft./sec.) 15.6
EAS = 150 KNOTS
$\hat{V}$=80 ft/s @ 81 ft
V_w = 13 ft/s
SENSOR HEIGHT IN FEET (AGL)
120
110
100
90
80
70
60
50
40
30
20
140 120 100 80 60 40 20 0 20 40 60 80 100 120 140
TANGENTIAL VELOCITY, V_θ, ft./sec.

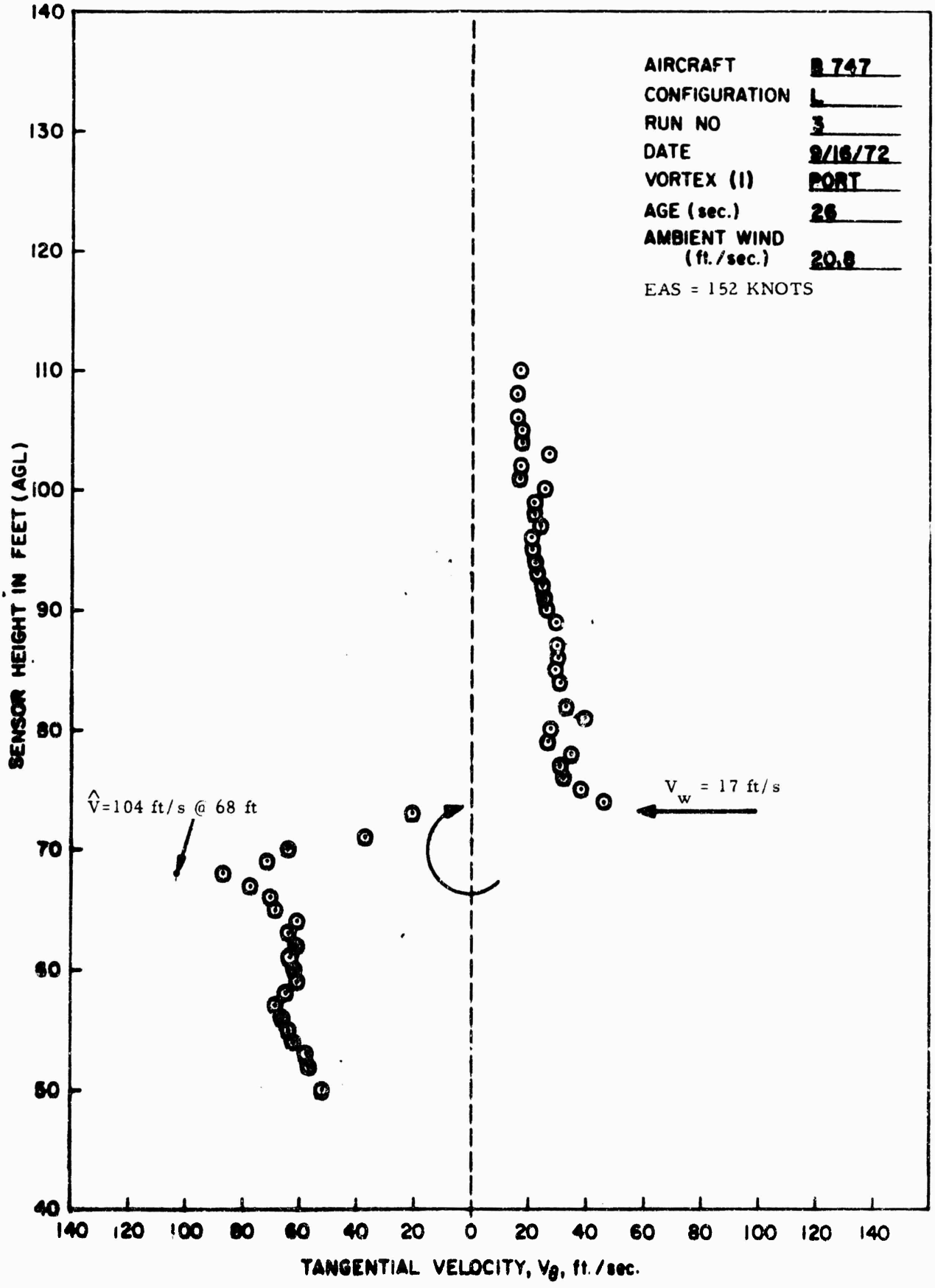
AIRCRAFT B 747
CONFIGURATION L
RUN NO 3
DATE 9/16/72
VORTEX (1) PORT
AGE (sec.) 26
AMBIENT WIND (ft./sec.) 20.8
EAS = 152 KNOTS
$\hat{V}$=104 ft/s @ 68 ft
V_w = 17 ft/s
SENSOR HEIGHT IN FEET (AGL)
TANGENTIAL VELOCITY, V_g, ft./sec.
140
130
120
110
100
90
80
70
60
50
40
140 120 100 80 60 40 20 0 20 40 60 80 100 120 140

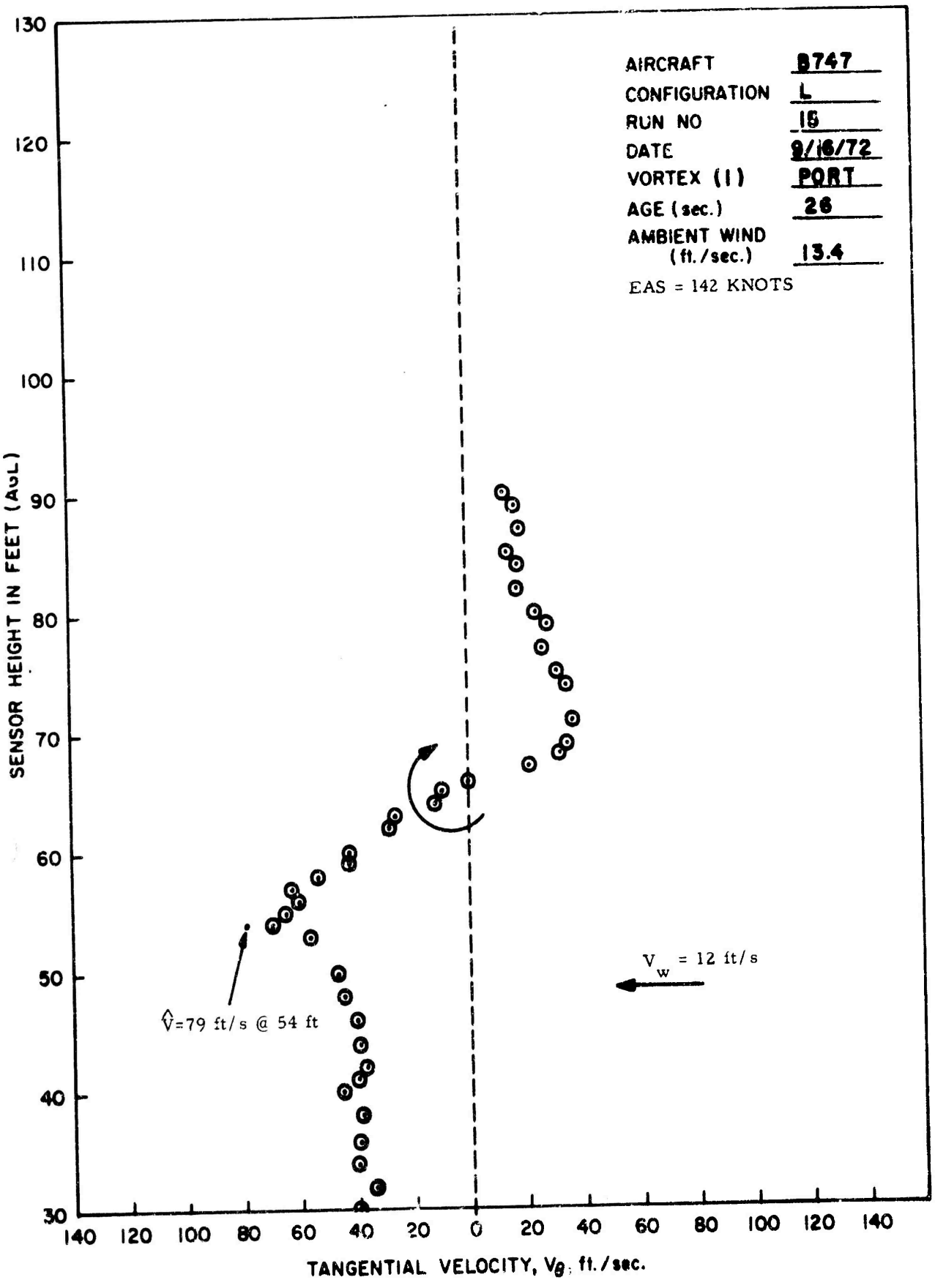
AIRCRAFT B747
CONFIGURATION L
RUN NO 15
DATE 9/16/72
VORTEX (1) PORT
AGE (sec.) 26
AMBIENT WIND (ft./sec.) 13.4
EAS = 142 KNOTS
SENSOR HEIGHT IN FEET (AGL)
130
120
110
100
90
80
70
60
50
40
30
140 120 100 80 60 40 20 0 20 40 60 80 100 120 140
TANGENTIAL VELOCITY, V_θ, ft./sec.
V_w = 12 ft/s
$\hat{V}$=79 ft/s @ 54 ft

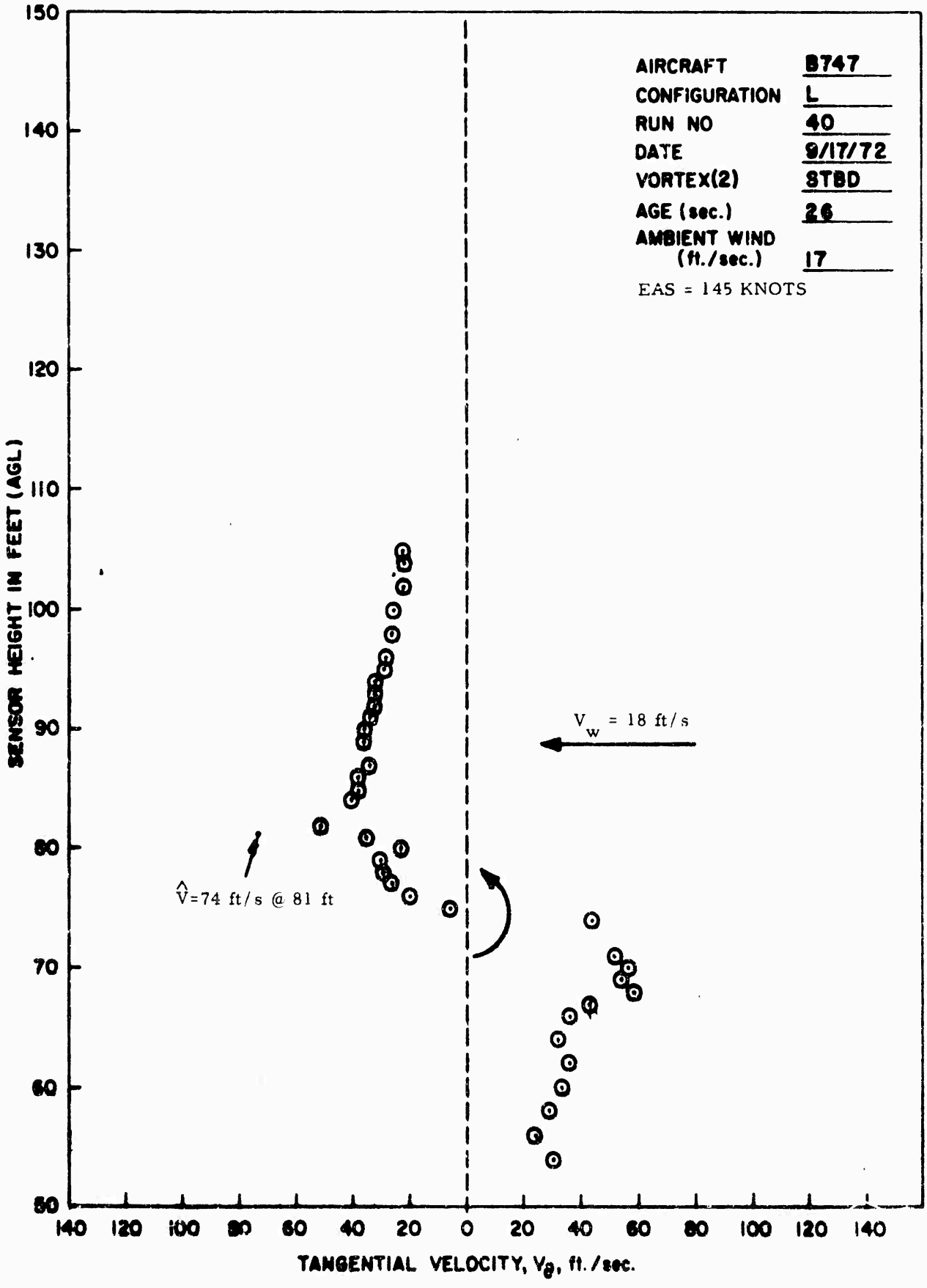
AIRCRAFT B747
CONFIGURATION L
RUN NO 40
DATE 9/17/72
VORTEX(2) STBD
AGE (sec.) 26
AMBIENT WIND (ft./sec.) 17
EAS = 145 KNOTS
V_w = 18 ft/s
$\hat{V}$=74 ft/s @ 81 ft
SENSOR HEIGHT IN FEET (AGL)
150
140
130
120
110
100
90
80
70
60
50
140 120 100 80 60 40 20 0 20 40 60 80 100 120 140
TANGENTIAL VELOCITY, V_θ, ft./sec.

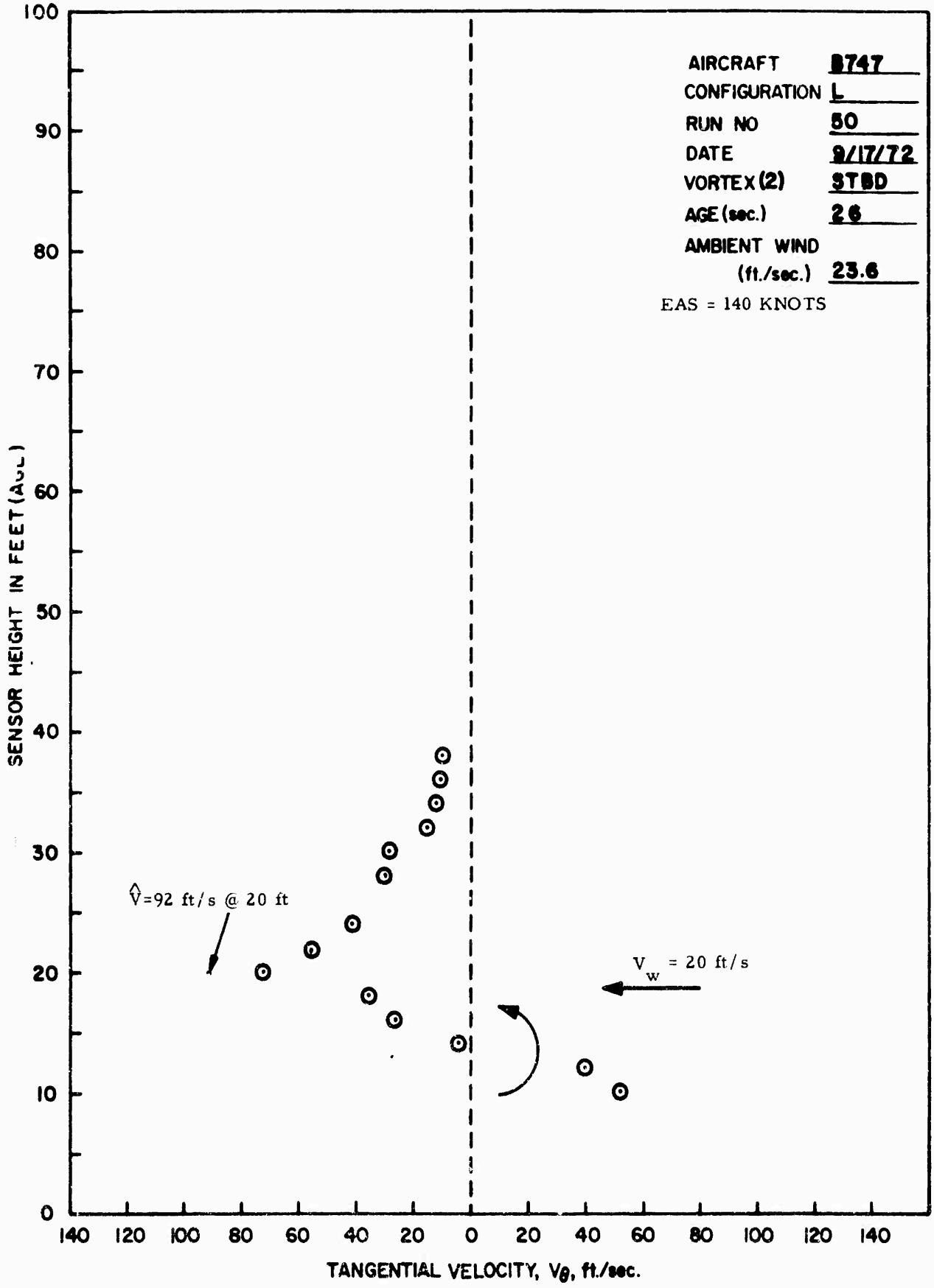
AIRCRAFT B747
CONFIGURATION L
RUN NO 50
DATE 9/17/72
VORTEX (2) STBD
AGE (sec.) 26
AMBIENT WIND (ft./sec.) 23.6
EAS = 140 KNOTS
SENSOR HEIGHT IN FEET (AGL)
TANGENTIAL VELOCITY, Vθ, ft./sec.
100
90
80
70
60
50
40
30
20
10
0
140 120 100 80 60 40 20 0 20 40 60 80 100 120 140
V=92 ft/s @ 20 ft
V_w = 20 ft/s

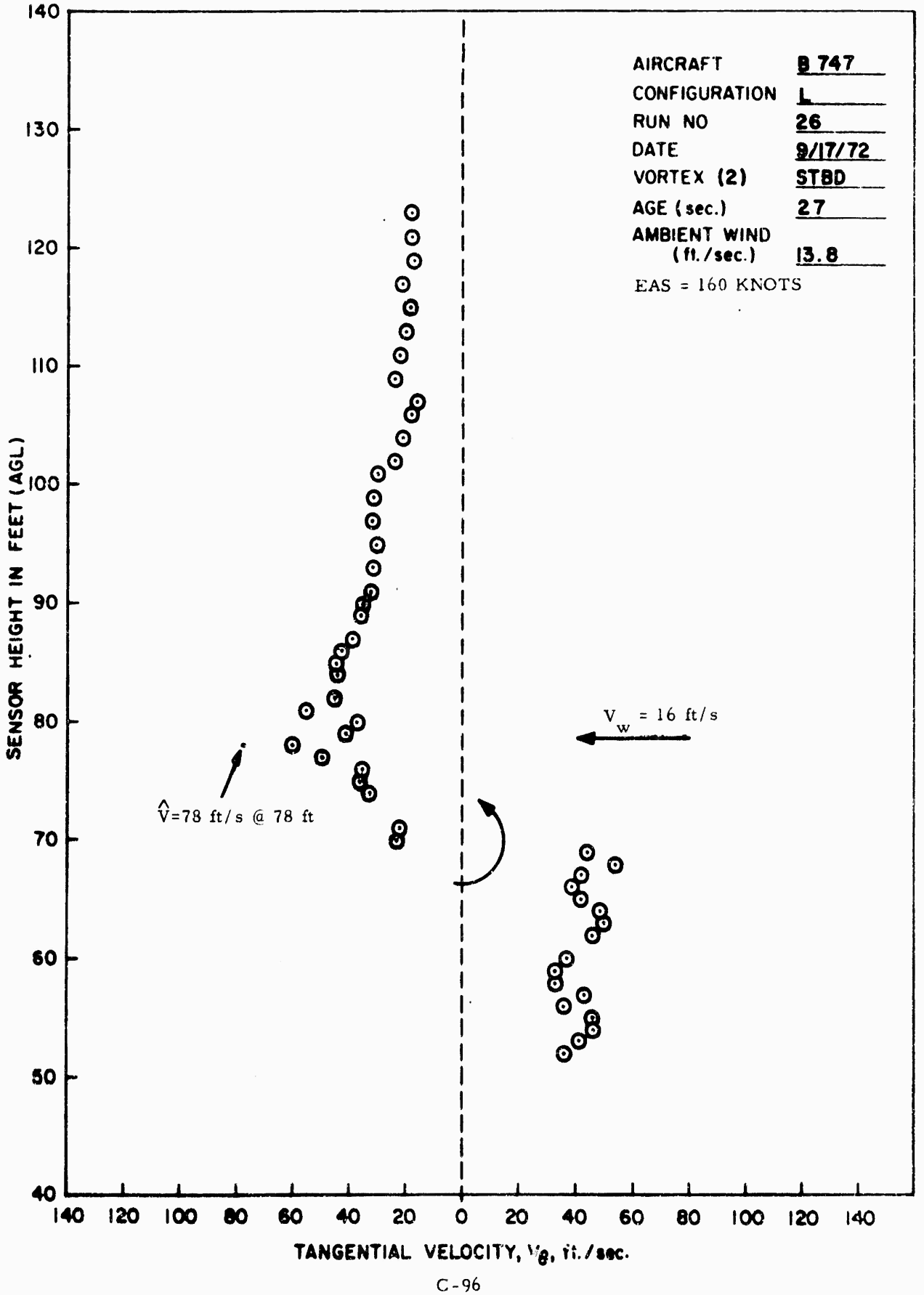
AIRCRAFT B 747
CONFIGURATION L
RUN NO 26
DATE 9/17/72
VORTEX (2) STBD
AGE (sec.) 27
AMBIENT WIND (ft./sec.) 13.8
EAS = 160 KNOTS
V_w = 16 ft/s
$\hat{V}$=78 ft/s @ 78 ft
SENSOR HEIGHT IN FEET (AGL)
TANGENTIAL VELOCITY, V_θ, ft./sec.
140
130
120
110
100
90
80
70
60
50
40
140 120 100 80 60 40 20 0 20 40 60 80 100 120 140

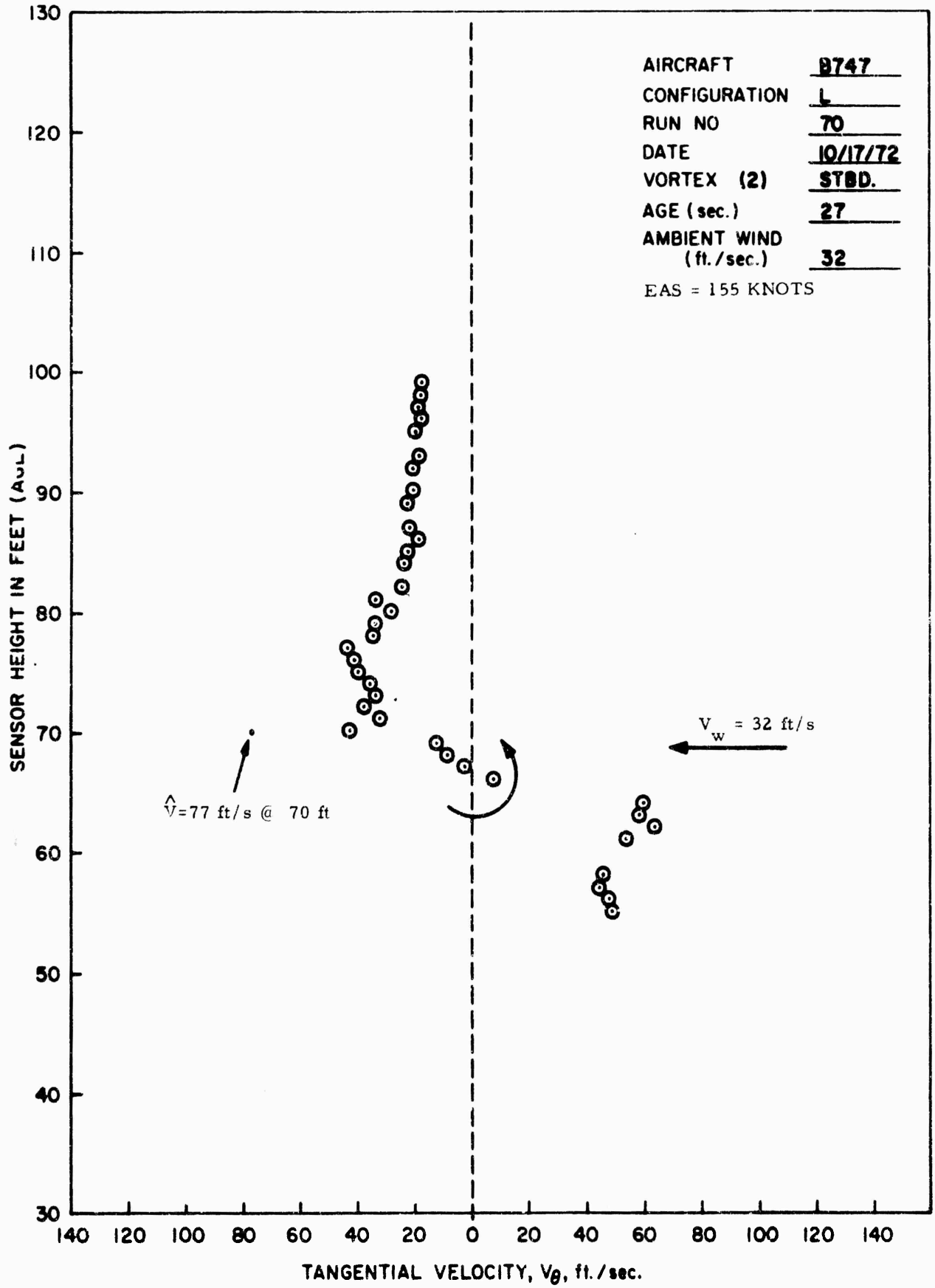
AIRCRAFT B747
CONFIGURATION L
RUN NO 70
DATE 10/17/72
VORTEX (2) STBD.
AGE (sec.) 27
AMBIENT WIND (ft./sec.) 32
EAS = 155 KNOTS
V_w = 32 ft/s
$\hat{V}$=77 ft/s @ 70 ft
SENSOR HEIGHT IN FEET (AGL)
TANGENTIAL VELOCITY, V_θ, ft./sec.
130
120
110
100
90
80
70
60
50
40
30
140 120 100 80 60 40 20 0 20 40 60 80 100 120 140

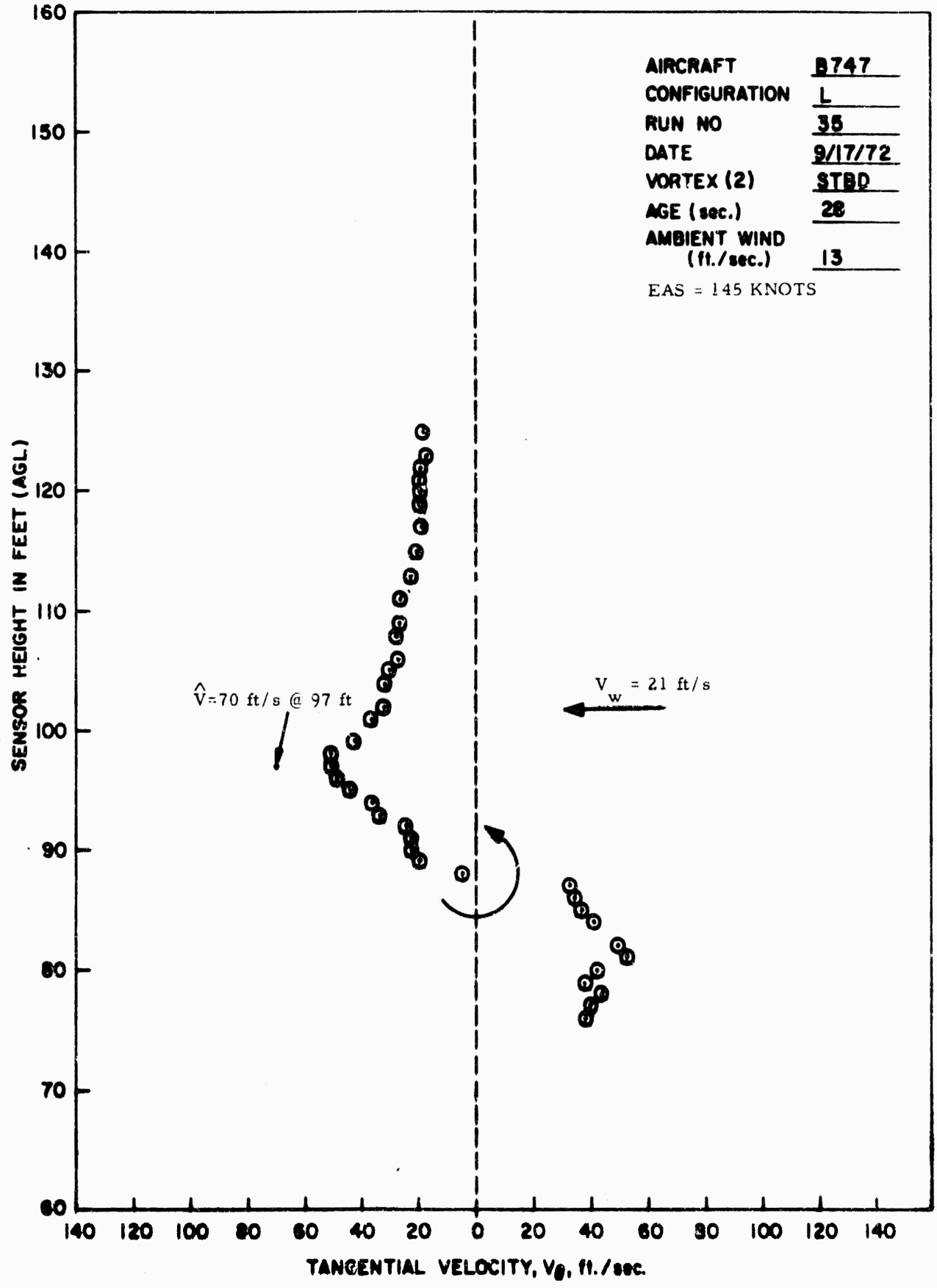
AIRCRAFT B747
CONFIGURATION L
RUN NO 35
DATE 9/17/72
VORTEX (2) STBD
AGE (sec.) 28
AMBIENT WIND (ft./sec.) 13
EAS = 145 KNOTS
$\hat{V}$=70 ft/s @ 97 ft
V_w = 21 ft/s
SENSOR HEIGHT IN FEET (AGL)
160
150
140
130
120
110
100
90
80
70
60
140 120 100 80 60 40 20 0 20 40 60 80 100 120 140
TANGENTIAL VELOCITY, V_θ, ft./sec.

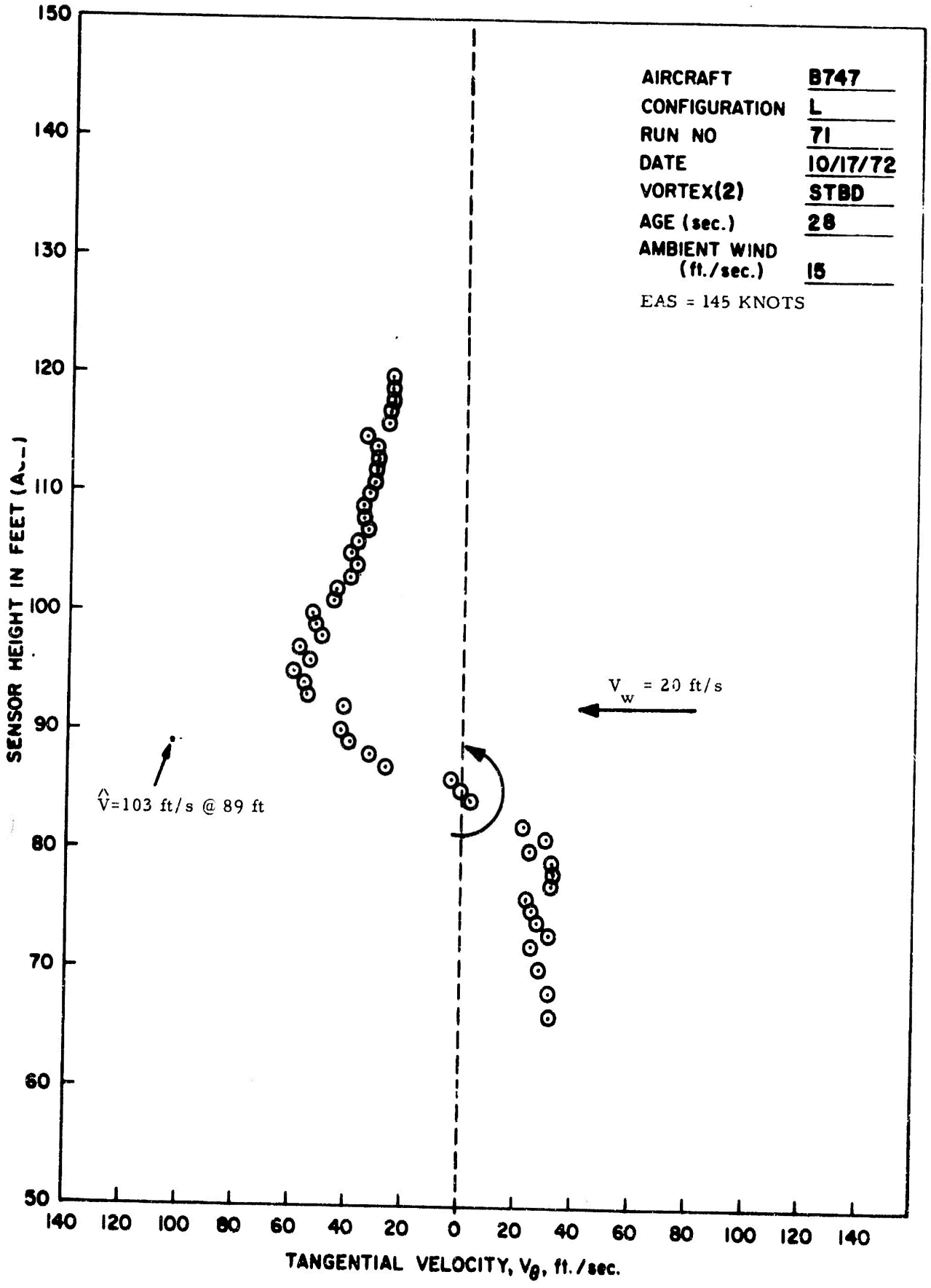
AIRCRAFT B747
CONFIGURATION L
RUN NO 71
DATE 10/17/72
VORTEX(2) STBD
AGE (sec.) 28
AMBIENT WIND (ft./sec.) 15
EAS = 145 KNOTS
V_w = 20 ft/s
$\hat{V}$=103 ft/s @ 89 ft
SENSOR HEIGHT IN FEET (AGL)
TANGENTIAL VELOCITY, V_θ, ft./sec.
150
140
130
120
110
100
90
80
70
60
50
140 120 100 80 60 40 20 0 20 40 60 80 100 120 140

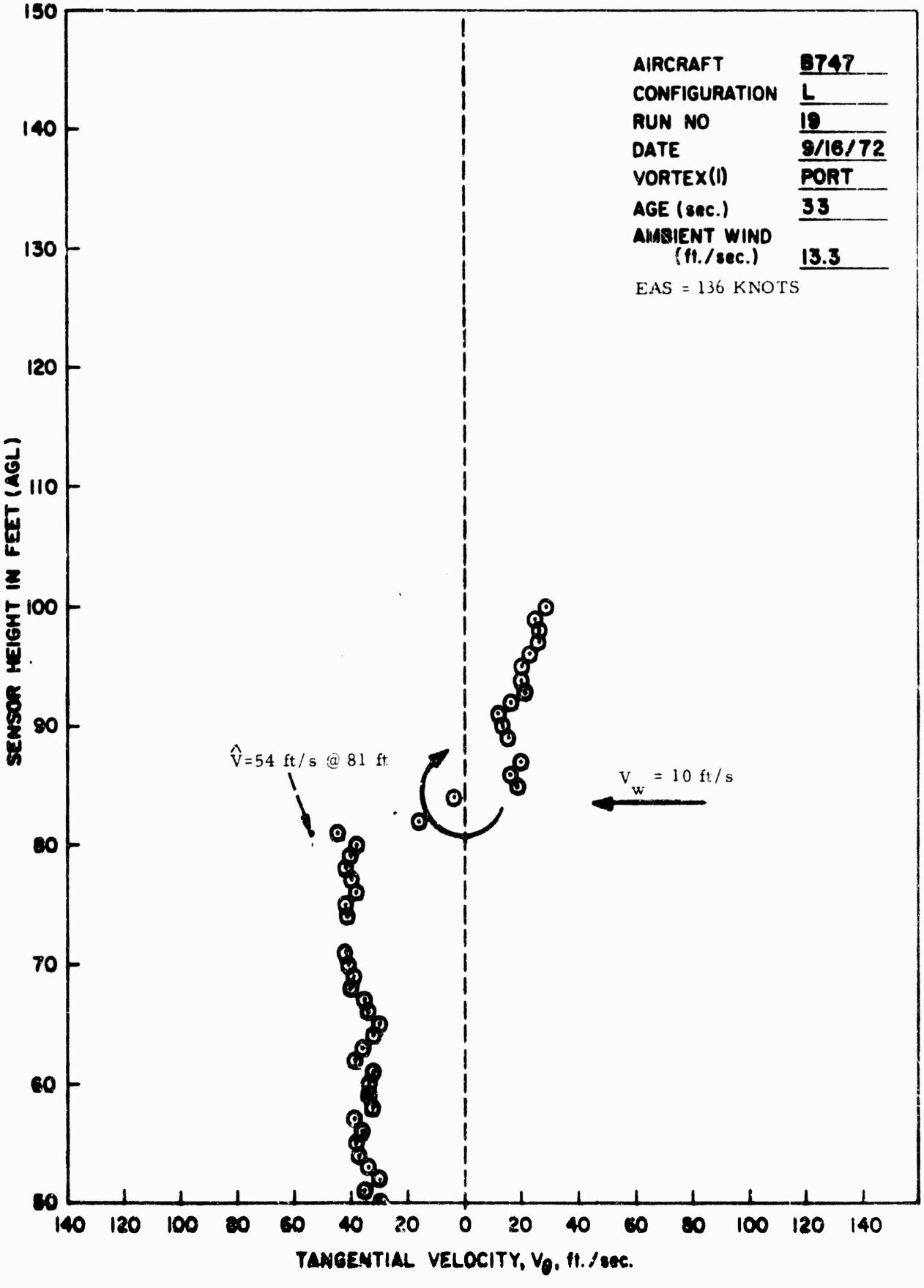
AIRCRAFT B747
CONFIGURATION L
RUN NO 19
DATE 9/16/72
VORTEX(1) PORT
AGE (sec.) 33
AMBIENT WIND (ft./sec.) 13.3
EAS = 136 KNOTS
$\hat{V}$=54 ft/s @ 81 ft
V_w = 10 ft/s
SENSOR HEIGHT IN FEET (AGL)
150
140
130
120
110
100
90
80
70
60
50
140 120 100 80 60 40 20 0 20 40 60 80 100 120 140
TANGENTIAL VELOCITY, V_θ, ft./sec.

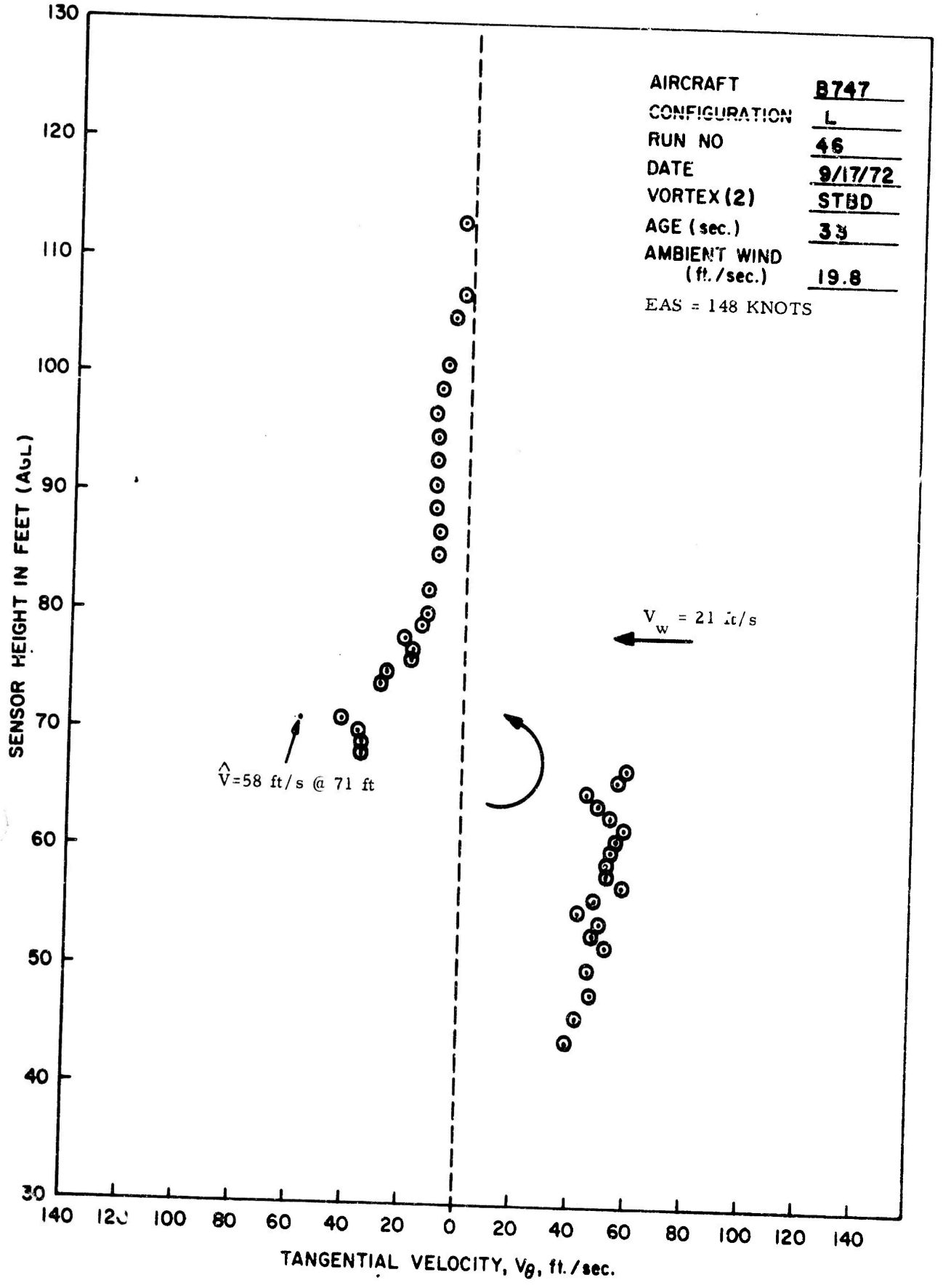
AIRCRAFT B747
CONFIGURATION L
RUN NO 46
DATE 9/17/72
VORTEX (2) STBD
AGE (sec.) 33
AMBIENT WIND (ft./sec.) 19.8
EAS = 148 KNOTS
V_w = 21 ft/s
$\hat{V}$=58 ft/s @ 71 ft
SENSOR HEIGHT IN FEET (AGL)
TANGENTIAL VELOCITY, V_θ, ft./sec.
130
120
110
100
90
80
70
60
50
40
30
140
120
100
80
60
40
20
0
20
40
60
80
100
120
140

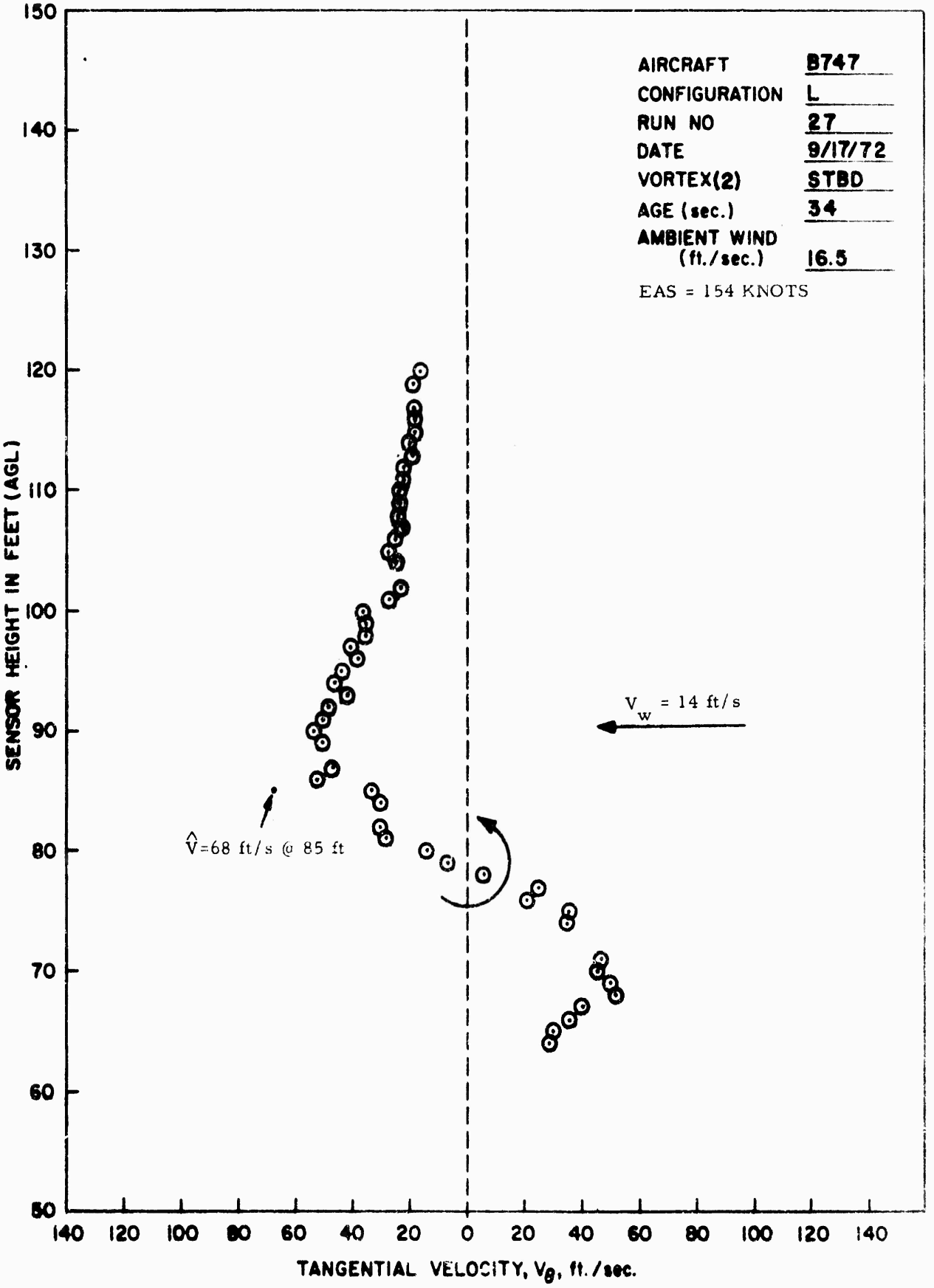
AIRCRAFT B747
CONFIGURATION L
RUN NO 27
DATE 9/17/72
VORTEX(2) STBD
AGE (sec.) 34
AMBIENT WIND (ft./sec.) 16.5
EAS = 154 KNOTS
V_w = 14 ft/s
$\hat{V}$=68 ft/s @ 85 ft
SENSOR HEIGHT IN FEET (AGL)
150
140
130
120
110
100
90
80
70
60
50
140 120 100 80 60 40 20 0 20 40 60 80 100 120 140
TANGENTIAL VELOCITY, V_θ, ft./sec.

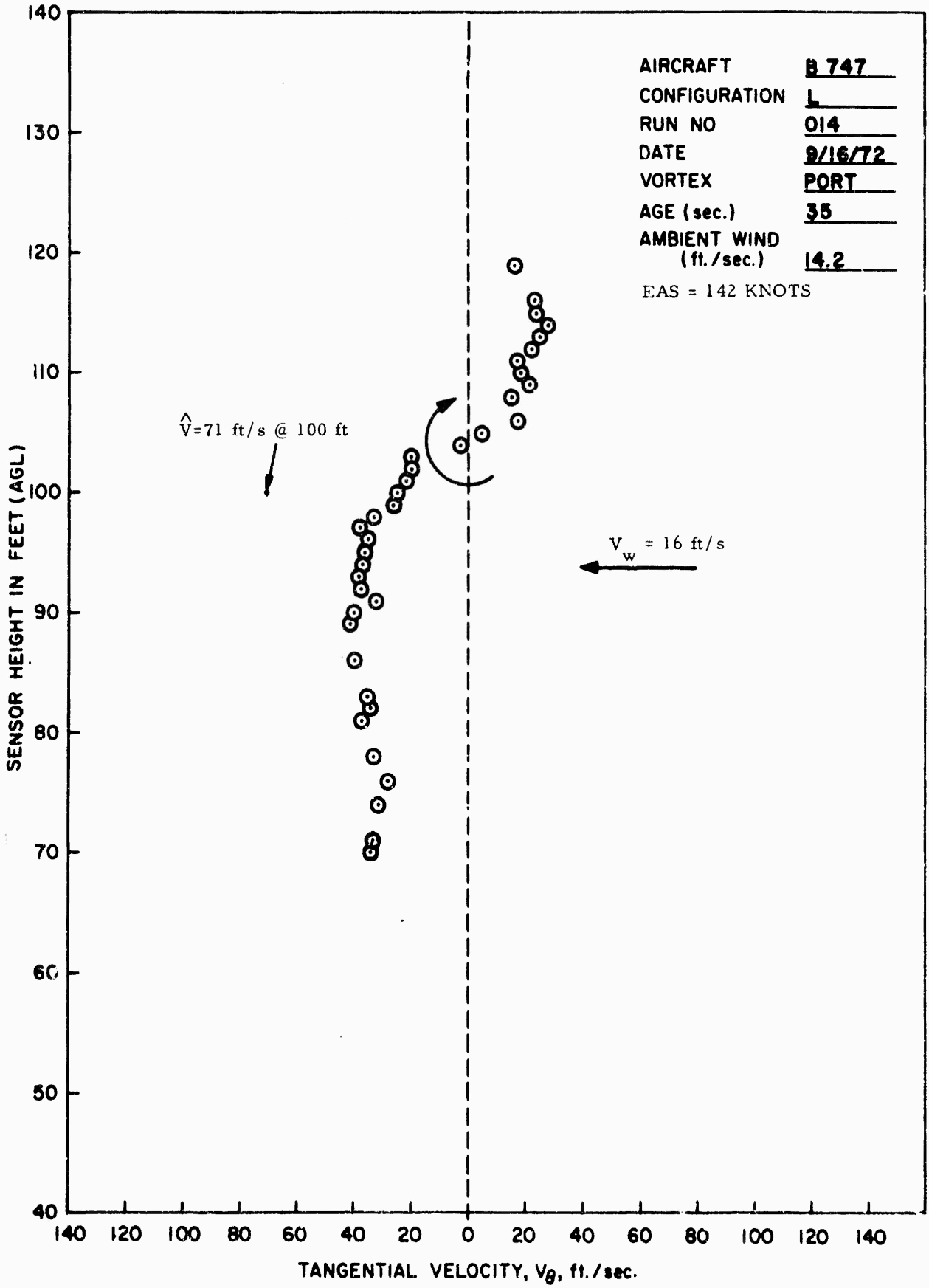
AIRCRAFT B 747
CONFIGURATION L
RUN NO 014
DATE 9/16/72
VORTEX PORT
AGE (sec.) 35
AMBIENT WIND (ft./sec.) 14.2
EAS = 142 KNOTS
$\hat{V}$=71 ft/s @ 100 ft
V_w = 16 ft/s
SENSOR HEIGHT IN FEET (AGL)
140
130
120
110
100
90
80
70
60
50
40
140 120 100 80 60 40 20 0 20 40 60 80 100 120 140
TANGENTIAL VELOCITY, V_θ, ft./sec.

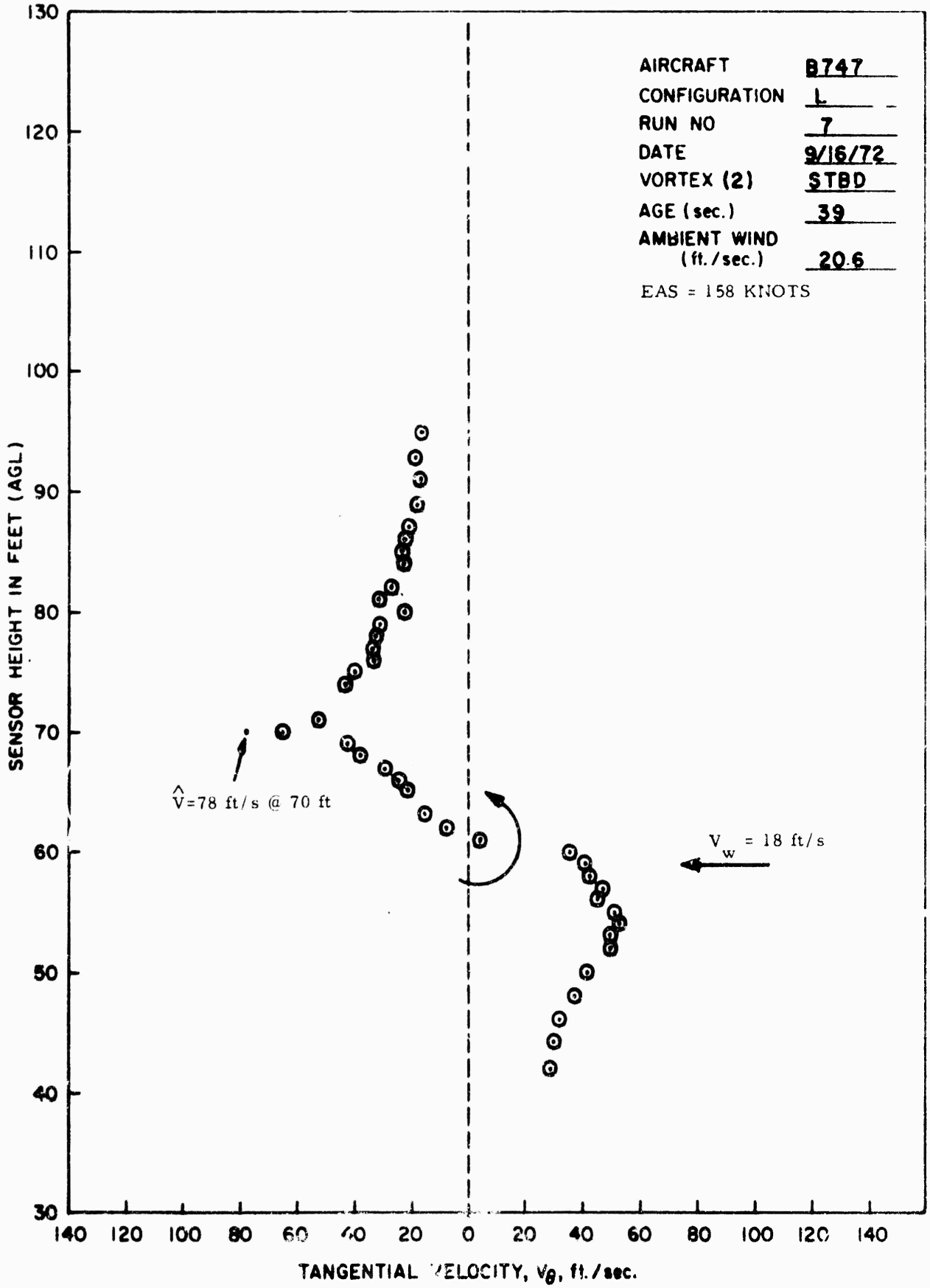
AIRCRAFT B747
CONFIGURATION L
RUN NO 7
DATE 9/16/72
VORTEX (2) STBD
AGE (sec.) 39
AMBIENT WIND (ft./sec.) 20.6
EAS = 158 KNOTS
SENSOR HEIGHT IN FEET (AGL)
130
120
110
100
90
80
70
60
50
40
30
140 120 100 80 60 40 20 0 20 40 60 80 100 120 140
TANGENTIAL VELOCITY, V_θ, ft./sec.
$\hat{V}$=78 ft/s @ 70 ft
V_w = 18 ft/s

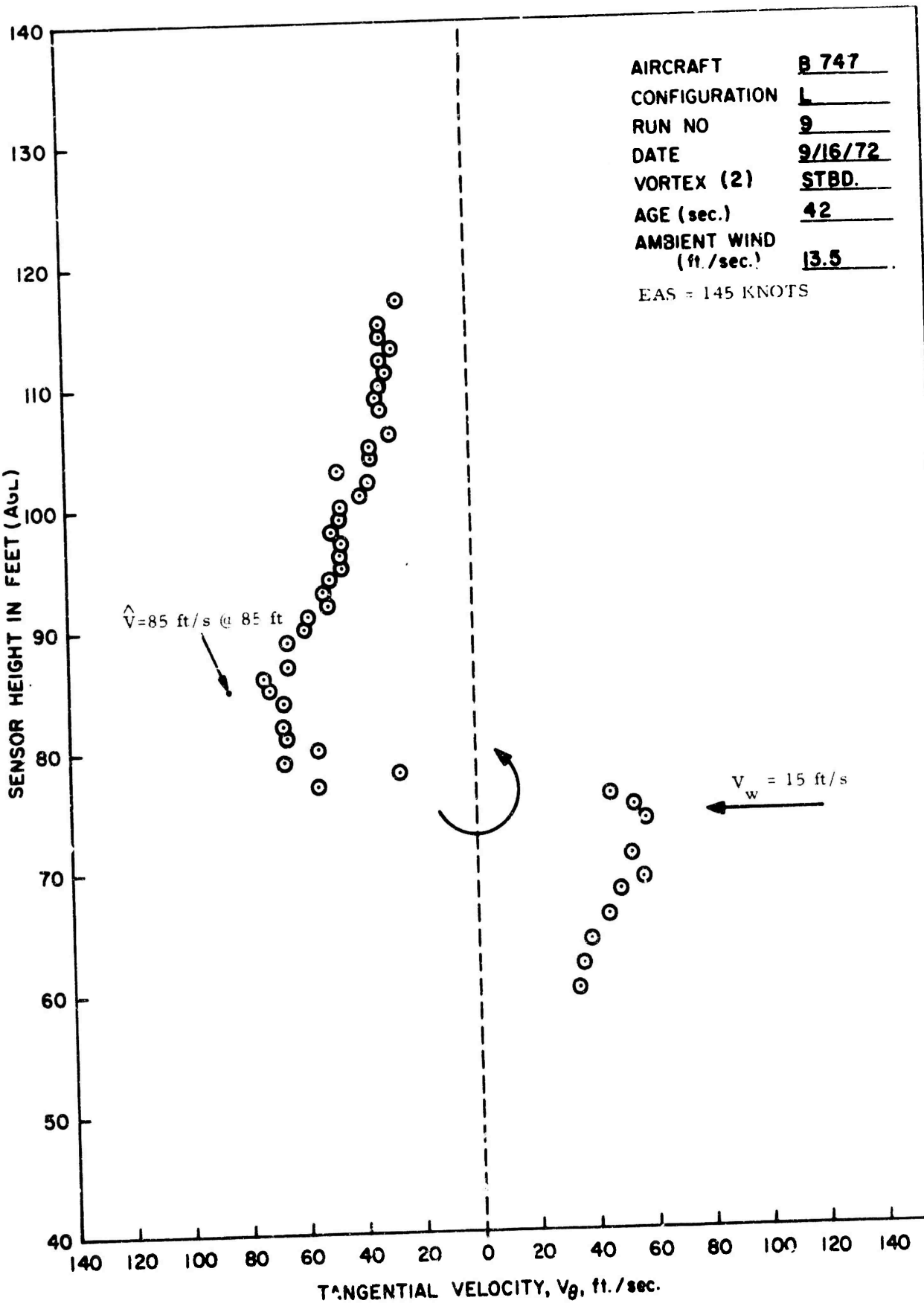
AIRCRAFT B 747
CONFIGURATION L
RUN NO 9
DATE 9/16/72
VORTEX (2) STBD.
AGE (sec.) 42
AMBIENT WIND (ft./sec.) 13.5
EAS = 145 KNOTS
$\hat{V}$=85 ft/s @ 85 ft
V_w = 15 ft/s
SENSOR HEIGHT IN FEET (AGL)
TANGENTIAL VELOCITY, V_θ, ft./sec.
140
130
120
110
100
90
80
70
60
50
40
140 120 100 80 60 40 20 0 20 40 60 80 100 120 140

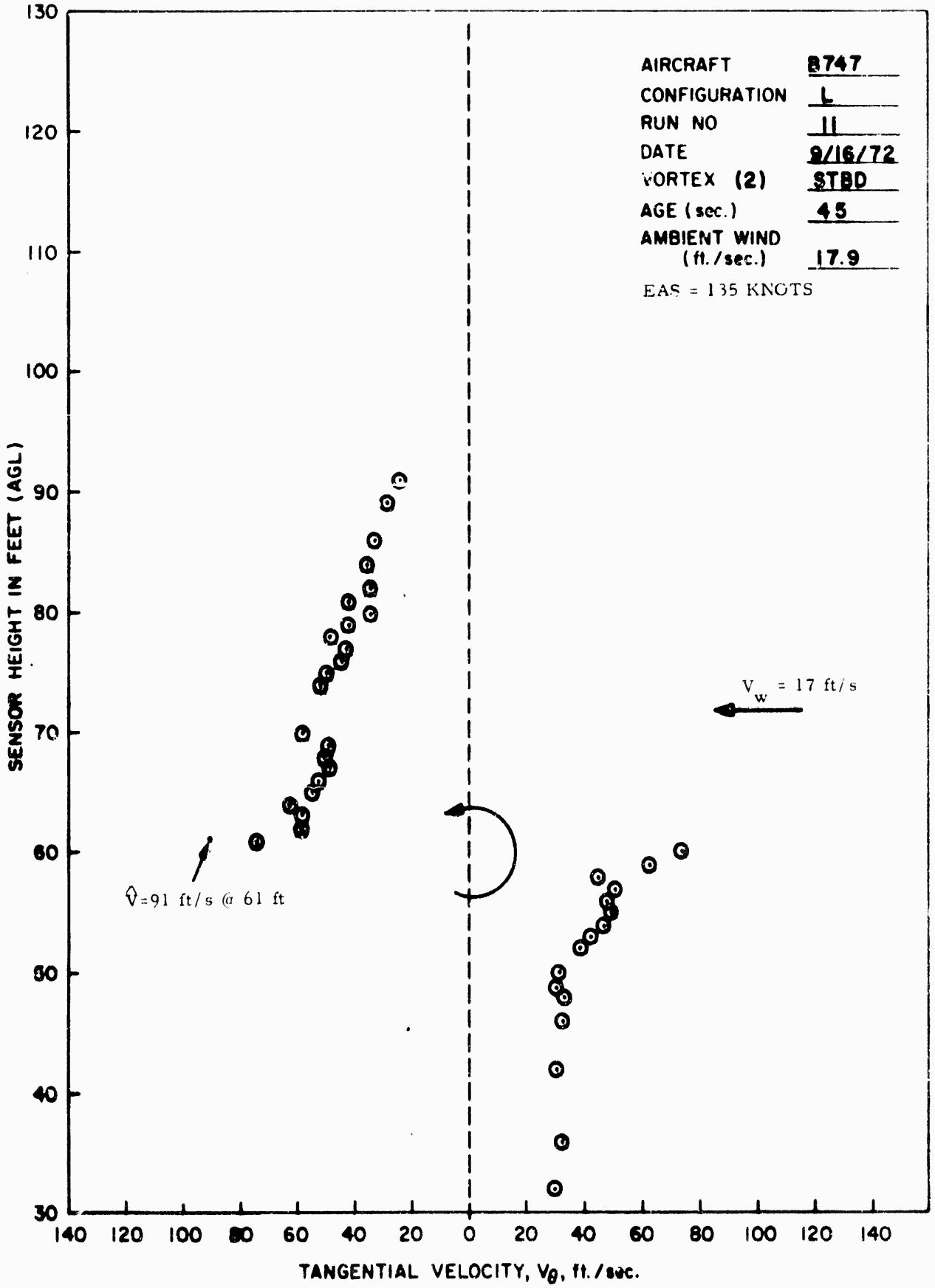
AIRCRAFT B747
CONFIGURATION L
RUN NO 11
DATE 9/16/72
VORTEX (2) STBD
AGE (sec.) 45
AMBIENT WIND (ft./sec.) 17.9
EAS = 135 KNOTS
V_w = 17 ft/s
◊=91 ft/s @ 61 ft
SENSOR HEIGHT IN FEET (AGL)
130
120
110
100
90
80
70
60
50
40
30
140 120 100 80 60 40 20 0 20 40 60 80 100 120 140
TANGENTIAL VELOCITY, V_θ, ft./sec.

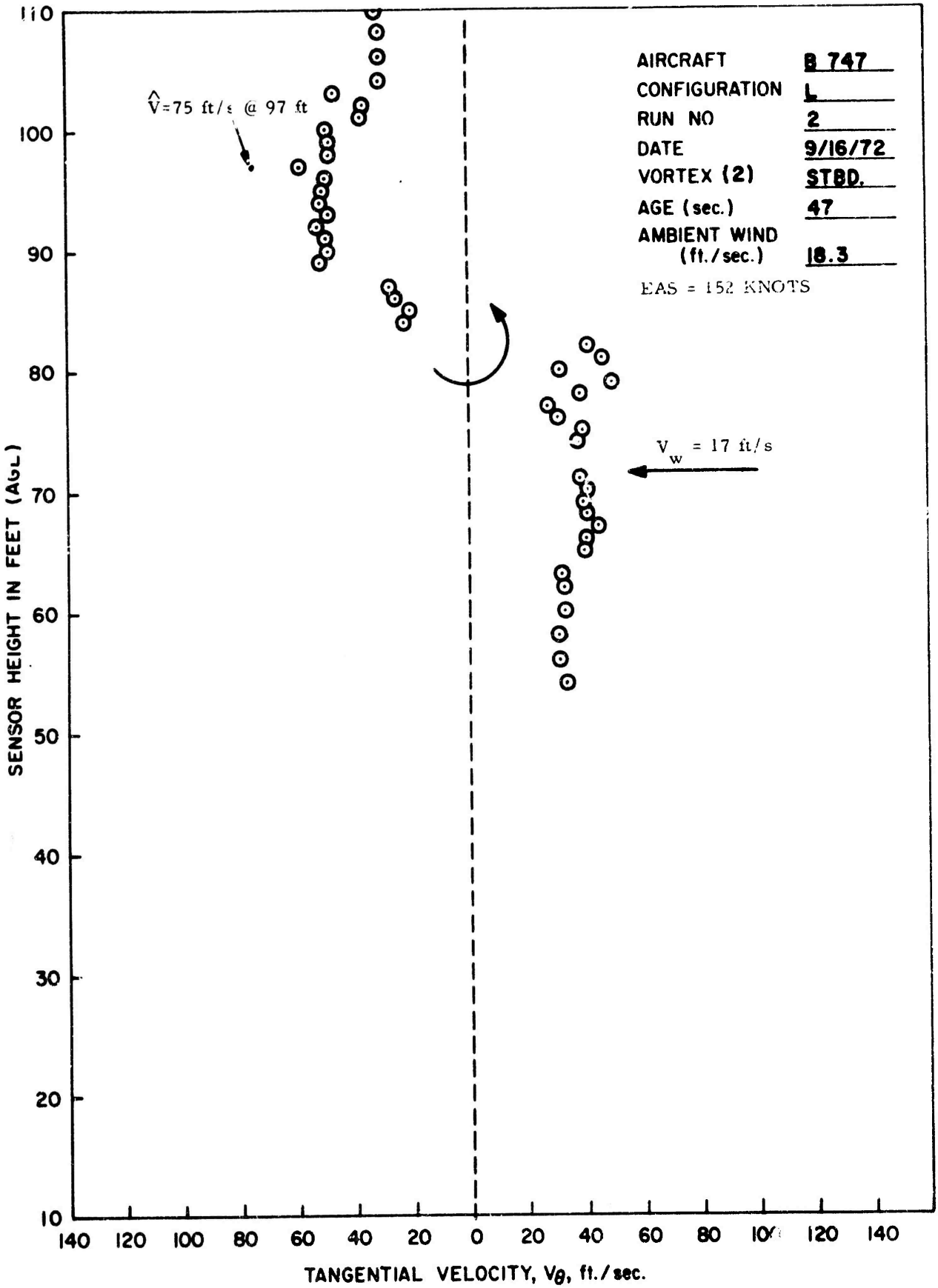
AIRCRAFT B 747
CONFIGURATION L
RUN NO 2
DATE 9/16/72
VORTEX (2) STBD.
AGE (sec.) 47
AMBIENT WIND (ft./sec.) 18.3
EAS = 152 KNOTS
$\hat{V}$=75 ft/s @ 97 ft
V_w = 17 ft/s
SENSOR HEIGHT IN FEET (AGL)
110
100
90
80
70
60
50
40
30
20
10
140 120 100 80 60 40 20 0 20 40 60 80 100 120 140
TANGENTIAL VELOCITY, V_θ, ft./sec.

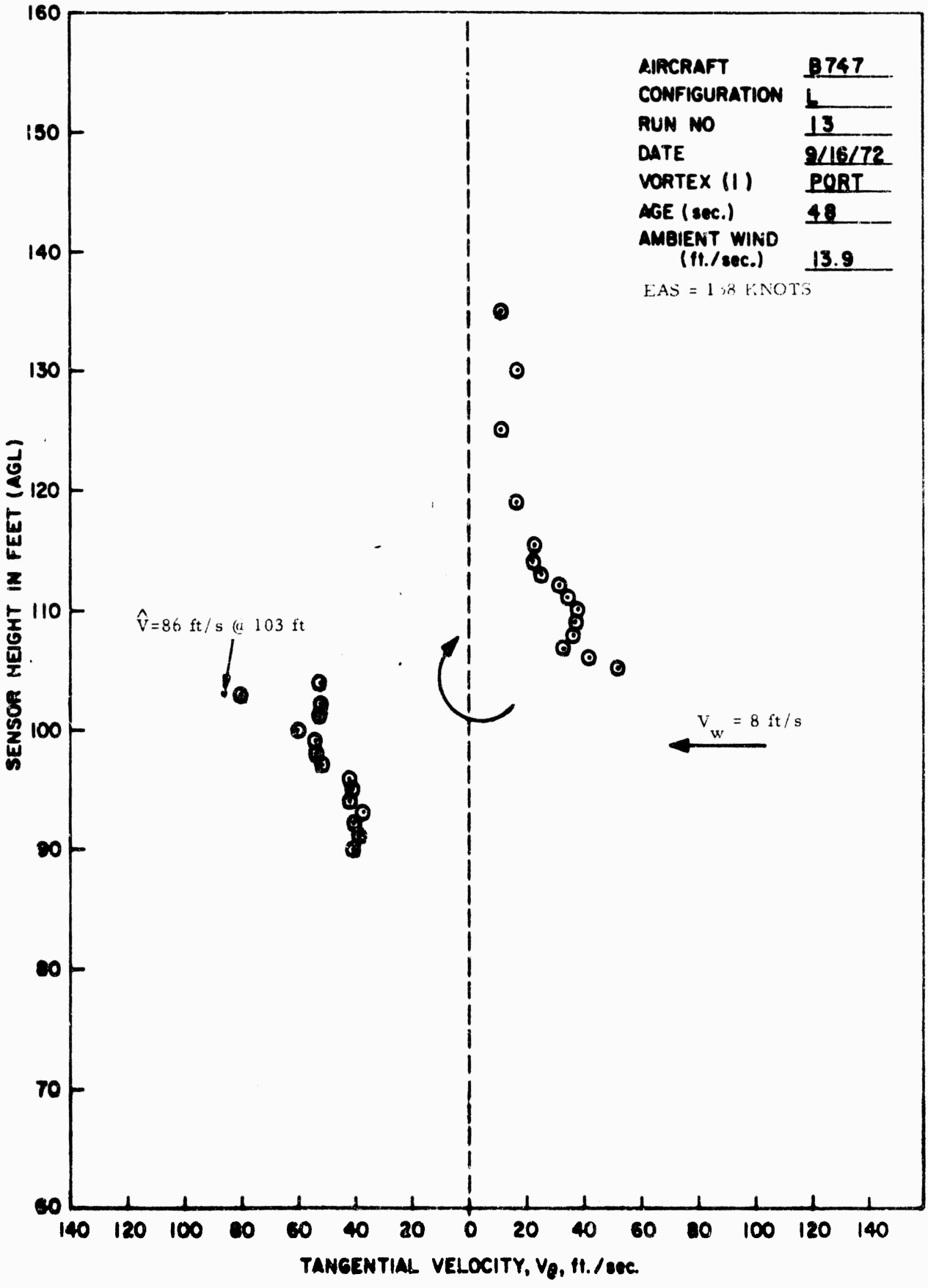
AIRCRAFT B747
CONFIGURATION L
RUN NO 13
DATE 9/16/72
VORTEX (1) PORT
AGE (sec.) 48
AMBIENT WIND (ft./sec.) 13.9
EAS = 158 KNOTS
$\hat{V}$=86 ft/s @ 103 ft
V_w = 8 ft/s
SENSOR HEIGHT IN FEET (AGL)
160
150
140
130
120
110
100
90
80
70
60
140 120 100 80 60 40 20 0 20 40 60 80 100 120 140
TANGENTIAL VELOCITY, V_θ, ft./sec.

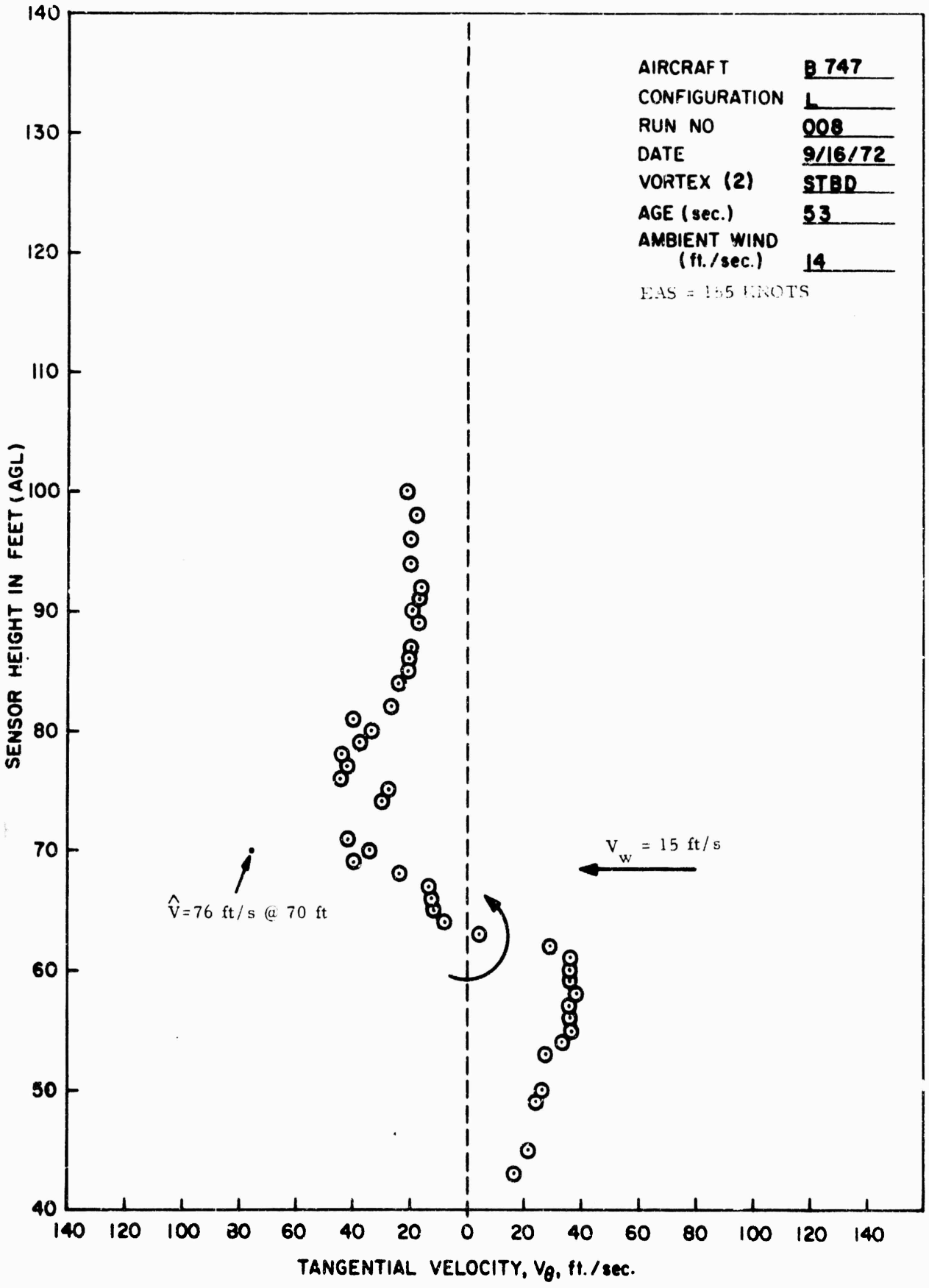
AIRCRAFT B 747
CONFIGURATION L
RUN NO 008
DATE 9/16/72
VORTEX (2) STBD
AGE (sec.) 53
AMBIENT WIND (ft./sec.) 14
EAS = 155 KNOTS
V_w = 15 ft/s
$\hat{V}$=76 ft/s @ 70 ft
SENSOR HEIGHT IN FEET (AGL)
TANGENTIAL VELOCITY, V_θ, ft./sec.
140
130
120
110
100
90
80
70
60
50
40
140 120 100 80 60 40 20 0 20 40 60 80 100 120 140

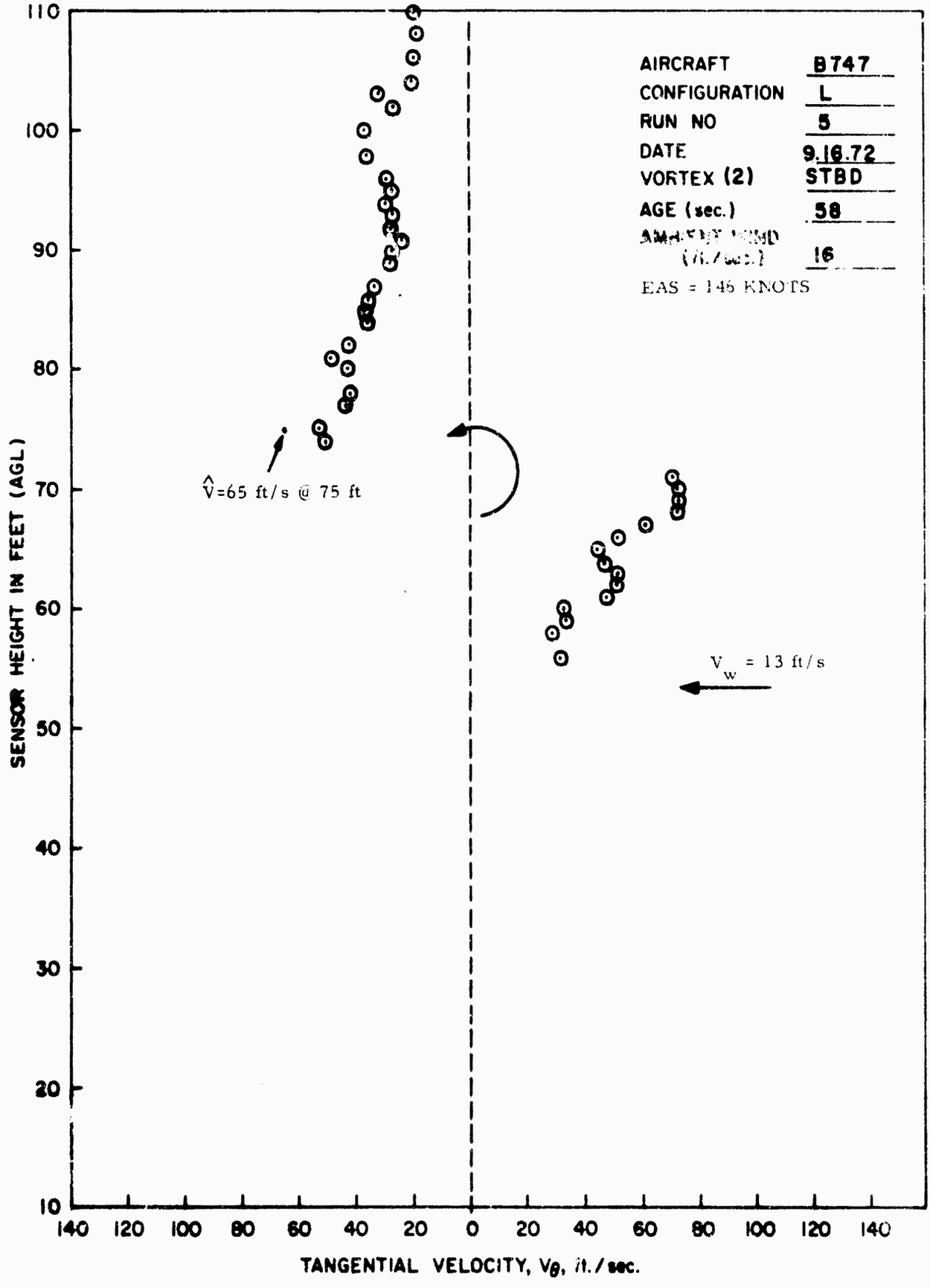
AIRCRAFT B747
CONFIGURATION L
RUN NO 5
DATE 9.16.72
VORTEX (2) STBD
AGE (sec.) 58
AMBIENT WIND (ft./sec.) 16
EAS = 146 KNOTS
$\hat{V}$=65 ft/s @ 75 ft
V_w = 13 ft/s
SENSOR HEIGHT IN FEET (AGL)
110
100
90
80
70
60
50
40
30
20
10
140 120 100 80 60 40 20 0 20 40 60 80 100 120 140
TANGENTIAL VELOCITY, V_θ, ft./sec.

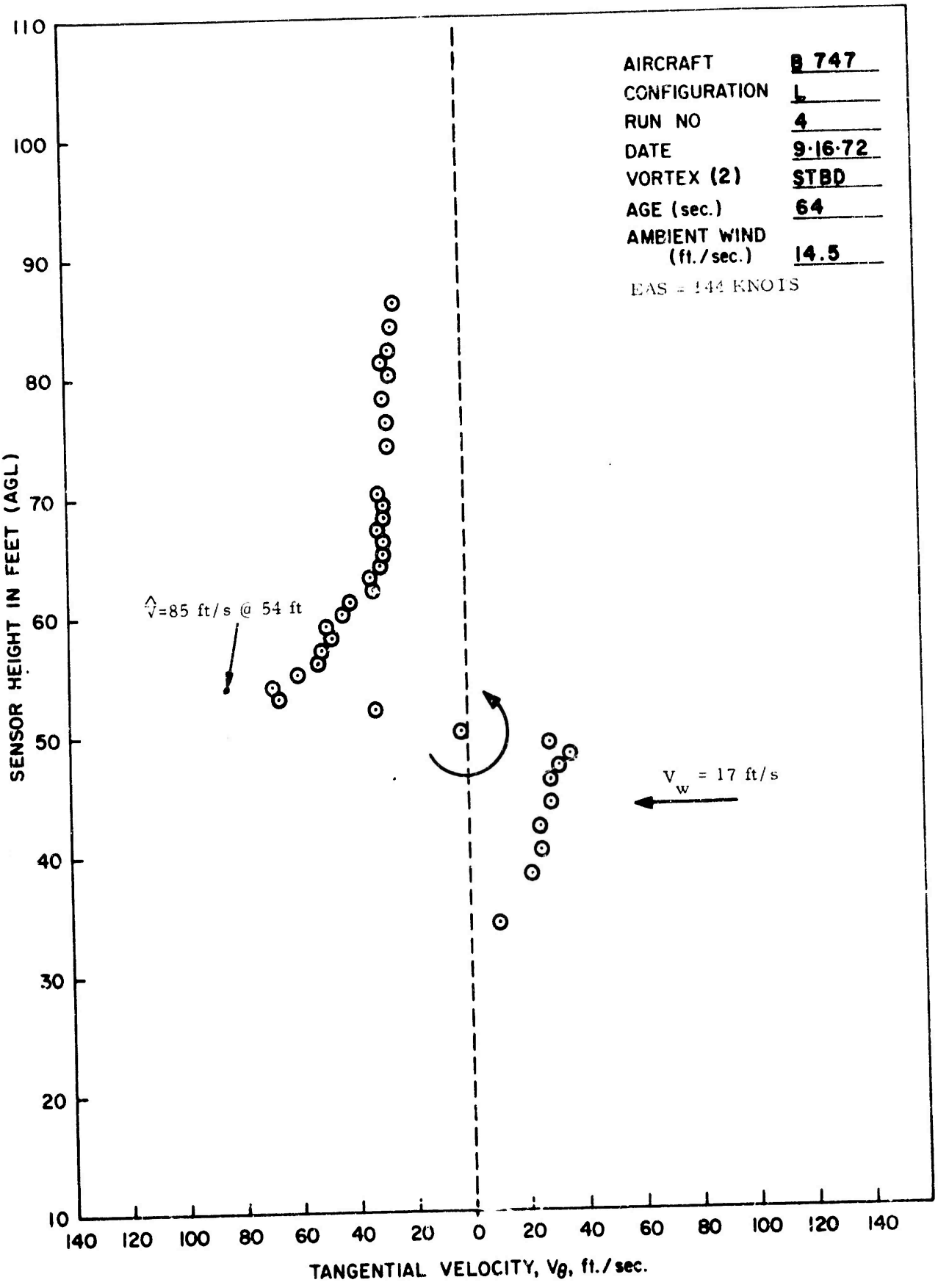
AIRCRAFT B 747
CONFIGURATION L
RUN NO 4
DATE 9·16·72
VORTEX (2) STBD
AGE (sec.) 64
AMBIENT WIND (ft./sec.) 14.5
EAS = 144 KNOTS
V̂=85 ft/s @ 54 ft
V_w = 17 ft/s
SENSOR HEIGHT IN FEET (AGL)
TANGENTIAL VELOCITY, Vθ, ft./sec.
110
100
90
80
70
60
50
40
30
20
10
140 120 100 80 60 40 20 0 20 40 60 80 100 120 140

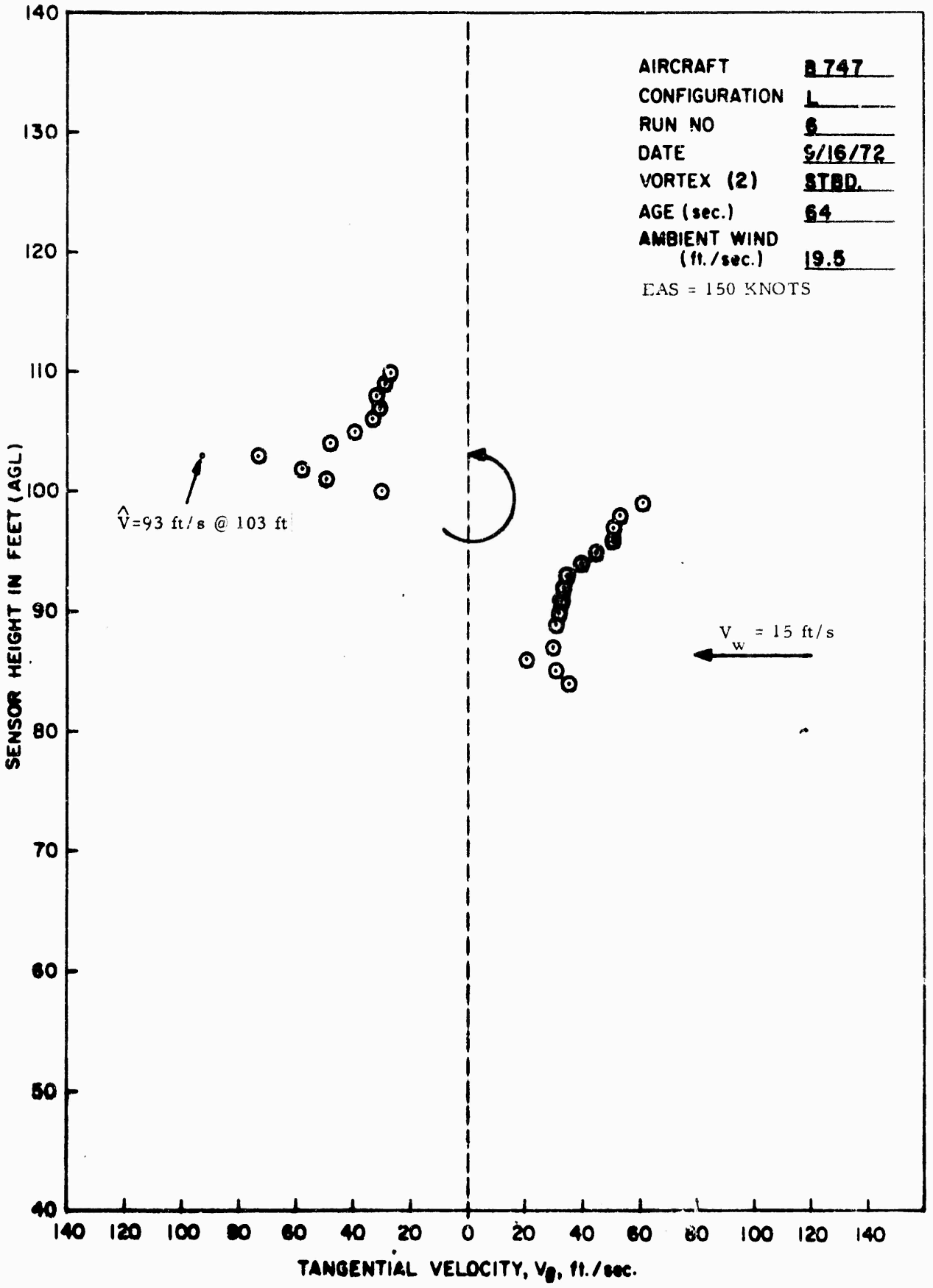
AIRCRAFT B 747
CONFIGURATION L
RUN NO 6
DATE 9/16/72
VORTEX (2) STBD.
AGE (sec.) 64
AMBIENT WIND (ft./sec.) 19.5
EAS = 150 KNOTS
$\hat{V}$=93 ft/s @ 103 ft
V_w = 15 ft/s
SENSOR HEIGHT IN FEET (AGL)
140
130
120
110
100
90
80
70
60
50
40
140 120 100 80 60 40 20 0 20 40 60 80 100 120 140
TANGENTIAL VELOCITY, V_θ, ft./sec.

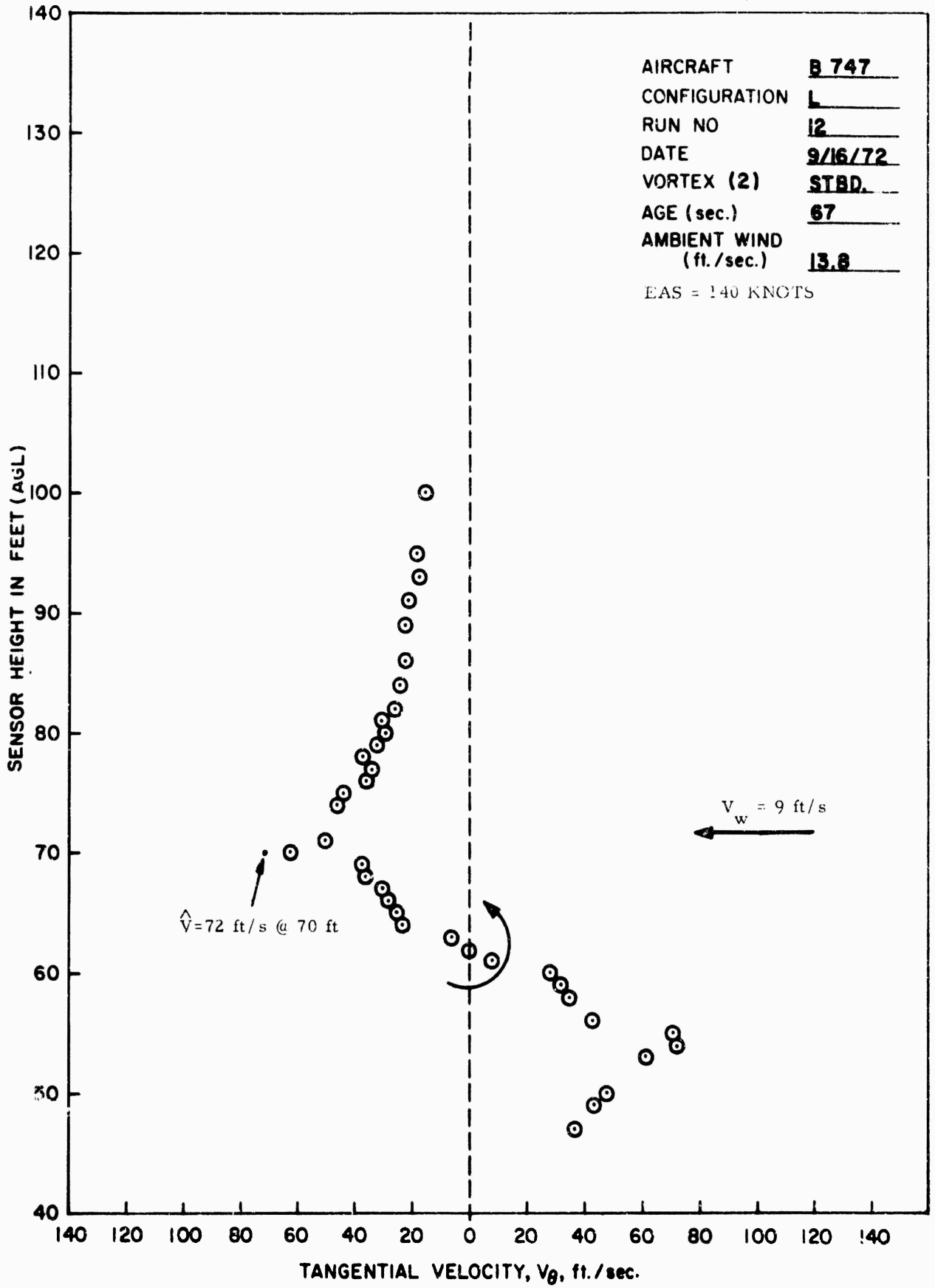
AIRCRAFT B 747
CONFIGURATION L
RUN NO 12
DATE 9/16/72
VORTEX (2) STBD.
AGE (sec.) 67
AMBIENT WIND (ft./sec.) 13.8
EAS = 140 KNOTS
V_w = 9 ft/s
$\hat{V}$=72 ft/s @ 70 ft
SENSOR HEIGHT IN FEET (AGL)
TANGENTIAL VELOCITY, V_θ, ft./sec.
140
130
120
110
100
90
80
70
60
50
40
140 120 100 80 60 40 20 0 20 40 60 80 100 120 140

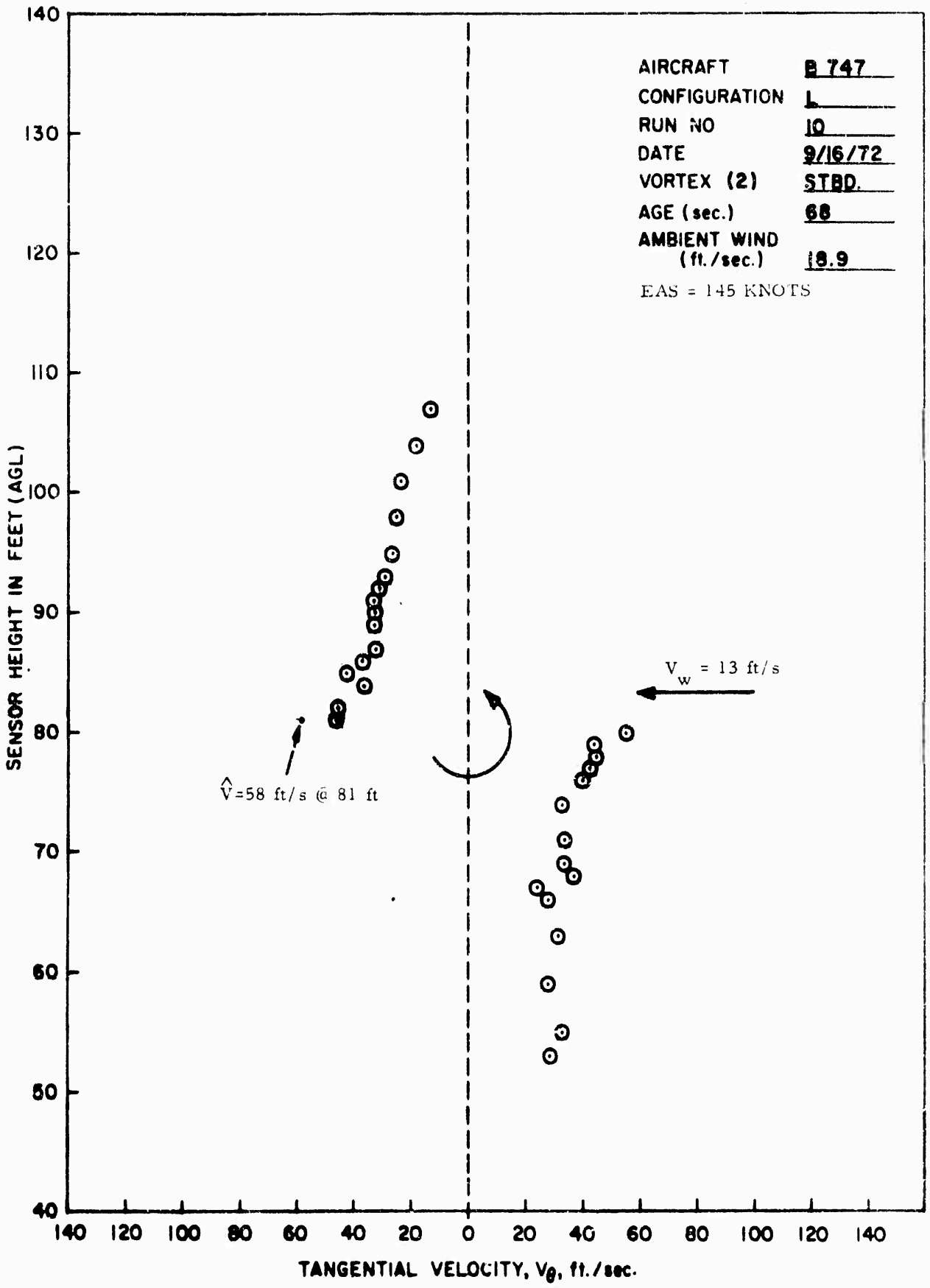
AIRCRAFT B 747
CONFIGURATION L
RUN NO 10
DATE 9/16/72
VORTEX (2) STBD.
AGE (sec.) 68
AMBIENT WIND (ft./sec.) 18.9
EAS = 145 KNOTS
V_w = 13 ft/s
$\hat{V}$=58 ft/s @ 81 ft
SENSOR HEIGHT IN FEET (AGL)
TANGENTIAL VELOCITY, V_θ, ft./sec.
140
130
120
110
100
90
80
70
60
50
40
140 120 100 80 60 40 20 0 20 40 60 80 100 120 140

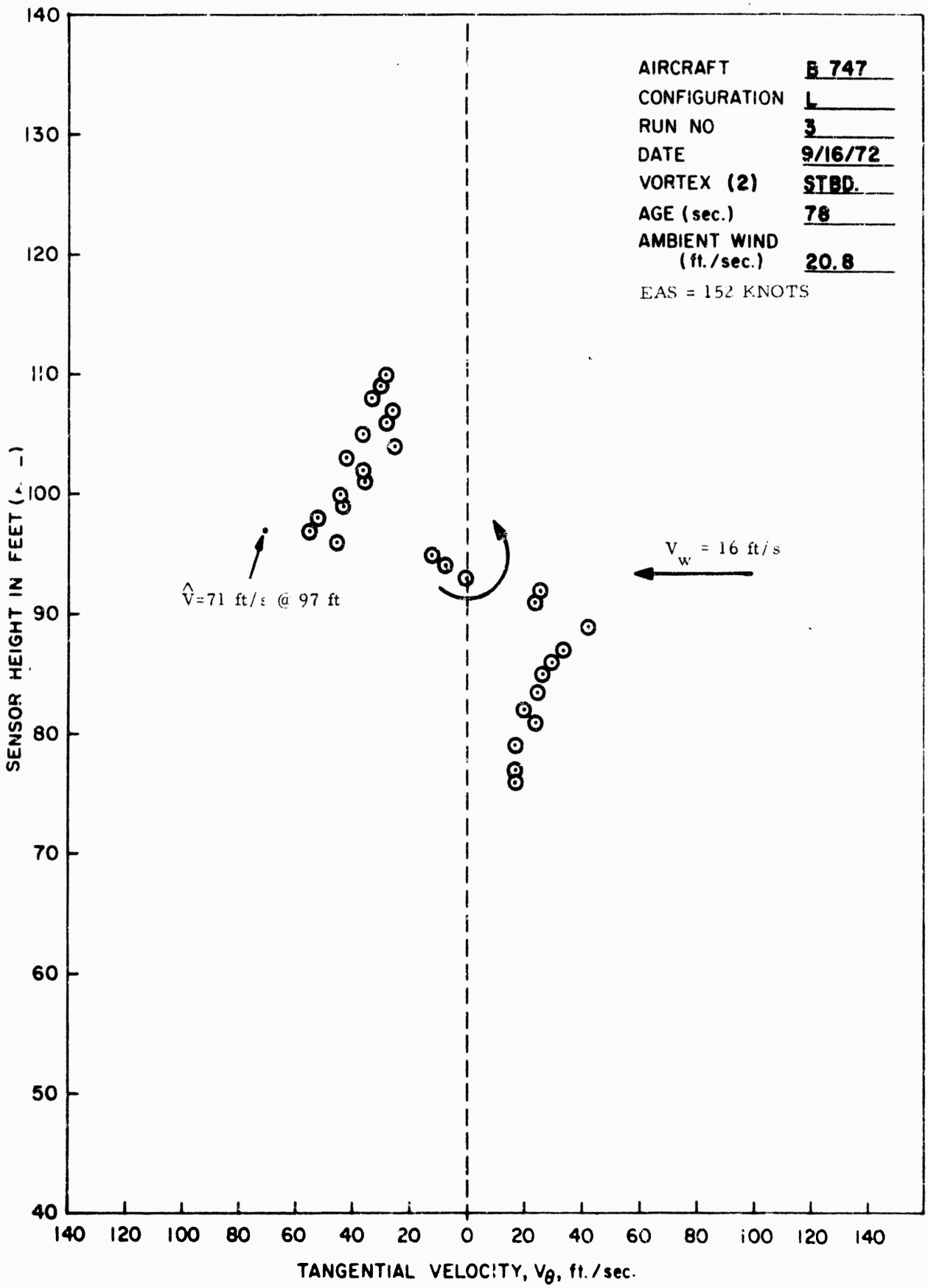
AIRCRAFT B 747
CONFIGURATION L
RUN NO 3
DATE 9/16/72
VORTEX (2) STBD.
AGE (sec.) 78
AMBIENT WIND (ft./sec.) 20.8
EAS = 152 KNOTS
V_w = 16 ft/s
$\hat{V}$=71 ft/s @ 97 ft
SENSOR HEIGHT IN FEET (A.G.L.)
140
130
120
110
100
90
80
70
60
50
40
140 120 100 80 60 40 20 0 20 40 60 80 100 120 140
TANGENTIAL VELOCITY, V_θ, ft./sec.

APPENDIX D

SUMMARY FLIGHT TEST DATA SHEETS

FLIGHT TEST DATA - BOEING 747 WAKE TURBULENCE

Run Number	1	2		4	5	6	7
Aircraft Position[1], ft.	390	267	448	291	296	261	176
Aircraft Height AGL[2], ft.	175	178	191	197	163	179	168
Equivalent Airspeed, Knots	150	152	152	144	146	150	158
Gross Weight, lb x 10^{-3}	538	536	534	532	530	528	526
Configuration[3]	L	L	L	L	L	L	L
Peak Recorded Absolute Velocity, First Vortex, ft/sec.	80	82	104	90	114	93	118
Peak Recorded Absolute Velocity, Second Vortex, ft/sec.	-	75	71	85	65	93	78
Vortex Height on Tower, First Vortex, ft.	89	84	74	91	84	78	109
Vortex Height on Tower, Second Vortex, ft.	-	83	93	50	74	100	61
Vortex Age (First) sec.	26	15	26	17	17	16	9
Vortex Age (Second) sec.	-	47	78	64	58	64	39
Mean Descent Rate, First Vortex, ft/sec.	3.31	6.27	4.50	6.24	4.65	6.31	6.56
Mean Descent Rate, Second Vortex, ft/sec.	-	2.02	1.26	2.30	1.53	1.23	2.74
Mean Lateral Velocity, First Vortex, ft/sec.	12.0	12.7	14.3	12.6	12.9	11.5	11.0
Mean Lateral Velocity, Second Vortex, ft/sec.	-	7.3	6.7	5.8	6.4	5.3	6.5
Crosswind Velocity Component, ft/sec.	3.5	6.4	10.9	8.4	9.3	11.0	9.5
Median Circulation $ft^2/sec.$	809	5720	5690	5984	5880	5701	5392

[1]Aircraft C/L lateral offset, ft. from tower base

[2]Determined when aircraft abreast of tower

[3]TO = Takeoff, HLDG = Holding, C = Cruise, L = Landing

FLIGHT TEST DATA - BOEING 747 WAKE TURBULENCE

Run Number	8	9	10	11	12	13	14
Aircraft Position[1], ft.	235	140	207	208	136	441	438
Aircraft Height AGL[2], ft.	187	184	168	206	225	234	224
Equivalent Airspeed, Knots	155	145	145	135	140	138	142
Gross Weight, lb x 10^{-3}	522	520	518	516	514	486	484
Configuration[3]	L	L	L	L	L	L	L
Peak Recorded Absolute Velocity, First Vortex, ft/sec.	110	145	110	83	76	86	71
Peak Recorded Absolute Velocity, Second Vortex, ft/sec.	76	85	58	91	72	-	-
Vortex Height on Tower, First Vortex, ft.	106	140	94	110	101	105	105
Vortex Height on Tower, Second Vortex, ft.	63	77	80	61	62	-	-
Vortex Age (First) sec.	13	6	12	13	16	48	35
Vortex Age (Second) sec.	53	42	68	45	67	-	-
Mean Descent Rate, First Vortex, ft/sec.	6.23	7.33	6.17	7.38	7.75	2.69	3.40
Mean Descent Rate, Second Vortex, ft/sec.	2.34	2.55	1.29	3.22	2.43	-	-
Mean Lateral Velocity, First Vortex, ft/sec.	12.2	10.5	10.8	10.1	3.7	7.6	10.3
Mean Lateral Velocity, Second Vortex, ft/sec.	5.9	5.2	4.2	6.3	3.2	-	-
Crosswind Velocity, Component, ft/sec.	8.6	8.8	8.7	10.5	5.6	5.7	8.0
Median Circulation $ft^2/sec.$	5455	5809	5786	6191	5947	5704	5521

FLIGHT TEST DATA - BOEING 747 WAKE TURBULENCE

Run Number	15	16	17	18	19	20	21
Aircraft Position[1], ft.	266	222	229	610	404	357	286
Aircraft Height AGL[2], ft.	189	178	187	338	321	334	397
Equivalent Airspeed, Knots	142	136	135	140	136	138	152
Gross Weight, lb x 10^{-3}	482	480	478	460	458	456	454
Configuration[3]	L	L	L	L	L	L	TO
Peak Recorded Absolute Velocity, First Vortex, ft/sec.	79	81	92	56	54	-	48
Peak Recorded Absolute Velocity, Second Vortex, ft/sec.	-	-	-	-	-	-	103
Vortex Height on Tower, First Vortex, ft.	66	91	96	-	84	-	-
Vortex Height on Tower, Second Vortex, ft.	-	-	-	-	-	-	99
Vortex Age (First) sec.	26	14	15	-	33	-	21
Vortex Age (Second) sec.	-	-	-	-	-	-	35
Mean Descent Rate, First Vortex, ft/sec.	4.73	6.21	6.07	-	7.18	-	-
Mean Descent Rate, Second Vortex, ft/sec.	-	-	-	-	-	-	8.51
Mean Lateral Velocity, First Vortex, ft/sec.	7.3	10.4	10.1	-	9.9	-	10.0
Mean Lateral Velocity, Second Vortex, ft/sec.	-	-	-	-	-	-	10.4
Crosswind Velocity, Component, ft/sec.	3.5	7.2	6.3	12.1	16.3	-	8.8
Median Circulation $ft^2/sec.$	5498	5717	5735	5322	5455	-	4838

FLIGHT TEST DATA - BOEING 747 WAKE TURBULENCE

Run Number	22	23	24	25	26	27	28
Aircraft Position[1], ft.	237	279	439	382	205	272	305
Aircraft Height AGL[2], ft.	322	275	320	175	185	126	172
Equivalent Airspeed, Knots	150	190	192	330	160	154	160
Gross Weight, lb x 10^{-3}	452	450	448	444	556	554	552
Configuration[3]	TO	HLDG	HLDG	C	L	L	TO
Peak Recorded Absolute Velocity, First Vortex, ft/sec.	-	-	-	35	91	77	165
Peak Recorded Absolute Velocity, Second Vortex, ft/sec.	-	-	139	32	78	68	139
Vortex Height on Tower, First Vortex, ft.	-	-	-	-	117	91	93
Vortex Height on Tower, Second Vortex, ft.	-	-	112	-	70	79	49
Vortex Age (First) sec.	-	-	-	-	11	14	13
Vortex Age (Second) sec.	-	-	32	-	27	34	28
Mean Descent Rate, First Vortex, ft/sec.	-	-	-	-	6.73	6.79	6.58
Mean Descent Rate, Second Vortex, ft/sec.	-	-	6.50	-	4.42	2.97	4.39
Mean Lateral Velocity, First Vortex, ft/sec.	-	-	-	-	11.6	13.9	17.5
Mean Lateral Velocity, Second Vortex, ft/sec.	-	-	16.1	-	10.4	10.3	13.6
Crosswind Velocity, Component, ft/sec.	20.0	17.5	16.7	17.7	12.9	16.9	-
Median Circulation $ft^2/sec.$	4881	3836	3779	2179	5629	5827	5588

FLIGHT TEST DATA - BOEING 747 WAKE TURBULENCE

Run Number	29	30	31	32	33	34	35
Aircraft Position[1], ft.	200	248	268	185	223	162	276
Aircraft Height AGL[2], ft.	175	177	186	183	172	164	128
Equivalent Airspeed, Knots	163	205	205	142	152	148	145
Gross Weight, lb x 10^{-3}	549	546	544	542	540	538	536
Configuration[3]	TO	HLDG	HLDG	L	L	L	L
Peak Recorded Absolute Velocity, First Vortex, ft/sec.	159	221	178	84	96	96	92
Peak Recorded Absolute Velocity, Second Vortex, ft/sec.	160	194	201	82	81	88	70
Vortex Height on Tower, First Vortex, ft.	121	114	127	125	105	130	103
Vortex Height on Tower, Second Vortex, ft.	78	65	110	74	60	77	87
Vortex Age (First) sec.	17	13	12	6	9	5	13
Vortex Age (Second) sec.	26	25	23	16	17	17	28
Mean Descent Rate, First Vortex, ft/sec.	9.00	5.25	5.36	9.67	7.44	6.80	1.92
Mean Descent Rate, Second Vortex, ft/sec.	6.06	4.67	3.33	7.27	6.59	5.12	1.46
Mean Lateral Velocity, First Vortex, ft/sec.	7.2	13.2	15.9	18.0	16.2	17.0	15.3
Mean Lateral Velocity, Second Vortex, ft/sec.	10.7	13.0	15.0	16.4	17.6	14.1	12.6
Crosswind Velocity, Component, ft/sec.	13.9	20.8	15.6	18.0	19.3	18.9	12.4
Median Circulation $ft^2/sec.$	5455	4314	4298	6182	5754	5888	5987

FLIGHT TEST DATA - BOEING 747 WAKE TURBULENCE

Run Number	36	37	38	39	40	41	42
Aircraft Position[1], ft.	240	236	243	227	279	240	293
Aircraft Height AGL[2], ft.	176	179	184	194	183	206	144
Equivalent Airspeed, Knots	152	152	150	152	145	145	165
Gross Weight, lb x 10^{-3}	534	532	530	528	507	504	502
Configuration[3]	L	L	L	L	L	L	TO
Peak Recorded Absolute Velocity, First Vortex, ft/sec.	80	86	93	-	65	72	109
Peak Recorded Absolute Velocity, Second Vortex, ft/sec.	78	85	72	-	74	80	93
Vortex Height on Tower, First Vortex, ft.	95	102	121	-	119	142	97
Vortex Height on Tower, Second Vortex, ft.	95	92	74	-	75	93	68
Vortex Age (First) sec.	11	10	8	-	11	8	14
Vortex Age (Second) sec.	23	22	19	-	26	15	29
Mean Descent Rate, First Vortex, ft/sec.	7.36	7.70	7.88	-	5.82	9.14	3.36
Mean Descent Rate, Second Vortex, ft/sec.	3.52	3.95	5.79	-	4.50	8.07	2.62
Mean Lateral Velocity, First Vortex, ft/sec.	14.8	15.9	20.8	-	18.4	20.4	15.4
Mean Lateral Velocity, Second Vortex, ft/sec.	13.8	14.2	16.8	-	13.7	21.1	12.8
Crosswind Velocity, Component, ft/sec.	14.5	14.5	14.7	-	15.0	24.5	13.4
Median Circulation ft^2/sec.	5690	5669	5723	-	5663	5630	4928

FLIGHT TEST DATA - BOEING 747 WAKE TURBULENCE

Run Number	43	44	45	46	47	48	49
Aircraft Position[1], ft.	292	330	249	231	216	229	224
Aircraft Height AGL[2], ft.	158	160	161	143	153	147	169
Equivalent Airspeed, Knots	162	190	195	148	140	140	140
Gross Weight, lb x 10^{-3}	500	498	496	494	492	490	487
Configuration[3]	TO	HLDG	HLDG	L	L	L	L
Peak Recorded Absolute Velocity, First Vortex, ft/sec.	136	183	186	80	68	79	72
Peak Recorded Absolute Velocity, Second Vortex, ft/sec.	129	164	172	58	46	71	78
Vortex Height on Tower, First Vortex, ft.	89	109	120	77	132	90	127
Vortex Height on Tower, Second Vortex, ft.	73	69	82	67	-	77	83
Vortex Age (First) sec.	11	11	10	8	9	7	6
Vortex Age (Second) sec.	21	21	20	33	-	21	13
Mean Descent Rate, First Vortex, ft/sec.	6.90	5.10	4.10	8.25	2.10	8.14	7.00
Mean Descent Rate, Second Vortex, ft/sec.	4.05	4.33	3.95	2.38	-	3.18	7.17
Mean Lateral Velocity, First Vortex, ft/sec.	19.5	23.0	17.2	19.3	15.4	21.7	24.5
Mean Lateral Velocity, Second Vortex, ft/sec.	17.6	19.4	16.3	9.3	-	14.6	23.2
Crosswind Velocity, Component, ft/sec.	20.5	23.5	21.2	15.4	19.0	16.3	13.9
Median Circulation $ft^2/sec.$	4999	4245	4120	5406	5692	5669	5634

FLIGHT TEST DATA - BOEING 747 WAKE TURBULENCE

Run Number	50	51	52	53	54	55	56
Aircraft Position[1], ft.	243	227	271	198	171	171	185
Aircraft Height AGL[2], ft.	143	145	162	152	151	177	184
Equivalent Airspeed, Knots	140	145	330	220	210	200	160
Gross Weight, lb x 10^{-3}	484	482	478	597	595	593	591
Configuration[3]	L	L	C	HLDG	HLDG	HLDG	L
Peak Recorded Absolute Velocity, First Vortex, ft/sec.	68	77	-	213	189	92	140
Peak Recorded Absolute Velocity, Second Vortex, ft/sec.	92	60	-	192	210	267	86
Vortex Height on Tower, First Vortex, ft.	85	103	-	112	124	120	142
Vortex Height on Tower, Second Vortex, ft.	14	54	-	82	69	94	100
Vortex Age (First) sec.	9	7	-	6	5	4	4
Vortex Age (Second) sec.	26	16	-	16	14	12	12
Mean Descent Rate, First Vortex, ft/sec.	7.25	6.00	-	6.67	4.50	14.25	10.50
Mean Descent Rate, Second Vortex, ft/sec.	4.96	5.70	-	4.38	4.56	6.91	6.46
Mean Lateral Velocity, First Vortex, ft/sec.	18.4	21.4	-	20.2	18.8	23.5	27.0
Mean Lateral Velocity, Second Vortex, ft/sec.	12.3	19.0	-	17.2	17.7	20.7	21.8
Crosswind Velocity, Component, ft/sec.	15.4	13.8	-	22.0	22.1	22.3	22.5
Median Circulation ft^2/sec.	5600	5384	-	4395	4589	4802	5983

FLIGHT TEST DATA - BOEING 747 WAKE TURBULENCE

Run Number	57	58	59	60	61	62	63
Aircraft Position[1], ft.	170	183	215	207	221	210	208
Aircraft Height AGL[2], ft.	170	184	166	158	154	103	121
Equivalent Airspeed, Knots	156	155	160	160	158	160	170
Gross Weight, lb x 10^{-3}	589	587	585	581	578	575	569
Configuration[3]	L	L	L	L	L	TO	TO
Peak Recorded Absolute Velocity, First Vortex, ft/sec.	-	103	87	102	145	140+	-
Peak Recorded Absolute Velocity, Second Vortex, ft/sec.	-	103	89	102	100	140+	-
Vortex Height on Tower, First Vortex, ft.	-	142+	103	120	102	90	-
Vortex Height on Tower, Second Vortex, ft.	-	98	77	53	66	90	-
Vortex Age (First) sec.	-	5	7	8	6	7	-
Vortex Age (Second) sec.	-	14	18	21	13	29	-
Mean Descent Rate, First Vortex, ft/sec.	-	10.50	7.88	5.43	8.66	1.30	-
Mean Descent Rate, Second Vortex, ft/sec.	-	6.14	4.94	5.25	6.77	.42	-
Mean Lateral Velocity, First Vortex, ft/sec.	-	21.2	19.7	16.3	24.0	19.0	-
Mean Lateral Velocity, Second Vortex, ft/sec.	-	18.6	16.2	13.5	22.9	9.9	-
Crosswind Velocity, Component, ft/sec.	-	25.0	16.1	16.7	16.4	18.0	-
Median Circulation $ft^2/sec.$	6116	6134	5922	5882	5925	5821	-

FLIGHT TEST DATA - BOEING 747 WAKE TURBULENCE

Run Number	64	65	66	67	68	69	70
Aircraft Position[1], ft.	197	440	334	449	439	404	428
Aircraft height AGL[2], ft.	119	172	220	259	213	229	204
Equivalent Airspeed, Knots	175	310	350	350	350	150	155
Gross Weight, lb x 10^{-3}	566	563	532	530	528	525	523
Configuration[3]	TO	C	HLDG	HLDG	HLDG	L	L
Peak Recorded Absolute Velocity, First Vortex, ft/sec.	104	-	-	-	137	80	85
Peak Recorded Absolute Velocity, Second Vortex, ft/sec.	73	-	-	86	109	85	77
Vortex Height on Tower, First Vortex, ft.	94	-	-	-	132	133	139
Vortex Height on Tower, Second Vortex, ft.	71	-	-	112	86	102	67
Vortex Age (First) sec.	6	-	-	-	15	14	19
Vortex Age (Second) sec.	32	-	-	18	24	21	27
Mean Descent Rate, First Vortex, ft/sec.	4.17	-	-	-	5.4	7.38	3.42
Mean Descent Rate, Second Vortex, ft/sec.	1.50	-	-	8.17	5.29	5.77	5.07
Mean Lateral Velocity, First Vortex, ft/sec.	20.0	-	-	-	24.1	23.4	18.5
Mean Lateral Velocity, Second Vortex, ft/sec.	8.6	-	-	29.2	21.5	22.9	18.7
Crosswind Velocity, Component, ft/sec.	-	-	20.9	22.5	18.0	21.8	24
Median Circulation $ft^2/sec.$	5239	2941	-	2452	2443	5669	5465

FLIGHT TEST DATA - BOEING 747 WAKE TURBULENCE

Run Number	71	72	73	74	75	76
Aircraft Position[1], ft.	416	482	440	402	394	354
Aircraft Height AGL[2], ft.	216	206	238	216	224	136
Equivalent Airspeed, Knots	145	155	150	150	205	300
Gross Weight, lb x 10^{-3}	521	519	517	513	510	507
Configuration[3]	L	L	L	L	HLDG	C
Peak Recorded Absolute Velocity, First Vortex, ft/sec.	69	84	-	96	126	78
Peak Recorded Absolute Velocity, Second Vortex, ft/sec.	103	106	-	78	-	72
Vortex Height on Tower, First Vortex, ft.	142+	82	-	142+	-	106
Vortex Height on Tower, Second Vortex, ft.	85	64	-	107	-	68
Vortex Age (First) sec.	17	17	-	12	-	9
Vortex Age (Second) sec.	28	24	-	19	-	15
Mean Descent Rate, First Vortex, ft/sec.	4.30	6.89	-	6.73	-	3.33
Mean Descent Rate, Second Vortex, ft/sec.	4.68	6.17	-	5.74	-	4.54
Mean Lateral Velocity, First Vortex, ft/sec.	19.9	23.8	-	27.0	-	35.4
Mean Lateral Velocity, Second Vortex, ft/sec.	17.6	23.3	-	25.2	-	31.4
Crosswind Velocity, Component, ft/sec.	10.7	13.3	-	21.6	-	43.5
Median Circulation $ft^2/sec.$	5820	5423	5583	5539	-	2737

APPENDIX E

VORTEX LATERAL TRANSPORT VELOCITY vs. X-WIND COMPONENT
PEAK RECORDED VELOCITY vs. ALTITUDE AT TOWER

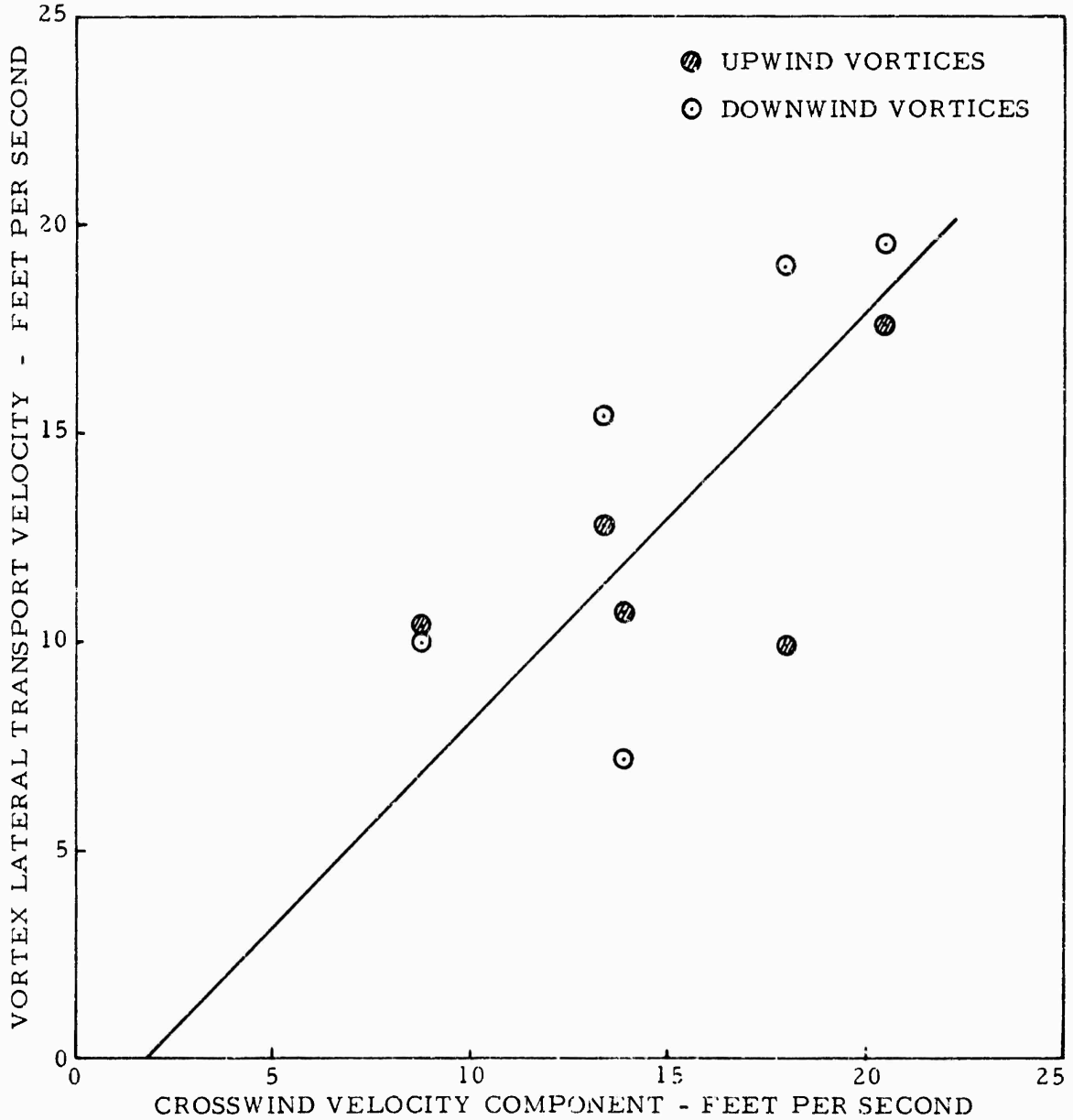

FIGURE E-1. VORTEX LATERAL TRANSPORT VELOCITY VS. CROSSWIND VELOCITY COMPONENT. TAKEOFF CONFIGURATION

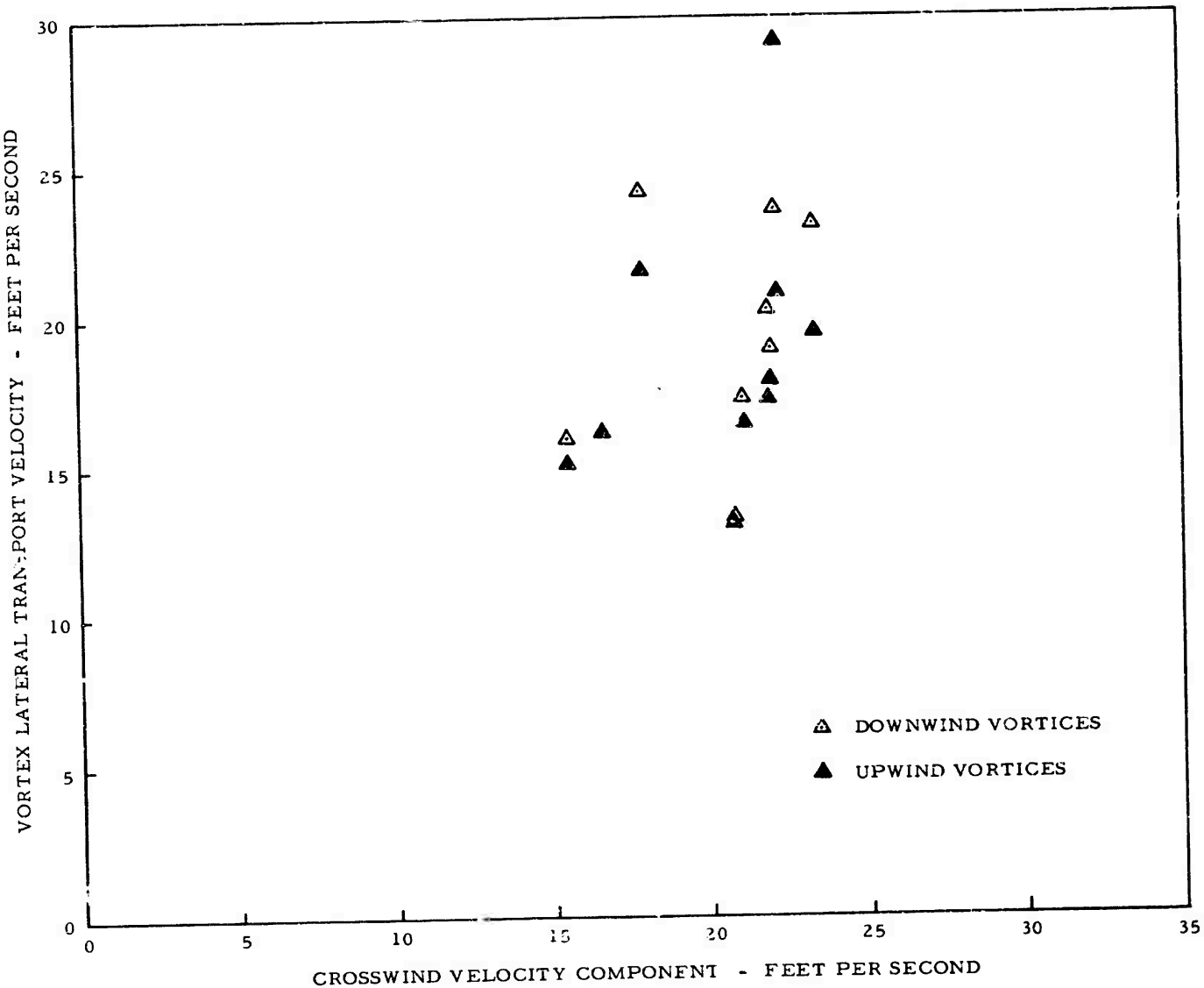

FIGURE E-2. VORTEX LATERAL TRANSPORT VELOCITY VS. CROSSWIND VELOCITY COMPONENT. HOLDING CONFIGURATION

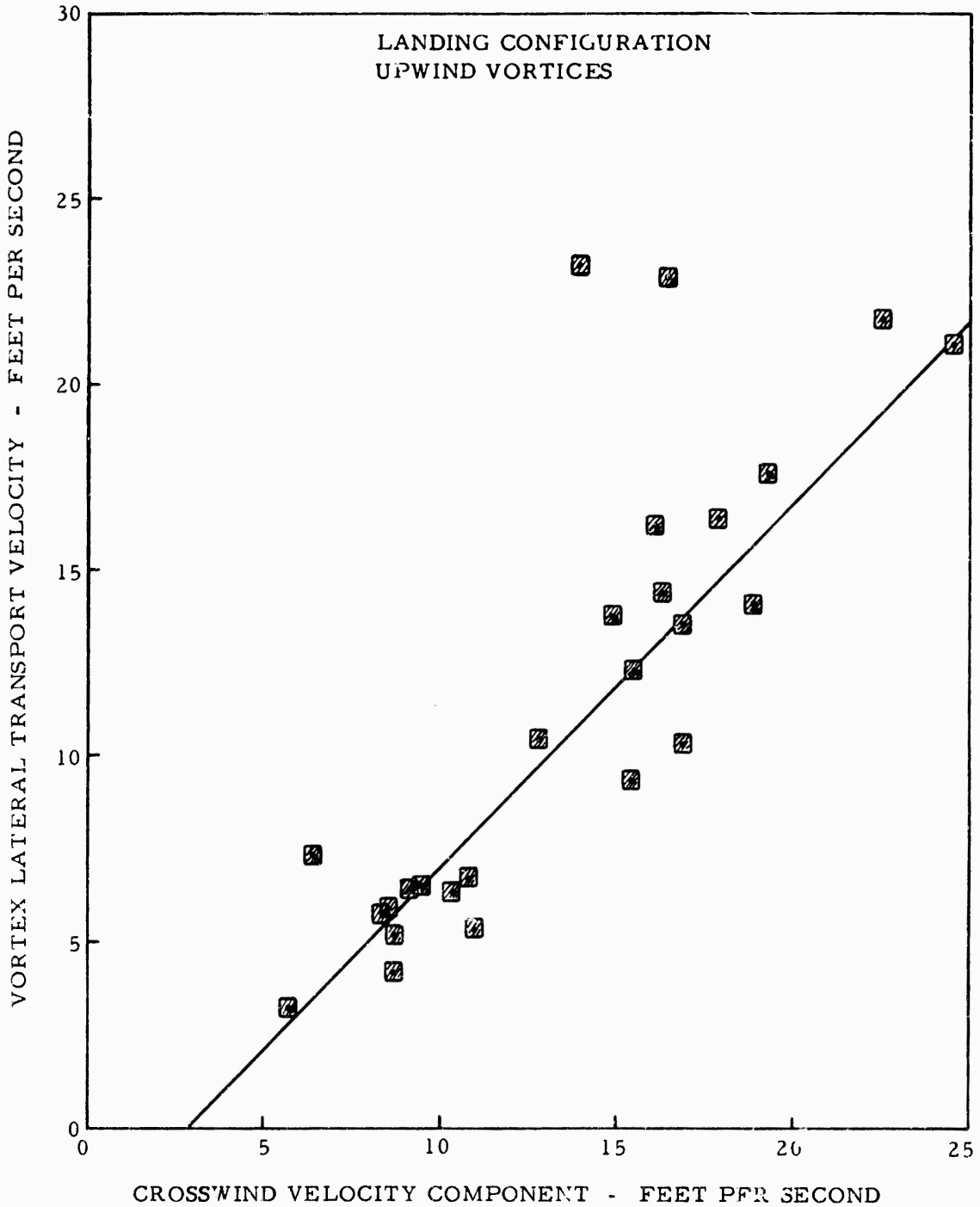

FIGURE E-3. VORTEX LATERAL TRANSPORT VELOCITY VS. CROSSWIND VELOCITY COMPONENT. LANDING CONFIGURATION - UPWIND VORTICES

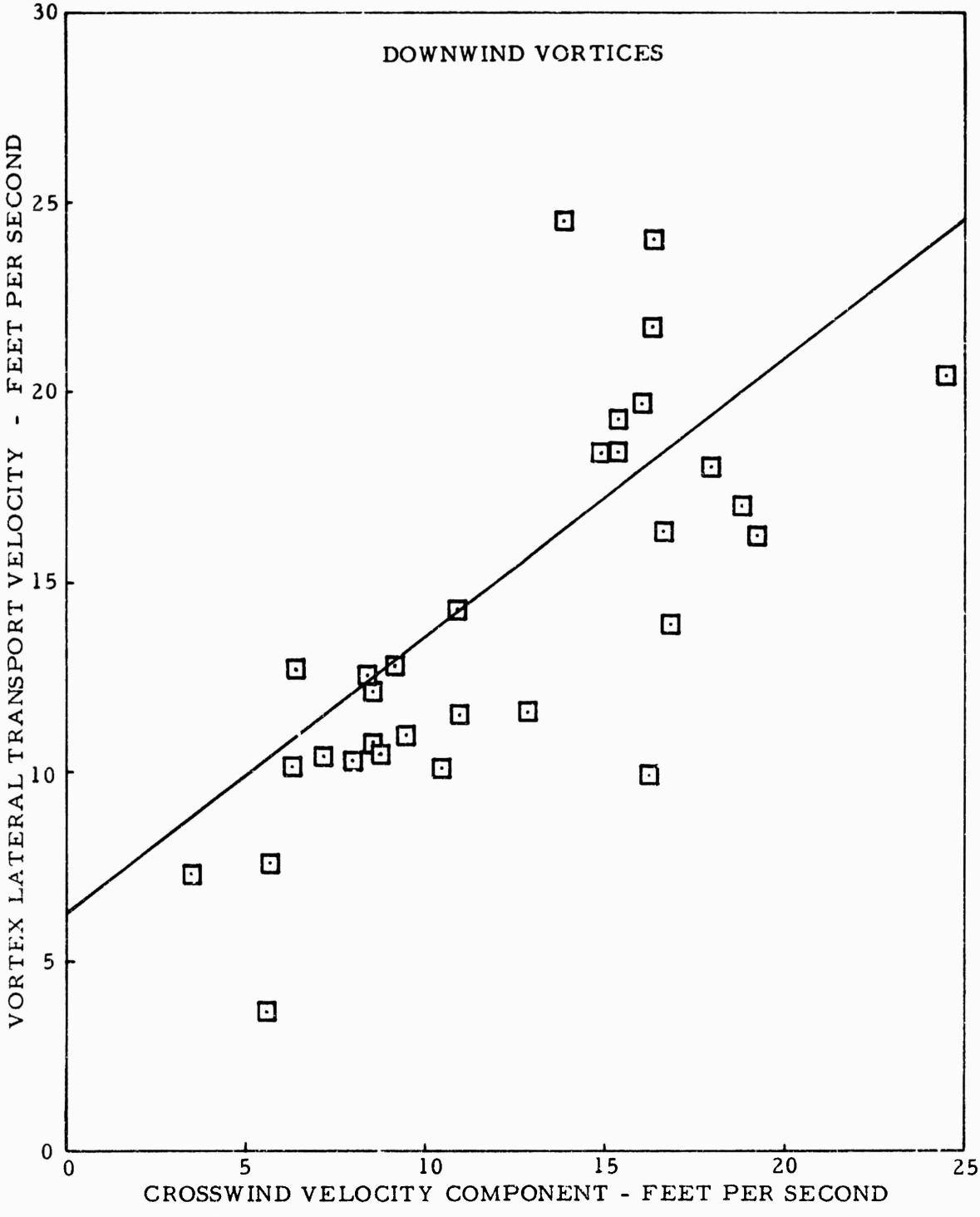

FIGURE E-4. VORTEX LATERAL TRANSPORT VELOCITY VS. CROSSWIND VELOCITY COMPONENT. LANDING CONFIGURATION - DOWNWIND VORTICES

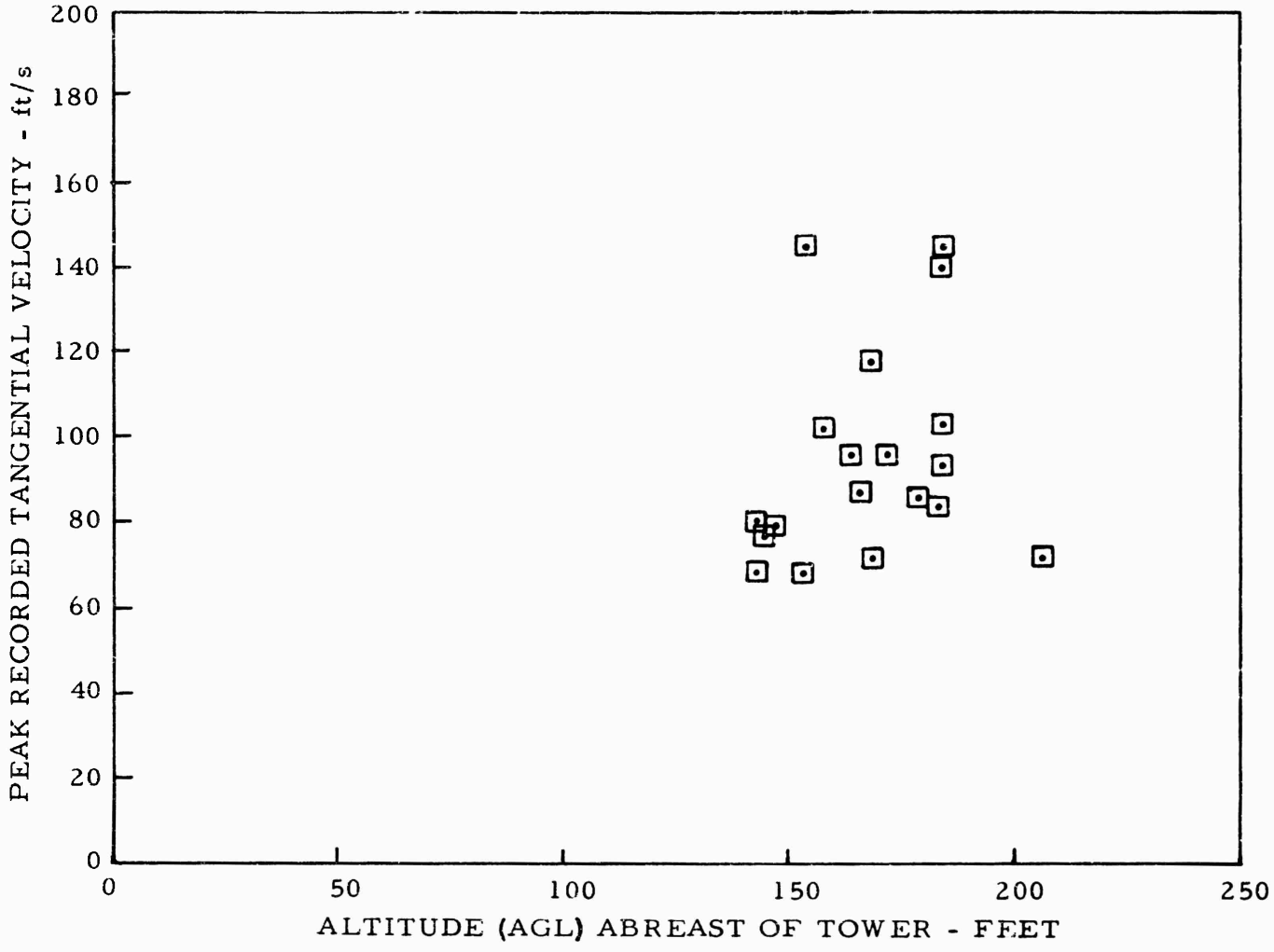

FIGURE E-5. PEAK RECORDED TANGENTIAL VELOCITY VS. AIRCRAFT ALTITUDE ABREAST OF TOWER. LANDING CONFIGURATION - DOWNWIND VORTICES, ZERO TO 10 SECONDS AGE

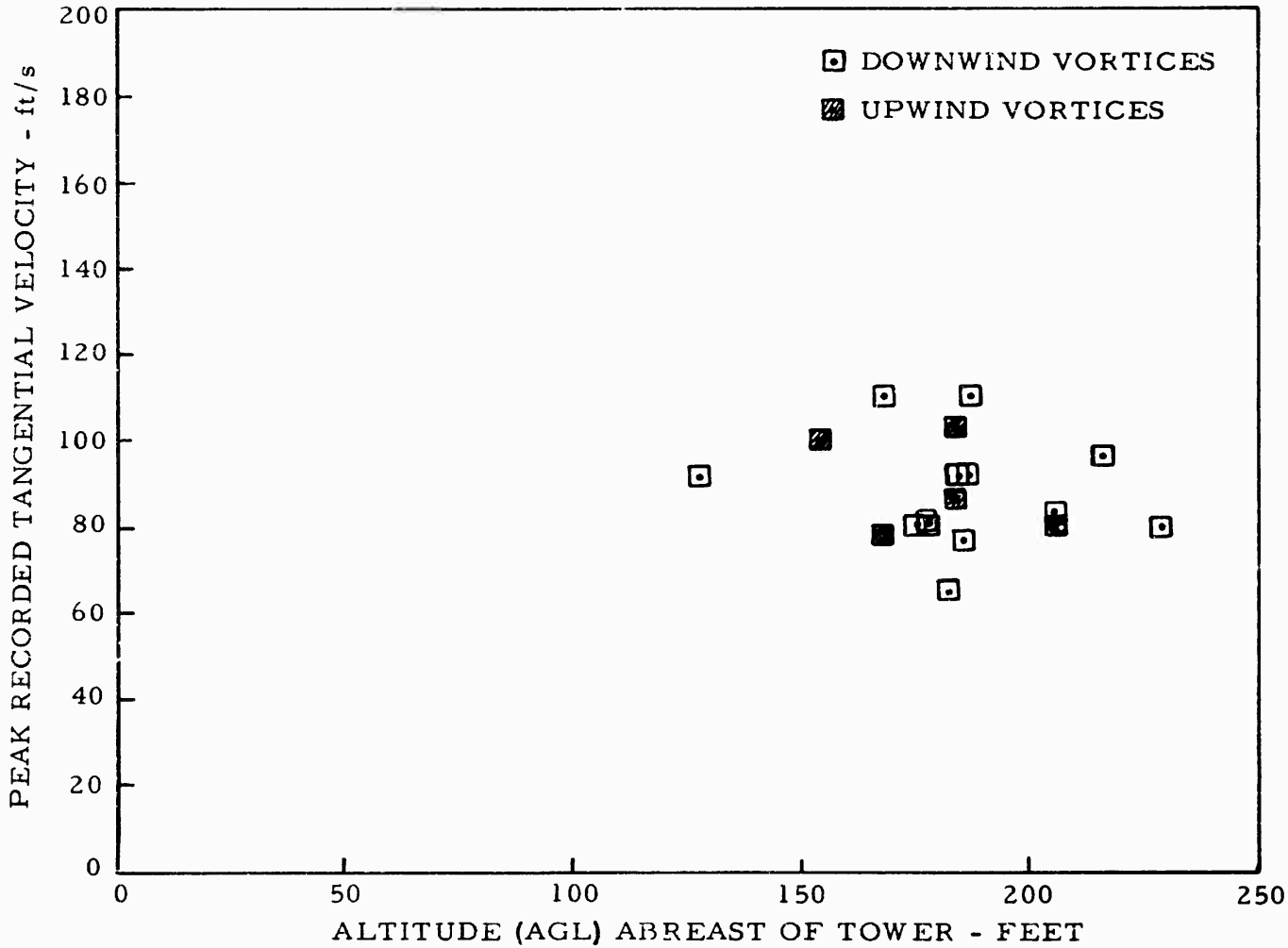

FIGURE E-6. PEAK RECORDED TANGENTIAL VELOCITY VS. AIRCRAFT ALTITUDE ABREAST OF TOWER. LANDING CONFIGURATION - UPWIND AND DOWNWIND VORTICES, 10 TO 15 SECONDS AGE

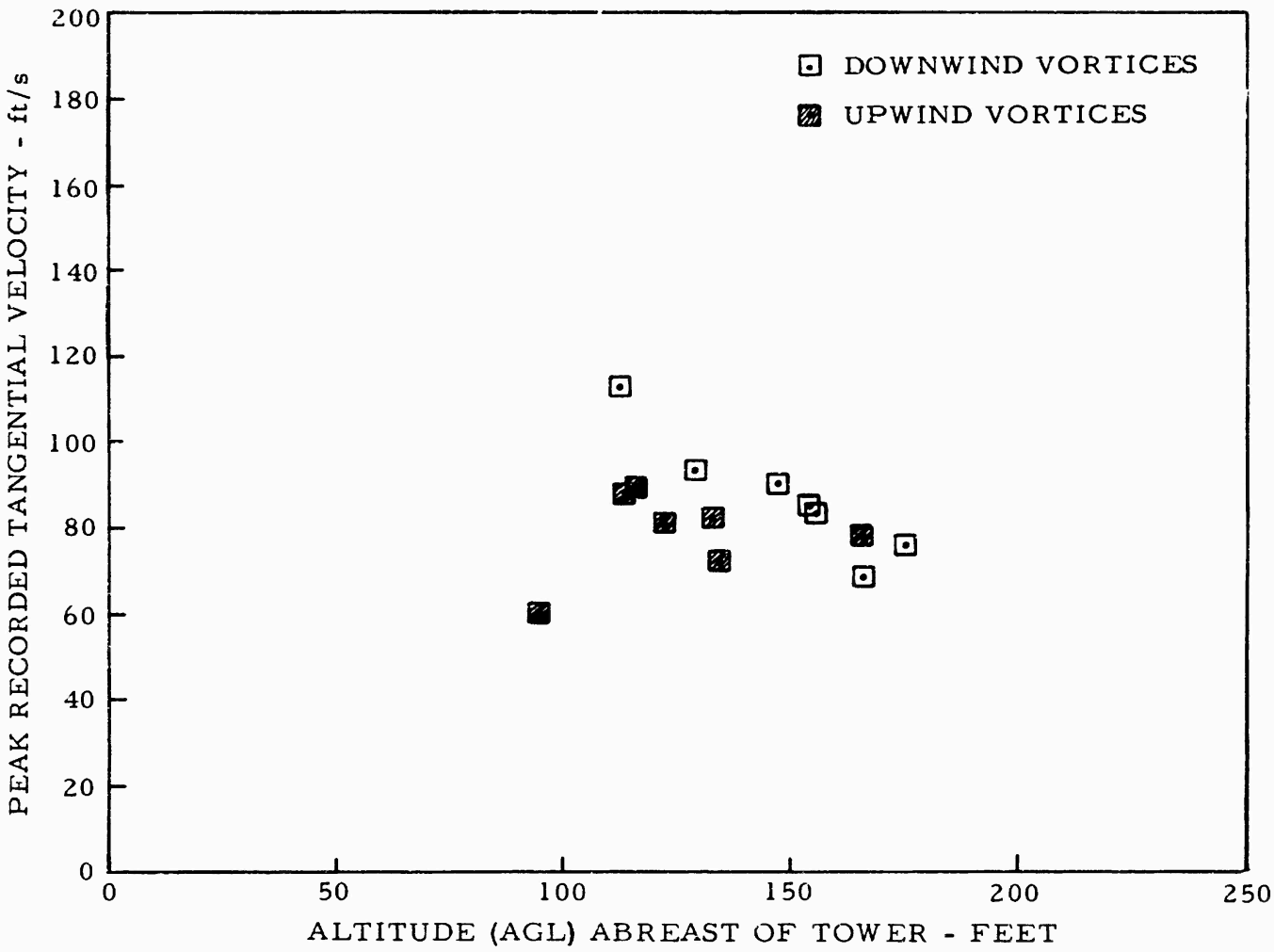

FIGURE E-7. PEAK RECORDED TANGENTIAL VELOCITY VS. AIRCRAFT ALTITUDE ABREAST OF TOWER. LANDING CONFIGURATION - UPWIND AND DOWNWIND VORTICES, 15 TO 20 SECONDS AGE

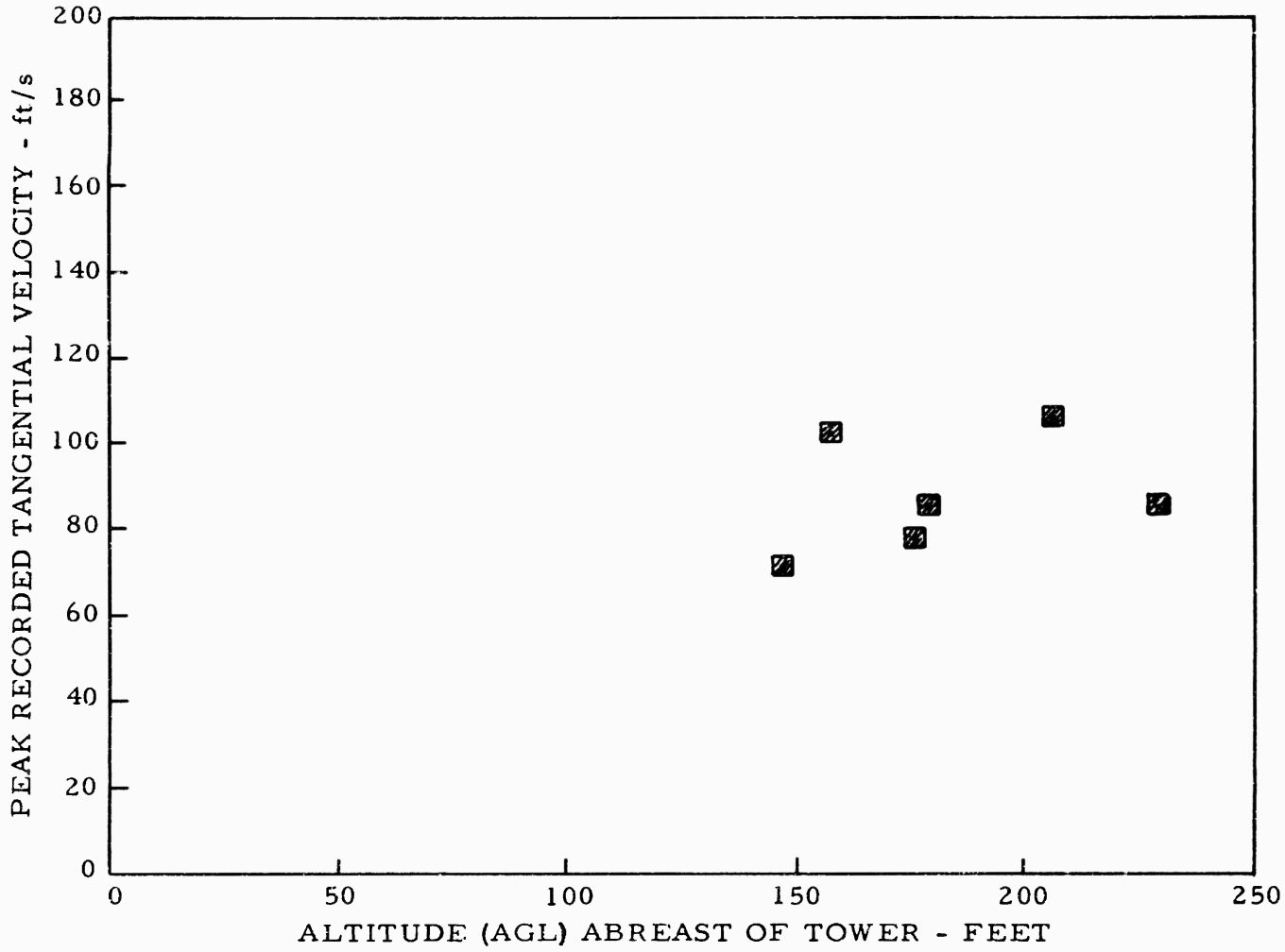

FIGURE E-8. PEAK RECORDED TANGENTIAL VELOCITY VS. AIRCRAFT ALTITUDE ABREAST OF TOWER. LANDING CONFIGURATION - UPWIND VORTICES, 20 TO 25 SECONDS AGE

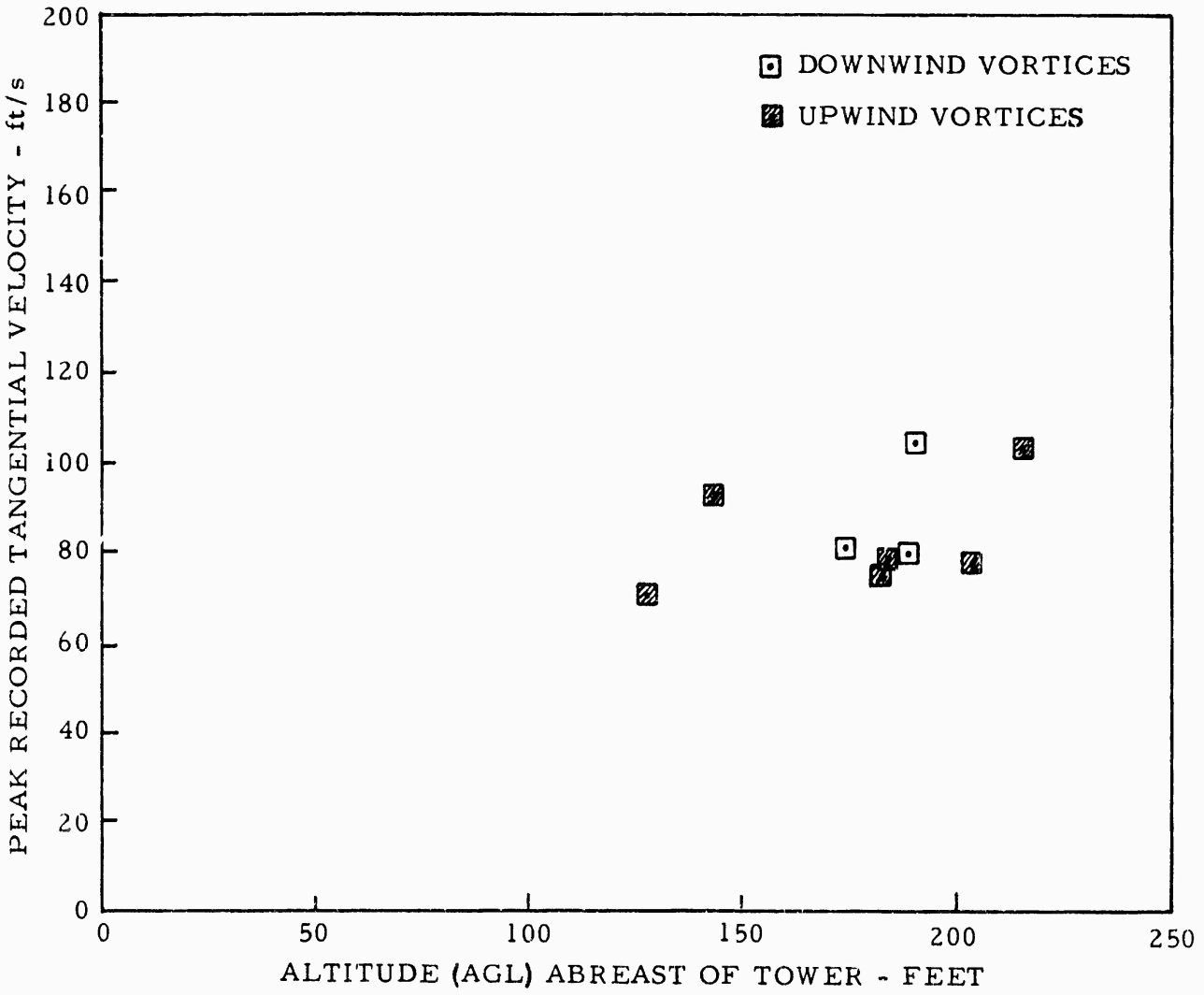

FIGURE E-9. PEAK RECORDED TANGENTIAL VELOCITY VS. AIRCRAFT ALTITUDE ABREAST OF TOWER. LANDING CONFIGURATION - UPWIND AND DOWNWIND VORTICES, 25 TO 30 SECONDS AGE

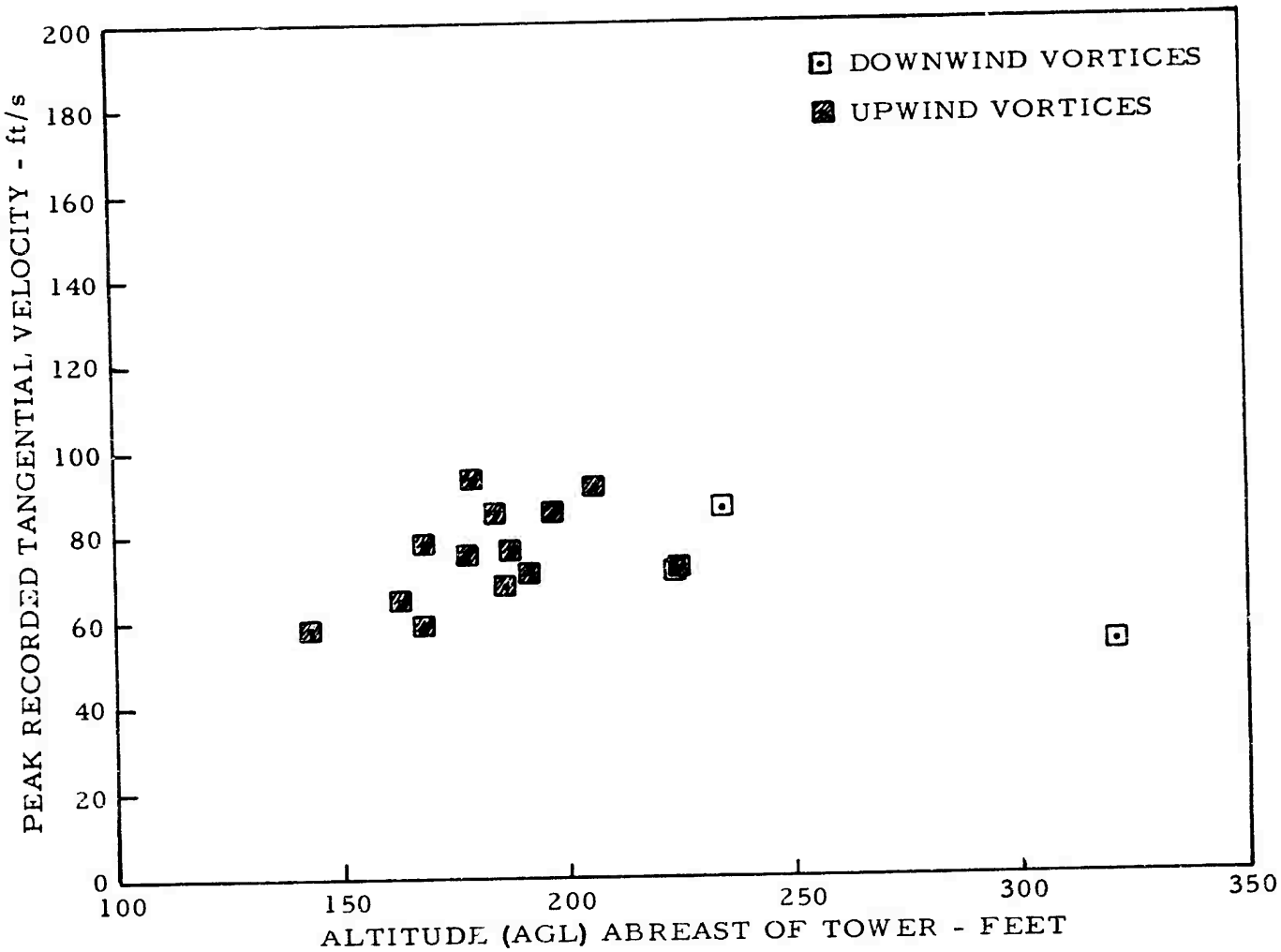

FIGURE E-10. PEAK RECORDED TANGENTIAL VELOCITY VS. AIRCRAFT ALTITUDE ABREAST OF TOWER. LANDING CONFIGURATION - UPWIND AND DOWNWIND VORTICES, > 30 SECONDS AGE

BOEING 747 VORTEX FLIGHT TESTS
LOW-ALTITUDE METEOROLOGICAL DATA
SEPTEMBER 16, 17, AND OCTOBER 17, 1972

	Runs 1-5			Runs 6-10		
Level ft	Temp °C	Vel. ft/s	Direc. °Mag.	Temp. °C	Vel. ft/s	Direc. °Mag.
23	20.5	14.7	256	20.8	15.5	257
45	20.6	14.8	256	20.7	17.5	266
70	20.6	15.7	263	20.8	17.5	274
100	20.6	15.5	236	20.7	19.5	247
140	20.7	16.6	273	20.6	18.8	274
23	21.5	14.6	257	20.9	17.6	274
45	21.4	17.1	258	20.9	19.5	279
70	21.5	17.0	264	21.0	18.2	283
100	21.5	18.3	245	20.9	20.6	255
140	21.5	18.8	285	20.9	18.9	280
23	21.1	17.5	260	21.0	13.6	262
45	21.2	20.0	262	20.8	14.1	261
70	21.3	18.7	266	20.8	12.9	264
100	21.4	20.8	240	20.9	14.0	241
140	21.4	20.3	273	20.8	15.8	277
23	18.1	13.1	254	20.3	12.3	254
45	18.1	13.8	260	20.1	12.7	263
70	18.2	12.8	266	20.1	12.3	267
100	18.2	14.5	240	20.1	13.5	241
140	18.1	13.1	270	20.0	15.9	277
23	18.8	14.8	259	22.2	17.0	256
45	18.9	15.8	262	22.0	17.8	261
70	18.9	14.6	265	22.0	16.0	267
100	19.0	16.0	233	22.0	18.9	239
140	18.9	13.5	269	21.9	15.5	276

Note: Runs 1 - 15 made between 0854 and 1044, 9-16-72.

BOEING 747 VORTEX FLIGHT TESTS
LOW-ALTITUDE METEOROLOGICAL DATA
SEPTEMBER 16, 17, and OCTOBER 17, 1972

	Runs 11-15			Runs 16-20		
Level ft	Temp °C	Vel. ft/s	Direc. °Mag.	Temp °C	Vel. ft/s	Direc. °Mag.
23	21.9	16.7	239	26.7	14.9	276
45	21.7	18.3	250	22.5	17.0	276
70	21.8	16.2	257	22.6	15.4	278
100	21.7	17.9	232	22.5	17.2	256
140	21.6	16.9	274	22.4	19.2	288
23	19.2	13.5	239	24.3	15.8	262
45	19.0	13.5	241	23.1	16.3	270
70	19.2	11.0	252	23.1	13.3	275
100	19.1	13.8	226	23.1	15.6	253
140	19.0	10.7	278	23.0	17.7	291
23	26.8	12.5	282	24.0	12.3	277
45	23.3	13.3	288	22.9	12.3	279
70	23.4	12.9	289	22.9	9.4	283
100	23.4	13.9	257	22.7	12.8	261
140	23.2	16.3	290	22.6	12.6	299
23	22.2	13.6	253	29.1	11.0	294
45	21.8	13.9	256	25.2	11.9	312
70	21.9	12.4	-	25.1	12.2	302
100	21.8	14.2	-	25.1	13.3	275
140	21.7	12.0	270	25.0	16.9	301
23	25.4	13.1	284	26.1	10.8	263
45	23.5	13.6	292	23.6	10.8	273
70	23.5	12.7	-	23.5	10.6	279
100	23.5	13.4	-	23.5	12.0	241
140	23.4	16.4	298	23.3	12.6	275

Note: Runs 1 - 15 made between 0854 and 1044, 9-16-72.
Runs 16 - 25 made between 1047 and 1205, 9-16-72.

BOEING 747 VORTEX FLIGHT TESTS
LOW-ALTITUDE METEOROLOGICAL DATA
SEPTEMBER 16, 17, AND OCTOBER 17, 1972

	Runs 21-25			Runs 26-30		
Level ft	Temp °C	Vel. ft/s	Direc. °Mag.	Temp. °C	Vel. ft/s	Direc. °Mag.
23	-	-	-	23.0	11.7	235
45	-	-	-	22.2	13.2	238
70	-	-	-	22.9	12.8	242
100	-	-	-	22.7	13.8	210
140	-	(13.2)	(270)	22.6	15.5	244
23	29.0	19.0	286	22.6	14.5	217
45	25.5	20.0	289	22.4	15.4	224
70	25.5	17.3	298	23.0	14.7	230
100	25.4	19.4	274	22.8	16.5	207
140	25.3	20.2	306	22.7	17.9	234
23	29.2	12.6	286	-	-	-
45	26.1	15.2	290	-	-	-
70	26.1	15.3	298	-	-	-
100	26.0	16.1	271	-	-	-
140	25.9	17.7	304	-	(7.3)	(240)
23	25.0	14.4	263	23.2	13.7	232
45	24.6	14.3	276	22.5	14.2	239
70	24.7	13.7	280	23.2	14.2	247
100	24.5	15.6	259	23.1	15.6	216
140	24.4	17.3	295	23.0	16.1	250
23	26.1	15.1	273	23.6	16.4	216
45	23.2	16.7	276	22.7	18.8	220
70	23.2	14.7	285	23.4	17.8	227
100	23.0	16.9	255	23.3	20.4	198
140	22.9	19.2	293	23.3	21.7	234

Note: Runs 16 - 25 made between 1047 and 1205, 9-16-72.
Runs 26 - 30 made between 0956 and 1011, 9-17-72.

BOEING 747 VORTEX FLIGHT TESTS
LOW-ALTITUDE METEOROLOGICAL DATA
SEPTEMBER 16, 17, and OCTOBER 17, 1972

	Runs 31-35			Runs 36-40		
Level ft	Temp °C	Vel. ft/s	Direc. °Mag.	Temp. °C	Vel. ft/s	Direc. °Mag.
23	24.8	14.3	222	-	-	-
45	23.0	15.7	230	-	-	-
70	23.6	16.2	238	-	-	-
100	23.5	16.7	211	-	-	-
140	23.4	18.2	251	-	(14.7)	(230)
23	24.2	18.2	228	-	-	-
45	23.1	19.8	234	-	-	-
70	23.7	19.9	241	-	-	-
100	23.7	22.2	212	-	-	-
140	23.5	20.9	251	-	(14.7)	(230)
23	24.4	15.1	218	-	-	-
45	23.4	16.6	228	-	-	-
70	23.9	17.4	236	-	-	-
100	23.8	18.7	207	-	-	-
140	23.7	21.3	243	-	(14.7)	(220)
23	24.7	15.9	217	-	-	-
45	23.7	17.8	225	-	-	-
70	24.2	16.4	232	-	-	-
100	24.1	19.4	204	-	-	-
140	23.9	19.8	237	-	(16.1)	(230)
23	-	-	-	28.4	13.8	239
45	-	-	-	27.3	14.5	246
70	-	-	-	27.0	16.5	254
100	-	-	-	27.0	17.0	224
140	-	(13.2)	(240)	26.7	19.2	259

Note: Runs 31 - 45 made between 1015 and 1200, 9-17-72.

BOEING 747 VORTEX FLIGHT TESTS
LOW-ALTITUDE METEOROLOGICAL DATA
SEPTEMBER 16, 17, AND OCTOBER 17, 1972

	Runs 41-45			Runs 46-50		
Level ft	Temp °C	Vel. ft/s	Direc. °Mag.	Temp. °C	Vel. ft/s	Direc. °Mag.
23	33.6	17.7	211	30.0	18.1	229
45	27.6	19.3	218	28.1	18.7	239
70	26.9	21.5	229	27.7	18.2	248
100	26.8	23.0	200	27.5	19.8	221
140	26.7	25.5	236	27.4	19.5	258
23	31.1	16.0	245	32.7	19.7	230
45	27.8	16.8	252	28.4	20.9	237
70	27.1	16.9	258	27.9	21.6	243
100	27.0	18.5	228	27.7	24.0	213
140	26.9	17.9	262	27.6	22.9	254
23	28.6	15.7	212	29.3	18.1	234
45	27.9	16.7	221	28.5	19.3	242
70	27.2	16.9	228	27.7	21.1	247
100	27.1	18.4	218	27.6	21.8	219
140	26.9	21.8	240	27.6	21.3	260
23	29.1	20.0	222	29.4	17.0	237
45	27.9	21.3	229	28.7	18.2	244
70	27.2	21.8	237	27.7	19.0	253
100	27.9	23.6	208	27.6	20.3	225
140	27.0	26.0	245	27.5	19.0	263
23	28.8	17.7	222	29.5	20.4	241
45	28.0	18.4	226	28.7	20.9	245
70	27.5	18.7	234	27.9	21.5	250
100	27.4	20.1	213	27.8	23.6	219
140	27.2	22.6	240	28.7	20.3	261

Note: Runs 31 - 45 made between 1015 and 1200, 9-17-72.
Runs 46 - 52 made between 1204 and 1229, 9-17-72.

BOEING 747 VORTEX FLIGHT TESTS
LOW-ALTITUDE METEOROLOGICAL DATA
SEPTEMBER 16, 17, AND OCTOBER 17, 1972

	Runs 51-55			Runs 56-60		
Level ft	Temp °C	Vel. ft/s	Direc. °Mag.	Temp. °C	Vel. ft/s	Direc. °Mag.
23	-	-	-	17.1	16.5	233
45	-	-	-	16.3	18.4	237
70	-	-	-	16.4	19.0	243
100	-	-	-	16.3	20.3	224
140	-	(14.7)	(240)	16.1	23.7	240
23	-	-	-	17.5	19.3	232
45	-	-	-	16.2	21.1	239
70	-	-	-	16.4	21.2	242
100	-	-	-	16.4	22.2	218
140	-	(14.7)	(220)	16.1	25.5	241
23	16.4	16.0	230	-	-	-
45	-	-	-	-	-	-
70	16.2	18.3	241	-	-	-
100	16.1	19.7	220	-	-	-
140	16.0	23.1	239	-	(25.0)	(220)
23	16.8	16.1	230	17.8	20.1	259
45	16.2	17.6	236	17.5	21.6	268
70	16.3	18.2	242	17.4	22.3	270
100	16.2	19.5	221	17.4	23.6	241
140	16.1	23.1	239	17.2	25.1	268
23	16.8	16.2	232	18.1	21.4	262
45	16.3	17.9	237	17.6	22.9	269
70	16.4	18.5	243	17.5	23.6	272
100	16.3	19.8	223	17.5	24.8	244
140	16.2	23.4	240	17.3	26.9	270

Note: Runs 46 - 52 made between 1204 and 1229, 9-17-72.
Runs 53 - 60 made between 0828 and 0901, 10-17-72.

BOEING 747 VORTEX FLIGHT TESTS
LOW-ALTITUDE METEOROLOGICAL DATA
SEPTEMBER 16, 17, AND OCTOBER 17, 1972

	Runs 61-65			Runs 66-70		
Level ft	Temp °C	Vel. ft/s	Direc. °Mag.	Temp. °C	Vel. ft/s	Direc. °Mag.
23	18.2	21.3	264	-	-	-
45	17.6	22.7	272	-	-	-
70	17.8	23.2	272	-	-	-
100	17.9	24.0	247	-	-	-
140	17.7	27.2	273	-	(23.0)	(260)
23	-	-	-	-	-	-
45	-	-	-	-	-	-
70	-	-	-	-	-	-
100	-	-	-	-	-	-
140	-	(22.0)	(255)	-	(29.0)	(270)
23	-	-	-	-	-	-
45	-	-	-	-	-	-
70	-	-	-	-	-	-
100	-	-	-	-	-	-
140	-	(37.0)	(250)	-	(23.0)	(270)
23	-	-	-	-	-	-
45	-	-	-	-	-	-
70	-	-	-	-	-	-
100	-	-	-	-	-	-
140	-	(29.0)	(250)	-	(29.0)	(270)
23	-	-	-	-	-	-
45	-	-	-	-	-	-
70	-	-	-	-	-	-
100	-	-	-	-	-	-
140	-	(22.0)	(250)	-	(32.0)	(270)

Note: Runs 61 - 76 made between 0906 and 1124, 10-17-72.

( ) - Indicates "spot" readings taken on backup instrumentation at time of passage of airplane by the tower. Height was 140 ft A.G.L.

\- - Indicates primary data missing or erroneous.

BOEING 747 VORTEX FLIGHT TESTS
LOW-ALTITUDE METEOROLOGICAL DATA
SEPTEMBER 16, 17, AND OCTOBER 17, 1972

Runs 71-76

Level ft	Temp °C	Vel. ft/s	Direc. °Mag.
23	-	-	-
45	-	-	-
70	-	-	-
100	-	-	-
140	-	(14.7)	(270)
23	-	-	-
45	-	-	-
70	-	-	-
100	-	-	-
140	-	(19.0)	(270)
23	-	-	-
45	-	-	-
70	-	-	-
100	-	-	-
140	-	(37.0)	(270)
23	-	-	-
45	-	-	-
70	-	-	-
100	-	-	-
140	-	(26.0)	(280)
23	-	-	-
45	-	-	-
70	-	-	-
100	-	-	-
140	-	(26.0)	(270)
23	-	-	-
45	-	-	-
70	-	-	-
100	-	-	-
140	-	(26.0)	(270)

Note: Runs 61 - 76 made between 0906 and 1124, 10-17-72.
( ) - Indicates "spot" readings taken on backup instrumentation at time of passage of airplane by the tower. Height was 140 ft A.G.L.
- - Indicates primary data missing or erroneous.

APPENDIX G

WINDSPEED AND DIRECTION AT 140 FEET, AIRPLANE TRACK, DATE, AND TIME OF RUNS

Run No.	Windspeed at 140 ft - ft/s	Wind Direction at 140 ft - °Mag.	Airplane Track °Mag.	Date	Time
1	16.6	273	105	9-16-72	0853
2	18.8	285	125	9-16-72	0857
3	20.3	273	125	9-16-72	0902
4	13.1	270	130	9-16-72	0906
5	13.5	269	132	9-16-72	0910
6	18.8	274	130	9-16-72	0914
7	18.9	280	130	9-16-72	0918
8	15.8	277	130	9-16-72	0922
9	15.9	277	130	9-16-72	0926
10	15.5	276	130	9-16-72	0931
11	16.9	274	132	9-16-72	0935
12	10.7	278	130	9-16-72	0939
13	16.3	290	130	9-16-72	1034
14	12.0	270	132	9-16-72	1039
15	16.4	298	130	9-16-72	1043
16	19.2	288	130	9-16-72	1048
17	17.7	291	132	9-16-72	1053
18	12.6	299	225	9-16-72	1130
19	16.9	301	226	9-16-72	1136
20	12.6	275	230	9-16-72	1141
21	(13.2)	(270)	228	9-16-72	1146
22	20.2	306	225	9-16-72	1151
23	17.7	304	222	9-16-72	1200
25	19.2	293	360	9-16-72	1205
26	15.5	244	120	9-17-72	0957
27	17.9	234	125	9-17-72	1000
28	(7.3)	(240)	125	9-17-72	1004
29	16.1	250	130	9-17-72	1008
30	21.7	233	128	9-17-72	1012
31	18.2	251	130	9-17-72	1016
32	20.9	251	130	9-17-72	1020
33	21.3	243	128	9-17-72	1024
34	19.8	237	130	9-17-72	1028
35	(13.2)	(240)	130	9-17-72	1032
36	(14.7)	(230)	130	9-17-72	1035
37	(14.7)	(230)	130	9-17-72	1039
38	(14.7)	(220)	130	9-17-72	1043
39	(16.1)	(230)	130	9-17-72	1047
40	19.2	259	130	9-17-72	1138
41	25.5	236	130	9-17-72	1142
42	17.9	262	130	9-17-72	1146
43	21.8	240	130	9-17-72	1150
44	26.0	245	130	9-17-72	1156
45	22.6	240	130	9-17-72	1200
46	19.5	258	130	9-17-72	1205
47	22.9	254	130	9-17-72	1209
48	21.3	260	130	9-17-72	1213

Run No.	Windspeed at 140 ft - ft/s	Wind Direction at 140 ft - °Mag.	Airplane Track °Mag.	Date	Time
49	19.0	263	130	9-17-72	1217
50	20.3	261	130	9-17-72	1221
51	(14.7)	(240)	130	9-17-72	1225
52	(14.7)	(220)	310	9-17-72	1229
53	23.1	239	132	10-17-72	0828
54	23.1	239	132	10-17-72	0832
55	23.4	240	132	10-17-72	0836
56	23.7	240	132	10-17-72	0841
57	25.5	241	130	10-17-72	0846
58	(25.0)	(220)	130	10-17-72	0851
59	25.1	268	128	10-17-72	0856
60	26.9	270	128	10-17-72	0901
61	27.2	273	130	10-17-72	0906
62	(22.0)	(255)	130	10-17-72	0912
63	(37.0)	(250)	125	10-17-72	0922
64	(29.0)	(250)	128	10-17-72	0926
65	(22.0)	(250)	305	10-17-72	0931
66	(23.0)	(260)	220	10-17-72	1034
67	(29.0)	(270)	220	10-17-72	1038
68	(23.0)	(270)	220	10-17-72	1041
69	(29.0)	(270)	222	10-17-72	1050
70	(32.0)	(270)	222	10-17-72	1055
71	(14.7)	(270)	223	10-17-72	1059
72	(19.0)	(270)	226	10-17-72	1104
73	(37.0)	(270)	230	10-17-72	1108
74	(26.0)	(280)	225	10-17-72	1114
75	(26.0)	(270)	225	10-17-72	1119
76	-	-	352	10-17-72	1124

Note: ( ) - Indicates "spot" readings taken on backup instrumentation at time of passage of airpiane by the tower. Height was 140 ft AGL.